SAMCO MONITORING GLOSSARY

STRUCTURAL DYNAMICS FOR VBHM OF BRIDGES

Helmut Wenzel, Hiroshi Tanaka

Vienna Consulting Engineers Holding GmbH, Vienna, Austria

E-mail: wenzel@vce.at Website: www.vce.at

Abstract

Part I, glossary, is an empirical collection of technical terms that appear in literature in association with the vibration-based health monitoring (VBHM) of bridges. The definition of terms is mainly aimed at intuitive understanding of the matter and little attention is paid for mathematical rigour or linguistic precision.

Understanding of the terms, however, particularly for the practical application of them, is sometimes easier with mathematical expressions. In order to help this aspect, three chapters of Part II present the basic mathematical formulation in dynamics, statistics and random vibration of structures, which are essentially related to the topic. Also attached are some notes on various types of damping characteristics and vibration tolerance criteria for practical purposes.

Part III is a brief description particularly on the wind-induced vibration of bridges and cables. The contents are obviously related to the rest of the document and yet they require a significant extent of different preparation, and are not necessarily familiar topics to all readers. Hence, it was considered useful to have a separate section.

Key words: *aerodynamics, analysis, ambient survey, bridges, cables, damping, definition, dynamics, extreme values, frequency, glossary, health monitoring, instability, measurement, modal parameters, probability, random vibration, simulation, spectral analysis, statistics, vortex, wind, wind tunnel.*

Table of Contents

PART I GLOSSARY OF TERMS FREQUNTLY EMPLOYED 4

PART II MATHEMATICAL FORMULATIONS IN DYNAMICS 47

Chapter 1 Elements of Structural Dynamics 47

1.1 Dynamics of SDOF Systems 47

1.2 Dynamics of Elastic Structures – Modal Analysis 53

1.3 Dynamics of MDOF Systems – Complex Eigenvalue Problems 53

1.4 Modal Parameter Identification Techniques 56

Chapter 2 Basic Tools in Statistics 62

2.1 Statistical Analysis of Random Processes 62

2.2 Statistical Treatment of Discrete Time Series 68

2.3 Commonly Used Probability Distributions 71

2.4 Errors Associated with Spectral Analysis 78

2.5 Spectral Windows 80

2.6 Wavelet Analysis 82

Chapter 3 Random Vibrations 84

3.1 SDOF Systems 84

3.2 Distributed Random Excitation 85

3.3 Extreme Value Analysis 86

3.4 Simulation Techniques 92

Chapter 4 Some Notes on Damping 94

4.1 Nature of Vibration Damping in General 94

4.2 Sources of Damping 94

4.3 Artificial Dampers 99

4.4 Effects of Vibrations on Human Bodies 106

4.5 Other Socio-Economic Impacts 111

PART III WIND INDUCED VIBRATION OF BRIDGES 116

Chapter 1 General Background 116

1.1 Early History of Bridge Aerodynamics 116

1.2 General Characteristics of Wind Induced Bridge Vibration 117

1.3 Development of Bridge Aerodynamics 118

1.4 Recent Trend in Bridge Aerodynamics 119

Chapter 2 Formulation of Aerodynamic Forces 121

2.1 Definition of Force Components 121

2.2 Quasi-Steady Aerodynamics 121

2.3 Unsteady Aerodynamic Force Coefficients....123
2.4 Transient Forces....125
Chapter 3 Aerodynamic Instability....128
3.1 Concept of Aerodynamic Instability....128
3.2 Historical Development of Bridge Flutter Analysis....128
3.3 3D Flutter Analyses....132
3.4 Galloping....135
3.5 Instability in Torsion....136
Chapter 4 Buffeting....139
4.1 General Characteristics....139
4.2 Analytical Prediction....139
4.3 Aerodynamic Admittance....145
4.4 Peak Factor....147
4.5 Time Domain Analysis....150
Chapter 5 Vortex Induced Oscillation....156
5.1 General Characteristics....156
5.2 Analytical Prediction....157
5.3 Typical box sections applicable to bridges....160
5.4 Control and Suppression....161
Chapter 6 Cable Aerodynamics....163
6.1 Classification of Cable Vibrations due to Wind....163
6.2 Vortex Induced Vibration, or Aeolian Oscillation....163
6.3 Buffeting due to Wind Gust....164
6.4 Galloping of Iced Cables....165
6.5 Vibrations Caused by Wake Interference....166
6.6 Parametric Excitation....167
6.7 Reynolds Number Related Drag Instability....168
6.8 Rain-Wind Induced Vibration....169
6.9 High-Speed Vortex Excitation of Dry, Inclined Cables....172
6.10 Dry Inclined Cable Galloping....173
Chapter 7 Wind Tunnel Tests....182
7.1 Similitude Requirements....182
7.2 Wind Tunnel Simulation of Natural Wind....187
7.3 Mathematical Simulations....192
7.4 Wind Tunnel Testing Techniques....195

PART I GLOSSARY OF TERMS FREQUNTLY EMPLOYED

Acceleration: The rate of change of velocity with respect to time.

It is often the quantity most easily detected in vibration measurement. If the motion is ideally simple harmonic, the magnitude of acceleration is given by the amplitude of vibration multiplied by the circular frequency squared. Note that the mean of acceleration is supposed to be zero. The estimation of vibration amplitude from measured acceleration often involves significant errors.

Accelerometer: An instrument used for measuring the acceleration.

In particular, low frequency, low amplitude accelerometers are suitable for the application in bridge dynamics. The common types of accelerometers for this application are piezoresistive, capacitive, and force balance accelerometers.

The accelerometer, in principle, is usually a high frequency spring-mass system, for which the elastic spring is often made of a cantilevered beam of metal or ceramic material, which bends under given acceleration. The displacement is measured by strain-sensitive gauges placed on the beam, or detected by the change of electric capacitance. The gauges are usually connected in a Wheatstone bridge.

Accounted Truth: What is claimed to be true with some theoretical and/or experimental explanations that are objectively acceptable.

J.L. Austin, a British philosopher of language, says, “To assert that a proposition *p* is true is to maintain that *p* corresponds to the facts”. In the field of natural science, though they can be still subjected to interpretations, these “facts” need to be scientific facts, which are expected to be explained by rigorous and robust theory or repeatable and replaceable experiments. Some other facts, for example from the religious point of view, may not be thus categorised.

ACM: Advanced Composite Materials.

Acoustic Emission (AE): The propagation of an elastic wave as the rapid release of energy associated with plastic deformation or development of defects within a stressed material.

AE analysis is a useful method for the investigation of local damage in materials. It has been successfully applied to detecting and locating faults in pressure vessels or leakage in storage tanks or pipeline systems, monitoring welding applications, corrosion processes, partial discharges from components subjected to high voltage and the removal of protective coatings. Research and development of AE applications are also in monitoring civil engineering structures, such as bridges, pipelines and offshore structures, and crack development in massive concrete structures and rocks.

Advanced Composite Materials (ACM): Materials which consist of a polymer matrix reinforced with high-strength fibres and, compared to other traditional materials, possess distinctly advantageous characteristics such as light weight and high strength.

Every composite has at least two components: reinforcements which are high-strength, high-stiffness fibres and are immersed in a matrix, which is usually a high-performance resin system and combine the reinforcement material together at a microscopic level. Three basic types of fibre reinforcement materials in use are carbon/graphite, glass fibres and aramid. Their major advantages in comparison to conventional materials include high strength and stiffness, light weight, fatigue strength, impact resistance and corrosion resistance.

Major users of ACM were traditionally the aerospace industry but the market has been gradually expending to sporting goods and civil engineering applications as well. Carbon fibre reinforced polymer (CFRP) is now extensively applied to bridges for strengthening, reinforcement and repairs.

AE: Acoustic Emission.

Aerodynamic Admittance Function: A transfer function to express how effectively the frequency characteristics of velocity fluctuation are picked up by the aerodynamic force components.

It is expected that the magnitude of this function is close to unity in low frequency range and quickly tapers off in higher frequencies. A classical example is the ***Sears function***, which reflects the frequency characteristics of aerodynamic lift force in relation to a sinusoidal fluctuation of vertical velocity component. In general, the aerodynamic admittance is not decided analytically and needs to be estimated experimentally.

Aerodynamic Instability: Dynamic instability of structures caused by aerodynamic forces.

A dynamic failure of aircraft wings caused by aeroelastic phenomena, called ***flutter***, was a serious engineering concern from the early days of flight. Though the excitation mechanism was not exactly identical, the collapse of the old Tacoma Narrows Bridge in 1940 was often compared to the aerofoil flutter. Galloping instability of ice-covered power transmission lines is another example of aerodynamic instability. The term *flutter* is, strictly speaking, restricted to the classical flutter which is a coupled motion in bending and torsion of streamlined bodies but is also used rather loosely without a clear definition. It sometimes means the catastrophic structural vibration caused by fluid dynamic forces, which are coupled with the body motion.

AI: Artificial intelligence.

Allowable Stress Design: A method to design structures such that allowable stresses are not exceeded when the structure is subjected to specified working loads.

Basically, an elastically computed stress from the combined nominal loads must be less than the material yield stress or the buckling stress divided by the safety factor.

Ambient Vibration Survey (AVS): A method to determine the dynamic characteristics of a structure by measurement of small vibrations, mostly micro-tremors, caused by existing disturbances such as earthquakes, wind and traffic, while the structure is in service.

In terms of data reliability, the forced vibration tests using shakers is probably the best method for the evaluation of dynamic characteristics of bridges. However, it usually requires a large operation, which is naturally costly, and could also mean an interruption of services. The ambient vibration survey, without any control on the input, is consequently an attractive alternative. This method is based on a few basic assumptions as follows: a) The input excitation is a broadband stochastic process which is adequately modelled by white-noise; b) The system characteristics are therefore well represented by the power spectral density function of dynamic response; c) The technique for measuring the dynamic response is sufficiently reliable; and d) The data acquisition and analysis are also sufficiently reliable. Hence, the reliability of this method is largely decided by these factors.

ANPSD: Averaged Normal Power Spectral Density.

ARIMA Model: Auto-regressive integrated moving average model.

It is one of the statistical forecasting techniques systemized by Box and Jenkins in 1976. The ARIMA time series analysis uses lags and shifts in the historical data to uncover patterns and predict the future.

Artificial Intelligence (AI): AI is intelligence exhibited by any manufactured systems. The term is often applied to general purpose computers which are expected to work on intelligent tasks that resemble to human activities.

AI methods are often employed in cognitive science research, which explicitly tries to model subsystems of human cognition, whereas AI research seeks to build more useful machines. ***Expert systems*** and ***neural networks*** are two of the most common techniques used for applied artificial intelligence

***Assessment: A set of activities performed to verify the reliability of an existing structure for future use.**

Averaged Normal Power Spectral Density (ANPSD): A method to identify all the possible natural frequencies participating in the vibration at a time by taking the average of all the normalized power spectral density functions obtained from the multi-point records.

The method was developed by Felber (1993) as a fast and effective way to identify many structural vibration modes participating in the vibration measured in ambient survey. It is a convenient way to display the most significant frequencies at a single spot in a series of motions in a certain direction. However, it should be noted that not all the peaks identified in this method necessarily correspond to the natural frequencies.

AVS: Ambient Vibration Survey.

Bayesian Statistics: A statistical method that handles all uncertainties by probability. It provides a different paradigm for both statistical inference and decision making from the conventional statistics.

The name is after Thomas Bayes (1702-61) but it may not be following particularly his idea. Bayes theorem states that the probability of A given B times the probability of B is equal to the joint probability of A and B, or $P(A|B) = P(A \cap B)/P(B)$.

The major difference between Bayesian statistics and other statistical methods is that the traditional statistics examine the probability of the data given a model or hypothesis, while Bayesian statistics examine the probability of a model given the data. This significantly enhances the power of statistical analysis. In particular, Bayesian methods make it possible to incorporate scientific hypothesis in the analysis by means of the prior distribution. It can be then applied to problems whose structure may be too complex for conventional methods to handle. The Bayesian paradigm is based on an interpretation of probability as a rational, conditional measure of uncertainty, which closely matches the sense of the word “probability” in ordinary language.

There are three particularly important terms used in Bayesian statistics: the prior and posterior probabilities and likelihood. The ***prior*** is the observer’s belief expressed by the probability $P(X)$ before any data (D) are observed. The ***posterior*** refers to the probability $P(X|D)$ after observed data have been taken into account. ***Likelihood*** is the probability with which D is expected to take place, that is the conditional probability $P(D|X)$ of the data given a particular model. Since the probability of D depends on the value of X, X is called the *parameter* of $P(D|X)$. Based on the Bayes theorem, the posterior probability is calculated as a product of the prior probability and likelihood divided by $P(D)$, which is called *evidence*. It also means that any events which were not observed are not involved in the computation. This is a key principle of Bayesian statistics: only what is actually observed is relevant in determining the probability that any particular model is true.

There has been a resurgence of Bayesian approaches in recent years and the methodology now plays a central role in many fields, from ***expert systems***, ***machine learning***, and ***pattern recognition***, to applications in finance and the law. The special situation, often met in scientific reporting and public decision making, where the only acceptable information is deduced from available documented data, is addressed by objective Bayesian methods, as a particular case. Thus it tells us, for example, the true likelihood of a person having an HIV infection if he tests positive, or that of person X being the murderer if his fingerprints turn up on the weapon.

Beating: A phenomenon where the magnitude of vibration varies with the differential frequency of the two component vibrations.

When two vibration components are present at the same time and same place and if their frequencies are very close to each other, the combined signal of them will vary its magnitude regularly with a rate equal to the difference of frequencies of these two components. This differential frequency is called the beat frequency.

Beaufort Scale: An empirical measure for the intensity of wind, based mainly on conditions of open sea waves.

The 12 scale measure was created by Sir Francis Beaufort, a British naval officer some two hundred years ago. The scale has been often referred to as a relatively easy method to indicate strength of wind also for non-naval use, and loosely related to the mean wind speed, too.

Boundary Layer Wind Tunnel: A kind of wind tunnel which has a long test section to develop turbulent boundary layer flow as the simulated natural wind.

It is a means to simulate micrometeorological characteristics of natural wind in model scale. The idea was originally developed by Martin Jensen, a Danish engineer, who experimentally arrived at the conclusion that "the phenomena induced by natural wind can be reproduced only when the model tests are performed in a boundary layer which was created in a similar way as the case of natural wind and also when the linear scale of its turbulence coincides with the linear scaling of other models placed in it". This scaling factor, h/z_0 , is now called the ***Jensen number***, where $h =$ a linear dimension of the model, and $z_0 =$ the roughness length of the flow.

The idea of the boundary layer wind tunnel was extensively developed by A.G. Davenport and J.E. Cermak in the North America for large scale industrial applications.

Bridge Management: A process and decision-making framework that covers maintenance and operation of bridges, in order to maintain the structural safety and serviceability of them in cost-effective ways, considering the changes in environment, public expectation and technological advances.

Buckling: An instability failure mode of a structure or its members under compression.

The critical buckling load is decided by the stiffness against deformation and the effective length of the member. Buckling can also take place in torsion, a combination of torsion and bending or only locally in a small portion of a structural member. Infamous collapse of the Québec Bridge in 1907 was a well-known example of buckling failure in bridge engineering.

Buffeting: Dynamic excitation or induced structural response caused by wind turbulence, which inherently exists in natural wind. Buffeting can be caused by turbulence that was created by existence of upstream objects, too.

It is usually considered and analyzed as a forced vibration caused by time-dependent aerodynamic forces due to velocity fluctuation. Buffeting is a stochastic vibration, that has a range of frequency components and vibration amplitude is randomly fluctuating. The magnitude of vibration is generally greater at higher wind speed. Consequence of having buffeting vibration is usually not catastrophic but long-time influence of it such as fatigue damage can be a serious engineering concern.

Bulk Modulus of Elasticity: Ratio of stress to change in volume of a material subjected to axial loading.

If the material is homogeneous and isotropic, the bulk modulus of elasticity (*K*) is related to Young's modulus (*E*) and Poisson's ratio (ν) by $K = E/3(1-2\nu)$.

Cable: A flexible metal wire or group of wires, used as a structural member against tensile force.

Cables employed as structural tension members are usually one of the following five types: a) A single piano wire; b) Seven-wire strand; c) Multi-wire helical strand; d) Parallel-wire strand; and e) Locked-coil strand. A piano wire has much higher tensile strength at the order of 3000 *MPa* and much smaller ductility than ordinary structural steel. Young's modulus is around 205 *GPa*. It is usually assembled to form wire strands.

The seven-wire strand consists of a single core wire and a single layer of six wires, all having the same pitch and direction of helix. The multi-wire helical strands are fabricated by successive spinning of layers generally in opposite direction of helix, whereas the parallel-wire strand has all wires straight and parallel so that there is no reduction of Young's modulus due to twist of wires. The parallel wires are suitable for main cables of long-span suspension bridges, for example. In the locked-coil strand, there are a number of different shapes of wires to form a strand with a smoother and tighter surface. This type is considered to be appropriate for relatively short span cable-stayed bridges.

Cables are primarily assumed to be perfectly flexible and resist only against tension. However, in reality, there is a bending stiffness. Because of its large flexibility, cable often exhibits a relatively large static deflection and, as a result, nonlinear structural characteristics. Once in vibration, cable has very low structural damping, usually an order of magnitude less than other types of structural members.

Cepstral Analysis: A nonlinear filtering technique in signal processing, often applied in speech analysis, when it is difficult to do de-convolution by applying linear filtering.

In many of the ***inverse problems***, it is experienced that the transfer function constructed by applying Fourier transfer technique for de-convolution is only with some ambiguity. However, it has been sometimes recognised that the cepstral analysis technique is useful in smoothing or desensitising the transfer function such that the reconstructed input/output data become clearer with minimum signal pollution.

Mathematically, when the Z–transform of a signal x_n is given by $X(z)$, the cepstrum of x_n is defined by the inverse Z–transform of the logarithm of $X(z)$.

Charpy Test: A method to test the material toughness by giving an impact to break a standard specimen.

The specimen is broken by the impact of a heavy pendulum hammer, which strikes the specimen at a fixed speed. The amount of energy absorbed by the high strain rate fracture is indicated by the remaining potential energy by the maximum height of the swing after the specimen is broken.

Comfort: A state of being relaxed and feeling no pain or worry.

The term is used in several different levels in the present context, such as in the ***comfort criteria***, when the structural serviceability and/or pedestrian level wind environment are to be considered. Stages of categories are usually based on the clients' freedom from concerns regarding their safety, danger of bodily harm, sickness, inconvenience and nuisance. They are also influenced by the position people are taking, such as walking, standing, sitting etc., personal health conditions and what they are wearing.

Convolution: A mathematical operator defined as the integral over all space of one function at *x* and another function at *x*–*u*.

The dynamic response of a structure due to external force is given by a convolution integral the ***impulse response function*** and the force function. In many problems in physics, when there is a linear system with the principle of superposition, a convolution appears.

Correlation: A measure to indicate how much two variables are statistically related.

Correlation is one of the most fundamental concepts in describing the statistical relationship between two signals. It can be the relationship between the excitation force and dynamic response, or between dynamic deflections at two different locations of the same structure, for example. As a special case, the correlation of a signal with the same signal itself, but with a given time interval in between, can be taken and in this case it is called the auto-correlation as opposed to the cross-correlation between two different signals.

The correlation between two signals can be described in various forms with different degree of sophistication, including the correlation functions, cross-spectral density functions and coherence.

Corrosion: Chemically induced damage to a material that results in deterioration of the material properties.

It is difficult to prevent corrosion totally but it needs to be minimized by proper choice of material and design, coatings and/or environmental control, if it is possible, since corrosion will eventually results in failure of the component. ***Stress corrosion*** is a type of failure mechanism that takes place particularly when material is under tensile stresses, which are often ***residual stresses*** in the material, above certain threshold value, together with the environmental conditions. It is particularly sensitive to temperature environment. The collapse of the Silver Bridge, a 680m long eye-bar chain suspension bridge over the Ohio River, in 1967 is known to be a result of stress corrosion.

Coulomb Damping: Nonlinear damping as a result of dry frictional rubbing that often exists due to sliding at structural joints and supports.

Creep: A slow flow of metal under large normal stresses or high temperature.

As a transient stress-strain status, it is called ***creep*** if strain is increasing under the same stress, whereas if the stress is decreasing under the same strain, it is called ***relaxation***. Method of determining creep or stress relaxation behaviour is called creep test. Standard creep testing procedures are defined by ASTM (American Society for Testing and Materials) standards.

Critical Damping: Magnitude of damping beyond which the energy dissipation is so large that vibratory motion does not exist any more.

In ordinary structural vibration, the magnitude of damping is indicated by the fraction of critical. For many of the civil engineering structures, the overall structural damping is the order of 1% of critical.

Critical Reynolds Number: Reynolds number at which the transition between laminar and turbulent flow takes place.

For the case of a circular cylinder against transverse flow, the transition is known to take place at $(\mathrm{Re})_{cr} = 2300$. However, in reality, the critical Reynolds number can only be indicated as a range of Re rather than a definite number, since it is easily influenced by many factors including the surface roughness of the cylinder and the level of flow turbulence. Experimentally, it is evidenced by sudden drop of drag force on the body and loss of more regular flow pattern in its wake.

***Damage: Unfavourable change in the condition of a structure that can affect structural performance.**

Damage Detection: On-site, non-destructive identification of structural damage.

Periodic visual inspections provide a generally economical means for assessing the structural conditions. However, they are inherently subjective so that the reliability of outcome is often less than desired. Also, most of non-visible degradation of the bridge would remain undetected by visual inspection alone.

The structural health monitoring (SHM) system should be inexpensive, non-invasive and automated, so that subjective differences by operator can be avoided. In particular, it must be able to detect all of significant structural damages without an exception.

The detection of damage is expected to be in four levels; a) If any damage is present? b) Where is it located? c) How severe the damage is? and d) How long the remaining service life of the structure would be?

Damping: The capacity of structures to dissipate energy imparted by the external forces.

The dissipation of dynamic energy during vibration results from many different sources, such as the imperfect elasticity and internal friction of structural materials, friction of structural members at their joints and support mechanisms, aerodynamic and hydrodynamic damping due to surrounding environment, the nonlinear structural characteristics, energy dissipation through foundation and substructures, and so on. In any of these, the theoretical evaluation of damping capacity is generally limited. For this reason, it is essentially important to consult to the results of the field experience as references.

Though the mechanism of damping is quite diverse, their overall effects on vibration is usually characterized by considering an equivalent viscous damping, crystallized in a single number of ***damping ratio*** (ζ) as a fraction of critical.

If the overall damping of the system is 1% of critical, for example, the free vibration amplitude will be reduced to a half after 11 cycles, whereas the 10% damping will reduce the amplitude to a half at each cycle. When damping is at or beyond critical, there is no vibration.

DAQ: Data Acquisition.

Data Acquisition (DAQ): Sampling and processing of signals, usually manipulated by a computer, to obtain desired information.

The components of data acquisition systems include appropriate sensors that convert any measurement parameters to electrical signals, which are acquired, displayed, analysed and stored on a PC by interactive control software and hardware.

Data Mining: Extraction of potentially useful, previously unknown, information from large databases.

It is the practice of automatically searching large stores of data for patterns, which would not be recognized otherwise. In this sense, it is also termed as *knowledge-discovery in databases*. Data mining grew as a result of very rapid developments in storing massive amounts of data and necessity for applying statistical analyses and search techniques to them for ***artificial intelligence***.

Decision Support System (DSS): An interactive computer-based information system that helps decision makers by compiling useful information from raw data, documents and other knowledge.

Started about a half century ago, DSS has developed as a powerful interactive concept with applications in any knowledge domain. It is now based on multi-disciplinary foundations, including database research, artificial intelligence, human-computer interaction, simulation methods, software engineering and telecommunications.

Degrees-of-freedom (DOF): The number of displacements for describing the characteristics of a given vibration.

The concept of DOF is applicable only in terms of mathematical modelling of vibration. The same vibration of a structure can be considered as multi-degree-of-freedom (MDOF) or it may be approximated as a single-degree-of-freedom (SDOF) system, depending on how the structure is conceptually modelled.

***Deterioration: Process that adversely affects the structural performance, including the reliability over time.**

Deterioration of structural performance can be caused by various reasons, such as:
1) Naturally occurring chemical, physical and biological actions;
2) Repeated actions such as those causing fatigue;
3) Normal or severe environmental influences;
4) Wear due to use; and
5) Improper operation and maintenance of the structure.

DFT: Discrete Fourier Transform.

Discrete Fourier Transform (DFT): Fourier transform of a discretely indexed series. Usually executed by the use of the fast Fourier transform algorithm, which is extremely efficient in computation.

DOF: Degree-of-freedom.

DSS: Decision Support System.

Ductility: The ability of a material to plastically deform without rupture.

Ductility is usually defined by tension tests but may also be considered in bending. More ductile materials show larger deformation before fracture, and hence, given the same strength and hardness, the material with the higher ductility would be more desirable. The lack of ductility is often termed ***brittleness***. The ductility of material may change if conditions are altered. A decrease in temperature tends to make the same material more brittle.

Dynamic Excitation: The extraneous sources which cause dynamic response of structures.
Civil engineering structures are usually designed to withstand the static loading, including dead load. However, in reality, the structures are often exposed to dynamic load as well. Main sources of dynamic excitation for bridge structures are: moving vehicles and pedestrians, wind, earthquakes, and possibly blast loading. It is standard design practice to cover these anticipated dynamic effects by either considering equivalent static forces or dynamic amplification factors, though sometimes more elaborate dynamic analyses would be required.

Earthquakes: Sudden movements of a part of the Earth's crust. They are often caused due to accumulated stress along the boundaries of rock plates or geological faults, which are slowly moving in geological time scale. Earthquakes release a large amount of strain energy, which radiates as seismic waves.

The Earth's crust, or mantle, is 50 to 100 km thick and a geological fracture may be deep below ground level. The origin of fracture is called the hypocentre and the point on the Earth's surface directly above the hypocentre is called the epicentre.

Earthquakes are sometimes caused by volcanic activities, too. Large earthquakes often result in catastrophic consequences damaging the infrastructure.

The magnitude of an earthquake is related to the amount of energy released by the geological rupture causing it, and often measured by the ***Richter scale***. The intensity of an earthquake, on the other hand, is a measure of the observed damage at a particular location, and is often given in the ***Modified Mercalli Intensity scale (MMI)***.

Eigen-frequency: Also called the *natural frequency*.

Eigen-mode: Characteristic shape of amplitude distribution when a structure is freely vibrating at one of its natural frequencies. Also simply called the *vibration mode*.

Elastic Hysteresis: Difference between strain energy required to generate a given stress in a material and elastic energy at that stress.

Hysteresis is caused when the dynamic strain of the system that does not instantly follow the applied stress, resulting in the stress-strain curve making a loop for each stress cycle. Since the area under the curve corresponds to the ***strain energy***, the area surrounded by the clock-wise loop is the energy dissipated as heat in a material in one cycle of vibration. Elastic hysteresis divided by elastic deformation energy is equal to damping capacity.

Elasticity: Ability of a material to return to its original shape when applied load that caused deformation is removed.

Elasticity is a concept opposed to ***plasticity***, which is a tendency to remain deformed. When a material is linearly elastic, the slope of the straight line portion of a stress-strain diagram is called the modulus, or coefficient, of elasticity. Since both stress and strain have the normal and shearing components in all three directions, in general, there can be 21 moduli of elasticity for any linearly elastic material. When the material is homogeneous and isotropic, because of symmetry, the number of elastic moduli is reduced to two.

Elongation: A ratio defined in a tensile test by the increase in gauge length measured after rupture to the original gauge length.

It is an important measure of the material's ductility and expected to be 35% or so for the case of ordinary mild steel. Elongation cannot be used to predict behaviour of materials subjected to sudden or repeated loading.

Environmental Noise: Unwanted sound that is loud, unpleasant, or unexpected.

It is disturbing, annoying, and even causing health or psychological problems to different extent, such as hearing damage, sleep disorder, high blood pressure or greater sense of frustration. It can come from a variety of sources such as factories, construction projects, vehicle traffic and aviation noise.

Philosophically, one difficult aspect of acoustic noise control is that the definition of noise itself is quite subjective; some sounds are considered noise by some but not by others. Even in music, there is rarely a consensus regarding what to be called noise amongst those who are involved.

On the other hand, noise control technology in reality is becoming a more and more serious engineering topic. Reduction of noise levels or controlling the airborne and structure-borne noise by the use of curtains and barriers, damping with absorbent materials, enclosure of sources or by isolation of vibrating structural elements are possible means often considered.

Expert System: A software-based artificial intelligence system which analyzes information and upgrades the quality and quantity of database for specified purposes.

The primary goal of expert systems is to make knowledge-based artificial intelligence that is available to decision makers. A major feature of the system is reliance on the database comparable to that of human experts, whose knowledge is based on a theoretical understanding of the problem and a collection of heuristic problem-solving rules obtained through professional experience.

Extensometer: A strain gauge. An instrument for measuring changes in linear dimensions.

Extreme Value Distributions: The limiting distributions for the extreme values, such as the maxima or minima, of a large collection of random observations.

In many civil engineering applications, concern often lies with the largest values of many events. This means that our attention is focussed upon the upper tail of the parent distribution of actual observations. Fisher and Tippett (1928) proved that there are only three forms of extreme value distributions. Extreme value analysis was largely developed and elaborated by Emil J. Gumbel (1891-1966), a German statistician.

Failure: The state or condition of a structure or its component that becomes unable to function for expected services.

Structural failure could occur because of various reasons, such as a) yielding; b) fatigue failure; c) corrosion failure; d) ductile or brittle fracture; e) creep rupture; or even too much deflection elastically, if the design was not appropriate or external loads exceed the expected magnitude.

Fast Fourier Transform (FFT): A highly efficient algorithm to compute the discrete Fourier transform (DFT) in high speed.

The method developed by Cooley and Tukey (1965) has been commonly used. However, some other algorithms are also known.

Fatigue: The adverse effect on metal of repeated cycles of stress.

The fatigue fracture is said to start with micro-cracks or defects, which cause a localised ***stress concentration***, resulting in growth or propagation of them but without any appreciable deformation of structure. Repetition of this process would cause decreased toughness, impact strength and tensile elongation and eventually failure of the material at considerably lower stress level than the original tensile strength. When the number of cycles-to-failure (N) is tested and plotted against the given constant stress level (S), it is called the ***S-N curve*** or ***Wöhler curve***, which allows designers to make a basic estimate of the expected life of the structural part against expected stresses.

Fatigue failure can be influenced by a number of factors including the level of stresses, number of cycles, size and shape of the structural component, condition of the surface and operating environment. There have been some infamous accidents where the cause was attributed to fatigue failures, including the 1842 railway disaster in Versailles, crashes of three de Havilland Comet jets in 1954, and the loss of Japan Airlines flight 123 in 1985.

FDA: Frequency Domain Analysis.

FFT: Fast Fourier Transform.

Fibre Optic Sensors: Highly sensitive sensors by the use of optical fibres.

When an optical fibre is bent, the light in the core no longer meets the cladding at an angle equal to or greater than the critical angle. This means that light escapes into the cladding and does not reach the other end of the fibre. It is called the *microbending loss* and the more the fibre is bent, the more loss takes place. The optical fibre thus works as a transducer by converting a measured quantity into a corresponding change in the optical radiation. Since light is characterised by intensity, phase, frequency and polarization, a change of any one or more of these parameters can be used for the detection of various quantities, such as temperature, stress and strain, angle of rotation or electromagnetic currents.

Some of the advantages of fibre optic sensors, on top of high sensitivity, are freedom from electromagnetic interference, wide bandwidth, compactness, geometric versatility and economy.

Fibre Stress: Stress through a point in a part in which stress distribution is not uniform, such as the maximum stress in both tension and compression at extreme surfaces for the case of beam bending.

Filter: An electronic device or mathematical algorithm to process a data stream by means of separating the frequency components of signals.

There are various types of filters, such as low-pass filters, high-pass filters and band-pass filters. For the monitored data, low-pass filters are used to cut-off high frequency noise and to prevent ailiasing, whereas the high-pass filters are used to reject low frequency noise such as the shift of zero reading.

Finite Element Method: A numerical method for solving static and dynamic problems of structures. It has been extensively applied to a variety of other engineering problems including fluid dynamics, heat transfer and material sciences.

The method was originally developed for working on dynamic analysis of aircraft structures. The basic idea is to subdivide a structure of any shape into a large number of simple elements. It is found that if the load-displacement equations for a single element are derived in matrix form, it is possible to use matrix algebra to combine the interacting effects of all the elements in a systematic and conceptually straightforward manner. Taking advantage of the rapid development of large capacity computers, the structural analysis thus became extremely simple and efficient.

Force Balance Accelerometer: A type of accelerometer which is widely used for the measurement of strong earthquake motions. It is based on the force-balance principle.

Instead of directly measuring the inertia force exerted upon the mass by detecting its displacement, the force-balance system measures the compensated inertia force, which is generated by an electromagnetic force transducer, so that the mass of the accelerometer moves as little as possible. The system is particularly suitable for the measurement in low frequency range. The available frequency bandwidth is, however, somewhat limited because of the phase delays caused by feedback servo loop.

Fourier Series: An infinite series of sine and cosine functions that can, if convergent, approximate a variety of periodic functions.

Fourier series can be further transformed to a series of exponential functions by the use of the Euler's formula. The study of functions given by Fourier series is called ***Fourier analysis*** or ***harmonic analysis***.

Fourier Transform: An integral transform particularly useful in relating the time domain and frequency domain variables for random vibration analysis.

Concept of the Fourier transform developed from a Fourier series, which is the decomposition of a periodic function. Fourier transform expands this concept to make it further applicable to the non-periodic functions. The analysis of measured data using the ***discrete Fourier transform (DFT)***, particularly in the form of the ***fast Fourier transform (FFT)***, is one of the most important techniques for the frequency domain vibration analysis.

Fracture Toughness: Ability of a material to resist crack propagation when subjected to shock load in an impact test.

Frequency Domain Analysis (FDA): Dynamic analysis processed by taking frequency, rather than time, as an independent variable.

Vibration analysis was originally established by taking both the external forces and resulted displacements as functions of time as an independent variable. However, when the random vibrations came into the scope and the statistical treatment of the problem became imminent, another way to look at the problem by taking frequency as a variable was found to be an attractive choice.

FDA, as opposed to the ***time domain analysis (TDA)***, is a way of processing dynamic analysis by decomposing the external forces into frequency components by applying Fourier transform and evaluates the structural response by superposing its frequency components. Even a non-periodic force can be included by pretending its period to be infinity.

Frequency Response Function (FRF): The ratio of the induced response to the excitation force, when an idealized SDOF system is subjected to a simple harmonic fluctuation force.

FRF, sometimes called the ***mechanical admittance function***, shows the sensitivity of a structural system to the excitation frequency. The peak response is reached when the excitation frequency coincides with the natural frequency and its magnitude is inversely proportional to the total damping of the system.

FRF: Frequency Response Function.

Froude Number: A dimensionless parameter that is decided by the ratio of fluid inertia force to vertical force due to gravity and/or buoyancy.

Froude number is defined by $Fr = V / \sqrt{gL}$, where V, L are the flow speed and a representative length, respctively, and $g =$ the acceleration due to gravity. Hence, it is the square-root of the ratio of the fluid inertia force to the gravity force. If the change of fluid density ρ is involved in the problem, the *densimetric Froude number* is defined by using the reduced gravity, $g' = g \cdot \Delta\rho / \rho$, in lieu of g.

It becomes an important parameter for describing the cases, such as dissipation of airborne particles or wind-induced response of cable-supported structures, where gravity is a dominant factor.

Fuzzy Logic: A problem-solving control system by introducing the concept of *partial truth* rather than expressing everything in binary terms.

The concept was introduced by L. Zadeh in 1965. Degrees of truth are often confused with being imprecise or probable but they are not. It allows for set membership values between and including 0 and 1, based on vague or even missing information, but arrives at a definite conclusion.

Fuzzy logic is, by some engineers, still said to be controversial but has been applied to many practical purposes including the fields of artificial intelligence, neural network and pattern recognition.

Global Positioning System (GPS): A world-wide radio-navigation system formed from a constellation of satellites and their ground stations. The system uses the network of reference points to calculate any positions on the ground accurately.

The GPS provides a means of measuring position or displacement that does not require the component that is being tested to be physically connected to a fixed reference location. The working principle of the GPS involves triangulation of the location using radio signals from satellites as reference points. Depending upon the direction of measurement, GPS accuracy ranges from metres to centimetres.

GPS: Global Positioning System.

Gust Factor: The ratio of the peak to the mean wind speed.

The same term is often used for the ratio of the peak to the mean of wind-induced dynamic response as well. Wind induced buffeting motion often has the ***peak factor*** of 3.5 to 4 and the coefficient of variation of about 0.3, resulting in the gust factor of approximately 2 or slightly higher than 2.

Hardness: Measure of a material's resistance to localized plastic deformation.

Most hardness tests involve indentation, but hardness may be reported as resistance to scratching or rebound of a projectile bounced off the material, too. It is a good indication of tensile and wear properties of a material.

Health Monitoring: Tracking of various aspects of a structure's performance and integrity in relation to the system's expected safety and serviceability.

It is desirable if the structural health monitoring system is inexpensive, non-invasive and also automated, so that subjective differences by operator can be avoided. In particular, neither the implementation nor operation of the system should involve closure of the bridge.

Carden & Funning (2004) lists the attempted levels of structural identification as follows: 1) Presence of damage in the structure; 2) Location of the damage; 3) Severity of the damage; and 4) Prediction of the remaining service life of the structure.

Impact Energy: Energy required to fracture a material that is subjected to shock loading as in an impact test.

Alternate terms are impact value, impact strength, impact resistance, and is usually measured by the energy absorbed in breaking the specimen in a single blow, as in the *Charpy test*. It is an indication of the toughness of the material.

Impulse Response Function (IRF): The ratio of the induced response to the excitation force, when an idealized SDOF system is subjected to a unit impulse load.

The ***convolution*** integral of IRF with an external force function, if available analytically, is called the ***Duhamel Integral***, which gives the induced response of the system by this force.

Frequency Response Function and Impulse Response Function make a Fourier transform pair.

Indicial Response Function: The response of an idealized quiescent SDOF system when it is subjected to a unit step load. Impulse response is obtained by differentiating the indicial response.

Infrastructure: A set of interconnected structural elements that provide the framework for supporting the entire structure.

The term is often used in a very broad range, as the ***social infrastructure***, including any life-sustaining social facilities required for municipal or public services, particularly for transportation systems such as roads, railways, airports and water surface transportation, public utilities such as flood control, fire services and waste management, emergency and security services, and even public education, health systems and social welfare.

***Inspection: On-site, non-destructive examination to establish the present conditions of the structure.**

A visible inspection performed on regular base is called the routine inspection and a more detailed inspection usually performed as a follow-up to a routine inspection to identify any deficiencies discovered is called the in-depth inspection.

Instability: A failure mode of a structure by losing its structural integrity in static or dynamic equilibrium.

Buckling is a static instability. There are also dynamic instability phenomena such as parametric excitation and/or self-excited vibrations.

Intensity: The relative strength of physical quantity, such as electricity, light, heat or sound, usually per unit area or volume of the space it is exposed.

It is a measure of the time-averaged energy flux transmitted. Intensity of signal fluctuation is often expressed by the coefficient of variation, which is the ratio of the root-mean-square to the mean value.

Inverse Problem: A task to identify system parameters based on observed output data.

Estimation of structural parameters from the measured vibration record is an example. It is exactly the inversed process compared to conventional response calculations in structural dynamics. Inverse problems exist in many disciplines such as remote sensing, medical imaging and non-destructive testing of materials.

A linear inverse problem is essentially expressed in the form of a Fredholm first kind integral equation and at least the idea is straightforward, but nonlinear problems are considerably more complex.

***Investigation: Collection and evaluation of information through inspection, document research, load testing and other experimental methods.**

IRF: Impulse Response Function.

Jensen Number: See the *Boundary Layer Wind Tunnel*.

Kalman Filter: An efficient recursive filter which estimates the state of a dynamic system from a series of incomplete measurements with noise.

It means that only the estimated state from the previous time step and the current measurement are needed for making an estimate for the current state. One example is to provide an accurate, continuously-updated information about the position and velocity of an object, given only a sequence of observations about its position, each of which includes some error.

Kalman filtering is an important topic in control systems engineering. A variety of Kalman filters has now been developed, including Kalman's original simple filter, the extended filter, the information filter, and a variety of square-root filters.

Kármán Vortices: A street of alternating vortices existing behind a circular cylinder which is exposed to the transverse flow. Also called the Kármán-Bédard vortex street.

Existence of a street of alternating vortices behind a circular cylinder which is exposed to the transverse flow was known for quite some time and studied by many including Strouhal, Lord Rayleigh and Bénard. However, the name of von Kármán has been frequently remembered because of his work on the stability of vortex arrangement. He considered two rows of alternating vortices behind a cylinder and mathematically considered a stability condition in terms of their geometric locations.

A very clear vortex street is usually recognisable at the Reynolds number range of 100 to 300 and these are the original Kármán vortices. However, even at much higher flow speed, even in the range beyond the critical Reynolds number, the existence of alternating vortex shedding behind a non-streamlined object has been widely recognised and they are also rather loosely called Kármán vortices.

An engineering significance of this vortex shedding is the ***vortex shedding excitation*** of structures.

Laser Doppler Vibrometer (LDV): A highly sensitive optical instrument to measure displacement and velocity of a moving object.

It consists of an optical head that emits laser light and a converter that processes the Doppler frequency of the reflected laser light. The voltage signal from the converter is proportional to the velocity at which the object moves. There are different types of LTD for a) out-of-plane vibration; b) in-plane vibration; and c) three-dimensional vibration. A non-contact way of measurement is a distinct advantage of the system, but care should be taken for the fact that the measured results are easily affected by the noise caused by the surface roughness of the target.

Least-Square Method: A process to quantitatively obtain a regression for a set of data by minimizing the sum of the deviations squared.

Polynomial functions are most commonly used for least-square curve-fitting. If more than one control parameters are involved, the multiple regression method can be applied, too.

Life Cycle: The total phases through which a structure passes from its birth to the time it ceases to exist. It involves all levels of engineering work, including design, construction, inspection, management, repair, improvement and demolition.

The concept has been developed from the needs to consider the overall performance of a structure, both in services and associated costs. The life-cycle assessment of a structure would include its cost-effectiveness, serviceability, environmental impacts and sustainability.

Limit State: A limit state is a set of performance criteria defined in terms of deflection, vibration levels etc. as a reference state that must be met by a structure under factored loading.

It is a concept used for design of structures in lieu of the older concept of ***allowable stress design***. The most common limit states are the serviceability limit state and the ultimate limit state.

Linear Variable Differential Transformer (LVDT): A type of electrical transformer used for measuring linear displacement without contacts.

LVDT is a commonly used, reliable position meter. It consists of a hollow metallic casing with solenoid coils around a tube and a ferromagnetic core shaft, which is attached to the object whose position is to be measured and moves freely back and forth along the axis of measurement. An alternating current is driven through the primary coil, causing a voltage to be induced in the solenoid coils and thus measure the travelling distance of the core.

Load: The applied forces which a structure is subjected to and expected to resist against.

It generally include the weight of the structure itself, traffic to be carried, effects of wind, earthquakes, temperature change, rain, snow, ice etc., and dynamic amplification of these loads due to their motion, possible collision and/or accidents.

***Load Testing: Test of the structure or its part by loading to evaluate its behaviour or properties, or to predict its load-bearing capacity.**

LVDT: Linear Variable Differential Transformer.

***Maintenance: Routine intervention to preserve appropriate structural performance.**

Markov Process: A statistical process whose relationship to the past does not extend beyond the immediately preceding observation, or its most recent value.

It could be also said that the random events whose likelihood depends on what happed last in this process. The stream of events with this character is called the ***Markov chain***. A game of Monopoly or Snakes and Ladders, whose moves are determined entirely by dice, is a Markov chain, in contrast to the Poker game, where the cards represent a memory of the past moves.

Mass Parameter: A dimensionless parameter to indicate the significance of structural mass.

Mass parameter can be defined in different ways depending on the nature of engineering problems. However, in case of the wind tunnel tests of a bridge model, for example, it is defined by $\mu = m/(\rho B^2)$, where $m =$ structural mass per unit length of the bridge, $\rho =$ the air density, and $B =$ the width of the bridge. If the issue is the bridge motion in torsion, another mass parameter, $\nu = J/(\rho B^4)$, would be more important, where $J =$ the polar mass moment of inertia per unit length of the bridge.

***Material Properties: Mechanical, physical or chemical properties of structural materials.**

Engineering properties sometimes required in the present context include the material density, yield strength, elongation, tensile strength, Young's modulus, Poisson's ratio, melting point, thermal expansion coefficient, specific heat capacity, electrical conductivity, etc.

MATLAB: A numerical computing environment, which is probably most widely used as a modern operating system. The same name can also mean its core language.

Short form of *MATrix LABoratory*. It was developed by Cleve Moler in the late 1970s and quickly spread and became popular through the community of applied mathematics. It allows easy matrix manipulation, plotting of functions and data, implementation of algorithms, creation of user interfaces, and interfacing with programs in other languages.

Maximum Likelihood Method: A procedure of finding the value of one or more parameters for the hypothetical probability distribution, or likelihood, to make it a maximum.

It is said to be a statistically robust method, or versatile and apply to most models and to different types of data. In addition, it provides efficient methods for quantifying uncertainty through confidence bounds.

The background theory is relatively simple. Suppose x is a random variable with PDF given by $p(x;\theta)$, where θ is an unknown parameter which needs to be estimated. After obtaining N independent observations, $\{x_r\}$ ($r = 1,2,.., N$), the likely function is defined by $L = \prod_{r=1}^{N} p(x_r;\theta)$ and the maximum likelihood estimator of θ is obtained by maximizing $L(x_1, x_2,..., x_N \mid \theta)$, or $\partial(\ln L)/\partial\theta = 0$. There can be more than θ involved in this process.

Melting Point: The temperature at which solid changes state from solid to liquid.

The temperature of the reverse change, liquid to solid, is referred to as the ***freezing point***. Unlike the boiling point, the melting point is relatively insensitive to pressure. The melting point of steel is approximately 1,700^{0}K.

Miner's Rule: A method to predict structural failure due to cumulative fatigue damage.

Fatigue loading is seldom of constant amplitude and hence the method of its assessment for the cumulative damage needs to consider the mean rate of crack propagation under variable-amplitude loading. This approach yields to an empirically derived expression by Palmgren (1924) and Miner (1945), which is given by $\sum_j n_j / N_j \geq 1$ as a failure condition, where n_j = the number of stress cycles with stress range σ_j and N_j = the number of stress cycles necessary to cause failure at stress range σ_j. It is a simple and convenient criterion but the usefulness of the Miner's rule is admittedly questionable.

Modal Mass: Participating mass.

Modal Parameters: The most fundamental information regarding vibration modes, namely the frequency of vibration, corresponding mode shape and damping.

The ultimate goal of ***vibration-based structural health monitoring*** is to determine the existence, location and extent of structural damage by identifying these modal parameters. Two key areas where the research efforts are required are on the following questions: a) if the measurements of these parameters yield consistently reliable results; and b) if the observed parameters are sensible reflection of structural damage that needs to be identified.

Often the measured ***modal data*** are influenced not only by possible structural damage but also other environmental factors such as the live load conditions, thermally-induced variations and amplitude dependence. Sometimes the results are limited by the availability of instrumentations, and error and noise in measurement and data analysis. Thus the measured modal data are either incomplete or with remaining uncertainties. It becomes necessary then to address this uncertainty by applying probabilistic approaches.

Modified Mercalli Intensity Scale: A widely accepted scale to indicate the intensity of an earthquake, which is a measure of the observed damage at a particular location.

It is based on a subjective assessment of the severity of an earthquake. The intensity varies with distance from the epicentre and local ground conditions. It should be remembered that the evaluated intensity is not necessarily proportional to the magnitude scale. It is analogous to the ***Beaufort scale*** for wind in that sense.

Moment Magnitude Scale: A method to indicate the magnitude of earthquakes as a possible replacement of the Richter scale. It is to measure the seismic moment, which relatable to the dimension of earthquake rupture and released energy.

The method was proposed by Hanks and Kanamori (1979) and defines the magnitude by $M = 2/3 \cdot (\log_{10} M_0 - 9.1)$, where M_0 is the seismic moment in $N \cdot m$. The seismic moment is a measure of the total energy that is transformed during an earthquake and only a very small fraction, typically 1.6×10^{-5}, is said to be converted into radiated seismic energy and registered on seismographs.

***Monitoring: Frequent or continuous observation or measurement of structural conditions or actions.**

Monte Carlo Method: A method to simulate a large variety of qualitative processes or to provide approximate solutions to mathematical problems by performing statistical sampling experiments on a computer by the use of random number generation.

The Monte Carlo method developed out of nuclear science, when the probabilistic problem of random neutron diffusion in fissile materials was a concern. The method is often envisaged as a statistical sampling technique to solve inherently probabilistic problems but it has been also applied to deterministic issues.

In the present context, it is referred to as a method to make use of random generation for the numerical simulation of functional relationships between random variables. It is known to be a useful and effective approach when the theoretical analysis of input-output relationship is too complicated, particularly in nonlinear problems.

Natural frequency: The frequency at which a structure is most easily excited.

Natural frequencies are uniquely decided by mass and stiffness of the structure and are rightfully termed the ***eigen-frequencies***. However, their magnitude also depends upon the way the structure vibrates, which is called the ***mode*** of vibration. For example, a bridge can vibrate in vertical bending, horizontal bending or in torsion. Even in vertical bending mode alone, the bridge can vibrate with its maximum dynamic deflection at the span centre, or with no deflection at the mid-span but the significant movement at the quarter-span points. Each vibration mode has its own natural frequency corresponding to it.

The mode of vibration is largely influenced by the way the structure is supported. The supporting conditions are called the ***boundary conditions***. For the design of the structure, they are usually assumed to be hinges, rollers, rigidly fixed, or sometimes elastic spring supports. However, these conditions, including the conditions of substructure and the ground, in reality are often somewhat different from their mathematical assumptions.

Natural frequencies are usually evaluated under the standard design conditions, in which the structure is free of live loads and extreme temperature effects. Since the instantaneous mass and stiffness of the structure in reality could be different from the design assumptions, the natural frequencies of the bridge in service can be different from the values calculated earlier.

Natural frequency is reduced a little with the increase of the system's ***damping***. However, in reality, this effect can be disregarded for the case of civil engineering structures. For example, even if the damping is as high as 10% of critical, the natural frequency is reduced by only 0.5% compared to the case with no damping.

The structure can be most easily excited into vibration if the excitation frequency coincides with, or is very close to, one of the natural frequencies. This phenomenon is called ***resonance***. If the excitation force contains many frequencies, the one close to the natural frequency would most effectively excite the structure. The sensitivity of a structure to different excitation frequencies is typically represented by the ***frequency response function (FRF)***, or the ***mechanical admittance function***.

When the structural system is ***nonlinear***, the natural frequencies are amplitude-dependent. For this case, the frequency observed at very small amplitude is usually defined as the natural frequency.

Neural Network: An analytical technique to explore the relationship between variables by creating a network system conceptually similar to the biological cognitive system.

Neural networks method is one of the data mining techniques, which is an analytical process to explore data in search of consistent patterns and/or systematic relationships between variables. The name obviously came from its resemblance to the biological cognitive system of brain and layers of neurons.

The method consists basically of three steps, the design of a specific object-oriented network architecture, the training of the system by the use of existing data, and the generation of predictions once the network is ready.

A distinct advantage of neural networks is that the method can be applied to any continuous input-output relationship without assuming hypotheses particular to the underlying model. On the other hand, there is an important disadvantage that the final outcome of the work depends upon the initial conditions of the network and the experience-based solution does not really give any insight to theoretical explanation of physics.

Noise: A random signal that does not convey any useful information.

The analysis of noise signal has been developed in the telecommunication field and became one of the most important tools in dynamics. A signal whose intensity is the same at all frequencies is called the ***white noise***, though an infinite-bandwidth white noise is a purely theoretical concept and, in reality, its frequency band has to be limited.

For acoustic aspect of noise, see the ***environmental noise***.

Nonlinear Vibration: When the structural restoring force and/or damping force are not linearly proportional to the displacement, or the external forces are amplitude dependent, the vibration becomes non-linear.

Nonlinear stiffness can be caused by material nonlinearity, such as plasticity, or structural nonlinearity, such as the case of cables. Structural damping ratio is usually higher when vibration amplitude is greater. In contrast, the aerodynamic damping is sometimes found drastically reduced, or even become negative, with greater vibration amplitude. This is because the excitation force is largely nonlinear with the displacement and/or displacement rate.

All of these factors indicate that the structural vibration is likely to be nonlinear, unless the dynamic amplitude is very small. However, we try to handle them with linear approximation so long as it is acceptable for practical purposes. Generally speaking, the nonlinear vibrations can be analysed only by applying numerical methods without closed form solutions.

Nyquist Frequency: The highest frequency beyond which the signal contents cannot be properly represented by the data in discrete form.

Any time signal can be measured usually only for a limited time period. Consequently, the analysed results of the sampled data from the original signal would be different from the expected results for which the whole infinite signal is intended. This difference is known as ***leakage***.

When the original continuous signal is sampled as a discrete time-series usually with a constant sampling time increment Δt, the signal contents with any frequencies higher than $f_N = 1/(2\Delta t)$ cannot be accurately represented because of the sampling resolution. f_N is called the Nyquist (or folding) frequency.

The problem caused by the choice of sampling time increment for digitizing the data is called ***aliasing***. In order to reduce these errors, it is considered prudent to low pass the original signal at, or preferably even below, the Nyquist frequency, before analysis.

Offset: A reading that is other than zero for a zero condition. Every reading thereafter is inaccurate by this amount, for which compensation is required.

Parameter Estimation: The process of finding parameter values that fit a mathematical model to experimental data.

Other terms such as ***system identification*** can be used for the present context. There are various heuristics developed for parametric estimation particularly in the field of control engineering, such as ***maximum likelihood***, ***predictive estimation*** and ***Kalman filtering***.

Parametric Excitation: A type of self-excited vibration where the stiffness term is time-dependent, resulting in the instability of the system depending on the combination of the system parameters.

Lateral vibration of struts and cables due to periodic fluctuation of axial force are two of the examples often referred to. The equation of motion takes the form of Mathieu's equation, whose solutions are known to become unstable under certain combinations of parameters.

Participating Mass: A part of the physical mass which is actually contributing to vibration. Also called the *modal mass*, since its magnitude depends upon the vibration mode.

Consider the sway vibration of an elevated mass, supported by an elastic column. If the structure vibrates in the fundamental mode of vibration, the heavy mass will vibrate with a large amplitude. However, when the structure vibrates in its second mode, the large amplitude is experienced by the thin column rather than the top mass. Hence, the effective mass contribution will be more substantial in the fundamental mode rather than the second mode, even if the physical mass distribution of the structure remains the same.

The modal mass is calculated by the integration of mass per unit length times the mode function squared, over the whole structure, and it is unique to each mode.

Pattern Recognition: The act of taking in raw data, extracting meaningful information to form the feature vectors out of them, and classifying the measured data into categories based on characterization of patterns.

It is a field within the area of machine learning or ***artificial intelligence***. It has been applied typically to the automatic speech recognition, classification of spam and non-spam email messages, and machine reading of hand-written postal codes on postal envelopes. Effective application of these techniques to structural parameter estimation is highly desired.

The most fundamental tasks in pattern recognition are a) to learn the probabilistic relationship between the feature vectors and presumed categories; and b) to make an inference as to which categories the recognized data should belong to, based on the Bayesian decision theory. Also developed in recent years is the application of ***neural network*** to pattern recognition as an effective tool for learning process.

Peak Counting: A method of cycle counting to reduce a statistical summary out of irregular time-histories by counting the number of peaks and valleys.

The valuable outcomes of the field observation of structural behaviour are usually given as lengthy and irregularly fluctuating time-histories of acceleration, stress, deflection and so on. An absolutely essential matter for engineers then is to reduce a small amount of useful information out of them for fatigue analysis, for example. Counting the number of cycles of the record fluctuation is one of them.

There are a number of methods to perform this operation, such as counting of ***peaks***, ***level crossings*** and ***ranges***, which are defined by the difference between two successive extremes. All of these are called *one parameter methods* whereas two parameter methods called the ***rainflow analysis*** is known to be a state-of-the-art counting method successfully applied to fatigue analysis. Note that the cycle counting yields amplitude distribution with no regard to frequency information.

Peak Factor: The ratio of dynamic peak to its root-mean-square value.

Not to be confused with the ***gust factor***. If the dynamic signal is a simple harmonic fluctuation, the peak factor should be $\sqrt{2}$. If the signal has the normal distribution of its magnitude, the peak factor is known to be approximately 3.6. Some peculiar random signals have very high peak factors. Wind induced suction, for example, on a tall building sometimes shows the peak factor of even higher than 10.

Piezoelectric Accelerometer: A type of accelerometer that uses solid-state strain gauge elements that are physically attached to cantilever beams and electrically connected to a Wheatstone bridge circuit.

Plasticity: Tendency of a material to remain deformed, after reduction of the deforming stress to a value equal to or less than its yield strength.

POD: Proper Orthogonal Decomposition.

Poisson's ratio: The ratio of transverse contraction strain to longitudinal extension strain in the direction of stretching force.

Virtually all common materials have Poisson's ratios in the range from 0 (such as cork) to 0.5 (such as rubber). Poisson's ratio of steel is approximately 0.29, resulting in the ratio of the Young's modulus to shear modulus to be 1.55.

Power Spectral Density (PSD): A function to represent a random process by the distribution of dynamic energy in terms of its frequency components.

PSD is a statistical function consisting of the average squared moduli of the Fourier transform at each frequency. It represents the random characteristics of the process in frequency domain. The ordinate of the function corresponds to the intensity of energy at that particular frequency and integration of PSD over the whole frequency range gives the variance of the process. Hence, the PSD function divided by the variance is called the ***normalised spectral density***.

When the structural system and excitation force are both linear and the principle of superposition is applicable, the PSD functions of input (force) and output (displacement) are related by the ***transfer function***, which is given by the square of the frequency response function (FRF).

Predictive Estimation: Parameter estimation consistent with Bayesian probability theory.

It seeks to minimize the average divergence between the estimated and true distributions. The divergence is measured by Kullback and Leibler's formula. The distribution which achieves minimum divergence corresponds to integrating out the unknown parameter. Hence, predictive estimation can be approximated by averaging over several different parameter choices.

Probability Distribution: A function to represent that the probability of an event is less than or equal to certain value.

The probability that the instantaneous value $X(t)$ is less than or equal to certain value x is defined by a function $P_X(\leq x)$, which is called the ***probability distribution function***, or ***cumulative distribution function (CDF)***, not to be confused with its derivative, which is the ***probability density function (PDF)***, $p_X(x)$.

Proper Orthogonal Decomposition (POD): A statistical method for system identification to provide modal decomposition.

It is essentially an attempt to extract characteristic information of a multivariate data set into an optimal set of uncorrelated variables called POD modes. The method was originally developed in analysing the spatial coherent structure in turbulent flow as a useful tool but it has been now applied to dynamics of structures, materials processing and many more fields of pattern recognitions, including feedback control design for smart material structures.

Proportional Limit: Highest stress at which stress is directly proportional to strain.

It is the highest stress at which the stress-strain diagram is a straight line. It is usually a little lower than the yield stress and is equal to the elastic limit for many metals.

PSD: Power Spectral Density.

Rainfall Analysis: A cycle counting method to define an equivalent series of peaks and troughs for convenience of fatigue life prediction.

The general approach in fatigue life prediction needs to relate a random load fluctuation in real life situation to the ***Wöhler curves***, which are based on laboratory experiments of simple specimens subjected to constant amplitude load. The rainflow cycle counting analysis is a method proposed to overcome this difficulty, originally by Endo et al. (1968) and has been developed by many researchers, including Downing (1972) Rychlik (1987) etc., to a state-of-the-art method in fatigue analysis for reducing lengthy irregular time-histories to a small amount of useful knowledge.

Random Decrement (RD) Technique: A technique to identify structural parameters by averaging out the random noise components.

RD was developed by H.A. Cole at NASA in the late 1960s, as an alternative technique to FFT, for identification of dynamic parameters and in-service damage detection of space structures. Its principle can be best explained by a simple example such as follows:

The random response of a structure at time $t_0 + t$ is composed of the following three parts: a) The component due to the initial displacement $x(t_0)$; b) The impulse response due to initial velocity $\dot{x}(t_0)$; and c) The zero-mean, random component due to random loading or noise in the period, t_0 to $t_0 + t$. If a time segment of $x(t)$ is picked up every time the triggering condition, such as $x(t) = a$, is satisfied, the average of these segments will be a free decay response from the initial displacement, a. It is because c) above will be eventually averaged out and become negligible, and the sign of the initial velocity is expected to vary randomly with time so the resulting initial velocity will be zero, and so is b).

The method has a merit in the sense that it requires relatively short data length, though it is also suitable for transforming long-term observations into a small amount of data. It requires a high rate of digitization, usually the order of magnitude higher than the representative frequency. Also, the method has to be carefully applied when there are two or more outstanding modes and frequencies coexisting. It is desirable to band-pass filter the data before processing to isolate an outstanding mode, if it is the case. Particularly when co-existing frequencies are closely spaced, the application of least-square curve fitting to obtain a multi-frequency signature has been recommended.

Random Process: The process which generates a sequence of indexed random variables, or the sequence itself.

It is also called the ***stochastic process***. The set of random variables is often a time sequence, $X(t)$, sampled from continuous analog signals. The entire collection of all possible sets of sequences is called the ***ensemble*** and an individual set is called a ***sample function*** or ***realized function*.** When the probability distribution of the random process does not evolve appreciably over a time of interest to the engineer, the process is called ***stationary***. When the temporal and ensemble averages of a random process are equal, the process is called ***ergodic***.

Random Vibrations: A type of vibration where the non-deterministic nature of excitation and/or of the structural system need to be counted for.

There are a number of examples. Wind induced vibration of tall buildings, earthquake excitation of buildings and dams, vibration of offshore oil drilling platforms by action of ocean waves and currents, aircraft vibration during its flight and taxiing, and traffic induced vibration of highway bridges are all random vibrations. Some of them are almost periodic but others are not. Some of them are stationary but others are not, transient or even impulsive. However, generally speaking, because of the non-deterministic nature of their processes, random vibrations are handled statistically.

RD: Random Decrement.

Reduced Frequency: A dimensionless expression of frequency often employed in wind engineering and aerodynamics.

Usually it is defined as $K = \omega B/U$, where $\omega = 2\pi f$ = the circular frequency, $B =$ a linear structural dimension, and $U =$ the mean wind speed. Sometimes, instead of the circular frequency ω, the frequency itself f is used for the definition. The inverse of the reduced frequency is often called the ***reduced velocity***.

Reduced Velocity: Inverse of the reduced frequency.

***Reference Period: Chosen period of time, which is used as a basis for assessing values of variables.**

***Rehabilitation: The work required to repair or upgrade an existing structure.**

Reliability: The probability that a structure will perform its intended functions during a specified period of time under stated conditions.

***Remaining Working Life: A remaining period of the expected life of an existing structure, which is intended or expected to operate with planned maintenance.**

***Repair: Improvement of the conditions of a structure by restoring or replacing existing components that have been damaged.**

Residual Stresses: Internal stress state of a structure or its components, as a result of the preceding thermal and/or mechanical processes such as pre-stressing or welding.

Reynolds Number: A dimensionless parameter that indicates the dynamic flow configuration in relation to the development of turbulence.

It is defined by $\mathrm{Re} = VL/\nu$, where V, L and ν are the mean flow speed, a characteristic length and the kinematic fluid viscosity. It is essentially the ratio of fluid inertia force to the viscous force. When Re is very small, the viscous force is large enough relative to the inertia force to suppress the development of turbulence and flow stays laminar, whereas when Re is large, it becomes turbulent. The transition between laminar and turbulent flow is often indicated by a critical Reynolds number, which depends on the exact flow configuration. For example, for the flow around a circular cylinder with a very smooth surface, the ***critical Reynolds number*** is known to be about 2300.

Richter Scale: A definition of earthquake magnitude proposed by Richter, who defined the magnitude by the logarithm of the largest displacement recorded by a standard seismograph.

The Richter scale *M* and the energy *E* released by an earthquake is approximately related by $\log_{10} E = 4.8 + 1.5M$, where *E* is measured in *joules*. Events with magnitude 5.0 or above can cause major damage to structures. The energy released by a 1 megaton hydrogen bomb is roughly equivalent to a magnitude 7.4.

It has been recognized that this scaling method has a saturation effect near 8.5 and it becomes difficult to differentiate the magnitude of events even when they are clearly different in size. Some seismologists now want to replace it with the ***moment magnitude scale***, which has been established more recently.

Risk Rating: A measure to classify the risk levels in different categories.

The risk levels are defined by assessing a) the potential threat, b) vulnerability of the existing or projected system, and c) the potential impact it could result.

Robustness: A desirable characteristic of a regulatory network to generate a certain qualitative response over a broad range of parameter values.

In the context of computer software or network system, it is the resilience of the system, especially when under stress or when confronted with invalid inputs. For example, the operating system is considered robust if it operates properly and correctly even when it starved of memory space, or confronted with an illegitimate application or bugs.

Safety: The condition of a structure being protected against failure, damage, error, accidents, or harm, in both causing and exposure.

Safety is the most overwhelming factor in structural design, construction and maintenance. However, in reality, it is a probabilistic concept and there is a need of a reliability method to decide if the condition is adequately acceptable. Reliability analysis based on appropriate modelling of parameters with reliability indices is a topic of ***Safety Engineering***.

***Safety Plan: A plan specifying the performance objectives, the scenarios to be considered for the structure, and all present and future measures such as design, construction, or operation such as monitoring, to ensure the safety of the structure.**

Scruton Number: A dimensionless parameter which indicates a combined effect of mass and damping on the vortex induced structural response.

Named after Kit Scruton, who was a pioneering British engineer in industrial aerodynamics, it is defined by $Sc = m\varsigma/(\rho D^2)$, in which $m =$ mass per unit length, $\varsigma =$ structural damping ratio, $\rho =$ fluid density, and $D =$ a representative linear dimension of the structure. Note that sometimes the Scruton number is defined by $2m\delta/(\rho D^2)$, which is 4π times greater than the above definition.

If the vortex excitation can be regarded as a resonance to a simply fluctuating excitation force, the induced peak response will be inversely proportional to the Scruton number.

Seismic Waves: Elastic waves that are caused by earthquakes and travel through the Earth. There are different types of waves, body waves and surface waves.

Seismic waves can be also caused by explosions on or under the ground surface. The mechanics of wave motion in solid media, particularly with geological strata, are very complex.

There are two different body waves, P-waves and S-waves. P-waves are longitudinal or compressive waves and travel at the speed of sound, which is about 1.5 km/s in water and 5 to 13 km/s in hard rocks. S-waves are transverse or shear waves. They travel at about 60% speed of P-waves, only through solid. With S-waves, the ground moves perpendicular to the direction of wave propagation. The body-wave amplitudes decay at the rate that is inversely proportional to the square of radial distance from the hypocentre.

Two kinds of surface waves, Rayleigh wave and Love wave, are known, that travel along the ground surface or inter-surface of media. Surface waves are often direct cause of severe catastrophic consequences of earthquakes. They give ground surface motion in vertical and horizontal direction, respectively. Surface waves travel with the speed a little slower than S-waves and their amplitudes decay much more slowly than the body-wave amplitude, with the rate proportional to the square-root of radial distance.

Sensor: A device that is designed to acquire information from an object and transform it into an electrical signal.

It usually consists of three parts: a) the sensing element, such as resisters, capacitor, transistor, piezoelectric materials, photodiode, etc.; b) equipment for signal conditioning and processing, such as amplification, linearization, compensation and filtering; and c) sensor interface to connect with other electronic components.

Service Life: The number of years a structure is intended to be in service.

Serviceability: The ability of a structure to be serving or capable of serving its intended purposes to the uses' satisfaction.

Shear Modulus: The ratio of the increase in stress to that of strain of a material subjected to shear loading.

For an isotropic, homogeneous elastic material, there are only two independent elastic moduli. The shear modulus (*G*), for this case, is related to Young's modulus (*E*) and Poisson's ratio (ν) by $G = E/2(1+\nu)$. For structural steels, $G \approx 80GPa$. The shear modulus of structural materials is determined by a twisting test, which is regulated in ASTM E-143.

SI Units: The *Systeme Internationale d'Unities*. An international system of units that was established in an attempt to simplify the language of science.

The system was an outcome of a resolution adopted at the 9^{th} General Conference of Weights and Measures, 1948, and has been gradually accepted by many countries over the world, replacing the traditional local unit systems. It is based on seven standard base units: length (*m*), mass (*kg*), time (*s*), electric current (*A*), temperature (*K*), luminous intensity (*cd*), and the amount of substance (*mol*), and all other units are derived from these. The system also specifies the standard prefixes to express multiples and submultiples, such as kilo (*k*), mega (*M*) and milli (*m*).

Signal Processing: A data analysing system which includes data filtering, frequency domain transformation and statistical analysis.

Similitude Requirements: Scaling requirements in engineering model tests so that the scale model test results could be interpreted with proper physical meaning.

The ***Buckingham*** Π ***-theorem*** states that a set of dimensionless parameters which consist of suitable combinations of the reference quantities are required to be invariant in model and prototype and with them the governing equations are also rendered dimensionless. However, the complete satisfaction of this requirement for all conceivable dimensionless numbers is possible only when the model and prototype are identical. It means that in any scale model tests, one or more of the similitude requirements need to be relaxed to make the model test possible. The real issue of experimental mechanics, therefore, becomes a matter of interpreting the test results, knowing that which of the requirements are actually distorted or disregarded in the tests.

The dimensionless numbers often treated in wind tunnel tests for bridge aerodynamics, for example, are ***Reynolds number***, ***Froude number***, ***Jensen number***, ***reduced frequency***, ***mass parameter***, ***damping ratio*** etc.

Simulation: The physical, mathematical or software-based modelling of a system and also of its behaviour as an interaction with the environment.

Smart Materials: Materials that have one or more property that can be significantly altered in a controlled fashion by external stimuli.

The external inputs can be stresses, temperature, moisture, pH, and electromagnetic fields, which are sensed and the response of the materials is actuated. There are many types of smart materials including piezoelectric materials and thermo-responsive materials.

Smart Structure: A structure that has the ability to alter its configuration or properties as a response to changes in environment.

The concept has been developed in the field of aerospace engineering but many possible applications in civil engineering structures have been explored and implemented. The use of piezoelectric materials and embedded or surface-mounted fibre optic sensor systems for monitoring the dynamic behaviour of structures to actuate the active damper system is one example. A smart structure needs to have three integral components besides the load carrying function - the sensors, the processor and the actuators.

S-N Curve: See the *Wöhler curve*.

Spectral Analysis: Dynamic analysis in terms of the frequency-based characteristics of the processes by the use of the auto- and cross-power spectral density functions (PSD).

Spectral Windows: Weighing functions to be applied in spectral analysis for processing only band-pass filtered data in frequency domain.

Windows are applied to obtain smoother spectra so that the physical interpretation of them would become easier. Basic requirements for the windows are: a) the integration of a window function over the whole frequency range should be unity; and b) the window function should be symmetric with respect to zero frequency. There are various types of window functions employed in engineering signal processing including the ***digital filters*** such as Hanning and Hamming windows.

Inverse Fourier transform of the spectral windows are called ***lag windows***, which are the windows in time domain and applicable to the autocorrelation functions.

Stationary Process: A stochastic process in which the probability density function (PDF) of a random variable does not change over time or position.

Stochastic Subspace Identification: A modal parameter identification method developed in a MATLAB environment, applicable to ambient vibration survey (AVS).

The method starts with a stochastic state-space representation of the dynamic behaviour of a structure under white noise excitation. The numerical procedures of matrix decomposition for identifying the state space model are all handled by built-in functions of MATLAB.

Strain Energy: Measure of energy absorption characteristics of a material under load up to fracture. It is equal to the area under the stress-strain curve, and is a measure of the toughness of the material.

Stress Concentration: A phenomenon where an object under load has higher than average local stresses due to its shape.

The types of shape that cause these concentrations are: cracks, sharp corners, holes and narrowing of the cross-section. Ratio of the greatest stress in the area to the corresponding average stress is called the ***stress concentration factor***.

Strouhal Number: A dimensionless parameter to indicate the frequency of alternating wake vortices.

Formulated by a Czech physicist, C.V. Strouhal, it is defined as $St = fD/U$, where f = the frequency of vortex formation, U = the flow speed, and D = a representative structural dimension, which is usually taken normal to the flow. The Strouhal number is generally a function of the ***Reynolds number***, $\mathrm{Re} = UD/\nu$. The Strouhal number of a two-dimensional circular cylinder, for example, is approximately 0.2 when the Reynolds number is in the sub-critical range. For ordinary plate-girder or box-girder bridge decks, the Strouhal number is typically in the range of 0.07 to 0.14.

Symmetry: A relationship of a form, pattern or style to its own mirror image, expressed by exact correspondence of the original to the opposite side of a dividing line or plane.

There is also a case of *point-symmetry*, where the same pattern correspondingly exists at a position that is 180° rotated about an axis. *Symmetry* is an extremely important element of thought in any artistic works. As an extended concept particularly in physics, *symmetry* sometimes means *invariance*. Note, however, that the mirror image may have different characteristics from the original, such as the case of *enantiomers*.

The autocorrelation function of a stationary process $x(t)$ is an even function, which is symmetric with respect to zero, or $R_X(-\tau) = R_X(\tau)$. It follows that, as a result, the power spectral density $S_X(f)$ of the same process becomes an even function of frequency. However, since the negative values of frequency does not make a good physical sense, the *one-sided* power spectral density, $G_X(f) = 2S_X(f) \quad 0 \le f < \infty$ (otherwise zero), is often defined only for the positive range of frequency. Note that the area under $G_X(f)$ for the positive frequency is equal to the whole area under the original $S_X(f)$.

System Identification: Technical determination of structural properties from the known response of the system.

Other terms such as ***modal identification*** or ***parameter estimation*** have been used for the same procedure in the present context. The goal of system identification is the opposite of classical dynamic analysis, where usually the structural properties are known and response of the system is to be determined under various excitations.

The approaches in system identification techniques are broadly classified into two groups; the time domain procedure, which includes the least-squares fitting and the random decrement method, deterministic as well as stochastic subspace identification method etc., and the frequency domain procedure by applying Fourier transform, which includes the half-power bandwidth method, the maximum likelihood method and so on.

***Target Reliability Level: The level of reliability required to ensure acceptable safety and serviceability.**

TDA: Time Domain Analysis.

Thermal expansion: Material characteristics specified by a linear expansion due to a unit increase in temperature.

A material constant defined by a strain corresponding to a unit increase in temperature is called the coefficient of thermal expansion. It is approximately 12×10^{-6} /^{0}C for structural steel and concrete.

Time Domain Analysis (TDA): Analysis of signals and their functions with respect to time as opposed to their handling in terms of frequency.

See also the ***frequency domain analysis (FDA)***.

Time Series: An ordered sequence of values of a variable at equally spaced time intervals.
Time series analysis is used for analysing and understanding the characteristics of discrete data systems sampled from continuous observations and also for fitting of time series models for forecasting of future values. There are many techniques of model fitting including Box-Jenkins ARIMA models and multivariate models.

Toughness: The ability of a metal to withstand shock loading.

The concept is the exact opposite of brittleness. Toughness can be explained as the ability of a metal to distribute within itself both the stress and strain caused by a suddenly applied load. It is usually measured by the ***Charpy test*** but its indication is relative, since toughness is also governed, in addition to the material composition, by the shape of the metal.

Trend removal: Removal of the data characteristics defined as any frequency component whose period is longer than the record length. Least square procedures or the average slope method are often used.

Ultimate Strength: Highest engineering stress developed in material before rupture. Normally, changes in area due to changing load and necking are disregarded in determining ultimate strength.

***Upgrading: Modifications to an existing structure to improve its structural performance.**

***Utilization Plan: A plan containing the intended uses of the structure, and listing the operational conditions of the structure including maintenance requirements, and the corresponding performance requirements.**

Vibration: The periodic to-and-fro motion of a structure or its members.

Vibration is characterised by three basic parameters: how quickly the motion is repeated (*frequency*), how large the magnitude of the motion is (*amplitude*), and how soon it dies out without new supply of excitation energy (*damping*).

Depending upon the sources of excitation, structural vibration in reality may be a regular periodic motion but is more likely stochastic in terms of both frequency and amplitude. The latter case is called the ***random vibration***, and it is often more convenient to handle the characteristics of vibration in statistical terms.

The ***adverse effects*** of structural vibration are examined from various aspects. The structure should not collapse, must maintain its structural integrity so that it does not lose its serviceability. Even if the structure is safe and able to serve, if it produces any discomfort to the users and/or causes any mechanical problems such as overstressing, malfunctioning or misalignment, it is not acceptable. Also, even if there is no immediate problem, any troubles in future such as structural fatigue damage, possibly even compound with material corrosion, must be

avoided as much as possible. The ***acceptance criteria*** are often defined by the combination of amplitude and frequencies but they are related to how often and how long the structure is exposed to dynamic excitation, too.
There are various sources of dynamic excitation for bridge vibrations, including earthquakes, wind, moving vehicles and pedestrians, and sometimes even unexpected impact loads such as ship collision on piers or machine operation and blasting.

Vortex Shedding Excitation: Vibration of a structure or its members excited by vortices of air flow created by the interaction of wind and the structure.

When an aerodynamically bluff body is exposed to wind, a trail of alternating vortices (the ***Kármán vortices***) is often found in its wake, formed by the flow separated from the body. There is also a fluctuating lift force acting on the body corresponding to the formation of vortices. As a result, when the frequency of vortex formation is close to the structure's eigen-frequency, there will be a resonant vibration. This is the most fundamental concept of vortex excitation. However, once the vibration starts, the body motion itself will influence on the flow behaviour, which results in the more complicated interaction of flow and structure.

Unlike the case of buffeting, the vortex excitation is usually observed in a limited range of wind speed and its amplitude decreases once it hits the peak value. The vibration is usually characterised by a narrow-band frequency spectrum and somewhat regular amplitude.

Wave: A vibratory motion or disturbance that propagates and yet is not usually associated with mass transport.

Mechanical waves propagate through continuous media, including air, liquid or solids, which are recognized as sound, ocean waves and seismic waves, for example. There are also electromagnetic radiations, including visible lights, infra or ultraviolet rays, gamma rays etc., which can propagate through vacuum.

All waves have common characteristics that are experienced as reflection, refraction, diffraction, interference, dispersion and rectilinear propagation, though possession of these characteristics is only a necessary condition to be waves.

Waves can be described using standard parameters such as frequency, wavelength, amplitude and period. Waves remaining in one place are called standing waves and waves moving are called travelling waves. Material particles in mechanical waves can be vibrating in the direction of wave propagation or perpendicular to it. They are termed longitudinal and transverse waves, respectively. In the case of ***seismic waves***, they are also called the P-wave and S-wave, respectively.

Wavelet Transform: A tool for decomposing a signal into its time- and scale-dependent components, in terms of so-called wavelet coefficients. It is suitable for the analysis of non-stationary data.

Fourier transform is a very versatile tool in signal analysis, but it is not suitable for identifying non-stationary aspects of the signal. For example, since Fourier transform is applied to the entire signal length, the result cannot indicate at what time in the signal a specific frequency existed. It is really a tool for frequency resolution but not for time resolution. It means that if the method is applied to structural health monitoring, the method may recognize damage occurrence, location, or even its severity, but not exactly when the damage happened.

Wavelet transform is basically an extended application of a windowing technique with variable-sized windows. It allows the use of long time intervals where low-frequency information is needed and shorter intervals for high-frequency information.

Wind Power Input: An expression for the magnitude of energy input due to wind. This expression is often used in the field of power line vibration.

The specific power input $\tilde{P}$ is defined by $\tilde{P} = P/(f^3 D^4 L) = 2\pi^2 \cdot m/D^2 \cdot (a/D)^2 \delta$, where $P =$ the power imparted by wind, $D =$ the cylinder diameter, $L =$ cable length, $m =$ the effective cable mass per unit length, $f =$ vibration frequency, $a =$ vibration amplitude, and $\delta =$ the net logarithmic decrement.

Wind Tunnel: An experimental facility to examine the interaction between wind flow and solid objects that are exposed to it by placing a model of the object in an artificially created air flow.

Wind tunnel tests are carried out for the measurement of wind flow around the body, wind-induced forces or pressure on the body and/or static and dynamic behaviour of the structure induced by wind. Since the determination of wind-structure interaction is not easily done by any analytical means, particularly for many of the civil engineering applications, wind tunnel tests are attractive alternatives. However, care should be taken for proper simulation of both structural models and wind flow conditions in carrying out these tests so that the test results would be properly interpreted to the situation in reality. A set of rules required for carrying out the tests is called the ***similitude requirements***.

A wind tunnel in which an artificially developed turbulent boundary layer flow is used as a simulation of natural wind is called the ***boundary layer wind tunnel*** (BLWT).

Windows: Weighing functions to be applied for required operations, such as band-pass filtering, smoothing and/or distortion of a given set of data.

Measurement of any data is a kind of windowing, too, since the measuring period cannot be infinitely long to cover the whole length of the original data, and the observed results are inevitably influenced by the characteristics of sensing devices such as the frequency response, resolution and precision of the measuring system.

The windowing operation can be carried out in time domain as well as the frequency domain. Windowing in time domain becomes convolution in frequency domain.

See also the ***spectral windows***.

Wöhler Curve: A graph of the magnitude of a cyclic stress (S) against the number of cycles (N) to the material's fatigue failure.

It is also called the ***S-N curve***. A Wöhler curve is derived from the coupon tests in the laboratory environment, where an ideal sinusoidal stress of constant amplitude is applied to failure. Each coupon tests generates a point on the plot, though in some cases the time to failure exceeds the anticipated time frame. The Wöhler curves allow designers to make a basic estimate of the expected life of the structural part against expected stresses.

Yield Point: The stress at which the metal changes from elastic to plastic in behaviour.

Structural steels usually exhibit the yield strength of 300 to 400 MPa. ***Offset yield strength*** is determined from a stress-strain diagram. It is the stress corresponding to the intersection of the stress-strain curve, and a line parallel to its straight line portion offset by a specified strain. Offset for metals is usually specified as 0.2%.

Young's Modulus: A ratio of increase in stress to that of strain, when stress and strain has a linear relationship.

Young's modulus of steel is usually taken as 200–210 *GPa*. When a material exhibits nonlinear stress-strain relationship, the definition of an equivalent Young's modulus is sometimes convenient. Young's modulus in dynamic situation may not be always equal to the static value.

Terms with * are definitions according to ISO 2394 and ISO 13822.

References:

Asmussen, J.C., Modal analyis based on the random decrement technique: Application to civil engineering structures, *Ph.D. thesis*, Aalborg University, 1997.

Balageas, D.L. (ed.) *Proc. 1st European Workshop on Structural Health Monitoring*, Paris, July 2002.

Brika, D. & Laneville, A., The power imparted by wind to a flexible circular cylinder in the wake of another stationary cylinder, *IEEE Trans. Power Delivery* (12) 1, 1997, pp.398-405.

Bullard, F., A brief introduction to Bayesian statistics, *NCTM*, 2001.

Carden, E.P. & Fanning, P., Vibration Based Condition Monitoring: a review, *Structural Health Monitoring* (3) 4, 2004, pp.355-377.

Chang, F.K. (ed.) *Proc. 4th Int. Workshop on Structural Health Monitoring*, Stanford, CA, Sept. 2003.

Cunha, Á. & Caetano, E., From input-output to output-only modal identification of civil engineering structures, *Proc. 1st Int. Operational Modal Analysis Conf.*, Copenhagen, Apr. 2005, pp.11-27.

De Roeck, G. & Peeters, B., Benchmark study on system identification through ambient vibration measurements, *Proc. 18th Int. Model Analysis Conf.* (IMAC) San Antonio, Texas, 2000, pp.1106-1112.

Doebling, S.W., Farrar, C.R. & Prime, M.B., A summary review of vibration-based damage identification methods, *The Shock and Vibration Digest* (30) 2, 1998, pp.91-105.

Farar, C.R., Doebling, S.W. & Nix, D.A., Vibration-based structural damage identification, *Phil. Trans. Roy. Soc. London* (A359) 2001, pp.131-149.

Felber, A.J., Development of a hybrid bridge evaluation system, Ph.D. thesis, University of British Columbia, Vancouver, 1993.

Hanks, T.C. & Kanamori, H., A moment magnitude scale, *J. Geophysical Research* (84) B5, 1979, pp.2348-2350.

Haritos, N. & Owen, J.S., The use of vibration data for damage detection in bridges: a comparison of system identification and pattern recognition approaches, *Structural Health Monitoring* (3) 2, 2004, pp.141-163.

Ibrahim, S.R., Random decrement technique for modal identification of structures, *J. Spacecrafts & Rockets* (14) 11, 1977, pp.696-700.

Ibrahim, S.R. & Miklucik. E.C., A method for the direct identification of vibration parameters from the free response, *Shock & Vibration Bulletin* (47) 4, 1977, pp.183-198.

Iliff, K.W., Aircraft parameter estimation, AIAA Dryden Lecture in Research for 1987, *NASA TM* 88281, 1987.

Kim, J.T. & Lyon, R.H., Cepstral analysis as a tool for robust processing, deverberation and detection of transients, *Mech. Systems & Signal Processing* (6) 1, 1992, pp.1-15.

Ljung, L., *System Identification: Theory for the User*, Prentice Hall PTR, 1999.

Madsen, H.O., Krenk, S. & Lind, N.C., *Methods of Structural Safety*, Prentice-Hall, 1986.

Mufti, A.A. (ed.) *Proc. 1st Int. Workshop on Structural Health Monitoring*, ISIS Canada Research Network, Winnipeg, Sept. 2002.

Peeters, B., System identification and damage detection in civil engineering, Ph.D. thesis, Katholieke Universiteit Leuven, Dec. 2000.

Peeters, B., Maeck, J. & De Roeck, G., Vibration-based damage detection in civil engineering: Excitation sources and temperature effects, *Smart Materials and Structures* (10) 2001, pp.518-527.

Reda Tana, M.M. et al., Introduction to the use of wavelet multi-resolution analysis for intelligent structural health monitoring, *Can. J. Civil Engineering* (31) 2004, pp.719-731.
Rychlik, I., A new definition of the rainflow cycle counting method, *Int. J. Fatigue* (9) 2, 1987, pp.119-121.
Salawu, O.S., Detection of structural damage through changes in frequency: a review, *Engineering Structures* (19) 9, 1997, pp.718-723.
Wenzel, H. & Pichler, D., *Ambient Vibration Monitoring*, Wiley & Sons, 2005.
Wu, Z.S. & Abe, M. (ed.) *Proc. 1st Int. Conf. on Structural Health Monitoring and Intelligent Infrastructure*, Tokyo, Nov. 2003, Balkema 2003.

List of entries listed in Part I

Acceleration
Accelerometer
Accounted truth
Acoustic emission (AE)
Advanced composite materials (ACM)
Aerodynamic admittance function
Aerodynamic instability
Allowable stress design
Ambient vibration survey (AVS)
ARIMA model
Artificial intelligence
Assessment
Averaged Normal power spectral density (ANPSD)

Bayesian statistics
Beating
Beaufort scale
Boundary layer wind tunnel
Bridge management
Buckling
Buffeting
Bulk modulus of elasticity

Cable
Cepstral analysis
Charpy test
Comfort
Convolution
Correlation
Corrosion
Coulomb damping
Creep
Critical damping
Critical Reynolds number

Damage
Damage detection
Damping
Data acquisition (DAQ)
Data mining
Decision support system (DSS)
Degree-of-freedom (DOF)
Deterioration
Discrete Fourier transform (DFT)
Ductility
Dynamic excitation
Earthquakes
Eigen-frequency
Eigen-mode
Elastic hysteresis

Elasticity
Elongation
Environmental noise
Expert system
Extensiometer
Extreme value distributions

Failure
Fast Fourier transform (FFT)
Fatigue
Fibre optic sensors
Fibre stress
Filter
Finite element method
Force balance accelerometer
Fourier series
Fourier transform
Fracture toughness
Frequency domain analysis (FDA)
Frequency response function (FRF)
Froude number
Fuzzy logic

Global positioning system (GPS)
Gust factor

Hardness
Health monitoring

Impact energy
Impulse response function (IRF)
Indicial response function
Infrastructure
Inspection
Instability
Intensity
Inverse problem
Investigation

Jensen number

Kalman filter
Kármán vortices

Laser Doppler vibrometer
Least-square method
Life cycle
Limit state
Linear variable differential transformer (LVDT)
Load
Load testing

Maintenance

Markov process
Mass parameter
Material properties
MATLAB
Maximum likelihood method
Melting point
Miner’s rule
Modal mass
Modal parameters
Modified Mercalli Intensity scale
Moment magnitude scale
Monitoring
Monte Carlo method

Natural frequency
Neural network
Noise
Nonlinear vibration
Nyquist frequency

Offset

Parameter estimation
Parametric excitation
Participating mass
Pattern recognition
Peak counting
Peak factor
Piezoelectric accelerometer
Plasticity
Poisson’s ratio
Power spectral density (PSD)
Predictive estimation
Probability distribution
Proper Orthogonal decomposition (POD)
Proportional limit

Rainflow analysis
Random decrement (RD) technique
Random process
Random vibrations
Reduced frequency
Reduced velocity
Reference period
Rehabilitation
Reliability
Remaining working life
Repair
Residual stresses
Reynolds number
Richter scale
Risk rating
Robustness

Safety
Safety plan
Scruton number
Seismic waves
Sensor
Service life
Serviceability
Shear modulus
SI units
Signal processing
Similitude requirements
Simulation
Smart materials
Smart structure
S-N curve
Spectral analysis
Spectral windows
Stationary process
Stochastic subspace identification
Strain energy
Stress concentration
Strouhal number
Symmetry
System identification

Target reliability level
Thermal expansion
Time domain analysis (TDA)
Time series
Toughness
Trend removal

Ultimate strength
Upgrading
Utilization plan

Vibration
Vortex shedding excitation

Wave
Wavelet transform
Wind power input
Wind tunnel
Windows
Wöhler curve

Yield point
Young's modulus

PART II MATHEMATICAL FORMULATIONS IN DYNAMICS

Chapter 1 Elements of Structural Dynamics

1.1 Dynamics of SDOF Systems

Depending on the purpose of the analysis, many structures can be simulated as a simple SDOF system. Degrees-of-freedom (DOF) is the number of displacements for describing the characteristics of a given vibration. However, the concept of DOF is applicable only in terms of mathematical modelling of vibration. The same vibration of a structure can be considered as multi-degree-of-freedom (MDOF) or it may be approximated as a single-degree-of-freedom (SDOF) system, depending on how the structure is conceptually modelled.

When a structure is modelled by a single-degree-of-freedom (SDOF) system of mass (*m*), stiffness (*k*) and viscous damping (*c*), subjected to an excitation force $F(t)$, the analysis of its dynamic displacement (z) can be formulated by the equation of motion as follows:

Equation of motion $$m\ddot{z} + c\dot{z} + kz = F(t) \qquad (1)$$

or $$m\left(\ddot{z} + 2\varsigma\omega_0\dot{z} + \omega_0^2 z\right) = F(t) \qquad (1a)$$

where $$\omega_0 = 2\pi f_0 = \sqrt{\frac{k}{m}}$$ Natural circular frequency (2)

$$\varsigma = \frac{c}{2\sqrt{mk}}$$ Damping ratio (3)

Natural frequency is characteristic to the structure since it is uniquely decided only by mass and stiffness. Natural frequencies of the structures are supposed to be evaluated under the standard design conditions of m and k, in which the structure is free of live loads and extreme temperature effects. However, since the instantaneous mass and stiffness of the structure in reality could be different from the design assumptions, it is worthwhile to note that the natural frequencies of the structure in service condition can be different from the values calculated by (2).

Free vibration When $F(t) = 0$, the general solution of (1) is given by

a) $\varsigma < 1$ (decaying vibration) $$z_H(t) = \exp(-\varsigma\omega_0 t)\left(A\sin\omega_D t + B\cos\omega_D t\right) \qquad (4)$$

where $$\omega_D = \omega_0\sqrt{1-\varsigma^2}$$ Frequency with damping (4a)

b) $\varsigma = 1$ (critical damping) $\quad z_H(t) = (At + B)\sin\omega_0 t$ (5)

c) $\varsigma > 1$ (over-damped) $\quad z_H(t) = \exp(-\varsigma\omega_0 t)\left(A\sinh\omega_N t + B\cosh\omega_N t\right)$ (6)

where $\quad \omega_N = \omega_0\sqrt{\varsigma^2 - 1}$ (6a)

The integral constants A and B are decided from the ***initial conditions***, $z_H(0)$ and $\dot{z}_H(0)$.

Damping can be defined as the capacity of structures to dissipate energy imparted by the external forces. The dissipation of dynamic energy during vibration results from many different sources, such as the imperfect elasticity and internal friction of structural materials, friction of structural members at their joints and support mechanisms, aerodynamic and hydrodynamic damping due to surrounding environment, the nonlinear structural characteristics, energy dissipation through foundation and substructures, and so on. In any of these, the theoretical evaluation of damping capacity is generally limited and it is essentially important to consult to the results of the field experience as references. Some practical notes on damping is added later in **Chapter 4**.

Though the mechanism of damping is quite diverse, their overall effects on vibration is usually characterized by considering an equivalent viscous damping, crystallized in a single number of *damping ratio* (ζ) as a fraction of critical. If the overall damping of the system is 1% of critical, for example, the free vibration amplitude will be reduced to a half after 11 cycles, whereas the 10% damping will reduce the amplitude to a half at each cycle. When damping is at or beyond critical, there is no vibration, as (5) or (6) above.

Natural frequency is reduced a little with the increase of the system's damping as in (4a). However, in reality, this effect can be disregarded for the case of civil engineering structures. For example, even if the damping is as high as 10% of critical, the natural frequency is reduced by only 0.5% compared to the case with no damping.

<u>Forced vibration</u>

a) By a ***simple harmonic excitation*** $F(t) = F_0\sin\omega t$ ($\omega = 2\pi f$) (7)

$$z_P(t) = M(\Omega,\varsigma)\cdot\frac{F_0}{k}\sin(\omega t - \beta) \quad (8)$$

where $\quad \Omega = \dfrac{\omega}{\omega_0} = \dfrac{f}{f_0}$ $\quad$ Frequency ratio (9)

$\beta = \tan^{-1}\dfrac{2\varsigma\Omega}{1-\Omega^2}$ $\quad$ Phase lag (10)

$M(\Omega,\varsigma) = \dfrac{1}{\sqrt{(1-\Omega^2)^2 + (2\varsigma\Omega)^2}}$ $\quad$ ***Dynamic load factor*** (11)

Dynamic excitation a structure is subjected to may not be exactly simple harmonic. However, by decomposing the external excitation function $F(t)$ to various frequency components by applying *Fourier analysis*, the structural response to each frequency component can be decided by (8) and hence the total response is given by a linear combination of all frequency response components, unless the system is nonlinear.

Generally the response of the system under excitation is given by $z(t) = z_P(t) + z_H(t)$.

- The dynamic load factor (or Magnification factor) takes its peak value

$$M_{\max} = \frac{1}{2\varsigma\sqrt{1-\varsigma^2}} \approx \frac{1}{2\varsigma} \qquad (12)$$

when $\Omega = \sqrt{1-2\varsigma^2} \approx 1$ or $\omega \approx \omega_0$ (***Resonance***). (13)

- More generally, when a simple harmonic excitation force is expressed by $F(t) = F_0 e^{i\omega t}$, the induced response of the system is given by $z_P(t) = \frac{H(\omega)}{k} F(t)$, where

$$\frac{H(\omega)}{k} = \frac{1}{k} \cdot \frac{1}{(1-\Omega^2) + i \cdot (2\varsigma\Omega)}$$ ***Frequency response function (FRF)***

(14)

Note that the dynamic load factor is the magnitude of FRF, or $\frac{|H(\omega)|}{k} = M(\Omega, \varsigma)$.

FRF is sometimes called the ***mechanical admittance function***. It shows the sensitivity of a structural system to the excitation frequency. The peak response is reached when the excitation frequency coincides with the natural frequency and its magnitude is inversely proportional to the total damping of the system.

b) Forced vibration induced by an ***impulse load*** $F(t) = F_0$ $(0 \le t \le \Delta t)$ is given by $z_P(t) = F_0 \cdot h(t)\Delta t$, where

$$h(t) = \frac{1}{m\omega_D} \exp(-\varsigma\omega_0 t) \sin \omega_D t$$ ***Impulse response function (IRF)***

(15)

- FRF and IRF make a ***Fourier transform*** pair, or

$$\frac{H(\omega)}{k} = \int_{-\infty}^{\infty} h(t) e^{-i\omega t} dt \quad \text{and} \quad h(t) = \frac{1}{2\pi} \int_{-\infty}^{\infty} \frac{H(\omega)}{k} e^{i\omega t} d\omega \qquad (16)$$

Fourier transform is an integral transform, which is particularly useful in relating the time domain and frequency domain variables for random vibration analysis. Concept of the Fourier transform developed from a Fourier series, which is the decomposition of a periodic function. Fourier transform expands this concept to make it further applicable to the non-periodic functions. The analysis of measured data using the ***discrete Fourier transform (DFT)***, particularly in the form of the ***fast Fourier transform (FFT)***, is one of the most important techniques for the frequency domain vibration analysis.

c) When the system is excited by an external load that can be expressed by a *known* function $F(t)$ ($t \geq 0$), the response is given by

$$z_P(t) = \int_0^t h(\tau)F(t-\tau)d\tau \qquad \textbf{Duhamel Integral} \qquad (17)$$

Mathematically, (17) is the general solution of (1), when $z(0) = \dot{z}(0) = 0$.

[Ex.1] When a SDOF system of mass m, stiffness k with no damping, is subjected to an external force $F(t) = F_0$ ($t \geq 0$), the induced response is given by

$$z_P(t) = \frac{F_0}{m\omega_0}\int_0^t \sin\omega_0(t-\tau)d\tau = \frac{F_0}{k}\left(1-\cos\omega_0 t\right)$$

[Ex.2] When $F(t) = F_0 \sin\omega t$ is applied to the same system, the response is

$$z_P(t) = \frac{F_0}{m\omega_0}\int_0^t \sin\omega\tau \sin\omega_0(t-\tau)d\tau = \frac{F_0}{k}\frac{\sin\omega t - \Omega\sin\omega_0 t}{1-\Omega^2}$$

Nonlinear Vibration

Equation of motion (1) describes the dynamics of a linear system. When the structural restoring force and/or damping force are not linearly proportional to the displacement or its time derivative, however, or the external forces are amplitude dependent, the vibration becomes *nonlinear*.

Nonlinear stiffness can be caused by material nonlinearity, or structural nonlinearity, such as the case of cables or strain hardening. Structural damping ratio is usually higher when vibration amplitude is greater. In contrast, the aerodynamic damping is sometimes found drastically reduced, or even becomes negative, with greater vibration amplitude. This is because the excitation force is largely nonlinear due to structural interaction with the surrounding fluid.

All of these factors indicate that very often the structural vibration is likely to be nonlinear in reality, unless the dynamic amplitude is very small, and the nonlinear vibrations can be analysed only by applying numerical methods without closed form solutions. However, we try to handle them with linear approximation so long as it is acceptable for practical purposes. An important discussion to be added to this topic, therefore, is to cover the characteristics of vibration that cannot be fully explained, or not explained at all, unless the linear approximation is removed.

Free vibration

Let us consider, as an example, a typical nonlinear equation of motion, where the restoring force has the slight strain hardening effect as follows:

$$m\ddot{z} + c\dot{z} + k(1+\varepsilon z^2)z = 0 \qquad (\varepsilon << 1) \tag{18}$$

or

$$\ddot{z} + 2\varsigma\omega_0\dot{z} + \omega_0^2(1+\varepsilon z^2)z = 0 \tag{18a}$$

Eq.(18) is called the Duffing's equation and its approximate solution is, by neglecting the damping, given by

$$z(t) \approx A\sin\left(1+\frac{3\varepsilon}{8}A^3\right)\omega_0 t \tag{19}$$

which indicates that the frequency of vibration, $\omega = \omega_0\left(1+\frac{3\varepsilon}{8}A^3\right)$, is amplitude dependent. As it is clear here, unlike the case of linear vibration, the eigen-frequency cannot be defined for a nonlinear system.

Forced vibration

Consider the same nonlinear system as before, which is now subjected to a simple harmonic excitation force. It is more natural to include the damping term for this case. The equation of motion becomes

$$\ddot{z} + 2\varsigma\omega_0\dot{z} + \omega_0^2(1+\varepsilon z^2)z = \frac{F_0}{m}\sin\omega_e t \tag{20}$$

If $\varepsilon = 0$, the case is linear and the steady-state response is given by

$$z(t) = A\sin(\omega_e t + \beta) \tag{21}$$

When $\varepsilon \neq 0$, because of the nonlinearity of the system, the resulted response is not limited only to the component at the excitation frequency but there are components of higher harmonics at the frequencies, such as

$$z(t) = \sum_{r=1,3,5..} A_r \sin(r\omega_e + \beta_r) \tag{22}$$

This is quite characteristic to nonlinear vibrations.

Also, the response at the excitation frequency behaves differently from the linear case. Let us assume that the solution to this case is somewhat similar to (21) except both A and β are functions of time. Since the steady-state vibration is determined by considering $\dot{A}(t) = \dot{\beta}(t) = 0$, it results that

$$\left(1-\Omega^2+\frac{3\varepsilon}{4}A^2\right)^2 A^2+\left(2\varsigma\Omega\right)^2 A^2=\left(\frac{F_0}{k}\right)^2 \tag{23}$$

$$\beta=-\tan^{-1}\left(\frac{2\varsigma\Omega}{1-\Omega^2+(3\varepsilon/4)A^2}\right) \tag{24}$$

where $\Omega=\omega_e/\omega_0$.

Eq.(22) indicates that, depending on the excitation frequency ω_e, the steady-state amplitude can take three different values. $A-\omega$ diagram (Fig.1.1) shows that one of them actually is an unstable limit cycle. Depending on ω_e, there is a sudden jump of amplitude (***jumping phenomenon***) and also the magnitude of steady state amplitude can be different for increasing and decreasing cases of ω_e, which is called the ***hysteresis phenomenon***. Generally speaking, when $\Omega\approx 1$, which is equivalent to the resonance condition for a linear system, there are somewhat similar phenomena for a nonlinear system, too, which is called the ***harmonic resonance***. However, unlike the case of linear systems, the harmonic resonance is accompanied by jumps and hysteresis, which are characteristic to nonlinear vibrations.

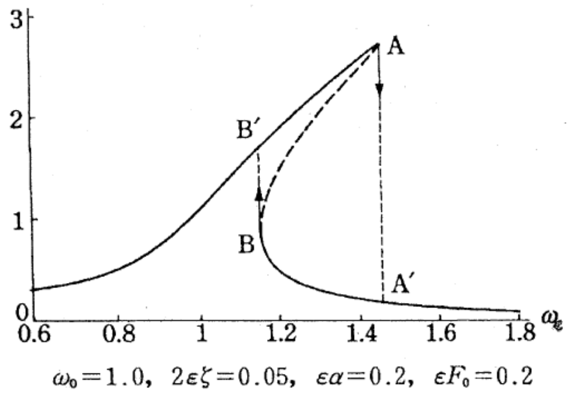

Fig.1.1

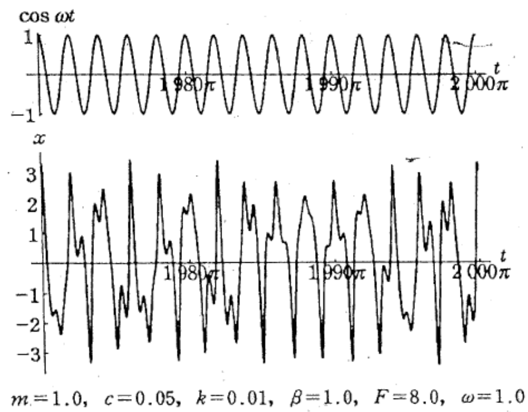

Fig.1.2

Chaotic vibration

Another characteristic aspect of nonlinear vibration is that, even if the system is deterministic, the system's response to a regular simple harmonic excitation can be quite random with a continuous frequency distribution. This is caused by the fact that the response of a strongly nonlinear system can be extremely sensitive to the difference of initial conditions for each cycle of vibration. An example is shown in Fig.1.2. This response vibration looks random but actually there are some regularity with it and is called the ***chaotic vibration***.

The state of this vibration can be fully described by the locus of $(x,\dot{x},t)$, which is called the ***phase portrait*** and this 3D space $(x,\dot{x},t)$ is called the ***phase space***. When the points are periodically taken with regular intervals along the phase portrait and a 2D projection of these points is made on the $x-\dot{x}$ plane, it is called the ***Poincaré map***. If the nonlinear motion of the system becomes stable and its motion is confined in a limited range, the Poincaré map will form a limited pattern, which is called an ***attractor***.

1.2 Dynamics of Elastic Structures – Modal Analysis

Once the dynamic finite element analysis is carried out of a structure and its natural frequencies and corresponding mode shapes are obtained as ω_r and $\phi_r(x)$ ($r = 1,2,..,N$), the dynamic response of the structure under a *known* external force $F(x,t)$ can be calculated as follows:

For the *r*-th mode of vibration of the structure, the equation of motion is

$$M_r(\ddot{q}_r + 2\varsigma_r\omega_r\dot{q}_r + \omega_r^2 q_r) = F_r(t) \tag{1}$$

where $M_r = \int_L m(x)\phi_r^2(x)dx$ Generalized mass (2)

$F_r(t) = \int_L F(x,t)\phi_r(x)dx$ Generalized force (3)

and the resulted response is given by $z(x,t) = \sum_{r=1}^{N} q_r(t)\phi_r(x)$ (4)

ς_r is the assumed damping for the *r*-th mode of vibration. The integrations $\int_L [.....]dx$ are to be carried out over the whole structure.

[Ex.] If the structure is a simply supported beam of span L with a uniformly distributed mass m and uniform bending stiffness EI, and the beam is subjected to the axial force T, the natural circular frequencies and corresponding mode shapes are given by

$$\omega_r = \left(\frac{r\pi}{L}\right)^2 \sqrt{\frac{EI}{m}} \sqrt{1 + \left(\frac{\gamma}{r\pi}\right)^2} \qquad \gamma^2 = \frac{TL^2}{EI}$$

and $$q_r(x) = \sin\frac{r\pi x}{L} \qquad (r = 1,2,3,...)$$

1.3 Dynamics of MDOF Systems – Complex Eigenvalue Problems

Considering a discrete model of *N*-degrees-of-freedom for a structure, the equation of motion can be written in a similar way as a SDOF system as follows:

$$[M]\cdot\{\ddot{z}\} + [C]\cdot\{\dot{z}\} + [K]\cdot\{z\} = \{F(t)\} \tag{5}$$

where $[M]$, $[C]$ and $[K]$ are the mass, damping and stiffness matrices, and $\{z\}$ and $\{F(t)\}$ are the displacement and the external force vectors, respectively.

Free vibration: The effect of damping can be ignored in free vibration analysis, or

$$[M]\cdot\{\ddot{z}\}+[K]\cdot\{z\}=\{0\} \tag{6}$$

Hence, by assuming $\{z(t)\}=\{\phi\}\cdot e^{i\omega t}$, the natural frequencies ω_r and associated eigenvector ϕ_r ($r=1,2,...,N$) are decided from

$$\left|[K]-\omega^2[M]\right|=0 \tag{7}$$

and

$$\left[[K]-\omega_r^2[M]\right]\cdot\{\phi_r\}=\{0\} \qquad (r=1,2,...,N) \tag{8}$$

has to be satisfied by the mode vector $\{\phi_r\}$, where one of the vector components, ϕ_{1r} for example, needs to be given arbitrarily and other components are decided relative to this value.

In case the external force is given as a linear function of structural displacement, $\{F(t)\}=[F_1]\cdot\{z(t)\}+[F_2]\cdot\{\dot{z}(t)\}$, by including these terms, the equation of motion has the homogeneous form as the case of free vibration, however with damping:

$$[M]\cdot\{\ddot{z}\}+[C]\cdot\{\dot{z}\}+[K]\cdot\{z\}=\{0\} \tag{6a}$$

For this case, the problem can be handled in the same way as before but the frequency equation will become more complicated, including the complex coefficients:

$$\left|[K]+i\omega[C]-\omega^2[M]\right|=0 \tag{7a}$$

It is more convenient to rewrite the equation (6a) as a ***state equation set*** as follows:

$$\{\dot{X}(t)\}=[A]\cdot\{X(t)\} \tag{9}$$

where

$$\{X\}=\begin{Bmatrix} z \\ \dot{z} \end{Bmatrix} \qquad [A]=\begin{bmatrix} \{0\} & [I] \\ -[M]^{-1}[K] & -[M]^{-1}[C] \end{bmatrix} \tag{10}$$

$\{X\}$and $[A]$ are a *2N×1* state vector and a *2N×2N* state matrix, respectively, and $[I]$ is a *N×N* unit matrix. By assuming a general solution as $\{X\}=\{\phi\}\cdot e^{st}$, the natural frequencies and damping are obtained as the complex eigenvalues of

$$\left[s[I]-[A]\right]\cdot\{\phi\}=\{0\} \tag{11}$$

where *s* and $\{\phi\}$ are the eigenvalue and eigen vector, respectively, and the natural circular frequency ω_r and the modal damping ratio ς_r in *r*-th mode are related to the eigenvalue $s = \alpha_r \pm i\beta_r$ ($r = 1,2,...,N$) by

$$\omega_r = \sqrt{\alpha_r^2 + \beta_r^2} \qquad \varsigma_n = -\frac{\alpha_r}{\sqrt{\alpha_r^2 + \beta_r^2}} \tag{12}$$

The *r*-th eigen mode of vibration $z_r(t)$ is expressed as

$$z_r(t) = 2\exp(-\varsigma_r \omega_r t)\left(C_{1r}\phi_r^R \cos\omega_{Dr} t - C_{2r}\phi_r^I \sin\omega_{Dr} t\right) \tag{13}$$

in which $\omega_{Dr} = \omega_r\sqrt{1-\varsigma_r^2}$, the complex eigen mode is $\phi_r = \phi_r^R \pm i\phi_r^I$, and C_{1r}, C_{2r} are decided from the initial conditions. Note that the *n*-th component of the displacement vector $z_r(t)$ is

$$\begin{aligned} z_{rn}(t) &= 2\exp(-\varsigma_r \omega_r t)\left(C_{1r}\phi_{rn}^R \cos\omega_{Dr} t - C_{2r}\phi_{rn}^I \sin\omega_{Dr} t\right) \\ &= 2\exp(-\varsigma_r \omega_r t)\sqrt{(C_{1r}\phi_{rn}^R)^2 + (C_{2r}\phi_{rn}^I)^2}\cos\left(\omega_{Dr} t + \theta_{rn}\right) \end{aligned} \tag{14}$$

where the phase lag $\theta_{rn} = \tan^{-1}\dfrac{C_{2r}\phi_{rn}^I}{C_{1r}\phi_{rn}^R}$ is found to be different for each *n*, which means that the maximum displacement for each mode (*n*) does not necessarily take place at the same time, or, unlike the case without damping, the mode of vibration is time-dependent or unsteady.

<u>Forced vibration</u>: Once the modal quantities, ω_r, ϕ_r ($r = 1,2,...,N$) are found, the modal equation of motion is established as

$$M_r\left(\ddot{q}_r + 2\varsigma_r\omega_r\dot{q}_r + \omega_r^2 q_r\right) = F_r^*(t) \tag{15}$$

where $M_r = \phi_r^T[M]\phi_r$ and $F_r^*(t) = \phi_r^T\{F(t)\}$ are the modal mass and modal excitation force, and the modal response is calculated as

$$q_r(t) = A_r \exp(-\varsigma_r\omega_r t)\cos(\omega_{Dr} t - \gamma_r) + \int_0^t F_r^*(\tau)h_r(t-\tau)d\tau \tag{16}$$

where $h_r(t) = \dfrac{1}{M_r\omega_{Dr}}\exp(-\varsigma_r\omega_r t)\sin\omega_{Dr} t$ is the Impulse Response Function (IRF) for *r*-th mode. A_r and γ_r are decided from the modal initial conditions as

$$A_r = \sqrt{\left(\frac{\dot{q}_{r0} + q_{r0}\varsigma_r\omega_r}{\omega_{Dr}}\right)^2 + q_{r0}^2} \qquad \gamma_r = \tan^{-1}\frac{\dot{q}_{r0} + q_{r0}\varsigma_r\omega_r}{\omega_{Dr} q_{r0}} \tag{17}$$

in which $q_{r0} = q_r(0) = \dfrac{\phi_r[M]}{M_r}\{z(0)\}$ and $\dot{q}_{r0} = \dot{q}_r(0) = \dfrac{\phi_r[M]}{M_r}\{\dot{z}(0)\}$ (18)

Then the total response is obtained as $z(t)=\sum_{r=1}^{L}\phi_r \cdot q_r(t) \qquad (L \le N)$ (19)

References:

Clough, R.W. & Penzien, J., *Dynamics of Structures*, McGraw-Hill, 1975/1993.
Smith, J.W., *Vibration of Structures: Applications in Civil Engineering Design*, Chapman & Hall, 1988.

1.4 Modal Parameter Identification Techniques

Structural health monitoring is our target, which is to track various aspects of a structure's performance and integrity in relation to the system's expected safety and serviceability. The attempted levels of structural identification are as follows: 1) Presence of damage in the structure; 2) Location of the damage; 3) Severity of the damage; and 4) Prediction of the remaining service life of the structure. It is desirable if the structural health monitoring system is inexpensive, non-invasive and also automated, so that subjective differences by operator can be avoided. In particular, neither the implementation nor operation of the system should involve closure of the bridge.

Vibration-based structural monitoring is considered in this context. Ideally we are trying to identify structural damages and deterioration from the measured modal parameters. Therefore, the goal of system identification is the opposite of classical dynamic analysis, where the structural properties are known and response of the system under assumed excitation is to be determined, as described in the previous section. For the present case, on the other hand, the structural parameters are to be identified from the measured response of the system.

The conventional modal identifications are based on structural response induced by known excitation such as a simple harmonic vibration imposed by an artificial excitation. For this case, the structural parameters are identified either from the free vibration decay traces, after the excitation is removed, or simply as a transfer function between input and output of the system. A difficulty of this method is to excite huge civil engineering structures for the measurement. The output-only modal identification, as opposed to the procedure based on input-output relationship, has been developed recently in order to avoid this difficulty, supported by technological development in accurate measurements of very low levels of dynamic response induced by ambient excitations.

Various techniques have been developed for determining the structural parameters. The most fundamental idea, however, is to assume mathematical models for the system and minimize the prediction errors by fitting models against the obtained output data. The prediction-error idetification approach contains some fundamental procedures, such as the least-squares fitting and the maximum-likelihood procedure. It is also closely related to other well-known methods in control engineering, such as the Bayesian maximum *a posteriori* estimation and Akaike's information criterion. So-called correlation approach is to carry out a similar procedure by taking correlation between the prediction errors and the output data. It contains the instrumental-variable technique, as well as several methods for rational transfer function models.

There is also the subspace approach, which is to identify state-space models. It consists of three steps: 1) estimating the *k*-step ahead predictors using the least-squares algorithm, 2) selecting the state vector from these, and finally 3) estimating the state-space matrices using these states and the least squares method.

(1) Conventional method applicable to free vibration records

In terms of data reliability, the forced vibration tests using shakers is probably the best method for the evaluation of dynamic characteristics of bridges. However, it usually requires a large operation, which is naturally costly, and could also mean an interruption of services. If this approach is available, the modal parameters are to be obtained from the free vibration record. Identification of natural frequencies is usually less problematic compared to the evaluation of damping. Emphasis is placed on identification of damping value in this section.

Log-decrement method is probably the most classical and straightforward method of identifying the system's damping. The damping ratio is obtained from the ratio of the vibration amplitudes over N consecutive waves:

$$\varsigma = \frac{1}{2\pi N} \log_e \left(\frac{A_j}{A_{j+N}} \right) \tag{1}$$

The reading is naturally more accurate with greater *N*. If the damping is very high, it becomes more difficult to expect good accuracy, since *N* cannot be too great. With $\varsigma = 0.15$, for example, the amplitude becomes 94% less after only three cycles. Even if the damping is not too high, damping often differs at different amplitude level. It may be better to formulate, hence, the calculation as follows:

$$\varsigma(A_j) = \frac{1}{8\pi} \log_e \left(\frac{A_{j-2}}{A_{j+2}} \right) \tag{2}$$

A little more elaborate way of determining ς is to find an envelope of $x(t)$, which is given by
$A(t) = \sqrt{\{x(t)\}^2 + \{\tilde{x}(t)\}^2}$, where $\tilde{x}(t)$ is the ***Hilbert transform*** of $x(t)$, defined by

$$\tilde{x}(t) = \int_{-\infty}^{\infty} \frac{x(u)}{\pi(t-u)} du \tag{3}$$

The log-decrement is an ideal method for laboratory tests, where the free vibration decay traces are available relatively easily. However, when it comes to the full scale on-site measurements, it is often difficult to obtain a good decay curve.

(2) Conventional methods applicable to ambient vibration tests

The ambient vibration survey, without any control on the input, is an attractive alternative to a large-scale forced vibration operation. It is a method to determine the dynamic characteristics of a structure by measurement of small vibrations, mostly micro-tremors, caused by existing disturbances such as earthquakes, wind and traffic, while the structure is in service. This method is based on a few basic assumptions as follows: a) The input excitation is a broadband stochastic process which is adequately modelled by white-noise; b) The system characteristics are therefore well represented by the power spectral density function of dynamic response; c) The technique for measuring the dynamic response is sufficiently reliable; and d) The data acquisition and analysis are also sufficiently reliable. Hence, the reliability of this method is largely decided by these factors. Errors for this case are caused by various sources such as noise contamination, coexistence of more than one predominant frequencies and nonlinearity or amplitude dependence of damping.

Half-power bandwidth method has been widely practised. The method is based on the fact that the width of the power spectral density of a SDOF system is proportional to the system's damping ratio. If the original data are given by $x(t) \approx e^{-\alpha t} \sin \omega_0 t$, $\alpha = \varsigma\omega_0$, the power spectral density (one-sided) becomes

$$G_x(\omega) = 4\alpha\left[\frac{1}{\alpha^2 + (\omega+\omega_0)^2} + \frac{1}{\alpha^2 + (\omega-\omega_0)^2}\right] \tag{4}$$

With its peak reading at

$$G_P = G_x(\omega_0) = \frac{4}{\alpha}\frac{2+\varsigma^2}{4+\varsigma^2} \approx \frac{2}{\alpha} \tag{5}$$

Since the half-peak readings, $G_P/2$, are given at $\omega = (1 \pm \varsigma)\omega_0$, the peak spectral width at half-power is given by $\Delta\omega = 2\varsigma\omega_0$.

This method cannot be free of all statistical errors associateed with the spectral analyses. A possible problem of this method is when the spectral peak is missing. In fact, there is a good chance not to have the reading of the exact spectral peak. If the peak is missing, the half-peak band width tends to be greater than the value in reality and the damping is likely to be overestimated.

Note also that if the peak is not of the power spectral density but the response amplitude itself, or the *dynamic amplification factor*, the frequency width $\Delta\omega$ should be taken at the peak divided by $\sqrt{2}$ rather than the half-power.

Autocorrelation decay method has been in use for quite some time, too. It was developed to cover the cases where the vibration data are contaminated by random noise. By taking the autocorrelation function of the given data, the outstanding SDOF will give a decaying harmonic function simply superposed on a quickly decaying non-oscillatory function caused by random noise. When the original data are given by

$$x(t) = A\exp(-\varsigma\omega_0 t)\sin\omega_0 t + n(t) \qquad n(t) = \text{noise} \tag{6}$$

The autocorrelation function is

$$R_x(\tau) = \frac{A^2}{2}\exp(-\varsigma\omega_0 t)\cos\omega_0 y + C(t) \quad (7)$$

where $C(t)$ is a quickly decaying function and the frequency and damping can be identified from the first term. This is a good method if a fairly long record is available, and also there is only one outstanding system frequency to be observed. If there are two or more closely-spaced system frequencies involved in the data, it becomes increasingly difficult to obtain an exact reading.

(3) <u>Random decrement method</u>

Random excitation by noise is a fact of life and cannot be excluded anyway. Random decrement approach is somewhat similar to the autocorrelation decay method. This is also a time domain method, developed at NASA for use in the aerospace industry [1]. The technique is straightforward. It consists of adding and averaging the segments of the data for pre-determined length, whenever the time series exceeds certain triggering level with the slopes alternating positive and negative. The process can be described as follows:

$$D_X(\tau) = \frac{1}{N}\sum_j x(t_j + \tau) \quad (8)$$

where $x(t_j) = x_s(const) \quad (j = 1,2,3...)$

$\dot{x}(t_j) \geq 0 \quad (j = 1,3,5...)$ and $\dot{x}(t_j) \leq 0 \quad (j = 2,4,6...)$

$D_X(\tau)$ is called the *random decrement signature* and, in fact, it is proved to be proportional to the autocorrelation coefficient $\tilde{R}_X(\tau)$. Generally speaking, these segments can be divided into the following three groups:

a) deterministic step response: $x_1(t) = x_0 e^{-\alpha t}\cos\omega_0 t$

b) deterministic impulse response: $x_2(t) = \frac{\dot{x}_0 + \alpha x_0}{\omega_0} e^{-\alpha t}\sin\omega_0 t$

c) transient random response: $x_3(t) = \frac{e^{-\alpha t}}{\omega_0}\int_0^t e^{-\alpha\tau} q(\tau)\sin\omega_0(t-\tau)d\tau$

The step response is due to an initial displacement x_0, the impulse response results from an initial velocity $\dot{x}_0$, and the random response is with any random component $q(t)$ in the forcing function. When the complete time history has been searched for these segments, they are overlaid and averaged together, b) and c) tend to average out to zero and only a) will remain, from which the damping and frequency are decided, or

$$x(t) = \frac{1}{N}\sum_{j=1}^{N}\{x_1(t_j) + x_2(t_j) + x_3(t_j)\} \rightarrow x_0 e^{-\alpha t}\cos\omega_0 t \quad (9)$$

The method has a merit in the sense that it requires relatively short data length. However, it also requires a high rate of digitization, usually $16f_0$ or more. Also, the method is not very effective when there are two or more outstanding system frequencies coexisting. It is highly recommended to band-pass filter the data before processing, if it is the case. Particularly when co-existing frequencies are closely spaced, the application of least-square curve fitting to obtain a multi-frequency signature has been recommended.

(4) <u>Maximum likelihood method</u>

This method applies a technique to fit an assumed spectral peak function by maximizing the joint probability of the sampled spectrum with it. In this process, the spectral peak is assumed to correspond to the mechanical admittance of an idealized SDOF system, which is given by

$$|H(f)| = \frac{1}{\sqrt{\left\{1-(f/f_0)^2\right\}^2 + (2\varsigma f/f_0)^2}} \tag{10}$$

and the response spectrum of the system under a white-noise excitation is given by

$$G_R(f) = |H(f)|^2 G_0 \tag{11}$$

Hence $$A_R = \int_0^\infty G_0 |H(f)|^2 df \approx \frac{\pi}{4}\frac{f_0 G_0}{\varsigma} \tag{12}$$

represents the area under the response spectrum. Now the idea of the method is to fit a spectral density function obtained from the original data with this idealized spectrum. After normalizing the fitting function as

$$F(f_r) = \frac{4\varsigma}{\pi}\frac{1}{\left\{1-(f/f_0)^2\right\}^2 + (2\varsigma f/f_0)^2} \tag{13}$$

the *likelihood function* $L(f_0, \varsigma)$ is defined as the product of $\{F(f)\}^\alpha$, or, by taking the logarithm of it,

$$Q(f_0, \varsigma) = \log_e L = \sum_{r=1}^{N} \{\alpha_r \log_e F(f_r)\} \tag{14}$$

The proper f_0 and ς are decided by maximizing the function Q. This condition is given by

$$\frac{\partial Q}{\partial f_0} = 0 \quad \text{and} \quad \frac{\partial Q}{\partial \varsigma} = 0 \tag{15}$$

However, since Q is to take its maximum when the above conditions are satisfied, as an actual operation, it is in fact easier to change the parameters f_0 and ς within a certain range and find out where Q becomes maximum rather than directly solving the above conditions (15) as a set of simultaneous equations.

A distinct advantage of this method is in the fact that it requires relatively a short record for analysis. It is also said to be relatively insensitive to variance errors. However, it requires larger computational effort relative to other simple methods.

References:

Asmussen, J.C., Modal analysis based on the random decrement technique: Application to civil engineering structures, *Ph.D. thesis*, Aalborg University, 1997.

Cole, H.A. Jr., On-line failure detection and damping measurements by random decrement signatures, *NASA-CR-2205,* Mar. 1973.

Ibrahim, S.R. & Miklucik. E.C., A method for the direct identification of vibration parameters from the free response, *Shock & Vibration Bulletin* (47) 4, 1977, pp.183-198.

Ljung, L., *System Identification: Theory for the User*, Prentice Hall PTR, 1999.

Chapter 2 Basic Tools in Statistics

2.1 Statistical Analysis of Random Processes

(1) Essential probability

The probability of event E is written as $P(E)$, or $P(E) = \Pr ob[E]$. There are three fundamental ***axioms of probability*** as follows:

When A is a random event	$0 \le P(A) \le 1$	(1)
When C is a certain event	$P(C) = 1$	(2)
Axiom of additivity	$P(A \cup B) = P(A) + P(B) - P(A \cap B)$	(3)

The probability of event A given the condition B is called the ***conditional probability*** and is written as $P(A \mid B)$. The ***Bayes' theorem*** states that

$$P(A \mid B)P(B) = P(A \cap B) = P(B \mid A)P(A) \quad (4)$$

(2) Statistics of a random variable

A sequence that consists of indexed random variables is called a ***random process***. The set of random variables is often a time sequence, $X(t)$, sampled from continuous analog signals. The entire collection of all possible sets of sequences is called the ***ensemble*** and an individual set is called a ***sample function***. When the probability distribution of the random process does not change appreciably over a time of interest, the process is called ***stationary***. When the temporal and ensemble averages of a random process are equal, the process is called ***ergodic***.

When a random signal does not convey any useful information, it is called ***noise***. The analysis of noise signal has been developed in the telecommunication field and became one of the most important tools in dynamics. A signal whose intensity is the same at all frequencies is called the ***white noise***, though an infinite-bandwidth white noise is a purely theoretical concept and, in reality, its frequency band has to be limited.

For a continuous random variable, $X(t)$ ($-\infty < t < \infty$), the following functions are defined:

Cumurative Distribution Function (CDF)	$P_X(x) = \Pr ob[X(t) \le x]$	(5)
Probability Density Function (PDF)	$p_X(x)dx = P_X(x+dx) - P_X(x)$	(6)

The probability distribution represents that the probability of an event is less than or equal to certain value x. These functions satisfy the followings:

$$P_X(-\infty) = 0 \quad \text{and} \quad P_X(+\infty) = 1$$
$$dP_X(x) = \Pr ob[X(t) \le x + dx] - \Pr ob[X(t) \le x] = P_X(x+dx) - P_X(x)$$

$$P_X(x) = \int_{-\infty}^{x} p_X(\xi)d\xi \qquad p_X(x) \geq 0$$

The ***Mean***, or average value of $X(t)$ is defined by

$$a_X = E[X(t)] = \int_{-\infty}^{\infty} x p_X(x)dx \tag{7}$$

When more than one simultaneous random processes, $X_k(t)$ ($k = 1,2,...,N$), are considered, the average value can be taken in two different ways as follows:

$$a_X(t) = \frac{1}{N}\sum_{k=1}^{N} X_k(t) \qquad \text{Ensemble average}$$

$$a_X(k) = \frac{1}{T}\int_0^T X_k(t)dt \qquad \text{Time average}$$

and the processes are called *ergodic*, when $a_X(t) = a_X(k) = a_X$.

The ***Moments*** of $X(t)$ are defined as follows:

n-th moments: $m_X^{(n)} = E[x^n] = \int_{-\infty}^{\infty} x^n p_X(x)dx$ (8)

n-th central moments: $\mu_X^{(n)} = E[(x - a_X)^n]$ (9)

The folowing magnitudes are defined using the moment functions:

$m_X^{(0)} = 1$ $\quad m_X^{(1)} = a_X$ $\quad m_X^{(2)} = \Psi_X^2$ (the mean square)

$\mu_X^{(0)} = 1$ $\quad \mu_X^{(1)} = 0$ $\quad \mu_X^{(2)} = \sigma_X^2$ (variance)

σ_X = standard deviation $\qquad c_X = \frac{\sigma_X}{a_X}$ = coefficient of variation

$\gamma_X^{(1)} = \frac{\mu_X^{(3)}}{\sigma_X^3}$ = coefficient of skewness $\qquad \gamma_X^{(2)} = \frac{\mu_X^{(4)}}{\sigma_X^4}$ = coefficient of kurtosis

It is sometimes convenient to transform the data $X(t)$ as

$$Z(t) = \frac{X(t) - a_X}{\sigma_X} \tag{10}$$

which results in $a_Z = 0$ and $\sigma_Z = 1$.

The ratio of dynamic peak to its root-mean-square value is called the *peak factor*. If the dynamic signal is a simple harmonic fluctuation, the peak factor should be $\sqrt{2}$. If the signal has the normal distribution of its magnitude, the peak factor is known to be approximately 3.6. Some peculiar random signals have very high peak factors. Wind induced suction, for example, on a tall building sometimes shows the peak factor of even higher than 10.

Standard Fourier series expansion

An infinite series of sine and cosine functions that can, if convergent, approximate a variety of periodic functions is called the ***Fourier series***. Fourier series can be further transformed to a series of exponential functions by the use of the Euler's formula. The study of functions given by Fourier series is called ***Fourier analysis*** or ***harmonic analysis***.

If $x(t)$ is periodic with a period T_p, $x(t)$ can be represented by the Fourier series as follows:

$$x(t) = \frac{A_0}{2} + \sum_{k=1}^{\infty}\left(A_k \cos\frac{2\pi kt}{T_p} + B_k \sin\frac{2\pi kt}{T_p} \right) \tag{11}$$

where

$$A_k = \frac{2}{T_p}\int_0^{T_p} x(t)\cos\frac{2\pi kt}{T_p}\,dt \qquad (k = 0,1,2...) \tag{12}$$

$$B_k = \frac{2}{T_p}\int_0^{T_p} x(t)\sin\frac{2\pi kt}{T_p}\,dt \qquad (k = 1,2,3...) \tag{13}$$

Correlation functions

Correlation is a measure to indicate how much two variables are statistically related. It is one of the most fundamental concepts in describing the statistical relationship between two signals. It can be the relationship between the excitation force and dynamic response, or between dynamic deflections at two different locations of the same structure, for examples.

As a special case, the correlation of a signal with the same signal itself, but with a given time interval in between, can be taken and in this case it is called the ***auto-correlation*** as opposed to the ***cross-correlation*** between two different signals.

The correlation between two signals can be described in various forms with different degree of sophistication, including the correlation functions, cross-spectral density functions and coherence.

Autocorrelation Function is defined as $R_X(\tau) = E[x(t)x(t+\tau)]$ (14)

And is normalized as $\tilde{R}_X(\tau) = \dfrac{R_X(\tau)}{\sigma_X^2}$ (Autocorrelation coefficient). (15)

Spectral Analysis

The dynamic analysis based on frequency characteristics of the processes, by the use of the auto- and cross-power spectral density functions, are called the ***spectral analysis***.

Power spectral density (PSD) is a function to represent a random process by the distribution of dynamic energy in terms of its frequency components. It is a statistical function consisting of the average squared moduli of the Fourier transform at each frequency. It represents the random characteristics of the process in frequency domain. The ordinate of the function corresponds to the intensity of energy at that particular frequency and integration of PSD over the whole frequency range gives the variance of the process.

When the structural system and excitation force are both linear and the principle of superposition is applicable, the PSD functions of input (force) and output (displacement) are related by the ***transfer function***, which is given by the square of the *frequency response function (FRF)*.

The ***spectral density function (SDF)*** is defined by the Fourier transform of the autocorrelation as

$$G_X(f) = 2\int_{-\infty}^{\infty} R_X(\tau)e^{-i\omega\tau}d\tau = 4\int_{0}^{\infty} R_X(f)\cos\omega\tau d\tau \qquad f = \frac{\omega}{2\pi} \tag{16}$$

Note that $$R_X(\tau) = \int_{0}^{\infty} G_X(f)\cos\omega\tau\frac{d\omega}{2\pi} \tag{17}$$

and $$R_X(0) = \int_{0}^{\infty} G_X(f)df = E[x^2] \qquad \omega = 2\pi f \tag{18}$$

The spectral density defined in eq.(16) is called ***one-sided***, becuase it is defined only in the positive range of frequency. The simple application of Fourier transform on the autocorrelation function will result in the *two-sided* spectral density $S_X(f) = S_X(-f)$ ($-\infty < f < +\infty$). Since the negative frequency does not make any physical sense, the spectral density is often redefined as follows:

$$G_X(f) = 2S_X(f) \ \ (0 \le f < \infty) \quad \text{otherwise zero} \tag{19}$$

As it is given above, the mathematical definition of spectral density function involves the ***Fourier transform***, which is an integral transform particularly useful in relating the time domain and frequency domain variables for random vibration analysis.
Concept of the Fourier transform developed from a Fourier series, which is the decomposition of a periodic function. Fourier transform expands this concept to make it further applicable to the non-periodic functions. The analysis of measured data using the ***discrete Fourier transform (DFT)***, particularly in the form of the ***fast Fourier transform (FFT)***, is one of the most important techniques for the frequency domain vibration analysis.

Two functions related by the Fourier transform, such as the autocorrelation function and spectral density function, make a *Fourier Transform Pair*, as follows:

$$F(\omega) = \int_{-\infty}^{\infty} f(t)\exp(-i\cdot\omega t)dt \tag{20}$$

$$f(t) = \frac{1}{2\pi} \int_{-\infty}^{\infty} F(\omega) \exp(i \cdot \omega t) d\omega \tag{21}$$

It should be noted that the Fourier transform is sometimes defined in somewhat different way:

$$F(\omega) = \frac{1}{\sqrt{2\pi}} \int_{-\infty}^{\infty} f(t) \exp(i \cdot \omega t) dt$$

$$f(t) = \frac{1}{\sqrt{2\pi}} \int_{-\infty}^{\infty} F(\omega) \exp(-i \cdot \omega t) d\omega$$

The resulted functions are naturally different by constant factors compared to the previous definition, but their physical meaning is the same as before.

(3) <u>Statistics of two time series</u> Consider $X(t)$ and $Y(t)$ $(-\infty < t < \infty)$.

On top of the probability functions for each of X and Y, now the following joint functions are defined:

Joint Probability Density Function

$$p_{XY}(x, y) = \frac{\Pr ob[x \le x(t) \le x + dx, y \le y(t) \le y + dy]}{dxdy} \tag{22}$$

Joint Cumulative Distribution Function

$$P_{XY}(x, y) = \Pr ob[x(t) \le x, y(t) \le y] \tag{23}$$

Note that $p_{XY}(x, y) = p(x)p(y)$ and $P_{XY}(x, y) = P(x)P(y)$, if $X(t)$ and $Y(t)$ are *statistically independent* of each other.

- ***Transformation of variables***

When the variable $X(t)$ has a known probablity density function $p(x)$, $Y = f(X)$ has the probability density function of $p(y) = p(x) \cdot |dx/dy|$.

When $x = f_1(r,s)$ and $y = f_2(r,s)$

$$p(r,s) = p(x,y)\frac{\partial(x,y)}{\partial(r,s)} = p(x,y) \cdot \begin{vmatrix} \partial x/\partial r & \partial x/\partial s \\ \partial y/\partial r & \partial y/\partial s \end{vmatrix}$$

Correlation functions and spectra are defined as follows:

Covariance $$C_{XY} = E[(x-a_X)(y-a_Y)] = E[xy] - a_X a_Y \quad (24)$$

and $$\rho_{XY} = \frac{C_{XY}}{\sigma_X \sigma_Y} \text{ (correlation coefficient) } \leq 1 \quad (25)$$

Cross-correlation Function $$R_{XY}(\tau) = E[x(t)y(t+\tau)] = R_{YX}(-\tau) \quad (26)$$

Cross-correlation Coefficient $$\tilde{R}_{XY}(\tau) = \frac{R_{XY}(\tau)}{\sigma_X \sigma_Y} \quad (27)$$

Cross-spectral Density Function

$$G_{XY}(f) = 2\int_{-\infty}^{\infty} R_{XY}(\tau)e^{-i\omega\tau}d\tau = C_{XY}(f) - i \cdot Q_{XY}(f) \qquad f = \frac{\omega}{2\pi} \quad (28)$$

Note that $$R_{XY}(\tau) = \int_0^{\infty} \{C_{XY}(f)\cos\omega\tau + Q_{XY}(f)\sin\omega\tau\}df \quad (29)$$

and $$R_{XY}(0) = E[x(t)y(t)] = \int_0^{\infty} C_{XY}(f)df \quad (30)$$

Also

$$C_{XY}(f) = 2\int_0^{\infty} \{R_{XY}(\tau) + R_{YX}(\tau)\}\cos\omega\tau d\tau = C_{XY}(-f) \quad (31)$$

$$Q_{XY}(f) = 2\int_0^{\infty} \{R_{XY}(\tau) - R_{YX}(\tau)\}\sin\omega\tau d\tau = -Q_{XY}(-f) \quad (32)$$

Coherence Function

$$coh_{XY}(f) = \gamma_{XY}^2(f) = \frac{|G_{XY}(f)|^2}{G_X(f) \cdot G_Y(f)} = \frac{\{C_{XY}(f)\}^2 + \{Q_{XY}(f)\}^2}{G_X(f) \cdot G_Y(f)} \quad (33)$$

Sometimes the following definitions are used instead of (33):

Root-coherence $$\sqrt{coh_{XY}(f)} = \gamma_{XY}(f) \quad (34)$$

Co-coherence $$cocoh_{XY}(f) = \frac{|C_{XY}(f)|}{\sqrt{G_X(f) \cdot G_Y(f)}} \quad (35)$$

2.2 Statistical Treatment of Discrete Time Series

Time series is an ordered sequence of values of a variable at equally spaced time intervals. The time series analysis is used for analysing and understanding the characteristics of discrete data systems sampled from continuous observations and also for fitting of time series models for forecasting of future values.

A continuous signal $X(t)\,(-\infty < t < \infty)$ is usually measured as a time series for only a limited time period, $0 \le t \le T$, and given by

$$x_j = X(t_0 + j\Delta t) \quad (j = 0,1,2,...,N) \qquad \text{in which} \qquad \Delta t = \frac{T}{N} \qquad (1)$$

where $T = N\Delta t =$ the total sampling time, $f_S = \frac{1}{\Delta t} =$ the sampling frequency, and the starting time can be chosen as $t_0 = 0$. Note that $f_C = \frac{1}{2\Delta t} = \frac{f_S}{2}$ is the ***Nyquist frequency***. N is usually taken as an even number. The meaning of the Nyquist frequency will be explained later.

The statistical terms required are, similar to those for a continuous signal, as follows:

Mean $$a_X = \frac{1}{N}\sum_{j=1}^{N} x_j \qquad (2)$$

n-tn central moments $$\mu_n = \frac{1}{N}\sum_{j=1}^{N}\left(x_j - a_X\right)^n \qquad (3)$$

Standard deviation $$\sigma_X = \sqrt{\mu_2} \qquad (4)$$

Data transformation can be applied in the same way as the case of continuous variable:

$$z_j = z(j\Delta t) = \frac{x_j - a_X}{\sigma_X} \qquad \Delta t = \frac{T}{N} \qquad (5)$$

resulting in $a_Z = 0$ and $\sigma_Z = 1$.

- ***Trend removal***

A correction is sometimes required to remove a trend in data, defined as any frequency component whose period is longer than the record length. One of the following methods is often applied:

<u>Average slope method</u> $$\hat{z}_j = z_j - \alpha_Z\left(t - \frac{T}{2}\right) \quad (j = 1,2,...,N) \qquad T = N\Delta t$$

where $\alpha_Z = \dfrac{1}{\Delta t \cdot \nu(N-\nu)} \left\{ \sum_{j=N-\nu}^{N} z_j - \sum_{j=1}^{\nu} z_j \right\}$ $\nu =$ the largest integer $\le \dfrac{N}{3}$

Least square method The desired fit is given by $\hat{z}_j = \sum_{k=0}^{K} b_k (j\Delta t)^k \; (j = 1,2,\ldots,N)$

where $\{b_k\}$ are to be chosen to minimize $Q(b) = \sum_{j=1}^{N} (z_j - \hat{z}_j)^2$. Hence

$$\frac{\partial Q}{\partial b_r} = 0 \quad \text{or} \quad \sum_{k=0}^{K} b_k \sum_{j=1}^{N} (j\Delta t)^{k+r} = \sum_{j=1}^{N} z_j (j\Delta t)^r \quad (r = 0,1,\ldots,K)$$

For $K = 1$, for example,

$$b_0 = \frac{2(2N+1)\sum_{j=1}^{N} z_j - 6\sum_{j=1}^{N} (jz_j)}{N(N-1)} \quad \text{and} \quad b_1 = \frac{12\sum_{j=1}^{N} (jz_j) - 6(N+1)\sum_{j=1}^{N} z_j}{\Delta t \cdot N(N-1)(N+1)}$$

$K \ge 4$ are not recommended.

Statistical Functions for a discrete process

The following definitions are made in parallel to the continuous processes:

Probability Mass Function (PMF) When the random variable Z is discrete

$$p_Z(z) = \Pr ob[Z = z] \tag{6}$$

Cumulative Distribution Function (CDF) $P_Z(z)$

$$P_Z(z) = \Pr ob[Z \le z] \tag{7}$$

Autocorrelation Function When the maximum lag number is m,

$$R_Z(k\Delta\tau) = \frac{1}{N-k}\sum_{j=1}^{N-k} z_j z_{j+k} \approx \frac{1}{N}\sum_{j=1}^{N-k} z_j z_{j+k} \qquad k = 0,1,\ldots,m << N \tag{8}$$

- The resolution bandwidth is decided by m as $B_e = \dfrac{1}{m\Delta t} = \dfrac{2f_C}{m}$ (9)

Autocorrelation coefficient $\tilde{R}_Z(k\Delta\tau) = \dfrac{R_Z(k\Delta\tau)}{\sigma_Z^2}$ (10)

Standard Fourier Series expansion If the sampled record $z(j\Delta t)$ ($j = 1,2,...,N$) is considered as a periodic function of a period $T_p = N\Delta t$, which is the total record length,

$$z_j = z(j\Delta t) = A_0 + \sum_{k=1}^{N/2} A_k \cos\frac{2\pi kj}{N} + \sum_{k=1}^{(N/2)-1} B_k \sin\frac{2\pi kj}{N} \tag{11}$$

where $A_0 = a_z = 0$, $A_k = \frac{2}{N}\sum_{j=1}^{N} z_j \cos\frac{2\pi kj}{N}$ ($k = 1,2,...,\frac{N}{2}-1$)

(12)

$$A_{N/2} = \frac{1}{N}\sum_{j=1}^{N} \cos j\pi, \quad B_k = \frac{1}{N}\sum_{j=1}^{N} z_j \sin\frac{2\pi kj}{N} \qquad (k = 1,2,...,\frac{N}{2}-1)$$

(13)

Discrete Fourier Transform (DFT)

Fourier transform of a discretely indexed series is called the ***discrete Fourier transform (DFT)***. The mathematical formulation is defined here but it is usually executed by the use of the fast Fourier transform algorithm, which is extremely efficient in computation.

$$Z_k = \sum_{j=0}^{N-1} z_j \exp\left(-i \cdot \frac{2\pi kj}{N}\right) \qquad (k = 0,1,...,N-1) \tag{14}$$

$$z_j = \frac{1}{N}\sum_{k=0}^{N-1} Z_k \exp\left(+i \cdot \frac{2\pi jk}{N}\right) \qquad (j = 0,1,...,N-1) \tag{15}$$

Spectral Density Function (SDF)

$$G_Z(f_k) = \frac{2\Delta t}{N}\left|\varsigma_k\right|^2 = \left(\sum_{j=0}^{N-1} z_j \cos\frac{2\pi kj}{N}\right)^2 + \left(\sum_{j=0}^{N-1} z_j \sin\frac{2\pi kj}{N}\right)^2 \tag{16}$$

SDF is usually obtained by applying the FFT routine program. ***Fast Fourier Transform (FFT)*** is a highly efficient algorithm for computing the discrete Fourier transform (DFT) in high speed. The method developed by Cooley and Tukey (1965) has been commonly used. However, some other algorithms are also known.

<u>Statistical functions for two discrete processes</u>

Assume that two standardized time series, x_j and y_j, are given, where $t_k = j\Delta t$, $\Delta t = \frac{T}{N}$.

Note that $a_X = a_Y = 0$ is assumed.

Cross-correlation Function When the maximum lag number is m,

$$R_{XY}(k\Delta t) = \frac{1}{N-k}\sum_{j=1}^{N-k} x_j y_{j+k} \approx \frac{1}{N}\sum_{j=1}^{N-k} x_j y_{j+k} \qquad k = 0,1,\ldots,m << N \quad (17)$$

Cross-correlation coefficient

$$\tilde{R}_{XY}(k\Delta t) = \frac{R_{XY}(k\Delta t)}{\sigma_X \sigma_Y} \quad (18)$$

Cross-spectral Density

Or, by considering the DFT of x_j and y_j as (14), the cross-spectral density function can be defined as follows:

$$G_{XY}(f_k) = C_{XY}(f_k) - i \cdot Q_{XY}(f_k) \qquad k = 0,1,\ldots,m << N \quad (19)$$

where

$$C_{XY}(f_k) = 2\Delta t \cdot \left\{ A_0 + 2\sum_{j=1}^{m-1} A_j \cos\frac{\pi kj}{m} + (-1)^k A_m \right\} \quad \text{Co-spectrum} \quad (20)$$

$$Q_{XY}(f_k) = 4\Delta t \cdot \sum_{j=1}^{m-1} B_j \sin\frac{\pi kj}{m} \quad \text{Quad-spectrum} \quad (21)$$

$$A_j = \frac{R_{XY}(j\Delta t) + R_{YX}(j\Delta t)}{2} \quad \text{and } B_j = \frac{R_{XY}(j\Delta t) - R_{YX}(j\Delta t)}{2} \quad (22)$$

The cross-spectral density is also usually directly computed through the FFT routine.

References:

Ang, A.H.S. & Tang, W.H., *Probability Concepts in Engineering Planning and Design* (in 2 vols.) John Wiley, 1975/1984.

Bendat, J.S. & Piersol, A.G., *Random Data: Analysis & Measurement Procedures*, John Wiley & Sons, 1971/1986.

Brigham, E.O., *The Fast Fourier Transform*, Prentice/Hall, 1974.

2.3 Commonly Used Probability Distributions

(1) Models based on simple discrete random trials – Binomial distribution

A series of random trials in which each trial is independent and yields the binary results, S (success) or F (failure), for example, is called the ***Bernoulli trials***. When the Bernoulli trials with the success rate p are repeated n times, the total number of successes X has a **Binomial distribution**, of which PMF is given by

$$p_X(x) = \binom{n}{p} p^x (1-p)^{n-x} \qquad (x = 0,1,2,...,n) \tag{1}$$

CDF, for this case, can be expressed as follows:

$$P_X(x) = \sum_{r=0}^{x} \binom{n}{r} p^r (1-p)^{n-r} = 1 - \frac{B_p(x+1, n-x)}{B(x+1, n-x)} \tag{2}$$

where $B(a,b)$ is the *beta function* and $B_p(a,b)$ is the *incomplete beta function* defined by

$$B(a,b) = \int_0^1 t^{a-1}(1-t)^{b-1}dt = \frac{\Gamma(a)\Gamma(b)}{\Gamma(a+b)} \qquad (a,b>0) \tag{3}$$

$$B_z(a,b) = \int_0^z t^{a-1}(1-t)^{b-1}dt \qquad (0<z<1) \tag{4}$$

The mean and variance of this distribution are given as follows:

$$a_X = E[X] = \sum_{x=-\infty}^{\infty} x p_X(x) = \sum_{x=0}^{n} x \binom{n}{x} p^x (1-p)^{n-x} = np \tag{5}$$

$$\sigma_X^2 = E[X^2] - E^2[X] = np(1-p) \tag{6}$$

N, the trial number at which the first S (success) occurs, has a ***Geometric distribution***, given by

$$p_N(n) = p(1-p)^{n-1} \qquad (n = 1,2,...) \tag{7}$$

With mean $a_N = \dfrac{1}{p}$ and variance $\sigma_N^2 = \dfrac{1-p}{p^2}$. a_N is also called the mean return period.

(2) Models based on random occurrences – Poisson distribution

Suppose that vehicles are randomly arriving at a specific location. Let $N(t)$ be a process that counts the number of arrivals occurring in $(0,t]$, which satisfies the following conditions:

The numbers of arrivals in non-overlapping intervals are independent of each other;
The mean rate of arrivals λ for a small Δt is defined as follows:

The probability of having exactly one arrival in Δt is proportional to Δt, or

$$P(1,\Delta t) = \Pr ob\left[N(t+\Delta t) = n+1 \mid N(t) = n\right] = \lambda \Delta t \tag{8}$$

The probability of more than one arrivals is negligible and vanishes when $\Delta t \to 0$. Hence, the probability of no arrivals in Δt is given by $1 - P(1,\Delta t)$, or

$$P(0,\Delta t) = \Pr ob\left[N(t+\Delta t) = n \mid N(t) = n\right] = 1 - \lambda \Delta t \tag{9}$$

The process starts at time zero with a count of zero, or $N(0) = 0$.

This is called a ***Poisson process***.

The PDF of $N(t)$, $p_N(n,t)$, is now derived. The probability of having the count n at time $t + \Delta t$ is either a) having the count n at time t and no new arrival in the following Δt, or b) having the count $n-1$ at time t and one new arrival in Δt. Therefore

$$\begin{aligned} p_N(n,t+\Delta t) &= p_N(n,t)\cdot P(0,\Delta t) + p_N(n-1,t)\cdot P(1,\Delta t) \\ &= p_N(n,t)\cdot(1-\lambda\Delta t) + p_N(n-1,t)\cdot \lambda\Delta t \end{aligned} \tag{10}$$

or
$$\frac{p_N(n,t+\Delta t) - p_N(n,t)}{\Delta t} = -\lambda \cdot p_N(n,t) + \lambda \cdot p_N(n-1,t)$$

Considering $\Delta t \to 0$, the following equation is established:

$$\dot{p}_N(n,t) + \lambda \cdot p_N(n,t) = \lambda \cdot p_N(n-1,t) \qquad (n = 1,2,\ldots) \tag{11}$$

By applying induction method
$$p_N(n,t) = \frac{(\lambda t)^n e^{-\lambda t}}{n!} \qquad (n \geq 0) \tag{12}$$

This is a ***Poisson distribution***, where both the mean and variance are

$$a_N(t) = \lambda t \qquad \text{and} \qquad \sigma_N^2(t) = \lambda t\,. \tag{13}$$

Exponential distribution

When T = the random time to the first arrival, the probability of $T > t$, which should be $1 - P_T(t)$, is the same as the probability of having no arrivals up to time t. Hence

$$1 - P_T(t) = \Pr ob\left[N(t) = 0\right] = \frac{(\lambda t)^0 e^{-\lambda t}}{0!} = e^{-\lambda t} \tag{14}$$

or, the cumulative distribution of T is hence given by the ***exponential distribution***

$$P_T(t) = \Pr ob(T \leq t) = 1 - \exp(-\lambda t) \tag{15}$$

and the density function is $p_T(t) = \lambda \cdot \exp(-\lambda t)$ $(t \geq 0)$ (16)

The mean and variance are $a_T = \frac{1}{\lambda}$ and $\sigma_T^2 = \frac{1}{\lambda^2}$ (17)

Gamma distribution

It is also of interest to ask for the distribution of the time S_k to the k th arrival of a Poisson process. Now, the times between arrivals, T_i $(i = 1,2,...,k)$ are independent and have exponential distribution with common parameter λ, and $X_k = T_1 + T_2 + ... + T_k$. From repeated application of the convolution integral, for any $k = 1,2,...$,

$$p_S(s) = \frac{\lambda(\lambda s)^{k-1} \exp(-\lambda s)}{\Gamma(k)} \qquad (s \geq 0) \qquad (18)$$

The mean and variance are $a_S = \frac{k}{\lambda}$ and $\sigma_S^2 = \frac{k}{\lambda^2}$ (19)

The cumulative distribution is expressed as

$$P_S(s) = \int_0^s p_S(s)ds = \frac{\Gamma(k, \lambda s)}{\Gamma(k)} \qquad (20)$$

where $\Gamma(k, x)$ is the *incomplete gamma function* defined by

$$\Gamma(k, x) = \int_0^x \exp(-u) \cdot u^{k-1} du \qquad (21)$$

(3) <u>Normal or Gaussian distribution</u>

The ***central limit theorem*** states that when the random variables $Y_j(k)$ ($j = 1,2,...,N$) are statically uncorrelated to each other, the distribution of $X(k)$ are asymptotically normally distributed when $N \to \infty$, where $X(k)$ are the total sums of these variables defined by

$$X(k) = \sum_{j=1}^{N} Y_j(k)$$

The ***normal** or **Gaussian distribution***, $N(a_{X,} \sigma_X^2)$, is given by

$$p_X(x) = \frac{1}{\sigma_X \sqrt{2\pi}} \exp\left\{ -\frac{(x-a_X)^2}{2\sigma_X^2} \right\} \tag{22}$$

or, by putting $Z = \frac{X - a_X}{\sigma_X}$, $$p_Z(z) = \frac{1}{\sqrt{2\pi}} \exp\left(-\frac{z^2}{2} \right) = N(0,1) \tag{23}$$

CDF is given by $$P_Z(z) = \frac{1}{\sqrt{2\pi}} \int_{-\infty}^{z} \exp\left(-\frac{\xi^2}{2} \right) d\xi = \frac{1}{2}\left\{ 1 + erf\left(\frac{z}{\sqrt{2}} \right) \right\} \tag{24}$$

where $$erf(x) = \frac{2}{\sqrt{\pi}} \int_0^x \exp(-t^2) dt = \frac{2}{\sqrt{\pi}} \left(x - \frac{x^3}{3} + \frac{x^5}{10} - \ldots \right) \tag{25}$$

is the *Gauss error function*.

The *n*-th central moment is $\mu_Z^{(n)} = E[z^{2n}] = \frac{n!}{2^{n/2}(n/2)!} \quad (n = 2,4,\ldots)$ (26)

resulting in $\gamma_Z^{(2)} = \frac{\mu_X^{(4)}}{\sigma_X^4} = 3$, which is so-called “standard” kurtosis or flatness.

When the joint behaviour of two or more variables is of interest, the multivariate normal distribution is most commonly considered. For two variables, a ***bivariate normal distribution*** is given as follows:

$$p_{XY}(x,y) = \frac{1}{2\pi\sigma_X\sigma_Y\sqrt{1-\rho_{XY}^2}} \exp\left\{ -\frac{Z_X^2 + Z_Y^2 - 2\rho_{XY} Z_X Z_Y}{2(1-\rho_{XY}^2)} \right\} \tag{27}$$

where $Z_X = \frac{x - a_X}{\sigma_X}$, $Z_Y = \frac{y - a_Y}{\sigma_Y}$ are standardized variables and $\rho_{XY} = \frac{C_{XY}}{\sigma_X \sigma_Y}$ = the correlation coefficient of *x* and *y*.

More generally, consider *N* random variables, $x_j(k)$ ($k = 1,2,..,N$). These variables may be correlated and their means, variances and covariances are defined by

$$\begin{aligned} a_j &= E[x_j(k)] \qquad \sigma_j^2 = E[(x_j(k) - a_j)^2] = C_{jj} \\ C_{ij} &= E[(x_i(k) - a_i)(x_j(k) - a_j)] \end{aligned} \tag{28}$$

The joint distribution is called an ***N-dimensional normal distribution***, whose density function is

$$p(x_1, x_2, ..., x_N) = \frac{1}{(2\pi)^{N/2}\sqrt{|C|}} \exp\left[\left(\frac{-1}{2|C|}\right)\sum_{i,j=1}^{N} |C_{ij}| (x_i - a_i)(x_j - a_j)\right] \quad (29)$$

where $[C]$ is the covariance matrix of the C_{ij}, $|C|$ is the determinant of $[C]$, and $|C_{ij}|$ is the cofactor of C_{ij} in determinant $|C|$, defined by the determinant of order *N-1*, formed by omitting the *i*-th row and *j*-th column of $[C]$ and multiplied by $(-1)^{i+j}$.

(4) Other normal-related distributions

Chi-square distribution

When Y_n is the sum of n squared independent normal random variables, its distributions are

PDF: $$p_Y(y) = \frac{(y)^{n/2-1}}{2^{n/2}\Gamma(n/2)} \exp\left(-\frac{y}{2}\right) \qquad y \geq 0 \quad (28)$$

CDF: $$P_Y(y) = \frac{\gamma(n/2, y/2)}{\Gamma(n/2)} \quad (29)$$

In the above expression, $\gamma(z,p) = \int_0^p e^{-t} t^{z-1} dt$, where $\mathrm{Re}[z] > 0$, is the *incomplete gamma function*. The mean and variance are n and $2n$, respectively, where $n = 1,2,...$. Is called the degree of freedom.

Rayleigh distribution

This is a distribution of $Y = \sqrt{X_1^2 + X_2^2}$, where both X_1 and X_2 are normal variables. If, for example, X_1 and X_2 are the NS and EW components of wind velocity vector and both of them are normally distributed, Y represents the magnitude of wind speed, regardless of the wind direction, whose distribution is characterised by

PDF: $$p_Y(y) = \frac{y}{\alpha^2} \exp\left(-\frac{y^2}{2\alpha^2}\right) \quad (30)$$

CDF: $$P_Y(> y) = \exp\left(-\frac{y^2}{2\alpha^2}\right) \quad (31)$$

The mean and variance are $a_X = \alpha\sqrt{\frac{\pi}{2}} \approx 1.253\alpha$ and $\sigma_X^2 = \alpha^2\left(2 - \frac{\pi}{2}\right)$. (32)

Weibull distribution

The Rayleigh distribution has only one parameter and sometimes it does not fit the data so well because of the lack of flexibility. The ***Weibull distribution*** tries to cover this deficit as follows:

PDF: $$p_X(x) = \frac{k}{c}\left(\frac{x}{c}\right)^{k-1} \exp\left\{-\left(\frac{x}{c}\right)^k\right\} \tag{33}$$

CDF: $$P_X(>x) = \exp\left\{-\left(\frac{x}{c}\right)^k\right\} \tag{34}$$

The mean and variance are

$$a_X = c\Gamma\left(1+\frac{1}{k}\right) \quad \text{and} \quad \sigma_X^2 = c^2\left\{\Gamma\left(1+\frac{2}{k}\right) - \Gamma^2\left(1+\frac{1}{k}\right)\right\} \tag{35}$$

The Weibull distribution coincides with the Rayleigh distribution when $c = \alpha\sqrt{2}$ and $k = 2$.

Reference:

Benjamin, J.R. & Cornell, C.A., *Probability, Statistics and Decision for Civil Engineers*, McGraw-Hill, 1970.

[Example] Distribution of hourly mean wind speed

The NS and EW components of mean wind velocity vector at any location are expressed by

$$X = U\cos\theta \quad \text{and} \quad Y = U\sin\theta$$

where U = the mean wind speed at this location, regardless of its direction, and θ = the wind azimuth angle taken from North. Unless there are strong topographical reasons, both X and Y are expected to have more or less the normal distribution as follows:

$$p_X(x) = \frac{1}{\sigma_X\sqrt{2\pi}}\exp\left(-\frac{x^2}{2\sigma_X^2}\right) \qquad p_Y(y) = \frac{1}{\sigma_Y\sqrt{2\pi}}\exp\left(-\frac{y^2}{2\sigma_Y^2}\right)$$

The joint probability of U and θ are, by definition, given by

$$p(U,\theta) = p(X,Y)\cdot\frac{\partial(X,Y)}{\partial(U,\theta)}$$

However, since X and Y are statistically independent, $p(X,Y) = p_X(x)p_Y(y)$ and

$$\frac{\partial(X,Y)}{\partial(U,\theta)} = \begin{vmatrix} \cos\theta & -U\sin\theta \\ \sin\theta & U\cos\theta \end{vmatrix} = U$$

Hence

$$p(U,\theta) = \frac{U}{2\pi\sigma_X\sigma_Y}\exp\left\{-\left(\frac{x^2}{2\sigma_X^2}+\frac{y^2}{2\sigma_Y^2}\right)\right\} \approx \frac{U}{2\pi\sigma^2}\exp\left(-\frac{U^2}{2\sigma^2}\right)$$

where $\sigma_X \approx \sigma_Y \approx \sigma\,(\text{const})$ is assumed. The PDF for both U and θ are given by

$$p(U) = p(U, 0 \le \theta < 2\pi) = \frac{U}{\sigma^2}\exp\left(-\frac{U^2}{2\sigma^2}\right) \qquad \sigma_U \approx 0.655\sigma$$

$$p(\theta) = p(0 \le U < \infty, \theta) = \frac{1}{2\pi}\int_0^\infty \frac{U}{\sigma^2}\exp\left(-\frac{U^2}{2\sigma^2}\right)dU = \frac{1}{2\pi}$$

This calculation suggests the Rayleigh distribution $P(U) = \exp\left(-\frac{U^2}{2\sigma^2}\right)$.

However, in reality, the meteorological observation has indicated that better agreement is expected with the Weibull distribution $P(U) = \exp\left\{-\left(\frac{U}{C}\right)^K\right\}$.

2.4 Errors Associated with Spectral Analysis

There are several sources of statistical errors when the procedure involves spectral analyses. Principal causes are a) bias error, b) variance error, and c) aliasing. There are also possibilities of having some intricacies caused by the presence of nonlinearities and non-stationarities in the data (Bendat & Piersol 1986).

<u>Bias error</u>

The ***bias term***, or the error caused by frequency resolution, of the estimated spectral density is, in terms of the normalized error, generally expressed by

$$\varepsilon_B\left[G_x(f)\right] = \frac{B_e^2}{24}G_x''(f) \approx -\frac{B_e^2}{3B_r^2} \tag{1}$$

where B_e = the narrow-band frequency resolution bandwidth for filtering, and B_r = the half-power bandwidth. This error can be decreased by decreasing the frequency resolution, or by increasing the number of points in the Fourier transform.

Variance error

The ***variance error*** is a straight result of estimating each value of an averaged power spectrum. Since the magnitude of each individual power spectral value is random, the average value of them should be also random. The distribution of these values is similar to a χ^2 distribution. The random error, or the standard error, is given by

$$\varepsilon_V\left[G_x(f)\right] = \frac{1}{\sqrt{N}} \tag{2}$$

where $N =$ the number of blocks used in the spectral estimates.

Ailiasing and Nyquist frequency

Ailiasing is a potenial source of error associated with sampling of digital data. Sampling of data is usually performed at equally spaced interval Δt. If Δt is too small, the data will be highly redundant. If, on the other hand, Δt is too far apart, the data cannot recognize the frequency components properly. For example, at least two samples per cycle are required to define a frequency component in the original data. Hence, the highest frequency that can be defined by sampling at a rate of $1/\Delta t$ (Hz) is $f_N = 1/(2\Delta t)$, which is called the ***Nyquist*** (or ***folding***) ***frequency***.

Nyquist frequency is the highest frequency beyond which the signal contents cannot be properly represented by the data in discrete form. Any time signal can be measured usually only for a limited time period. Consequently, the analysed results of the sampled data from the original signal would be different from the expected results for which the whole infinite signal is intended. This difference is called ***leakage***.
The problem caused by the choice of sampling time increment for digitizing the data is called ***aliasing***. In order to reduce these errors, it is considered prudent to low pass the original signal at, or preferably even below, the Nyquist frequency, before analysing.

It is difficult to make a general statement regarding the error caused by non-stationarity and/or non-linearity which could exist in the data. Non-stationarity, for example, almost always exist even in wind-induced structural response, which is often analysed assuming the local stationarity. Some sort of engineering judgement has to be called before the measured data are adopted for analysis.

Leakage

Leakage caused by digitizing can be considered in the following way, too. Suppose there is a continuous time signal $X(t)$ ($-\infty < t < \infty$) and its Fourier transform is defined by $\Psi(f)$ ($-\infty < f < \infty$). The measurement of $X(t)$ can be done only for a limited period ($0 \le t \le T$), which is mathematically equivalent to apply a window function $w(t)$ to the signal as $x(t) = w(t)X(t)$ ($-\infty < t < \infty$) . $w(t)$ is a temporal weighting function defined by

$$w(t) = 1 \quad \text{for} \quad |t| \le T/2$$

and $= 0 \quad \text{for} \quad |t| > T/2$ (3)

Thus the Fourier transform of $x(t)$ is given by the convolution integral

$$\xi(f) = \int_{-\infty}^{\infty} \Psi(\alpha) W(f - \alpha) d\alpha \qquad -\infty < f < \infty \tag{4}$$

where

$$W(f) = \frac{\sin 2\pi f T}{2\pi f} \qquad -\infty < f < \infty \tag{5}$$

is the Fourier transform of $w(t)$. The difference of $\xi(f)$ from $\Psi(f)$ is the leakage.

Reference:

Bendat, J.S. & Piersol, A.G., *Random Data: Analysis & Measurement Procedures*, John Wiley & Sons, 1971/1986.

2.5 Spectral Windows

Spectral windows are weighing functions to be applied in spectral analysis for processing only band-pass filtered data in frequency domain. Windows are applied to obtain smoother spectra so that the physical interpretation of them would become easier. Basic requirements for the windows are: a) the integration of a window function over the whole frequency range should be unity; and b) the window function should be symmetric with respect to zero frequency.

Inverse Fourier transform of the spectral windows are called ***lag windows***, which are the windows in time domain and applicable to the autocorrelation functions.

In general, the sample spectra have a lot of fluctuations and smoothing of data by the use of weighted average is often applied to reduce these fluctuations. A very simple data window in the time domain is to apply the *moving average method*, which is to move the centre point of a window and keep taking the average of data over its width *b*, or

$$f(t) \quad \Rightarrow \quad \bar{f}_b(t) = \frac{1}{b} \int_{t-b/2}^{t+b/2} f(\tau) d\tau \tag{1}$$

Rectangular pulse window $w(t) = 1/b \quad (|t| \le b/2)$ (2)

Since $w(t-\tau) = 1/b \quad \text{for} \quad t - b/2 \le \tau \le t + b/2$
$= 0 \quad \text{otherwise}$

hence

$$\bar{f}_b(t) = \int_{-\infty}^{\infty} f(\tau) w(t-\tau) d\tau \qquad \text{(Convolution)} \tag{3}$$

and its Fourier transform is given by the product $F(f)W(f)$, where $F(f)$ and $W(f)$ are Fourier transform of $f(t)$ and $w(t)$, respectively. $W(f)$ is given by

$$W(f) = \int_{-\infty}^{\infty} w(t)\exp(-i \cdot 2\pi ft)dt = \frac{\sin \pi bf}{\pi bf} = dif(bf) \qquad (4)$$

$dif(x) = \dfrac{\sin \pi x}{\pi x}$ is called the *diffraction function.*

Spectral window Smoothing of spectra themselves can be done by applying a window as

$$\overline{S}(f) = \int_{-\infty}^{\infty} S(g)W(f-g)dg \qquad (5)$$

It is required that $\int_{-\infty}^{\infty} W(f)df = 1$ and $W(f) = W(-f)$ so that the area $\int_{-\infty}^{\infty} S(f)df =$ const.

The shape of the window can be rectangle but there are many other types. However, what matters most is the effective width of the window over which the averaging takes place. It is often defined by

$$B_e = \left\{ \int_{-\infty}^{\infty} W^2(f)df \right\}^{-1} \qquad (6)$$

which is b for the rectangular window. $W(f)$ has its peak value of unity at $f = 0$ and reduces to zero at $f = 1/b$. Hence it is practically a low-pass filter. However, in the range of $f > 1/b$, there are small ups and downs of this function and these fluctuations are called the ***side lobes***.

Filter is a term used for an electronic device or mathematical algorithm to process a data stream by means of separating the frequency components of signals. There are various types of filter functions employed in engineering signal processing including the ***digital filters*** such as Hanning and Hamming windows.

<u>*Hanning Window*</u> When the raw estimate of a power spectral density is given as $G_k(f)$ by applying eq.(22) of **2.2**, where $k = 1,2,...,m$, a smooth estimate of G_k by the use of Hanning window is given as follows:

$$\begin{aligned} \overline{G}_0 &= 0.5 \cdot (G_0 + G_1) \\ \overline{G}_k &= 0.25 \cdot G_{k-1} + 0.50 \cdot G_k + 0.25 \cdot G_{k+1} \qquad k = 1,2,..,m-1 \\ \overline{G}_m &= 0.5 \cdot (G_{m-1} + G_m) \end{aligned} \qquad (7)$$

This window is frequently used before applying a fast Fourier transform to avoid aliasing artifacts. It was developed by Julius von Hann and known widely because of good leakage characteristics such as low peak side-lobe height and a rapid decay rate for side lobes far from the centre lobe.

Hamming Window is another type of digital filter, remembered by the name of R.W. Hamming, and also widely employed. It is defined by the following equation in lieu of eq.(7).

$$\overline{G}_k = 0.23 \cdot G_{k-1} + 0.54 \cdot G_k + 0.23 \cdot G_{k+1} \qquad k = 1,2,..,m-1 \quad (8)$$

2.6 Wavelet Analysis

Wavelet transform is a tool for decomposing a signal into its time- and scale-dependent components, in terms of so-called wavelet coefficients. It is an extended idea from the Fourier transform so that it is more suitable for the analysis of non-stationary data.

Fourier transform is a very versatile tool in signal analysis, but it is not suitable for identifying non-stationary aspects of the signal. For example, since Fourier transform is applied to the entire signal length, the result cannot indicate at what time in the signal a specific frequency existed. It is really a tool for frequency resolution but not for time resolution. It means that if the method is applied to structural health monitoring, the method may recognize damage occurrence, location, or even its severity, but not exactly when the damage happened.
Wavelet transform does not have a single set of basis functions like the Fourier transform, which utilizes only the sine and cosine functions. Instead, wavelet transform has infinite possibility of choosing basis functions. Thus the wavelet analysis provides immediate access to information that can be obscured by other time-frequency methods such as Fourier analysis.

Wavelet transform is basically an extended application of a windowing technique with variable-sized windows. It allows the use of long time intervals where low-frequency information is needed and shorter intervals for high-frequency information.

Wavelet coefficients are calculated by applying a chosen wavelet function to the signal as

$$W_x(a,b) = \frac{1}{\sqrt{|a|}} \int_{-\infty}^{\infty} x(t) \psi^{\bullet}\left(\frac{t-b}{a}\right) dt \qquad (1)$$

Here, $W_x(a,b)$ are wavelet coefficients of the signal $x(t)$, at position (or shift) b and scale a. Scale a is inversely proportional to frequency f. $\psi^{\bullet}$ is the complex conjugate of the wavelet function $\psi(t)$. The inverse transform is expressed as

$$x(t) = \frac{1}{C_\psi} \int_{-\infty}^{\infty} \int_{-\infty}^{\infty} W_x(a,b) \frac{1}{\sqrt{a}} \psi\left(\frac{t-b}{a}\right) \frac{dadb}{a^2} \qquad C_\psi = \int_{-\infty}^{\infty} \frac{|\Psi(\omega)|^2}{|\omega|} d\omega < \infty \qquad (2)$$

C_ψ is called the admissibility constant. $\Psi(\omega)$ is the Fourier transform of $\psi(t)$.

The discrete wavelet transform of discrete time sequence $x(n)$ is defined by

$$C_{j,k} = \frac{1}{2^{j/2}} \sum_n x(n) \psi_{j,k}(n) \quad \text{where} \quad \psi_{j,k}(n) = \frac{1}{2^{j/k}} \psi\left(\frac{n}{2^j} - k\right) \tag{3}$$

in which $\psi(n)$ is the wavelet function and j, k are called the scaling coefficient and shifting coefficient, respectively. $C_{j,k}$ represent the corresponding wavelet coefficients. The inverse transform for this case is given by

$$x(n) = \sum_j \sum_k C_{j,k} \psi_{j,k}(n) \tag{4}$$

References:

Newland, D.E., *An Introduction to Random Vibrations, Spectral & Wavelet Analysis*, Addison Wesley Logman, 1993 (3rd ed.).

Torrence, C. & Compo, G.P., A practical guide to wavelet analysis, *Bull. Am. Meteorological Soc.* (79) 1, 1998, pp.61-78.

Chapter 3 Random Vibrations

General references:

Wirsching, P.H., Paez, T.L. & Ortiz, H., *Random Vibrations: Theory and Practice*, John Wiley & Sons, 1995.
Yang, C.Y., *Random Vibration of Structures*, Wiley, 1986.

3.1 SDOF Systems

When a SDOF system, that is characterized by the frequency response function $H(f)/k$, is subjected to a random excitation $F(t)$, the system's response $x(t)$ is calculated as follows:

Mean response: $$a_X = \frac{a_F}{k} \quad \text{(Static response)} \tag{1}$$

Response spectrum: $$G_X(f) = \frac{|H(f)|^2}{k^2} G_F(f) \tag{2}$$

where $G_F(f) =$ Excitation spectrum (one-sided)

The root-mean square response σ_x is evaluated by the following integration:

$$\sigma_X^2 = \int_0^\infty G_X(f)df = \frac{1}{k^2}\int_0^\infty |H(f)|^2 G_F(f)df \tag{3}$$

The peak response is usually estimated as $$\hat{x} = a_X + g_X \sigma_X \tag{4}$$

where $$g_X = \sqrt{2\log_e \nu T} + \frac{\gamma}{\sqrt{2\log_e \nu T}} \qquad \gamma = 0.5772... \tag{5}$$

is the peak factor. $T =$ the evaluation period, and $\nu =$ the cycling rate, defined by

$$\nu = \frac{1}{\sigma_X}\sqrt{\int_0^\infty f^2 G_X(f)df} \tag{6}$$

[Example] **<u>A random point load F(t) located at *z = a* on an elastic beam</u>**

By the modal analysis, the beam response is expressed as $x(z,t)=\sum_r \phi_r(z)q_r(t)$. Hence the variance of the response is approximately $\sigma_X^2(z)\approx\sum_r \phi_r^2(z)\cdot\overline{q_r^2}$, in which the modal variance is

$$\overline{q_r^2}=\frac{\phi_r^2(a)}{M_r\omega_r^2}\int_0^\infty |H_r(f)|^2 G_F(f)df \tag{7}$$

where $|H_r(f)|^2=\dfrac{1}{(1-\Omega_r^2)^2+(2\varsigma_r\Omega_r)^2}$ and $\Omega_r=\dfrac{\omega}{\omega_r}$.

ω_r and ς_r represent the circular frequency and damping ratio for the *r*-th mode of vibration.

$G_F(f)$ is the power spectral density of the random force $F(t)$. If, for example, the excitation spectrum is given by a *white noise* G_0 ($0<f<\infty$), eq.(7) reduces to the following:

$$\overline{q_r^2}=\frac{\phi_r^2(a)}{M_r\omega_r^2}G_0\cdot\frac{\pi f_r}{4\varsigma_r}=\frac{0.7854 f_r}{K_r\varsigma_r}\cdot\phi_r^2(a)\cdot G_0 \tag{8}$$

If there are more than one loadings, $F(a_j,t)$ ($j=1,2,...,N$), being applied to the system, the response spectrum is given by

$$\overline{q_r^2}=\sum_{i=1}^{N}\sum_{j=1}^{N}\frac{\phi_r(a_i)\phi_r(a_j)}{M_r\omega_r^2}\int_0^\infty |H_r(f)|^2 G_F(a_i,a_j;f)df \tag{9}$$

where , the cross-spectrum $G_F(a_i,a_j;f)$ can be perhaps approximated by

$$G_F(a_i,a_j;f)=\sqrt{G_F(a_i,f)G_F(a_j,f)}\cdot\gamma_F^2(a_i,a_j;f) \tag{10}$$

3.2 Distributed Random Excitation

When an elastic structure is subjected to a distributed random excitation force $F(z,t)$, the response spectrum in *r*-th mode of vibration is, by extending the concept of eq.(9), as follows:

$$\overline{q_r^2} = \frac{1}{M_r \omega_r^2} \int_0^\infty |H_r(f)|^2 \int_L \int_L G_F(z_1, z_2; f) \phi_r(z_1) \phi_r(z_2) dz_1 dz_2 df \qquad (1)$$

For the case of distributed random load on an elastic beam, often $G_F(z, f)$ does not vary with the space coordinate and the cross-correlation can be simplified as

$$G_F(z_i, z_j; f) = G_F(f) \cdot \gamma_F^2(\Delta_{ij}, f) \qquad (2)$$

where $\Delta_{ij} = |z_i - z_j|$ is the distance between z_i and z_j. Then

$$\sigma_X^2(z) \approx \sum_r \frac{\phi_r^2(z)}{M_r \omega_r^2} \int_0^\infty |H_r(f)|^2 |J_r(f)|^2 G_F(f) df \qquad (3)$$

in which

$$|J_r(f)|^2 = \int_L \int_L \gamma_F^2(\Delta_{12}, f) \phi_r(z_1) \phi_r(z_2) dz_1 dz_2 \qquad (4)$$

is called the *joint acceptance function*.

3.3 Extreme Value Analysis

Extreme Value Distributions are the limiting distributions for the extreme values, such as the maxima or minima, of a large collection of random observations. In many civil engineering applications, concern often lies with the largest values of many events. This means that our attention is focussed upon the upper tail of the parent distribution of actual observations. Fisher and Tippett (1928) proved that there are only three forms of extreme value distributions. Extreme value analysis was largely developed and elaborated by Emil J. Gumbel (1891-1966), a German statistician.

(1) <u>Estimation of extremes from the parent distribution</u>

Consider the random variables X_j ($j = 1,2,..,N$) and the maximum of them, $Y = \max[X_j]$. The probability that Y does not exceed a certain value y in n discrete events is expressed by using the cumulative distribution function of the parent population as

$$P_Y(< y) = \{P_X(< y)\}^n \qquad (1)$$

For a large value of y, $P_X(> y)$ is generally very small. Hence

$$1 - P_Y(> y) = \{1 - P_X(> y)\}^n \approx 1 - n \cdot P_X(> y)$$

or

$$P_Y(> y) \approx n \cdot P_X(> y) \qquad (2)$$

[Example] **Annual maximum wind speed**

If $P_Y(>y)$ is the annual maximum of the observed hourly mean wind speed exceeding y, the inverse of it is the *return period* R. The distribution of hourly mean wind is often expressed by Weibull distribution as

$$P_X(>y) = \exp\left\{-\left(\frac{y}{C}\right)^K\right\} \tag{3}$$

Hence, the annual maximum wind can be expressed as

$$y(R) = C\{\log_e(nR)\}^{1/K} \qquad (n \approx 10^3) \tag{4}$$

(2) Type I distribution

Suppose *n* samples are randomly taken from the parent group. The parent size is so large that its distribution will not be influenced by taking samples away. At each sampling, the maximum value of the case is retained while the others are returned to the distribution. The sampled maxima will make their own distribution after repeating this process and the resulted distribution will be increasingly removed from the parent, when n increases. This corresponds to the extreme value distribution.

Fisher and Tippett (1928) proved that there are only three limiting functional forms of extreme value distributions, which are similar with a difference caused by the properties of the upper tail of the parent distribution. Gumbel called them *asymptotes* because they are approached asymptotically when $n \to \infty$.

The first of three, often called the ***Type I distribution***, is derived when the distribution of X is

1) unlimited in the positive direction; and
2) the upper tail falls off in an exponential manner as $P_X(<x) \approx 1 - \exp\{-g(x)\}$, where $g(x)$ is an increasing function of x.

The cumulative function is given by

$$P_{\hat{X}}(<\hat{x}) = \exp[-\exp\{-\alpha(\hat{x}-u)\}] \qquad (-\infty < \hat{x} < \infty) \tag{5}$$

where $u =$ mode, or the most probable value, and $\alpha =$ the dispersion. The density function is

$$p_{\hat{X}}(\hat{x}) = \frac{dP_{\hat{X}}(<\hat{x})}{d\hat{x}} = \alpha\exp[-\alpha(\hat{x}-u) - \exp\{-\alpha(\hat{x}-u)\}] \qquad (-\infty < \hat{x} < \infty) \tag{6}$$

and mean: $a_{\hat{X}} = u + \dfrac{\gamma}{\alpha}$ $\gamma = 0.5772...$ (Euler's const.)

variance: $\sigma_{\hat{X}}^2 = \dfrac{\pi^2}{6\alpha^2}$

Hence, the two parameters can be decided as follows:

$$u = a_{\hat{X}} - \frac{\gamma}{\alpha} \approx a_{\hat{X}} - 0.450\sigma_{\hat{X}} \qquad \frac{1}{\alpha} = \frac{\sqrt{6}}{\pi}\sigma_{\hat{X}} \approx 0.7797\sigma_{\hat{X}} \tag{7}$$

(3) Type II and III distributions

Type II distribution can be applied when the parent distribution of variables is limited on the left at zero, but unlimited to the right in the tail of interest. The probability functions of extremes $\hat{x}$ are then defined by

$$P_{\hat{X}}(<\hat{x}) = \exp\left\{-\left(\frac{u}{\hat{x}}\right)k\right\} \qquad \hat{x} \geq 0 \tag{8}$$

$$p_{\hat{X}}(\hat{x}) = \frac{k}{u}\left(\frac{u}{\hat{x}}\right)^{k+1} \exp\left\{-\left(\frac{u}{\hat{x}}\right)^k\right\} \qquad \hat{x} \geq 0 \tag{9}$$

The j-th moment is given by $E[\hat{x}^j] = \int_{-\infty}^{\infty} \hat{x}^j p_{\hat{X}}(\hat{x})d\hat{x} = u^j \Gamma\left(1 - \dfrac{j}{k}\right)$ (10)

resulting in

$$a_{\hat{X}} = u \cdot \Gamma\left(1 - \frac{1}{k}\right) \qquad k > 1 \tag{11}$$

$$\sigma_{\hat{X}}^2 = u^2 \cdot \left\{\Gamma\left(1 - \frac{2}{k}\right) - \Gamma^2\left(1 - \frac{1}{k}\right)\right\} \qquad k > 2 \tag{12}$$

Note that if X has Type II distribution with parameters u_x and k, $Y = \log_e X$ has the Type I distribution with parameters $u_y = \log_e u_x$ and $\alpha = k$.

Type III distribution is usually applied to a model dealing with smallest values. Assuming the variables as $X \geq 0$, the probability distribution of the minima is actually identical to the Weibull distribution.

(4) Probability of threshold crossing

The expected number of up-crossing the level $x = a$ per unit time, a stationary random process $X(t)$ is expected to make, according to Rice (1945), is given by

$$N_X^+(a) = \int_0^\infty \dot{x} \cdot p(a, \dot{x}) d\dot{x} \tag{13}$$

where $p(x, \dot{x}) =$ the joint probability density function of x and $\dot{x}$. For a Gaussian stationary random process with zero-mean, $p(x, \dot{x}) = p(x)p(\dot{x})$ where the probability density function is given by

$$p_X(x) = \frac{1}{\sqrt{2\pi}\sigma_X} \exp\left(-\frac{x^2}{2\sigma_X^2}\right)$$

Hence $$N_X^+(a) = p_X(a)\int_0^\infty \dot{x} \cdot p(\dot{x}) d\dot{x} = \sqrt{2\pi}\nu\sigma_X \cdot p_X(a) \tag{14}$$

where $$\nu = \frac{1}{2\pi}\frac{\sigma_{\dot{X}}}{\sigma_X} = \frac{1}{\sigma_X}\left\{\int_0^\infty f^2 G_X(f) df\right\}^{1/2} = N_X^+(0) \tag{15}$$

is the zero up-crossing frequency and is called the *cycling rate*, which is often considered as the expected frequency of the process. $G_X(f)$, when the power spectral density is given by $X(t)$.

By substituting (15) into (14), the number of up-crossing can be expressed as

$$N_X^+(a) = \frac{1}{2\pi}\frac{\sigma_{\dot{X}}}{\sigma_X} \exp\left(-\frac{a^2}{2\sigma_X^2}\right) \tag{16}$$

Note that $N_X^+(a)$ decreases when the threshold a goes higher. For a given σ_X, the crossing rate increases as the root-mean-square velocity $\sigma_{\dot{X}}$ increases.

Concept of Narrow-Band Envelope

Experience tells us that, if the process is narrow-band, with the mid-band frequency of f_m, most arrivals occur in clusters approximately one cycle period apart, but there may be a substantial length of time between clusters. The waiting times are obviously not exponentially distributed for this case. For engineering design, we are often interested in the first time crossing and subsequent crossings in the same cluster are less important. To address this situation, Rice introduced the concept of ***envelope function*** $R(t)$. The up-crossing rate of the envelope is obtained in a similar way as before and

$$N_R^+(a) = \sqrt{2\pi}\frac{a}{\sigma_X}\sqrt{\nu^2 - f_m^2} \exp\left(-\frac{a^2}{2\sigma_X^2}\right) \tag{17}$$

Note that the envelope up-crossing is zero if ν and f_m coincide.

References:

Fisher, R.A. & Tippett, L.H.C., Limiting forms of the frequency distribution of the largest or smallest member of a sample, *Proc. Cambridge Phil. Soc.* (24) 1928, pp.180-190.

Gumbel, E.J., *Statistics of Extremes*, Columbia Univ. Press, 1958.

Kotz, S. & Nadarajah, S., *Extreme Value Distributions*, Imperial College Press, 2000.

Rice, S.O., Mathematical analysis of random noise, *Bell Syst. Tech. J.* (23) 1944, pp.282-332 & (24) 1945, pp.46-156; reprinted in Wax, N., *Selected Papers on Noise and Stochastic Processes*, Dover, 1954.

(5) Concept of First-Passage Failure

Basic formulation

Consider a stationary random stress process $S(t)$ and the strength of material defined by $R(t)$. Note that $R(t)$ is generally a deterministic function of time. The up-crossing of $S(t)$ past $R(t)$ in a small time increment Δt forms a point process, whose rate of arrival is described by a Poisson process. Then, it follows that the probability of not having an up-crossing in Δt is

$$P(Y < R) = \exp\left[- N_R^+(t) \cdot \Delta t\right] \tag{18}$$

Considering the service life span of the structure to be T, and $\Delta t = T/k$, where $k \to \infty$ and $\Delta t \to 0$, the probability of not having an up-crossing in T is given by

$$P(Y < R) = \prod_{j=1}^{k} \exp\left[- N_R^+(t_j)\Delta t\right] = \exp\left\{- \sum_{j=1}^{k} N_R^+(t)\Delta t\right\} \to \exp\left\{- \int_0^T N_R^+(t)dt\right\} \tag{19}$$

Hence, the probability of failure is defined by

$$P_f = 1 - \exp\left\{- \int_0^T N_R^+(t)dt\right\} \tag{20}$$

where, if $X(t)$ is a Gaussian process, $N_R^+(t)$ is given by eq.(16) or

$$N_R^+(t) = \nu \cdot \exp\left[-\frac{1}{2}\left\{\frac{R(t) - a_S}{\sigma_S}\right\}^2\right] \tag{21}$$

[Example 1] If R is, and hence N_R^+ is, constant, $p_f \approx N_R^+ T$.

[Example 2] If $X(t)$ is a narrow-band Gaussian process with the central frequency f_m,

since $\nu = f_m$, it results in $p_f \approx f_m T \cdot \exp\left\{-\frac{1}{2}\left(\frac{R-a_S}{\sigma_S}\right)^2\right\}$.

(6) Cycle Counting

The valuable outcomes of the field observation of structural behaviour are usually given as lengthy and irregularly fluctuating time-histories of acceleration, stress, deflection and so on. An absolutely essential matter for engineers then is to reduce a small amount of useful information out of them for fatigue analysis, for example. Counting the number of cycles of the record fluctuation is one of them.

There are various methods to perform this operation, such as counting of peaks, level crossings and ranges, which are defined by the difference between two successive extremes. All of these are called *one parameter methods* whereas two parameter methods called the *rainflow analysis* is known to be a state-of-the-art counting method successfully applied to fatigue analysis. Note that the cycle counting yields amplitude distribution with no regard to frequency information.

Peak counting is a relatively simple method where the local maxima above mean are identified, each maximum is paired with a local minimum of the same magnitude, and thus an equivalent time history is obtained.

Range cycling is a method where the range, defined by the difference between two successive local extremes, is counted as a half cycle

Rainflow cycle counting

The general approach in fatigue life prediction needs to relate a random load fluctuation in real life situation to the Wöhler curves, which are based on laboratory experiments of simple specimens subjected to constant amplitude load. The rainflow cycle counting analysis is a method proposed to overcome this difficulty, first proposed by Endo et al. (1968) and has been developed by many researchers including Downing (1972), Rychlik (1987) etc. and now regarded as a state-of-the-art estimator in fatigue analysis. The basic way of counting can be explained by Fig.3.1, which is a strain time history plotted against time, where the time is vertically downward and the line connecting the strain peaks are imagined to be a series of pagoda roofs, on which rain water drips and falls.

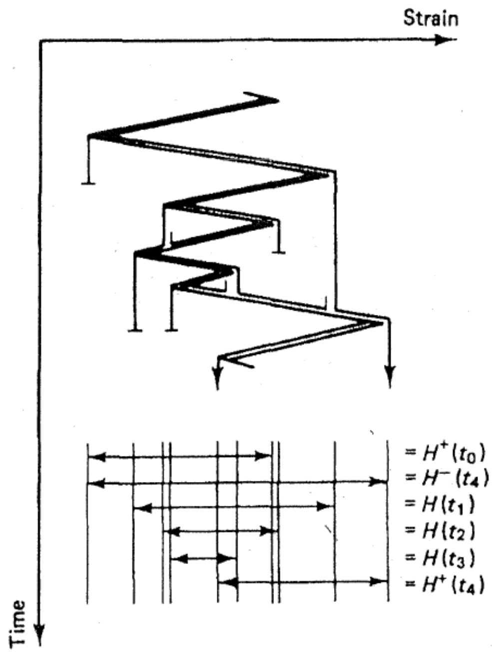

Fig.3.1 (after Rychlik)

Several rules are imposed on defining the half-cycles are counted:

1. Rainflow begins at the inside of each strain peak and strain trough.
2. A rainflow must stop if it meets another flow from the roof above.
3. A rainflow goes on, unless it is stopped, to the tip of the roof and drips down.
4. The rainflow initiating at each trough is allowed to drip down and continue, but stops when it comes opposite to a trough, which is more negative than where it originated.
5. The rainflow initiating at each peak is allowed to drip down and continue, but stops when it comes opposite to a peak, which is more positive than where it originated.

Thus a random time series is now reduced to an equivalent pair of reversals. A counting matrix, as a result, is obtained where the number of occurrences of closed cycles from a certain level of displacement to another is established for convenience of fatigue life prediction.

References:

Downing, S.D. & Socie, D.F., Simple rainflow counting algorithms, *Int. J. Fatigue* (4) 1, 1982, pp.31-40.

Madsen, H.O., Krenk, S. & Lind, N.C., *Methods of Structural Safety*, Prentice-Hall, 1974.

Rychlik, I., A new definition of the rainflow cycle counting method, *Int. J. Fatigue* (9) 2, 1987, pp.119-121.

Veit, R. & Wenzel, H., Measure-data based lifetime estimation of the Europabrücke due to traffic load, *Proc. 11th Int. EG-ICE Workshop*, Weimar, 2004.

3.4 Simulation Techniques

Once the characteristics of a random process, the observed dynamic excitation for example, are identified, it is useful to simulate the process by a mathematical function or a time series for the future prediction of the process. There have been various simulation techniques developed and investigated by many researchers and the followings are typical examples.

(1) <u>Application of Fourier Series</u>

When $x(t)$ is a stationary Gaussian random process with $a_x = 0$, and its power spectral density function is given by $G_x(\omega)$, a sample function of $x(t)$ can be approximately simulated by the following expression:

$$x^d(t) = \sum_{k=1}^{N} \sqrt{2G_x(\omega_k)\Delta\omega} \cdot \cos(\omega_k t + \phi_k) \tag{1}$$

where $\omega_k = \omega_L + \left(k - \frac{1}{2}\right)\Delta\omega \qquad \Delta\omega = \frac{\omega_U - \omega_L}{N} \qquad (k = 1,2,..., N)$

(2)

ω_U and ω_L are the upper and lower bounds of $G_x(\omega)$, the phase angles ϕ_k are randomly produced mutually independent variables with a flat distribution in the range of $0 \le \phi_k < 2\pi$, and N is a sufficiently large integer. For the production of random variables X that follows the cumulative distribution function $P_X(x)$, the Monte Carlo method can be applied.

If the random process to be simulated is non-stationary, such as the case of earthquake waves, the model function can be assumed as $f(t) = g(t) \cdot x(t)$, where $g(t)$ is a known deterministic function of time. For this case, a simulated sample function can be simply expressed by $f^d(t) = g(t) \cdot x^d(t)$.

(2) Application of ARIMA time series

Reference:

Box, G.P. & Jenkins, G.M., *Time Series Analysis: Forecasting and Control*, Holden-Day, 1976.

Chapter 4 Some Notes on Damping

4.1 Nature of Vibration Damping in General

The capacity of structures to dissipate energy imparted by the external forces is one of the most basic knowledge required in the dynamic analysis of buildings, towers, bridges and other civil engineering structures. For built-up structures, energy dissipation may result from various sources. Bleich & Teller [1] listed the following sources:

1. The imperfect elasticity of the structural materials;
2. Plastic yielding and friction due to small relative displacements in the structural joints;
3. Internal friction of the materials such as concrete;
4. Friction in the expansion joints of the floor structure or at the pedestals;
5. Friction at the end bearings of the trusses and girders;
6. Aerodynamic and hydrodynamic damping.

Some other sources can be also considered [8]. For example:

7. The nonlinear structural characteristics such as of cables;
8. Energy dissipation through foundation on the ground and any other substructures;
9. Artificial dampers installed on the structures, etc.

Theoretical approaches are possible to some extent for estimating the damping effects on dynamic behaviour of structures from each origin based on some basic experimental information. Nevertheless, because of the complexity and interactions of these mechanisms, actual measurements for the structures in reality are essentially important for finding the overall damping capacity of compound structures.

4.2 Sources of Damping

Brief discussion on various sources of damping is given below. References such as 6, 12 or 16 can be recommended for further study if there is a need. The magnitude of damping in this article is given as damping ratio (ς), or the fraction of critical.

(1) <u>Material Damping</u>

Intrinsic material damping always exists due to plastic and visco-elastic behaviour of structural materials. This appears in conventional viscous type and the following values, as the damping ratio (ς) or the fraction of critical damping, are generally accepted from a number of experimental results:

Steel	ς = 0.001 to 0.004
Concrete	0.010 to 0.020

Wood	0.020 to 0.025

At increasing stresses, if the limit of proportionality is exceeded, this deviation will cause extra damping. Damping capacity in material can be defined as the ratio of the energy ΔW dissipated on one cycle of oscillation to the maximum amount of energy W accumulated in that cycle (Fig.4.1), or

$$\Delta W = \oint F dx = \int_0^T F \frac{dx}{dt} dt \qquad (1)$$

In case a hysteresis loop occurs because of the material non-linearity as shown in Fig.4.2, the area (A) enclosed by the loop indicates the amount of energy dissipated during each complete cycle.

Note that when the stress is related to the strain and strain rate by

$$\sigma = E'\varepsilon + \frac{E''}{\omega}\frac{d\varepsilon}{dt} \qquad (2)$$

the stress-strain *hysteresis loop* becomes an ellipse as shown in Fig.4.2 and $A = \oint \sigma d\varepsilon$.

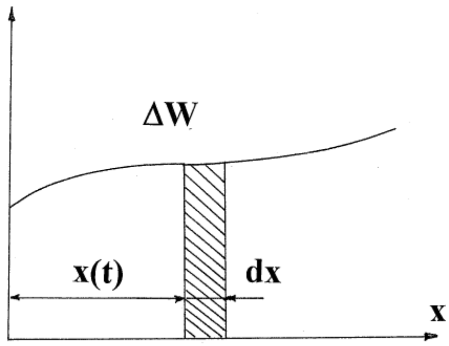

Fig.4.1

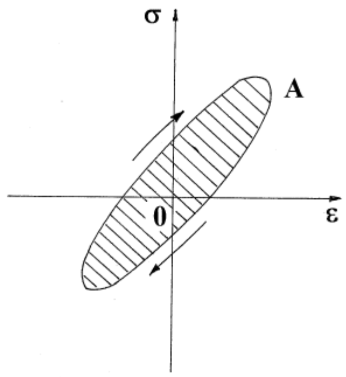

Fig.4.2

There is a group of special metal alloys called ***high damping alloys*** developed to have very high damping characteristics. In these special alloys, the gain in damping is often at the expense of stiffness, strength, durability, corrosion resistance, cost, machinability, or long-term stability and they are usually not suitable for construction purposes. They are often highly nonlinear and temperature sensitive, too. One example is a material called *Sonoston*, which is commercially available [7].

It is worthwhile to mention about the ***composite materials.*** These are combinations of two or more materials in a macroscopically homogeneous level. Fibres of a material may be embedded uniformly in either single or multi-directions or short fibres randomly embedded in a matrix etc. Boron fibres in aluminum or titanium matrix, carbon fibres in epoxy matrix are typical examples.

Often the aim of making composite materials is to increase the stiffness and/or reduce the overall density of the material and the change of damping characteristics is not in its scope. There are disadvantages, too, such as low natural resistance to erosion and impact damages, high costs, difficulty in repairing etc. Damping is not necessarily high but often highly nonlinear.

There are also materials categorized as the ***viscoelastic materials***. Many polymeric and glassy materials exhibit high viscoelastic damping [4,5].

(2) Coulomb Frictional Damping

Significant amount of energy can be dissipated by friction at structural joints, such as bolted, riveted or simply placed with their surfaces contacting each other, between components of the structure, cladding joints, masonry facades, composite floors and so on. The magnitude of damping force for these cases is directly proportional to the coefficient of friction (μ), the unit pressure (P_N) between surfaces and the area of contact (S), or

$$F_f = \mu S P_N \tag{3}$$

Typical values for coefficient of friction are as follows:

brassvs. steel	μ = 0.15
steel vs. steel	0.15
leather vs. steel	0.35
nylon vs. metal	0.30
teflon vs. metal	0.05

In general, the static coefficient tends to be greater than its dynamic counterpart. In case of steady state vibration, the relative velocity becomes equal to zero twice during each cycle and thus the effective coefficient of friction falls between two extremes. The values listed above reflect this condition to an extent.

Free vibration with Coulomb damping is completely damped out at time T_e which is given by

$$\frac{T_e}{T_o} = \frac{y_o k}{4F_f} \tag{4}$$

where T_0 = the natural period of vibration
k = stiffness
y_0 = initial amplitude

(3) Radiation Damping through Foundation

This is due to the propagation of energy away from the structure into the infinite soil mass. The magnitude of radiation damping depends on the soil properties and also on the size of the sub-structure.

Several examples of soil stiffness in terms of an equivalent spring constant (k) and damping ratio (ς) associated with various modes of vibration of a rigid circular footing on an idealized elastic half-space are given as follows [6]:

Vertical	$k_z = \dfrac{4Ga}{1-\nu}$	$\varsigma_z = \dfrac{0.425}{\sqrt{B_z}}$	$B_z = \dfrac{1-\nu}{4}\dfrac{m}{\rho a^3}$	(5a)
Rocking	$k_\phi = \dfrac{8Ga^3}{3(1-\nu)}$	$\varsigma_\phi = \dfrac{0.15}{(1+B_\phi)\sqrt{B_\phi}}$	$B_\phi = \dfrac{3(1-\nu)}{8}\dfrac{I_\phi}{\rho a^5}$	(5b)
Horizontal	$k_x = \dfrac{32(1-\nu)}{7-8\nu}Ga$	$\varsigma_x = \dfrac{0.288}{\sqrt{B_x}}$	$B_x = \dfrac{7-8\nu}{32(1-\nu)}\dfrac{m}{\rho a^3}$	(5c)
Rotational	$k_\theta = \dfrac{16}{3}Ga^3$	$\varsigma_\theta = \dfrac{0.50}{1+2B_\theta}$	$B_\theta = \dfrac{I_\theta}{\rho a^5}$	(5d)

in which m = mass on the half space I = mass moment of inertia on the half space
a = radius of the footing G = shear modulus of the elastic media
ν = Poisson's ratio of the elastic media ρ = density of the elastic media

As an approximation for various other forms of footings, an equivalent radius a of the footing can be taken by equating the actual contact area to πa^2.

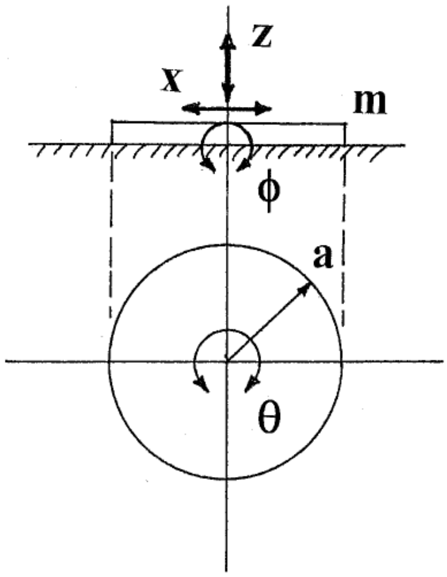

Fig.4.3

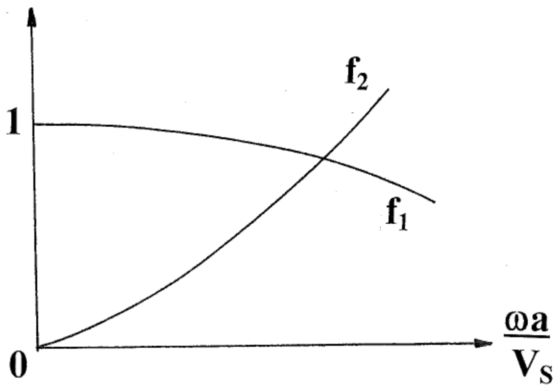

Fig.4.4

However, the dynamic stiffness should be, generally speaking, a function of the excitation frequency. Hence, it is more generally given in the form of a complex function

$$K(\omega) = k[f_1(\omega) + i \cdot f_2(\omega)] \qquad (6)$$

and $C = 1/K$ is called the *dynamic compliance*. f_1 and f_2 are generally given as functions of $\omega a/V_S$ as typically shown in Fig.4.4, where $V_S = \sqrt{G/\rho}$ [3]. Damping ratio is then given by $\varsigma = f_2/2f_1$. There have been a number of studies carried out for the derivation of dynamic stiffness, including radiational damping, in the form of eq.(6) for different forms of footings, pile foundations and effects of embedment. They belong to the category called soil-structure interaction problems. The analytical solutions are often complicated, involving so-called *mixed boundary condition problems*, which can be simplified by assuming the contact pressure distribution under the footing.

It should be noted that the static case corresponds to $\omega \to 0$, resulting in $f_1 \to 1$ and $f_2 \to 0$.

(4) Aerodynamic Damping

The aerodynamic damping is typically caused by a "fan" action of a structure as it moves through wind. The damping in still air is generally negligible whereas it is a big factor for the case of ***Hydrodynamic damping***.

The magnitude of aerodynamic damping is more or less proportional to wind speed but is dependent upon the vibration amplitude, too. It significantly varies with the geometrical shape of the structure. The amount of this damping is often the order of 1% and 5% of critical for buildings and bridges, respectively, but it could be even negative in some instances leading to the aerodynamic instability.

Consider the linear aerodynamic force acting on a SDOF system. The equation of motion is given by

$$m\frac{d^2x}{dt^2} + c\frac{dx}{dt} + kx = \frac{\rho V^2}{2} A \cdot \left(F_R x + F_I \frac{dx}{dt} \right) \qquad (7)$$

or

$$m\frac{d^2x}{dt^2} + \left(c - \frac{\rho V^2 A F_I}{2} \right)\frac{dx}{dt} + \left(k - \frac{\rho V^2 A F_R}{2} \right) x = 0 \qquad (7a)$$

where m, c, k are the mass, damping and stiffness of the system, respectively, A is the area of the body exposed to wind, ρ and V are air density and wind speed, and F_R and F_I are the aero-dynamic force coefficients.

From eq.(7a), if $F_I > 2c/(\rho V^2 A)$, the total damping becomes negative. It means that once the vibration starts of this structure, its amplitude will grow endlessly leading to its destruction. This is a case of aerodynamic instability or *flutter*. Similarly, if $F_R > 2k/(\rho V^2 A)$, the total stiffness becomes negative and the structure becomes unstable and will be also destroyed. This phenomenon is called *divergence*. Generally speaking, F_R and F_I are given as functions of the reduced wind speed

$V_r = V/(f\sqrt{A})$, where f is the frequency of the vibration and, for this case, is likely to be very close to the natural frequency. Generally speaking, aerodynamic force coefficients have to be experimentally obtained. However, when the wind speed is much higher than the moving speed of the body itself, so-called *quasi-steady* assumption can be introduced, which is to say that the aerodynamic forces at any instant depends only upon the instantaneous position of the body at that particular moment and the temporal memory effect or the history of the motion can be ignored. If this assumption is justified, the aerodynamic damping can be given as follows:

lift: $$\varsigma_{z,aero} = \frac{\rho VA}{4m\omega_z}\frac{dC_L}{d\alpha} \quad (8a)$$

drag: $$\varsigma_{x,aero} = \frac{\rho VA}{2m\omega_x}C_D \quad (8b)$$

pitch: $$\varsigma_{\theta,aero} \propto \frac{\rho VA^{3/2}}{4\Theta\omega_\theta}\frac{dC_M}{d\alpha} \quad (8c)$$

where ω_z, ω_x, ω_θ are the natural circular frequencies in lift, drag and pitching motions, respectively, m and Θ are mass and mass moment of inertia of the body, and C_L, C_D, C_M are the coefficients of the aerodynamic lift force, drag force and pitching moment, respectively.

4.3 Artificial Dampers

(1) <u>Concept of Vibration Control</u>

Vibration control can be achieved either by a) reducing the external disturbances applied to the structure, or by b) increasing the damping force to dissipate dynamic energy out of the system. Improvement of aerodynamic performance by choosing and adjusting the geometrical details or adding edge fairings (Fig.4.5), corner vanes and vortex-killers have been often employed to avoid adverse dynamic effects of wind [19]. These are typical of the first category. Base isolation to reduce the seismic response of structures also belongs to this category.

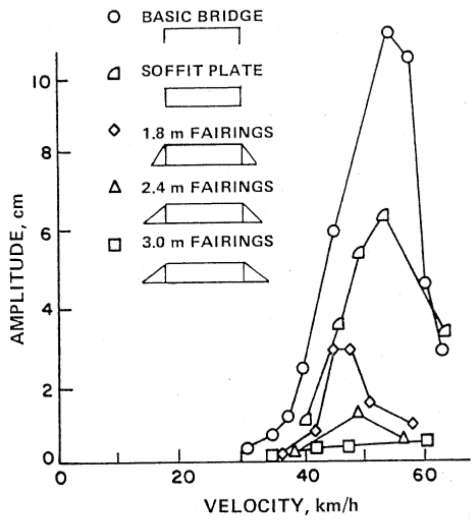

Fig.4.5

It is obviously not possible to completely isolate the structure from the ground motion. However, the idea is to allow having the relative displacement between the base and the ground to an extent so that the transmission of the base excitation from the ground would be reduced (Fig.4.6).

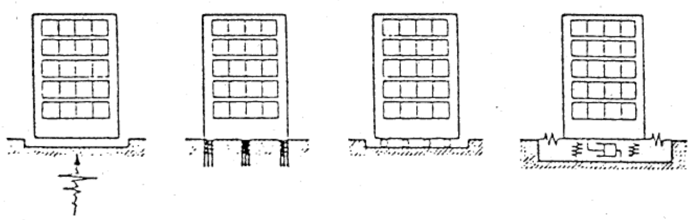

Fig.4.6

At the same time, it is a usual practice to expect some sort of damping with the isolation mechanism so that a part of dynamic energy, which is usually proportional to the relative velocity, could be dissipated. If this is achieved by inserting any damping system with the isolation mechanism, the addition of artificially increased damping belongs to the second category.

More typical of the second category is the installation of the artificial dampers. They can be simply an addition of viscous materials or frictional mechanisms at the movable joints. The World Trade Center Towers, New York, had nearly 10,000 viscoelastic damper elements installed in their frames in each building. Artificial dampers can be also a fairly complicated mechanical system, which may need to be operated by supplying additional energy from outside. The damper system which requires the additional energy for controlling structural vibrations is called an ***active control*** system [16,18]. Gyro-stabilizer, a system to stabilize the rolling motion of a ship by rotating a gyroscope, is an example of active control system. Many of the artificial dampers often listed in references such as shock absorbers, hanging chains, water sloshing basins etc. (Fig.4.7), on the other hand, usually do not require any energy supply from outside. Their action is triggered by the vibration of the primary structure itself and the induced action accordingly works in dissipating energy. This type of damper is called a ***passive control*** system. Tuned mass dampers can be either active or passive.

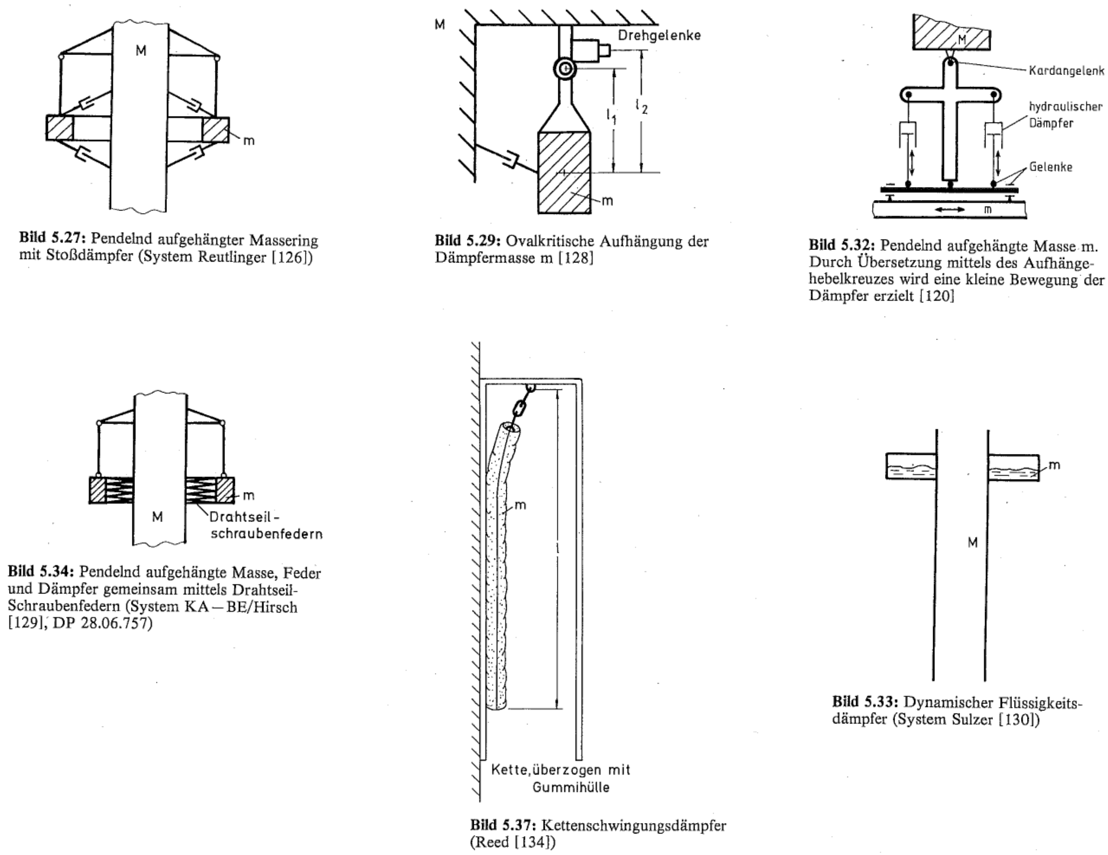

Fig.4.7 Various types of passive dampers (From [11])

(2) <u>Passive Dampers</u>

Simplest kinds of passive control dampers include ***hydraulic shock absorbers*** which are often used for the bridge stay cables and installation of either viscoelastic- or hysteresis-type ***shear dampers*** applied to the building frames to augment seismic resistance capacity. There is also a group of ***impact dampers***. These dampers are not particularly complicated in principle. Rather special dampers worthwhile noting are the tuned mass dampers (TMDs) and liquid sloshing dampers (LSDs). Both of them work on the same mechanical principle which involves an auxiliary vibratory system, using a solid mass (TMD) or liquid mass (LSD).

<u>Tuned Mass Dampers</u>

The idea of the tuned mass damper (TMD) is to have a small auxiliary system of a mass-spring-damper whose natural frequency is tuned to the frequency of the primary system or the structure so that the vibration energy of the primary structure can be absorbed and dissipated by the auxiliary system. The original idea was extensively discussed by Den Hartog [2] for the case of a simple harmonic excitation. In civil engineering applications, however, the excitation forces are usually better defined as a random process with certain band-width and hence the choice of physical parameters for the design of TMDs need to reflect this reality to make them effective.

In the last thirty years or so, TMDs have been applied to some of the major structures including, the Centrepoint Tower, Sydney, the CN Tower, Toronto, the John Hancock Tower, Boston, and the Citicorp Center, New York, and also for stabilizing various structures particularly during erection before the structure has reached its full design stiffness.

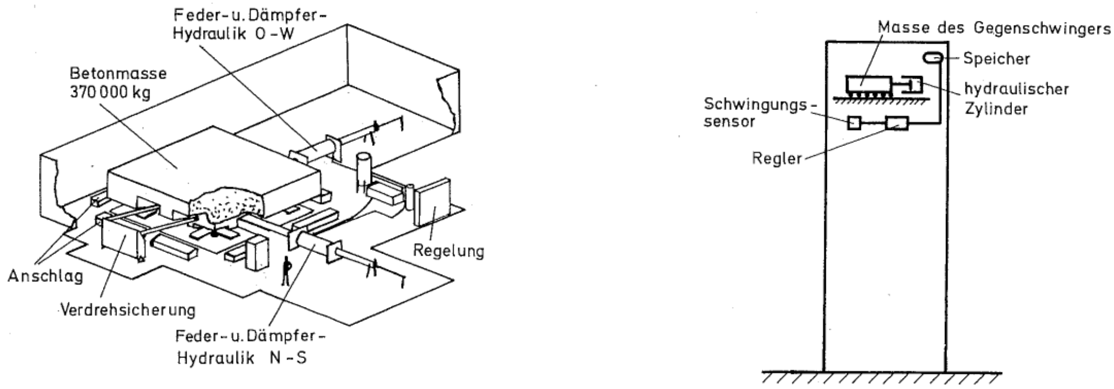

Fig.4.8 Tuned mass damper, the Citycorp Center, New York

Considering the difference in nature of external excitations, the optimized physical parameters for the design of TMDs can be summarized as follows [22]:

Table 4.1 Optimized design parameters for TMDs under various excitations.

	$\beta = \omega_T / \omega_S$	ς_T (Damper's damping)	ς_{eff} (Total damping)	Optimization *
Harmonic Excitation	$\frac{1}{1+\mu}$	$\sqrt{\frac{3}{8}\cdot\frac{\mu}{1+\mu}}$	$\frac{1}{2}\sqrt{\frac{\mu/2}{1+\mu/2}}$	1)
Harmonic Ground motion	$\frac{1}{\sqrt{1+\mu}}$	$\sqrt{\frac{3}{8}\cdot\frac{\mu}{1+\mu/2}}$	$\frac{1}{2}\sqrt{\frac{\mu(1+\mu)}{2}}$	2)
Free vibration	$\frac{1}{1+\mu}$	$\sqrt{\frac{\mu}{1+\mu}}$	$\frac{1}{2}\sqrt{\frac{\mu}{1-\mu/4}}$	3)
Self-excited vibration	$\frac{1}{\sqrt{1+\mu}}$	$\frac{1}{2}\sqrt{\frac{\mu}{1+\mu/2}}$	$\frac{1}{2}\sqrt{\frac{\mu(1+\mu)}{1+\mu/2}}$	4)
Random Excitation	$\frac{\sqrt{1+\mu/2}}{1+\mu}$	$\frac{1}{2}\sqrt{\frac{\mu(1+3\mu/4)}{1+3\mu/2}}$	$\frac{1}{4}\sqrt{\frac{\mu(1+\mu)}{1+3\mu/4}}$	5)

where ω_T = natural circular frequency of the damper

ω_S = natural circular frequency of the structure

ς_T = damping ratio of the damper itself

ς_{eff} = overall modal damping including the effect of the damper

μ = damper mass / modal mass of the structure (<< *1*).

* Optimization for the design of the damper is

1) by maintaining the response as low as possible for any excitation frequencies.
2) by maintaining the response as low as possible for any excitation frequencies.
3) by maximizing the modal damping.
4) by maximizing the acceptable negative damping.
5) by minimizing the root-mean-square response.

There are a few important aspects to be remembered for the application of tuned mass dampers.

TMDs are most effective when structures are under steady excitations since they require some time to transfer vibration energy before they start dissipating it. They are less effective, therefore, under unsteady excitations such as impulsive loading and earthquakes.

TMDs tend to be very effective when its frequency is exactly synchronized. However, a slight deviation in such design parameters could significantly reduce their effectiveness. Since a degree of uncertainty in estimation of natural frequencies, for example, is inevitable, the lack of robust performance is a weakness of this type of dampers.

For many civil engineering structures where the modal mass is quite large, a required auxiliary mass for the damper system may become enormous. Also, in order to have the damper effectively functioning, a large stroke of damper movement may be required. By restricting this stroke, the damper will not be fully effective.

In order to cover these deficiencies, the TMD system designed and installed in the Citicorp Center Building, New York, was made to be an active control system. The damper is essentially a hydraulic servo system which controls the motion of a mass which weighs 400 tons, supported hydrostatically in two mutually perpendicular directions. The damper-system mass is equal to about 1% of the building mass. The spring stiffness is pneumatic and the provided damping is of hydraulic type [10].

Tuned Liquid Dampers

Instead of using a solid mass, liquid can be used in the same concept as TMDs and, for this case, it is called the tuned liquid damper (TLD). For this case, the gravity field provides the restoring force on the water mass which performs sloshing motion in a container and hence it is also called the ***tuned sloshing damper***. TLDs have been used in aerospace industry and for marine vessels for quite some time. The use of liquid could be even more advantageous in the following ways:

- It works even for a very slight disturbance, for which TMDs are sometimes ineffective because of the frictional resistance at its solid surface.
- The damper system itself is not complicated and usually less expensive.
- One damper can be effective for the structural movement in two or more directions.
- Easy to install and easy to relocate.
- Easy to maintain and unlikely to have any aging problems such as fatigue failures.

Just like in TMDs, TLDs also require proper frequency tuning and appropriate choice of damper's own damping to have the system work effectively. There are basically two types of TLDs as follows:

Shallow liquid in a relatively small container [14]:

Energy dissipation is due mainly to surface wave breaking with large vibration amplitude for this case and the synchronization of damper's frequency does not have too much influence on the overall effectiveness. However, with smaller amplitude, damping effect is quite sensitive to the frequency tuning. The nonlinear surface wave theory is known to predict natural frequencies with good accuracy unless wave breaking is involved.

Deep water contained in a large tank [17]:

The motion of water becomes a relatively smooth sloshing, for which Housner's sloshing model can be applied. However, in order to increase damper's damping, various grids, nets and barriers are usually inserted to create turbulence, which also somewhat increases the sloshing frequency. Since theoretical prediction of damping is difficult at any rate, its effectiveness largely relies on experimental evaluation.

Another application of the same principle is TLCD, the ***tuned liquid column damper***, which is basically to have a liquid column such as a U-tube and utilizes it as an auxiliary mass. Its frequency can be controlled by adjusting pressure of air room above water surface and damping is changed by inserting an orifice in the tube.

(3) Active Dampers

Active control of structures has been applied for aircraft and spacecraft for sometime but its application to civil engineering structures has only a short history so far [16,18]. However, considering the fact that they are generally more capable of controlling vibrations with different frequencies and vibration modes compared to the passive type dampers, it can be expected that they would be used more extensively in future [24]. Some of the successful applications so far include the First National City Corporation Building, New York [10], as mentioned earlier, and the Crystal Tower, Osaka [20]. Also, for the last ten years or so, the active vibration dampers have been often applied to control vortex shedding excitation of suspension bridge pylons during erection in Japan. It was found to be particularly advantageous to use active dampers for these cases since the natural frequencies are almost continuously changing and also because it was desirable to install relatively small dampers which are effective in two or more vibration modes simultaneously.

There is another category of active dampers which is to install the aerodynamic active control devices to reduce wind induced motion of buildings and bridges. Mechanically controlled additional flaps are known to be quite effective in controlling the occurrence of flutter instability of wings and streamlined shallow box girders [21].

References

1. Bleich, F. & Teller, L.W., Structural damping in suspension bridges, *Trans. ASCE* (117) 1952, Paper 2486.
2. Den Hartog, J.P., *Mechanical Vibrations*, McGraw-Hill, 1956 (4th ed.).

3. Hsieh, T.K., Foundation vibrations, *Proc. Inst. Civil Engers* (22) 1962, pp.211-226.
4. Oberst, H., Reduction of noise by the use of damping materials, *Trans. Roy. Soc.* (A263) 1968, pp.441-.
5. Grootenhuis, P., Vibration control with viscoelastic materials, *Environmental Engineering, Proc. SEE* (38) 1969.
6. Richart, F.E., Hall, J.R. & Woods, R.D., *Vibrations of Soils and Foundations*, Prentice-Hall, 1970.
7. Jones, D.I.G. & Trapp, W.J., Influence of additive damping on resonance fatigue of structures, *J. Sound & Vibration* (17) 2, 1971, pp.157-185.
8. Van Koten, H., *Damping of building structures*, Report No. BI-74-64, Inst. TNO voor Bouw-materialen en Bouwconstructies, Delft, The Netherlands, 1974.
9. Ayoride, E.O. & Warburton, G.B., Minimizing structural vibrations with absorbers, *Earthquake Engng & Structural Dynamics* (8) 1980, pp.219-236.
10. Petersen, N.R., Design of large scale tuned mass dampers, *Structural Control* (ed. Leipholz, H.H.E.) North-Holland Publ. Co., 1980, pp.581-596.
11. Ruscheweyh, H., *Dynamische Windwirkung an Bauwerken*, Vol.2, Bauverlag, 1982.
12. Nashif, A.D., Jones, D.I.G. & Henderson, J.P., *Vibration Damping*, John Wiley & Sons, 1985.
13. Modi, V.J. & Welt, F., Damping of Wind Induced Oscillations through Liquid Sloshing, *J. Wind Engineering & Industrial Aerodynamics* (30) 1988, pp.85-94.
14. Fujino, Y., Pacheco, B.M. & Sun, L.M., Fundamental study on tuned liquid damper – A new damper for building vibrations, *Proc. Symp on Serviceability of Buildings*, Ottawa, 1988.
15. Blevins, R.D., *Flow-Induced Vibration*, Van Nostrand Reinhold, 1990 (2nd ed.).
16. Soong, T.T., *Active Structural Control: Theory and Practice*, Longman Sci. & Tech., 1990.
17. Ueda, T., Fujiwara, T. & Nakagaki, R., Suppression of wind induced oscillation by tuned sloshing dampers in the free-standing tower of a cable-stayed bridge, *Proc. Int. Symp. for Innovation in Cable-Stayed Bridges*, Fukuoka, 1991, pp.207-216.
18. Hirsch, G.H., Damping measures to control wind-induced vibrations, *Aerodynamics of Large Bridges* (ed. Larsen) Balkema, 1992, pp.1-50.
19. Wardlaw, R.L., The improvement of aerodynamic performance, *ditto.* pp.59-70.
20. Nagase, T. & Hisatoku, T., Tuned-pendulum mass damper installed in the Crystal Tower, *The Structural Design of Tall Buildings* (1) 1992, pp.35-36.
21. Kobaashi, K. & Nagaoka, H., Active control of flutter of a suspension bridge, *J. Wind Engng & Industrial Aerodynamics* (41) 1992, pp.143-153.
22. Fujino, Y. & Abé, M., Design formulas for tuned mass dampers based on a perturbation technique, *Earthquake Engng & Structural Dynamics* (22) 1993, pp.833-854.
23. Korenev, B.G. & Reznikov, L.M., Dynamic Vibration Absorbers: Theory and Tech-nical Applications, John Wiley & Sons, 1993.
24. François, A., De Man, P., Bossens, F. & Preumont, A., State of the art review of MR fluids technology and semi-active control, *CaSCo Workpackage No.1*, 2000.

4.4 Effects of Vibrations on Human Bodies

(1) <u>Human Sensitivity to Motion and Stresses</u>

The motion and mechanical stresses resulting from the exposure of the human body to vibrations can have several different effects such as: a) direct interference with physical activities or functions; b) mechanical damage or destruction; and/or c) secondary effects as changes in organism [1].

***Mechanical Interference*:** Some types of displacement, velocity and/or acceleration are known to be very disturbing to sensory and neuromuscular activities such as reading, speaking and position controls. For example, the disturbance of visual acuity is recognized in certain frequency ranges and is also found to become proportionally serious to vibration amplitude.

***Mechanical Damage*:** Mechanical damage of the human body arises under application of the accelerative forces in the form of either shock or vibration. Among these are bone fracture, lung damage, injury to the inner wall of the intestine, brain injury, cardiac damage, ear damage, tearing or crushing of soft tissues, and some types of chronic injury such as tendon or joint strains and interruption of circulatory system. The response of humans to mechanical vibration is often frequency dependent, particularly at or near the resonant frequency with the visceral organs. It is also likely that there is heating of the body when it is shaken hard.

***Biological Responses*:** Mechanical stresses and motions may stimulate various receptor organs or may excite parts of the nervous system and hormonal activity. These changes are difficult to measure since they can be somewhat subjective, too. Nevertheless, considerable indirect evidence exists for the reality of these response patterns such as fatigue, changes in work capacity, ability to maintain attentiveness etc. Also, there are acute emotional reactions such as fear or unpleasantness which lead to automatic or deliberate compensation or protective behaviour.

(2) <u>Human Tolerance Criteria based on ISO Standard</u>

A general guideline for the evaluation of human exposure to whole-body vibration has been developed as *ISO 2631*. Three different levels of human discomfort are distinguished as follows [2]:

The ***reduced comfort boundary*** applies to tolerable disturbance during ordinary life activities such as eating, reading or writing.

The ***fatigue-decreased proficiency boundary*** gives the level at which recurrent vibrations would cause fatigue to personnel and reduction of efficiency as a consequence.

The ***exposure limit*** defines the maximum vibration tolerable with respect to human health and safety and is much higher than other two.

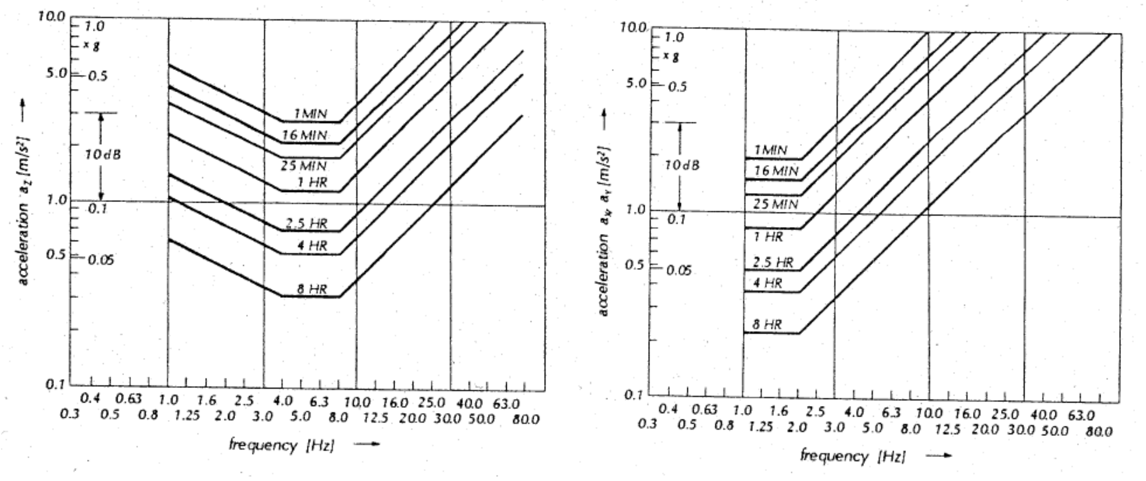

Fig. 4.9

The bounds given in Fig.4.9 are for the *fatigue-decreased proficiency boundaries*. The *exposure limits* are obtained roughly by multiplying by *2* and the *reduced-comfort boundaries* are given approximately by dividing by *3*. These bounds also depend on the direction of incidence to the human body. The reference coordinates are shown in Fig.4.10. The criteria given here are in terms of an effective acceleration, which is the root-mean-square value over the exposure time T.

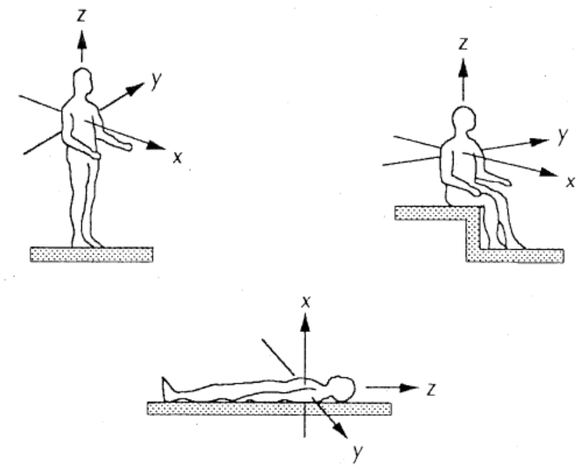

Fig.4.10

(3) Design Criteria for Acceptable Comfort

Obviously the knowledge of physical tolerance or human perception itself does not automatically decide any *acceptance* level applicable to everybody. For example, Melbourne [3] has pointed out that "the least tolerant appear to be those people doing office work, with apartment dwellers seemingly more tolerant and tower-top diners even more." It also depends on visual and auditory cues that heighten occupant awareness. It is the level and frequency of unacceptable motion that is critical to the development of structural design criteria.

In reality, the criteria for body injuries or clear disturbances for physical functions are far beyond our considerations. Needless to say about their safety, the civil engineering structures are expected to serve people without giving any serious discomfort. What is at stake, therefore, is not only an individual's perception but also the resulted state of mind. This is not a very easy condition to define since it is not only a function of acceleration and frequency but also there is a variety of physiological and psychological factors influencing on it. However, the line has to be drawn somewhere.

Influencing factors include the individual's position (moving, standing, sitting or lying), preoccupation and knowledge, existence of any visual or auditory cues, and health conditions on this particular day and so on. There has been a number of early experimental investigations carried out regarding the tolerable peak accelerations for people as functions of frequency [1,4]. Fig.4.11 is a crude summary of them. However, these studies cover only the frequency range down to *1 Hz*. There are not many studies explored the region below *1 Hz* and a good summary of them has been presented by Melbourne [5] and is reproduced in Fig.4.12.

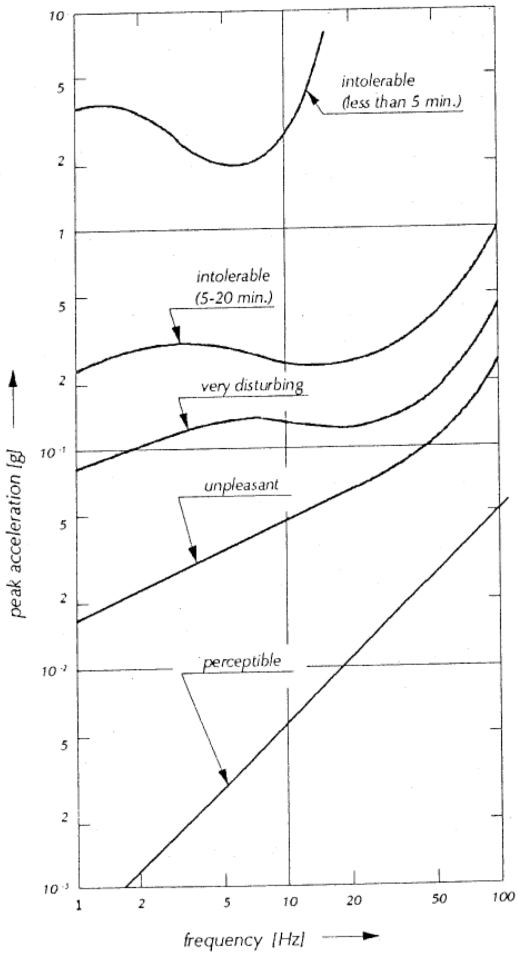

Fig.4.11

Note that the acceleration of Fig.4.12 is given in root-mean-square (rms), which should be multiplied by $\sqrt{2}$ in theory to be compared with peak values of Fig.4.11, since the motions referred to in Fig.4.12 are all presumably sinusoidal. However, Melbourne suggests the use of *2 ~ 2.5* instead as an appropriate factor to be multiplied.

In particular, it is worth noting the results produced by Chen & Robertson [6], which were the work carried out for the design of the World Trade Center Towers, New York. As indicated in Fig.4.12, the results show a substantial range of people's difference in perception – the perception range of the whole population spans about a decade of accelerations. Also the “lower threshold” indicated by Irwin [7] appears to present a good lower limit to motion perception.

Chang [8] has given a similar comparison of results from various sources as shown in Fig.4.13, though the outcome is a little less conclusive. Khan & Parmelee [9], in connection to the design of the John Hancock Center, Chicago, carried out an experimental programme to investigate accelerations on subjects in various body positions and found that the difference between individuals’ perception tends to be more significant than the effects of body positions. It indicates *4 milli-g* for a perception level and *20 milli-g* as a disturbing level for the frequency of *0.13 Hz*, which fit well with others.

Regarding particularly on wind-induced motion of tall buildings, the prediction method of structural response was basically established by the end of 1970s but their acceptability criteria were not yet established then. Reed et al. [10] were probably the first to work on this issue systematically. The study suggested the rms acceleration should not exceed *5 milli-g* for a return period of *6 years* if an office building wants to avoid significant vacancy.

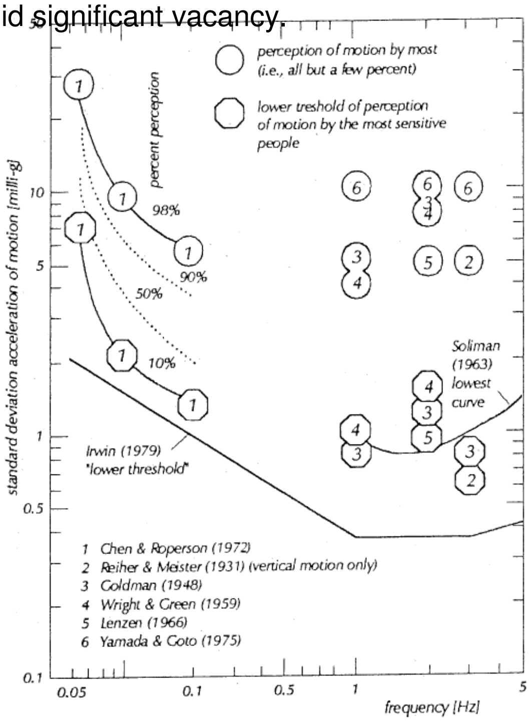

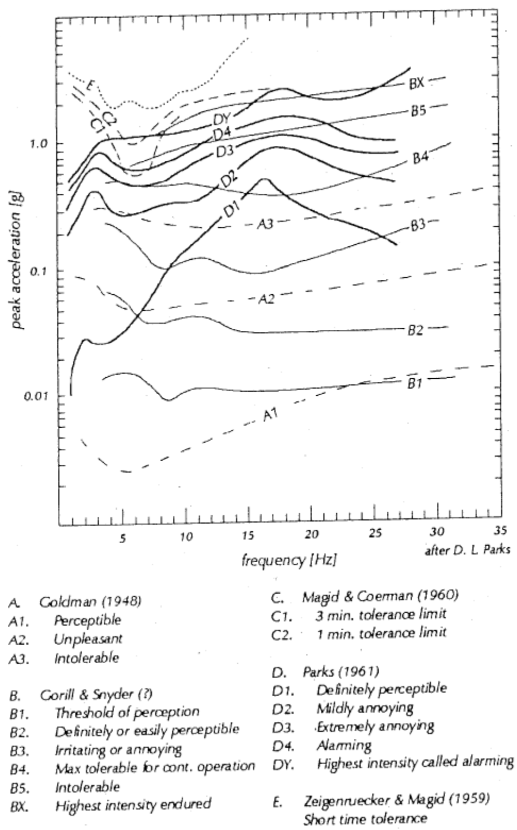

Fig.4.12 (From [4])

Fig.4.13 (From [8])

Based on a number of full-scale observations and experiments, Irwin [6,11] developed a general expression to indicate the level of human occupancy comfort as follows:

$$\sigma_a = \exp(-3.56 - 0.41 \cdot \log_e n) \tag{1}$$

where σ_a = root-mean-square acceleration [m/s^2]
n = frequency with an approximately normal distribution [Hz]

Eq.(1) has been quoted by ISO [12] as a satisfactory magnitude indicating a level of acceleration at which "about *2%* of the occupants will comment adversely". Melbourne [3] further developed the peak acceleration criteria for the return period of less than *10 years* as follows:

$$\hat{a} = \sqrt{2\log_e nT}\left\{0.68 + \sqrt{\log_e R}/5\right\}\exp\left(-3.56 - 0.41 \cdot \log_e n\right) \qquad (2)$$

where $\hat{a}$ = peak acceleration in the horizontal plane [m/s^2]
R = return period [*years*]
T = evaluation period of wind storm
(= *600 s*)

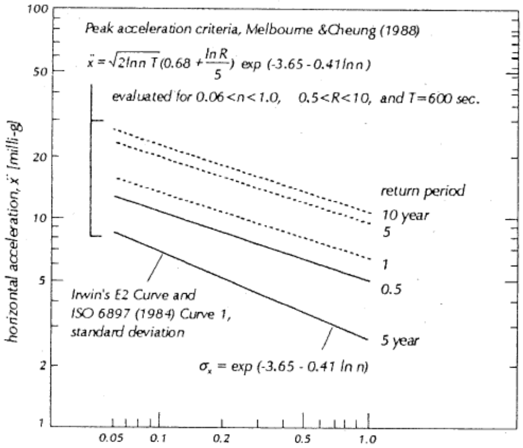

Fig.4.14 (From [13])

Both equations (1) & (2) are presented in Fig.4.14 [13]. Further to these, Isyumov et al. [14] have come up with tentative guidelines as shown in Table 4.2 considering the importance of visual and auditory cues. These guidelines do not recognize the importance of any frequency dependence.

Nevertheless, Melbourne regards [5] that it would at least avoid any building motion perception problems, though admittedly more work is needed to evaluate these effects exactly.

Table 4.2: Tentative guidelines for wind-induced motions in tall buildings [14]

Category of structures	Acceptable hourly peak values	
	Yearly event	10 year event
Peak resultant accelerations (top floor) should be	(*milli-g*)	(*milli-g*)
at or below:	5-7	10-15
Residential	7-9	15-20
Hotels	9-12	20-25
Office		
Peak torsional velocity (top floor) should be at or below:	(*milli-g*)	(*milli-g*)
All	1.5	3.0

References

1. Harris, C.M. & Crede, C.E., *Shock and Vibration Handbook*, McGraw-Hill, 1976 (2nd ed).
2. International Standard Organization, *Guide for evaluation of human exposure to whole-body vibration*, ISO 2631, 1980.

3. Melbourne, W.H. & Cheung, J.C.K.C., Designing for serviceable accelerations in tall buildings, *Proc. 4th Int. Conf. on Tall Buildings*, Hong Kong & Shanghai, 1988, pp.148-155.
4. Wiss, F. & Parmelee, R.A., Human perception of transient vibrations, *J. Structural Div., ASCE* (100) ST4, 1974, pp.773-787.
5. Melbourne, W.H., Comfort criteria for wind-induced motion in structures, *Structural Engineering International* (8) 1, 1998, pp.40-44.
6. Chen, P.W. & Robertson, L.E., Human perception thresholds of horizontal motion, *J. Structural Div., ASCE* (98) ST8, 1973, pp.1681-1695.
7. Irwin, P.A., Human response to dynamic motion of structures, *The Structural Engineer* (9) 56A, 1979, pp.237-244.
8. Chang, F.K., Human response to motions in tall buildings, *J. Structural Div., ASCE* (98) ST6, 1973, pp.1259-1272.
9. Khan, F.R. & Parmelee, R.A., Service criteria for tall buildings for wind loading, *Proc. 3rd Int. Conf. Wind Effects on Bldgs & Structures*, Tokyo, 1971, pp.401-408.
10. Hansen, R.J., Reed, J.W. & Vannarcke, E.H., Human response to wind-induced motion of buildings, *J. Structural Div., ASCE* (99) ST7, 1974, pp.1589-1605.
11. Irwin, P.A., Motion in tall buildings, *Proc. Conf. on Tall Bldgs & Urban Habitat*, Chicago, 1986, pp.759-778.
12. International Standard Organization, *Guidelines for the evaluation of the response occupants of fixed structures, especially buildings and off-shore structures, to low frequency horizontal motion (0.063 to 1 Hz)*, ISO 6897, 1984.
13. Melbourne, W.H. & Palmer, T.R., Accelerations and comfort criteria for building undergoing comply motions, *J. Wind Engng & Industrial Aerodynamics* (41) 1992, pp.105-116.
14. Isyumov, N., Motion perception tolerance and mitigation, *Proc. 5th World Congress of Council on Tall Bldgs & Urban Habitat*, Amsterdam, 1995.

4.5 Other Socio-Economic Impacts

(1) <u>Production-Quality Criteria</u>

The acceptance criteria for vibrations of civil engineering structures need to be looked at from various aspects. First of all, the structure should not collapse and must maintain its structural integrity so that it does not lose its serviceability. Second, even if the structure is safe and able to serve, if it produces any discomfort to the customers and/or causes any mechanical problems such as overstressing, malfunctioning or misalignment, it is not acceptable. Third, even if there is no immediate problem, any troubles in future such as structural fatigue damage, possibly even compound with material corrosion, must be carefully avoided.

The acceptance criteria for structural vibrations therefore need to be established in three categories: a) structural criteria; b) physiological criteria; and c) production-quality criteria. The criteria related to human tolerance and perception described in the previous section correspond to the second category. For industrial or scientific work in particular, more purpose-oriented criteria need to be established and this is the reason of the third category. However, in reality, there cannot be any universally acceptable criteria in this aspect.

There are number of national and international codes and recommendations in literature, such as *ISO 2372 & 2373* (1974). However, it is difficult to come up with a unified regulation out of them. Specific data on individual types of machinery are also available in references such as [1,2]. Acceptance criteria particularly in relation to the use of machinery and equipment developed by Korenev & Rabinovič (1980) has been listed by Bachmann & Ammann [3] and reproduced in Table 6.1 below as an example.

Table 4.3: Acceptance criteria for the use of machinery and equipment.

Category of apparatus	Peak acceleration (*mm/s²*) Freq. range: *1 ~ 10 Hz*	Max. velocity (*mm/s*) Freq. range: *10 ~ 100 Hz*
I (Highly sensitive optical instruments, Mechanical measuring instruments etc.)	*6.3*	*0.1*
II (Normally sensitive machinery for Grinding, milling etc.)	*63*	*1*
III (Little sensitive machinery for metal-Working to usual precision)	*250*	*4*
IV (Insensitive machinery such as blowers, Vibratory machines etc.)	*>250*	*>4*

(2) Structural Aspects

Structural criteria need to be considered with several different levels of consequences in mind. They are

a) The level of damages which could accumulate to eventual fatigue failure;
b) Development of permanent damages such as plastic deformations and cracks;
c) Serious damages to make the structure unserviceable; and
d) Collapse of the structure.

Bachmann & Ammann [3] list the following parameters as the elements to be counted for structural criteria:

a) Type and quality of the structural materials, ductility in particular;
b) Type of construction;
c) Properties of the foundation;
d) Main dimensions of the principal load-bearing members;
e) Age of the structure;
f) Duration of the vibration effects; and
g) Characteristics of vibration, namely frequency, amplitude and damping.

There are no standard criteria which can be uniformly applied over the world. The proposed draft of ISO Standard [4], for example, divides the structures into four different categories and gives the criteria to be considered in the form of pseudo-spectra, or the response velocity versus frequency. Fig.4.15, for example, shows the criteria for vibration limits for structures subjected to blasting, adopted by U.S. Bureau of Mines [5]. The diagram shows simultaneous values of displacement, velocity and acceleration and the limiting condition for each of these quantities forms an envelope on this diagram. Points falling above this envelope violate the failure conditions. Two shaded zones describe the possibility of structural damage, particularly to walls for this case, which may be caused by steady-state vibrations.

Another chart showing the safety limits of structural vibration (Fig.4.16) for the frequency range of up to *50 Hz* is quoted from [6]. It should be noted that the vibration limits are often given in terms of velocity but it is more appropriate to give it in accelerations when the structures are in higher frequency range.

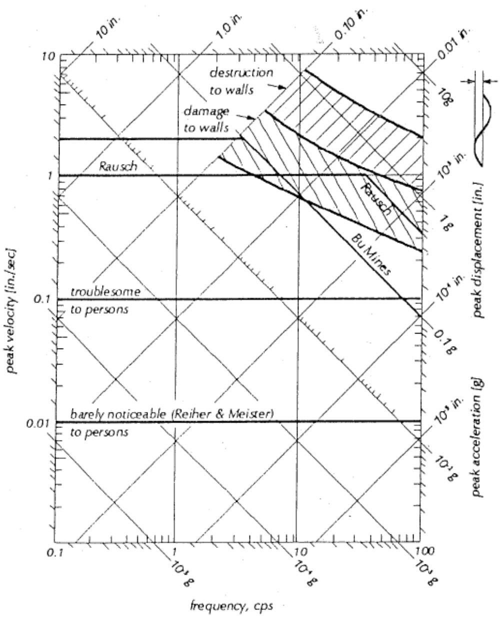

Fig.4.15 (From [5])

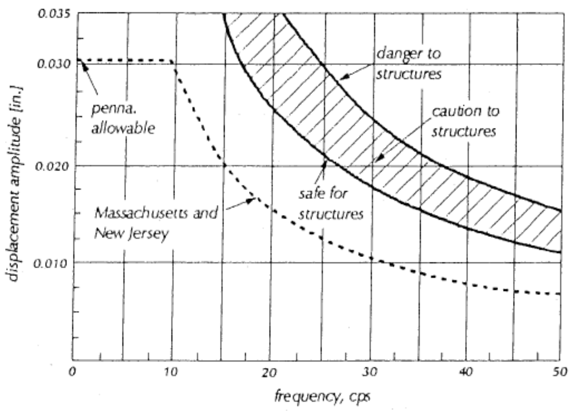

Fig.4.16 (From [6])

(3) More Contemporary Criteria

Bachmann & Ammann [3] has made a concise survey of various regulations and codes of practice regarding the structural criteria. German and Swiss codes, as typical examples, are as follows:

Standard DIN 4150 (1983)

Structural Category	Peak velocity limits	
	Frequency range (*Hz*)	Velocity (*mm/s*)
Industrial buildings	$f \le 10$	20
Residential buildings	$10 < f \le 50$	$15 + f/2$
Vulnerable buildings	$50 < f \le 100$	$30 + f/5$

Standard SN 640312 (1978)

Structural Category	Machinery / Traffic loads		Blasting load	
	Frequency (Hz)	Velocity limits (m/s)	Frequency (Hz)	Velocity limits (m/s)
I (Industrial structures)	$10 \rightarrow 30$ $30 \rightarrow 60$	12 $12 \rightarrow 18$	$10 \rightarrow 60$ $60 \rightarrow 90$	30 $30 \rightarrow 40$
II	$10 \rightarrow 30$ $30 \rightarrow 60$	8 $8 \rightarrow 12$	$10 \rightarrow 60$ $60 \rightarrow 90$	18 $18 \rightarrow 25$
III	$10 \rightarrow 30$ $30 \rightarrow 60$	5 $5 \rightarrow 8$	$10 \rightarrow 60$ $60 \rightarrow 90$	12 $12 \rightarrow 18$
IV (Vulnerable buildings)	$10 \rightarrow 30$ $30 \rightarrow 60$	3 $3 \rightarrow 5$	$10 \rightarrow 60$ $60 \rightarrow 90$	8 $8 \rightarrow 12$

(4) <u>Overall Acceptance Levels</u>

Having reviewed various existing criteria, Bachmann & Ammann [3] suggest the overall acceptance levels as follows:

Table 4.4: Overall acceptance levels as structural criteria (From [3])

Structures	Acceptance level	Comments
Pedestrian structures	$a \leq 5\text{~}10$ % g	Normally the lower value does not produce discomfort.
Office buildings	$a \leq 2$ % g	DIN and BS may yield quite different values.
Gymnasia (Sports halls)	$a \leq 5\text{~}10\ \%\ g$	The higher value recommended only if • Acoustic effect is small, and • Only participants are on or near the vibrating floor.
Dancing and concert halls	$a \leq 5\text{~}10$ % g	The same as for gymnasia.
Factory floors	$v \leq 10$ mm/s	Stricter bounds required for high-quality production factories.

There are some examples appended to this table including footbridges and some public buildings. As it is clearly stated in the book [3], their intention was to provide with a “crude but simple global criteria”, which of course should be applied with caution but is quite helpful particularly for provisional studies.

Fig.4.17 is a tentative proposal as an overall summary of the present study. Generally speaking, the discomfort criteria are much stricter than the structural criteria and hence become more critical for structural design purposes. The discomfort criteria presented in Fig.4.17 approximately corresponds to the curve *Unpleasant* in Fig.5.3, the peak acceleration criteria for *R = 5 years* in Fig.5.6 and about the middle line of the *Chen & Robertson bounds* for the lower frequency range. It is only a crude indicator, of course, and cannot be applied blindly to all structures. Care should be taken when the required services of the structure are particularly sensitive to the environmental tranquility since the production-quality criteria listed in **(1)** are not considered for Fig.4.17.

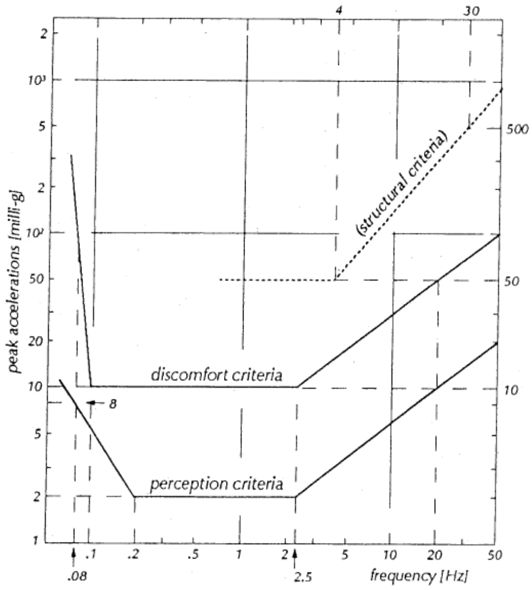

Fig.4.17

References

1. Major, A., *Dynamics in Civil Engineering: Analysis and Design*, Akademial Klado, Budapest, 1980.
2. Harris, C.M. & Crede, C.E. (ed.), *Shock and Vibration Handbook*, McGraw-Hill, 1976 (2nd ed).
3. Bachmann, H. & Ammann, W., *Vibrations in Structures*, Structural Engineering Documents 3e, IABSE, 1987.
4. International Standard Organization, *Mechanical vibrations and shock measurement and evaluation of vibration effects on buildings*, ISO/DIS 4866, 1984.
5. Richart, F.E., Hall, J.R. & Woods, R.D., *Vibrations of Soils and Foundations*, Prentice-Hall, 1970.
6. Leet, L.D., *Vibrations from Blasting Rocks*, Harvard Univ. Press, 1960.

PART III WIND INDUCED VIBRATION OF BRIDGES

Chapter 1 General Background

1.1 Early History of Bridge Aerodynamics

On this topic, what many people would have in mind immediately is the collapse of infamous Tacoma Narrows suspension bridge, which took place 65 years ago. All of the large bridges, long-span cable-supported bridges in particular, designed and built since then have been more or less haunted by the memory of Tacoma. Meanwhile there has been a remarkable technical progress both in experimental mechanics and analytical means on the subject. A brief review of its history is attempted here. Attention is also focused upon finding out what are still left as the problems to be addressed.

(1) <u>Static action of wind</u>

Wind has been an important factor since ancient time for the design of house buildings and town planning. However, it was only in the 18th century, the wind force was first considered in a more scientific way in relation to the structural design. John Smeaton, known as the first Civil Engineer in England, presented the *Table of Wind Forces* to the Royal Society of London in 1759. The Smeaton's table was ahead of times and, despite of its good quality, its significance was not much appreciated by engineers in general of his days or even a century later. In the 19th century, when wrought iron became a popular new material, the size of structures grew to an extent so that wind force on them became a more serious issue. The failure of the Firth of Tay Bridge in 1879 left a great scar in engineers' mind regarding the recognition of wind load. Clearly, this was a turning point in the history of bridge aerodynamics.

(2) <u>Failure of the first Tacoma Narrows</u>

The second turning point in the history of bridge aerodynamics was the collapse of the Tacoma Narrows Bridge in 1940. With the centre span of 854 *m*, Tacoma was one of the largest bridges of the day. The bridge was designed for the lateral wind load of 2.4 *kPa*, which is equivalent to roughly 50 *m/s* of wind speed. What happened in reality, however, was that the bridge kept vibrating in vertical bending modes in much lighter wind, even during its construction. On November 7, 1940, the usual bending vibration suddenly changed to a violent motion in torsion and the bridge collapsed at the wind of less than 20 *m/s*. It was not a matter of static wind load but a matter of dynamic instability.

It is fair to state that no bridge before Tacoma was designed specifically against the dynamic action of wind. It is not to say that no bridge had collapsed due to dynamic action of wind. In the gale of November 30, 1836, one of the four 78 m spans of the

Brighton Chain Pier in England collapsed. A report of this incident included remarkable llustration of severe torsional motion and ultimate deck failure. One would be surprised to see a striking resemblance between these sketches and photographs of the Tacoma failure, which took place a century later.

(3) <u>Application of Deflection Theory</u>

In fact, the progress of modern suspension bridges throughout the first 200 years of history was a continuous struggle against wind action. Many of the major suspension bridges constructed in the 19th century, the Menai Straits Bridge by Thomas Telford to start with, were either destroyed or severely damaged by wind. John Röbling was one of the successful engineers who managed to overcome this difficulty by adding a heavy girder and numerous stay cables to ensure high overall rigidity of the structure. The Niagara Railway Bridge (1855) and the Brooklyn Bridge (1883) were his monumental achievements.

The challenge of bridge building is often indicated by its span length. It is interesting to observe how the maximum bridge span length developed in the last 200 years. Most of them were achieved by suspension bridges. A rather sudden increase of maximum span length appeared in early 1930's, supported by the application of the *deflection theory*. When Prof. Melan developed a new theory taking the bridge deck deflection into stress analysis, his idea was perhaps simply to carry out more exact stress calculation. However, once this was applied to the design of suspension bridges, its interpretation could have been quite different: "*The more flexible the stiffening girder is, the less stress it has to carry*".

Faithful application of this philosophy to an extreme end in rather simplistic philosophy led to the design of the George Washington Bridge (1931), which practically had no stiffening girder at all. This was the first bridge with a clear span of over 1000 meters. The achievement of Golden Gate (1937) was possible only with this philosophy. Emergence of suspension bridges with plate girder stiffening such as Bronx-Whitestone (1939) and Tacoma (1940) was also along the same line. At this point, at the same time, a precious teaching of Röbling on the "stability due to heavy weight" was not paid much respect. The unfortunate incident of Tacoma thus happened.

There has been another very rapid development of maximum bridge span in recent years. This has been made possible by many factors but what should be emphasized in particular are the progress of high-strength steels and welding techniques together with the development of electronic computers and calculation techniques. At the same time, the number of engineers working for the design and construction of these bridges is no comparison to a half century ago.

1.2 General Characteristics of Wind Induced Bridge Vibration

There are various types of wind-induced dynamic response of bridges. They have been revealed through difficult experience, measurements and experimental investigations. The difference of response is caused by different mechanism of aerodynamic action or its interaction with the structure and it very much depends upon the types of structures, too. They can be classified typically as shown in Table 1.

Table 1 – Various types of wind induced structural response

Types of response			***Examples***
Static behaviour	Lateral deflection / Lateral buckling		Suspension bridges
	Overturning		Towers, Tall buildings
	Negative pressure		Flat roofs, Window panes
	Instability	Buckling	Shell structures
		Divergence	Light beams
Dynamic response	Buffeting		Tall buildings, Bridge decks
	Vortex excitation		Chimneys, Bridge decks
	Instability	Galloping	Ice-covered cables
		Instability in torsion	Bridge decks
		Flutter	Aerofoils

Listed examples are not necessarily of bridge structures. The difference between three types of dynamic response is of particular importance. They can be identified in two different ways: one is in terms of response curve which is the change in magnitude of response amplitude versus wind speed, and another is the dynamic characteristics. Effects of damping can be clearly indicated in the former way whereas the statistical treatment of the latter, the spectral analysis, is generally most informative.

1.3 Development of Bridge Aerodynamics

(1) <u>After Tacoma till now</u>

Immediately following the collapse of Tacoma, an intensive investigation into the aerodynamic stability of suspension bridges was initiated by Farquharson in U.S.A., later joined by von Kármán and Vincent. Their pioneering activities using bridge models in wind tunnels were not only productive, including the reconstruction of the more successful second Tacoma Narrows Bridge and improved aerodynamic performance of other major bridges such as Golden Gate, George Washington and Bronx-Whitestone, but also became a precedent for many other research activities on wind resistant design of large suspension bridges all over the world. Somewhat similar activities were carried out by Frazer, Scruton and others in U.K., aiming at the building of Severn and Forth crossings after WW II.

In this early period, the most important matter was not to repeat the same mistake as the old Tacoma. Naturally, the emphasis was placed on finding out the *critical wind speed* where the dynamic instability may occur for a given deck cross-section and to make sure that this critical threshold is higher than the anticipated wind speed in design.

There were theoretical analyses, too, including the application of flutter theory by Bleich (1949), lateral buckling analysis by Hirai (1947), buffeting analysis by Davenport (1958) etc. Theoretical analyses would naturally require the knowledge of aerodynamic forces on bridge decks. There has been a significant development of measuring techniques associated with these activities. Rapid development of electronic computers and computing technology is very much hand-in-hand with them for more sophisticated analyses. Application of statistical reliability theory is also a significant development in this field.

(2) Simulation of natural wind

Wind tunnels were originally developed by civil engineers at the end of the 19th century. However, following the successful flight experience by Wright Brothers, it became a major experimental tool particularly in the field of aeronautics. In the post-war era, when civil engineers started using wind tunnels, naturally they tested bridge models in conventional aeronautical wind tunnels with idealized uniform smooth air flow rather than with simulated natural wind. It was a contribution of Danish engineers, Nøkkentved and Jensen, who brought in the concept of simulating natural wind, that is necessary in order to properly reproduce wind induced response in model tests.

Following Jensen's pioneering work (1958), Davenport in Canada further developed the concept of the boundary layer wind tunnel in the 1960′s. Davenport applied a large scale simulation of strong natural wind to many major structures including the World Trade Center Towers, N.Y., Sears Building, Chicago, and CN Tower, Toronto. Bridges were not exceptions. The Thomas MacKay suspension bridge in Halifax, Nova Scotia, was probably the first bridge that was tested in properly scaled turbulent boundary layer wind, including its deck construction stage.

1.4 Recent Trend in Bridge Aerodynamics

It is probably acceptable to state now that bridges can be designed without repeating the problem of the old Tacome Narrows. However, the bridge engineers today have their own issues to deal with, where the focal points of Bridge Aerodynamics have somewhat shifted from before.
One of the most remarkable developments in long-span bridges in the last four decades or so is the fact that cable-stayed bridges are becoming more competitive in their span length with classical suspension bridges, while the latter have also increased the maximum span length drastically. When the span is increased, naturally the wind stability becomes a more serious issue. This is not only for the completed bridges but also, if not more so, through their erection stages.
General trend in the field of Bridge Aerodynamics in recent years include the following topics:

a) Security of serviceability conditions – the engineering attention is not only for ensuring the survival of the bridge as a structure but also the consideration of better serviceability of the structure as a part of the social infrastructure, including the safety for transportation and prevention of long-term problems such as fatigue damages.

b) Aerodynamics of bridges during erection – conditions during construction are found generally less favourable and yet this issue has been traditionally less focussed in research. It includes the consideration of rational design conditions and vibration control measures.

c) Another focal point of wind study for bridges is a dynamic problem of structural members, cables in particular. There have been a number of reports on stay-cable vibrations. Cables are extremely flexible and their structural damping is generally very low compared to other structural components. They are, as a result, much more vulnerable to dynamic wind actions. Accumulated structural damage due to vibration needs to be identified and properly looked after, too.

d) Advances in cost-effective design tend to impose more stringent requirements not only for qualitative but also for quantitative wind study results. It is also preferable to have response predictions not only conservatively for design purposes but as realistic as possible so that they make better comparison with the full-scale observations.

e) Contemporary research topics include:

   Comparative benchmark study of various wind tunnel testing methods;
   Full scale measurement and verification of predictions;
   Numerical simulation of wind for response calculation in time domain, including the question regarding the applicability of computational fluid dynamics;
   Identification of flutter derivatives for commonly used road deck configurations and effects of turbulence on them;
   Refinement of buffeting theory for more accurate response prediction;
   Consideration of wind yaw angles;
   Dynamics of cables, particularly on galloping of inclined stay cables;
   Fundamental mechanism of vortex induced oscillations;
   Further development of vibration control methods, etc..

References:

Larsen, A. (ed.) *Aerodynamics of Large Bridges*, Balkema, 1992.
Larsen, A. & Esdahl, S. (ed.) *Bridge Aerodynamics*, Balkema, 1998.
Miyata, T. et al. (ed.) *Long-Span Bridges and Aerodynamics, Sprinter*, 1999.
Paxton, R. (ed.), *100 Yrs of the Forth Bridge*, Thomas Telford, 1990.
Scott, R., *In the Wake of Tacoma*, ASCE Press, 2001.
Steinman, D.B. & Watson, S.R., *Bridges and Their Builders*, Dover, 1957.
Wyatt, T.A. et al. (ed.) *Bridge Aerodynamics*, Thomas Telford, 1981.

Chapter 2 Formulation of Aerodynamic Forces

2.1 Definition of Force Components

When a three-dimensional (3D) structure is exposed to an air flow, three force components, the lift, drag and side forces, and three moment components, the pitching, yawing and rolling moments, can be generally considered. However, in many wind engineering problems, it is not necessary to consider all six of these components, and a two-dimensional (2D) alternative is considered as a convenient mathematical model.

The strip theory assumption, originally introduced for aerofoils, is usually the method applied for bridges. Since a bridge is usually extended in one direction along its span and our primary concern is its behaviour when wind comes perpendicular to the span axis, instead of looking at the whole structure, often a 2D slice (or strip) of unit bridge length, cut off by two planes in the mean wind direction, is to be considered. The idea is the same as the plane strain analysis in the 2D theory of elasticity.

For this case, there are only three components needed to be considered; lift force, drag force and pitching moment, since each spanwise station is considered as though it were a portion of an infinite span bridge with uniform spanwise properties. Corresponding to these, the displacements taken into consideration are (h, p, α) in the lift, drag and pitching directions, respectively. In the following section, only these three directions are counted for the formulation of aerodynamic force components.

Corresponding to these force components, the following dimensionless coefficients are often introduced and called the lift force, drag force and pitching moment coefficients, respectively:

$$C_L = \frac{L}{\rho \bar{U}^2 / 2 \cdot B} \qquad C_D = \frac{D}{\rho \bar{U}^2 / 2 \cdot B} \qquad C_M = \frac{M}{\rho \bar{U}^2 / 2 \cdot B^2} \tag{1}$$

where $\bar{U} =$ the mean wind speed taken normal to the bridge axis, $\rho =$ the air density, $B =$ the width of the bridge deck, and $L, D, M =$ the 2D lift force, drag force and pitching moment for the deck of unit length exposed to wind, respectively.

2.2 Quasi-Steady Aerodynamics

Another assumption often introduced is the quasi-steady approximation, which is to say that the aerodynamic forces at any time are dependent only on the instantaneous position of the body relative to wind at that particular moment. In other words, the temporal memory effect or the history of the motion in the aerodynamic model is to be ignored.

The strip theory approximation discussed above is unambiguous and its appliocation is generally accepted. However, this is not true for the quasi-steady approximation. It

is an acceptable assumption for relatively high wind speed case but clearly unacceptable, for example, in case of vortex excitations.
When the quasi-steady approximation is applied, three aerodynamic force components are given by

$$L = \frac{\rho \overline{U}_{rel}^2}{2} B C_L \qquad D = \frac{\rho \overline{U}_{rel}^2}{2} B C_D \qquad \text{and} \qquad M = \frac{\rho \overline{U}_{rel}^2}{2} B^2 C_M \qquad (2)$$

where $\overline{U}_{rel}$ is the relative wind speed given by $\overline{U}_{rel} = \overline{U} + u - \dot{p}$. The velocity vector is given by ($\overline{U} + u, v, w$). The force and moment coefficients are, as their first approximation given by

$$C_F = C_F(\alpha) + \frac{dC_F}{d\alpha}\alpha_{rel} \qquad (F = L, D, M) \qquad (3)$$

where α_{rel} is the relative angle of attack as follows:

$$\alpha_{rel} = \alpha - \frac{\dot{h} + nB\dot{\alpha} - w}{\overline{U} + u - \dot{p}} \approx \alpha - \frac{\dot{h} - nB\dot{\alpha} - w}{\overline{U}} \qquad (4)$$

where n is a dimensionless factor representing the position, where the aerodynamic lift force acts upon. For a thin aerofoil at low reduced frequency, for example, $n \approx 0.25$. The force components can be expressed as follows:

$$F = \overline{F} + F_f + F_b \qquad (F = L, D, M) \qquad (5)$$

The first term is the static component and is given by

$$\overline{L} = \frac{\rho \overline{U}^2}{2} B C_L(\alpha) \qquad \overline{D} = \frac{\rho \overline{U}^2}{2} B C_D(\alpha) \qquad \overline{M} = \frac{\rho \overline{U}^2}{2} B^2 C_M(\alpha) \qquad (6)$$

The second term is the motion-dependent component, which is

$$\begin{aligned}
L_f &= \frac{\rho \overline{U}^2}{2} B \left\{ \frac{dC_L}{d\alpha}\alpha - 2C_L \frac{\dot{p}}{\overline{U}} + \frac{dC_L}{d\alpha}\frac{\dot{h} - nB\dot{\alpha}}{\overline{U}} \right\} \\
D_f &= \frac{\rho \overline{U}^2}{2} B \left\{ \frac{dC_D}{d\alpha}\alpha - 2C_D \frac{\dot{p}}{\overline{U}} + \frac{dC_L}{d\alpha}\frac{\dot{h} - nB\dot{\alpha}}{\overline{U}} \right\} \\
M_f &= \frac{\rho \overline{U}^2}{2} B^2 \left\{ \frac{dC_M}{d\alpha}\alpha - 2C_M \frac{\dot{p}}{\overline{U}} + \frac{dC_M}{d\alpha}\frac{\dot{h} - nB\dot{\alpha}}{\overline{U}} \right\}
\end{aligned} \qquad (7)$$

and the last term, buffeting force term, is given by

$$L_b = \frac{\rho \overline{U} B}{2} \left\{ 2C_L \cdot u(t) + \frac{dC_L}{d\alpha} \cdot w(t) \right\}$$

$$D_b = \frac{\rho \bar{U} B}{2}\left\{2C_D \cdot u(t) + \frac{dC_D}{d\alpha} \cdot w(t)\right\}$$
$$M_b = \frac{\rho \bar{U} B^2}{2}\left\{2C_M \cdot u(t) + \frac{dC_M}{d\alpha} \cdot w(t)\right\} \quad (8)$$

The first terms relate only to the static displacement and can be set aside for the dynamic analysis. The slope of force coefficients are taken at the vicinity of the static angle. If the cross-section is symmetric with respect to the horizontal plane, C_L, C_M and $dC_D/d\alpha$ are close to zero, and hence

$$L(t) \approx \frac{\rho \bar{U}^2}{2} B \frac{dC_L}{d\alpha}\left\{\alpha - \frac{\dot{h} - nB\dot{\alpha}}{\bar{U}}\right\} + \frac{\rho \bar{U} B}{2}\frac{dC_L}{d\alpha} \cdot w(t)$$
$$D(t) \approx -\rho \bar{U}^2 B C_D \dot{p} + \rho \bar{U} B C_D \cdot u(t) \quad (9)$$
$$M(t) \approx \frac{\rho \bar{U}^2}{2} B^2 \frac{dC_M}{d\alpha}\left\{\alpha - \frac{\dot{h} - nB\dot{\alpha}}{\bar{U}}\right\} + \frac{\rho \bar{U} B^2}{2}\frac{dC_M}{d\alpha} \cdot w(t)$$

2.3 Unsteady Aerodynamic Force Coefficients

The motion-dependent force components can be expressed more generally, including the virtual mass effects, as follows:

$$\begin{Bmatrix} L_f \\ D_f \\ M_f \end{Bmatrix} = \begin{bmatrix} L_{\dot{h}} & L_{\ddot{h}} & L_{\dot{\alpha}} & L_{\ddot{\alpha}} & L_{\dot{p}} & L_{\ddot{p}} \\ D_{\dot{h}} & D_{\ddot{h}} & D_{\dot{\alpha}} & D_{\ddot{\alpha}} & D_{\dot{p}} & D_{\ddot{p}} \\ M_{\dot{h}} & M_{\ddot{h}} & M_{\dot{\alpha}} & M_{\ddot{\alpha}} & M_{\dot{p}} & M_{\ddot{p}} \end{bmatrix} \cdot \begin{Bmatrix} \dot{h} \\ \ddot{h} \\ \dot{\alpha} \\ \ddot{\alpha} \\ \dot{p} \\ \ddot{p} \end{Bmatrix} \quad (10)$$

The components of the coefficient matrix are generally called the aerodynamic derivatives and are given as functions of the reduced velocity

$$V_r = \frac{\bar{U}}{\omega B} \quad (11)$$

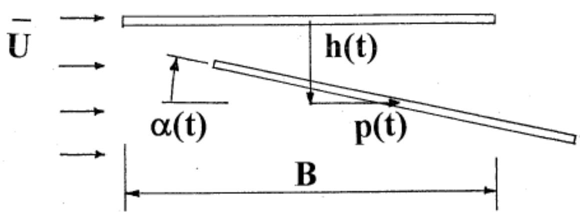

or the reduced frequency

$$K = \frac{1}{V_r} = \frac{\omega B}{\bar{U}} \quad (12)$$

The analytical expressions for the derivatives have been obtained only for a few very limited cases: one is the case of an idealized flat plate performing a simple harmonic motion in coupled heave-pitch mode with infinitesimal amplitudes and zero mean angle of attack. Another simple case analytically resolved is the lift force on a flat plate, induced by a sudden stepwise position change, $h=1$ and $\alpha=1$, respectively, when it is exposed to an uniform air flow with zero angle of attack.

For other cases, the aerodynamic derivatives need to be determined experimentally. Usually a simple harmonic oscillatory motion is assumed. For this case, though the velocity term is 90° out-of-phase, the acceleration and displacement terms are put together, since they are in the same phase. The following expression by Scanlan has been widely accepted:

$$\begin{Bmatrix} L_f \\ D_f \\ M \end{Bmatrix} = \frac{\rho \bar{U}^2 B}{2} \begin{bmatrix} KH_1^* & KH_2^* & K^2H_3^* & K^2H_4^* & KH_5^* & K^2H_6^* \\ KP_5^* & KP_2^* & K^2P_3^* & K^2P_6^* & KP_1^* & K^2P_4^* \\ BKA_1^* & BKA_2^* & BK^2A_3^* & BK^2A_4^* & BKA_5^* & BK^2A_6^* \end{bmatrix} \begin{Bmatrix} \dot{h}/\bar{U} \\ B\dot{\alpha}/\bar{U} \\ \alpha \\ h/B \\ \dot{p}/\bar{U} \\ p/B \end{Bmatrix} \tag{13}$$

where eighteen aerodynamic derivatives, $H_1^*, H_2^*, ..., A_6^*$, are functions of the reduced frequency, $K = \omega B/\bar{U}$. For the case of the flat plate aerodynamics, the aerodynamic derivatives are given as follows:

$$\begin{aligned} H_1^* &= -\frac{\pi}{k}F(k) & H_2^* &= -\frac{\pi}{4k}\left\{1+F(k)+\frac{2}{k}G(k)\right\} \\ H_3^* &= -\frac{\pi}{4k^2}\{2F(k)-kG(k)\} & H_4^* &= \frac{\pi}{2}\left\{1+\frac{2}{k}G(k)\right\} \\ A_1^* &= \frac{\pi}{4k}F(k) & A_2^* &= \frac{\pi}{16k}\left\{-1+F(k)+\frac{2}{k}G(k)\right\} \\ A_3^* &= \frac{\pi}{8k^2}\left\{\frac{k^2}{8}+F(k)-\frac{k}{2}G(k)\right\} & A_4^* &= -\frac{\pi}{4k}G(k) \end{aligned} \tag{14}$$

$$H_5^* = H_6^* = A_5^* = A_6^* = 0 \quad \text{and} \quad P_j^* = 0 \quad (j = 1,2,..,6)$$

in which $F(k)$ and $G(k)$ are the real and imaginary parts of the Theodorsen function, defined by using the Hänkel functions, $H_\nu^{(2)}(k) = J_\nu(k) - i \cdot Y_\nu(k)$ ($\nu = 0,1$), as follows:

$$C(k) = F(k) + i \cdot G(k) = \frac{H_1^{(2)}(k)}{H_1^{(2)}(k) + i \cdot H_0^{(2)}(k)} \tag{15}$$

or
$$F(k) = \frac{J_1(k)[J_1(k)+Y_0(k)] + Y_1(k)[Y_1(k)-J_0(k)]}{[J_1(k)+Y_0(k)]^2 + [Y_1(k)-J_0(k)]^2} \tag{16}$$

$$G(k) = -\frac{Y_1(k)Y_0(k) + J_1(k)J_0(k)}{[J_1(k)+Y_0(k)]^2 + [Y_1(k)-J_0(k)]^2} \tag{17}$$

by using the Bessel functions, $J_\nu(k)$ and $Y_\nu(k)$ ($\nu = 0{,}1$), where $k = K/2$ is traditionally used as the reduced frequency.

2.4 Transient Forces

The definition of these aerodynamic derivatives, however, assumes that the body in motion is performing a simple harmonic coupled oscillation, just like the case of an aerofoil flutter analysis, with infinitesimal amplitudes. Hence they are not directly applicable to the description of any transient motion, which can be obtained by a convolution of any forcing function with indicial admittance.

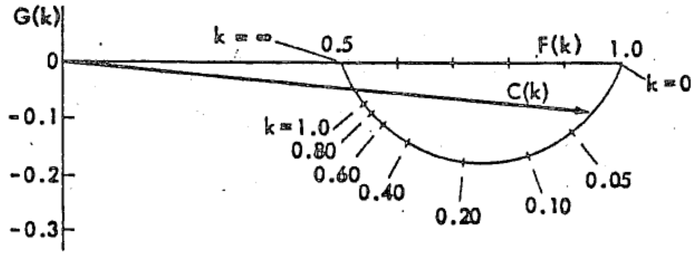

[Vector diagram of C(k)]

When a thin two-dimensional aerofoil of the chord length B is placed in a uniform flow $\overline{U}$ and the angle of attack α is suddenly given as a step-wise increase from zero, only a half of the final lift force would become effective immediately and another half of the lift force will be gained asymptotically

$$L(\tau) = \pi\rho\overline{U}^2 B\alpha \cdot \Phi(\tau) \tag{18}$$

where $\tau = 2\overline{U}t/B > 0$ is the dimensionless time. $\Phi(\tau)$ is called the Wagner function and is approximately given by

$$\Phi(\tau) = 1 - 0.165\exp(-0.0455\tau) - 0.335\exp(-0.300\tau) \tag{19}$$

The Wagner function is related to the Theodorsen function by the inverse Laplace transform as

$$\Phi(\tau) = L^{-1}\left[\frac{C(-is)}{s}\right] \tag{20}$$

This relationship implies that the indicial lift and steady state sinusoidal lift term form a Laplace transform pair. Since the Laplace transform of an exponential function is given by a rational form, or

$$L\left[e^{at}\right] = \frac{1}{s-a} \tag{21}$$

it has been established that the unsteady aerodynamic force terms in general can be approximated by a series of partial function forms of the Laplace variable (Karpel

1981). The most common form of the approximate functions, currently used for each unsteady generalized force coefficient, is the Roger's formulation given as follows (Roger 1977):

$$[A_p] = [Q_1] + [Q_2]p + [Q_3]p^2 + \sum_{j=1}^{N} \frac{p}{p+\gamma_j}[R_j] \tag{22}$$

Another fundamental formulation is when the lift force is induced by a suddenly applied constant upward gust $w_0(t)$, which is given by

$$L(\tau) = \pi\rho\overline{U}^2 B \frac{w_0}{\overline{U}} \cdot \Psi(\tau) \tag{23}$$

where $\tau = 2\overline{U}t/B$ is again the dimensionless time and $\Psi(\tau)$ is the indicial admittance and is called the Küssner function for this particular case. Küssner function is somewhat similar to Wagner function, except it starts from zero at time zero and approaches asymptotically its steady-state value of unity when $\tau \to \infty$. If the gust is of an arbitrary vertical velocity distribution $w(t)$, the lift becomes a convolution, or the Duhamel integral, involving the derivative of Küssner function, which is equivalent to the impulse response function, as

$$L(\tau) = \pi\rho\overline{U}^2 B \int_0^\infty w(\tau - s)\Psi'(s)ds \tag{24}$$

In particular, if the gust variation takes a sinusoidal form, $w(s) = w_0 \exp(iks)$, where $k = \omega B/2\overline{U}$, the lift force becomes

$$L(s) = \pi\rho\overline{U}^2 B \frac{w(s)}{\overline{U}} \cdot \Theta(k) \tag{25}$$

where $\Theta(k)$ is the Sears function, which is related to the Küssner function by

$$\Theta(k) = \int_0^\infty \Psi'(s)\exp(-iks)ds$$
$$= ik\int_0^\infty \Psi(s)\exp(-iks)ds \tag{26}$$

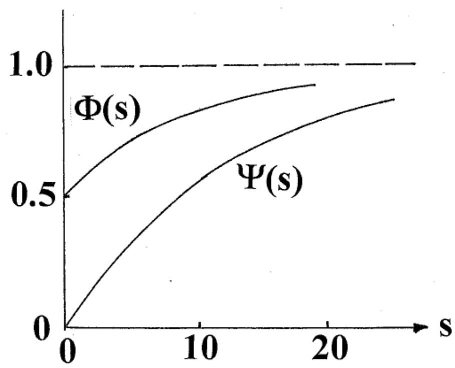

The concept of convolution integral explained above becomes an important tool for the time domain analysis.

References:

Biggs, J.M., Wind Forces on Structures, Final Report of the Task Committee, *Trans. ASCE* (119) 1954.

Fung, Y.C., *An Introduction to the Theory of Aeroelasticity*, Wiley, 1955; Dover, 1969.

Jaeger, J.C. & Newstead G.H., *An Introduction to the Laplace Transformation with Engineering Applications*, Methuen, London, 1949.

Jain, A., Jones, N.P. & Scanlan, R.H., Coupled flutter and buffeting analysis of long-span bridges, *Proc. ASCE* (122) ST7, 1996, pp.716-725.

Karpel, M., Design of active and passive flutter suppression and gust alleviation, *NASA Contractor Rept.* 3482, 1981.

Roger, K.L., Airplane math modeling methods for active control design, *AGARD-CP*-228, 1977.

Scanlan, R.H. & Simiu, E., *Wind Effects on Structures: Fundamentals and Applications to Design*, Wiley, 1999 (3rd ed.).

Scruton, C., *An Introduction to Wind Effect on Structures*, Oxford Univ. Press, 1981.

Theodorsen, T. & Garrick, I.E., Mechanism of flutter: A theoretical and experimental investigation of the flutter problem, *NACA TR* 685, 1940.

Chapter 3 Aerodynamic Instability

3.1 Concept of Aerodynamic Instability

Consider, as an example, a twisting motion of a beam. If the external excitation is a pitching moment defined in 2.2, the 2D equation of motion is as follows:

$$J\ddot{\phi} + C\dot{\phi} + K\phi = \frac{\rho \overline{U}^2}{2} B^2 C_M(\phi, \dot{\phi}, \ldots) \tag{1}$$

where J = the polar mass moment and C and K are appropriate damping and stiffness terms of the structure. C_M is not known. However, as a simple expression, if $C_M = a\phi + b\dot{\phi}$

$$\ddot{\phi} + 2\varsigma_S \omega_T \dot{\phi} + \omega_T^2 \phi = \frac{\rho \overline{U}^2 B^2}{2J}\left(a\phi + b\dot{\phi}\right) \tag{2}$$

where $\omega_T = \sqrt{K/J}$ and $\varsigma_S = C/(2J\omega_T)$.

or $$\ddot{\phi} + 2(\varsigma_S + \varsigma_a)\omega_T \dot{\phi} + \omega_T^2 (1 - S_a)\phi = 0 \tag{3}$$

where $$\varsigma_a = -\frac{\rho \overline{U}^2 B^2}{4\omega_T J} b(U_r) \qquad S_a = \frac{\rho \overline{U}^2 B^2}{2J\omega_T^2} a(U_r) \qquad U_r = \frac{\overline{U}}{B\omega_T} \tag{4}$$

Since the aerodynamic derivatives a and b are not known, Eq.(3) indicates that there is a possibility of having two types of aerodynamic instability as follows:

$\varsigma_S + \varsigma_a < 0$ $\rightarrow$ negative damping $\rightarrow$ flutter
$S_a > 1$ $\rightarrow$ negative stiffness $\rightarrow$ divergence

3.2 Historical Development of Bridge Flutter Analysis

(1) <u>Flutter and unsteady aerodynamics</u>

Though dynamic failures of aircraft wings caused by aeroelastic phenomena were observed from the early days of flight, a real development of the nonstationary airfoil theory did not occur till 1920s. An analytical expression of the aerodynamic lift force on a harmonically oscillating flat plate was first given by Birnbaum in 1922 as an application of the Prandtl's theory of bound vortices. Through the following decade, the analysis of unsteady aerodynamic forces on an oscillating two-dimensional plate attracted significant interests of aerodynamicists such as Wagner, Glauert, Küssner, Duncan and Collar and the most complete solution to this problem was presented by

Theodorsen in 1935. Similar solutions were also given in Europe by Küssner and Schwartz, Cicala, Schmieden, Ellenberger, etc. but the solution by Theodorsen (1930) has been most extensively used.

The collapse of the original Tacoma Narrows Bridge was, from the time immediately following the incident, frequently compared to galloping of iced cables or flutter of aircraft wings. Bleich (1949) tried to analyse the incident as a flutter by applying the Theodorsen's aerodynamic formulation to the bridge and found that the critical flutter speed thus calculated was considerably higher than that of Tacoma Narrows. It was obvious that the airfoil flutter coefficients calculated by the potential flow theory were not directly applicable to much more aerodynamically bluff sections such as this bridge.

Bleich tried to cover this defect by modifying the Theodorsen's expression by considering an additional lift force term corresponding to the effects of vortex formation from the leading edge of the deck but was not very successful. Pugsley commented at this point that experimentally determined aerodynamic coefficients rather than Theodorsen's would be of more help in future. He was right. In later days, when the use of streamlined shallow box girders as a suspension bridge stiffening girder became quite popular, having inspired by successful application of them for both Severn and Lillebælt crossings in late 1960s. In these cases, the flow separation is much less than the sections such as Tacoma, and ironically Bleich's original calculation with the Theodorsen's force can actually yield a reasonably good approximation.

(2) Experimental determination of unsteady aerodynamic forces

Theodorsen's analysis was based on the potential flow theory, which assumes that flow is to follow the solid surface of the body. However, there is another category of flutter instability in which the flow separation is involved as an essential feature of it. The phenomenon of stall flutter became an issue particularly as instability of propellers and turbine blades. Severe drop of critical flutter speeds, predominance of pitching or torsional vibration and strong non-linearity in response are known to be its characteristics.

In the absence of any analytical means to determine unsteady aerodynamic forces for stalled wings, where the flow separation is involved, an extensive experimental evaluation of them has been attempted since 1930s. There are basically two ways to do it. One is to make a direct measurement of aerodynamic force components by dynamometers, strain gauges and so on when the body is give a specific motion, and the other way is to calculate the force indirectly from the induced motion of the body. The same principles have been applied to both airfoils and bridge deck sections.

Försching applied the direct method for the measurement of unsteady aerodynamic forces on various prisms but Ukeguchi et al. (1966) were probably the first for applying it to bridge deck sections. Rigid bridge deck models were mechanically driven into a simple harmonic motion with a range of specific frequency and amplitude in two-dimensional air stream and the reactions at the model supports were detected. This is a method which was extensively applied by Halfman (1952) to airfoil aerodynamics. The forced vibration technique was further extended particularly in Japan to cover various aerodynamically bluff sections and also to investigate nonlinear characteristics of them. A recent development of high-speed pressure scanning techniques has made it possible to do practically a simultaneous measurement of dynamic pressure signals at many ports and real-time integration of them. An application of this technique to the forced vibration method has opened up another promising avenue for effective measurement of unsteady aerodynamic forces (King, Davenport & Larose 1991).

As opposed to the direct measurement, the indirect measurement of aerodynamic forces by detecting the induced response of models in air flow generally requires less-complicated experimental set-ups but more careful conditioning of them. Application of this method in bridge aerodynamics was initiated by Scanlan & Sabzevari (1967) and has been widely practiced over the world. A more sophisticated development of this method is an application of the system identification (SI) techniques which has been developed almost simultaneously in Europe, USA and Japan in recent years; (Poulsen et al. 1999, for example).

Most of these measurements have been done in two-dimensional, smooth air flow and the force coefficients are assumed to be given by linear combinations of displacements and their first derivatives with respect to time. Some attempts have been made to investigate the effects of turbulence and non-linearity on the derivatives but the process and outcomes are still too complicated for practical applications.

(3) Formulation of 2D flutter analysis

Once the unsteady aerodynamic forces are established, the critical conditions for the onset of aerodynamic instability can be determined. The most traditional way for this analysis is by applying the strip assumption, where the interaction between air stream and the body is to be decided in a two-dimensional section perpendicular to the longitudinal axis of the structure. Consequently, any three-dimensional effects along the longitudinal axis of the structure are assumed to be negligible. The equation of motion is given as follows:

$$\begin{bmatrix} m & 0 \\ 0 & J \end{bmatrix} \begin{Bmatrix} \ddot{h} \\ \ddot{\alpha} \end{Bmatrix} + \begin{bmatrix} C_h & 0 \\ 0 & C_\alpha \end{bmatrix} \begin{Bmatrix} \dot{h} \\ \dot{\alpha} \end{Bmatrix} + \begin{bmatrix} K_h & 0 \\ 0 & K_\alpha \end{bmatrix} \begin{Bmatrix} h \\ \alpha \end{Bmatrix} = \begin{Bmatrix} L_h \\ M_\alpha \end{Bmatrix} \tag{5}$$

The drag-ward motion was considered to be insignificant following the tradition of airfoils. Another restriction usually assumed in a conventional flutter analysis is the fact that the unsteady aerodynamic forces are all given as functions of the reduced frequency $K = \omega B / \overline{U}$ assuming that the body is performing a simple harmonic motion both in heaving and pitching simultaneously with the same frequency (f) and infinitesimal amplitudes. Hence, in (5) above, the left-hand side is all established with respect to time and yet the aerodynamic force terms are actually given in the frequency domain. It means that the equation is applicable only when the body is performing this particular motion as follows:

$$h(t) = h_0 \exp(i\omega t) \qquad \alpha(t) = \alpha_0 \exp(i\omega t) \tag{6}$$

By substituting (6) into (5), the flutter conditions, $\overline{U}_F$ and ω_F, are decided and this process is called the flutter analysis.

(4) Simple formulae for 2D flutter

It was a heavy task to carry out the numerical calculation required for the flutter analysis in pre-computer days. Because of a tedious process required for its calculation, various simplification of flutter calculation was considered. For the case of a thin airfoil, the calculation needs to be done just once for ever for a range of structural parameters, since the aerodynamic tools are established uniquely. An extensive parametric study was carried out and an approximate equation to give the flutter speed was proposed by Theodorsen and Garrick (1940) for airfoils. For the case of bridge decks, similar attempts were made by several researchers and, amongst them, Selberg's formulation has been most frequently referred to:

$$\overline{U}_F = \kappa B f_T \sqrt{\frac{r^*}{\mu}\left\{1-\left(\frac{f_V}{f_T}\right)^2\right\}} \tag{7}$$

where $$r^* = \frac{r}{B} \qquad r = \sqrt{\frac{J}{m}} \quad \text{and} \quad \mu = \frac{\rho B^2}{m} \tag{8}$$

$m, J =$ the mass and mass moment per unit deck length, $f_V, f_T =$ the fundamental natural frequencies in bending and torsion, respectively. The coefficient κ was introduced to accommodate the difference of flutter speed due to the cross-sectional shape of the bridge deck and is unity for a flat plate. Selberg (1963) suggested the κ-values for some aerodynamically bluff sections and different angles of attack. Similar approaches were taken by Klöppel and Weber, Rocard, Frandsen and others in this period.

(5) Time domain versus frequency domain analyses

Bridge flutter analysis was traditionally carried out in the frequency domain but there have been some attempts to do it in the time domain as well. Scanlan et al. (1974) first worked on solving the problem entirely in the time domain, introducing the indicial functions which were put forward earlier in the aeronautical field. The idea was also extended to the coupled mode flutter by Bucher and Lin (1988). One of the difficulties then was to make a proper functional fit to define indicial functions corresponding to the experimentally obtained aerodynamic derivatives, particularly when the cross-sections are far from streamlined. It is only recently that much effort has been invested in developing efficient time domain formulations of the unsteady aerodynamic forces that could be combined with finite element models of the structure and could include all the non-linearities that have been disregarded in the past. This development has been associated with the planning of very long bridge projects such as Akashi, Storebælt and Messina.

Miyata et al. (1995) clearly presented the advantages of the time domain approach, particularly when it is combined with a finite element modelling of the structure, for the prediction of bridge behaviour under wind action. The formulation used by them was a conventional quasi-steady aerodynamics with the strip assumption. Much the same approach was also taken by Kovacs et al. (1992). Diana et al. (1992), on the other hand, developed a corrected quasi-steady theory by introducing the concept of an equivalent linearization of force coefficients for each reduced velocity. This formulation has been proved to be adequate in many ways, except that it does not deal with the aerodynamic memory effects and the span-wise coherence of the lift forces.

Another model for the self-excited forces is a method to approximate the unsteady aerodynamic forces by rational functions which can be regarded as the Laplace transformed functions (Tiffany & Adams 1988). The idea, in principle, is the same as the use of indicial functions. This method was extensively applied as a state-space method by Xie (1985) to analyse the 3D multi-mode bridge flutter. Similar approaches have been also taken by Lin and Li, Q.C. (1993), Boonyapingyo et al. (1994), Fujino et al. (1995) and so on.

3.3 3D Flutter Analyses

(1) Direct method and modal method

Application of flutter analysis for three-dimensional structures, without the use of strip assumption, has a relatively short history. The calculation can be performed in two different ways: one is to apply the unsteady aerodynamic forces, either in the frequency domain or in the time domain, directly to a 3D finite element model of the structure (direct method); another is to consider the structural response separately in various vibration modes and assemble them (mode superposition method).

The direct method was formulated by Miyata and Yamada (1990) leading to a complex eigenvalue problem by the use of aerodynamic derivatives in the frequency domain. The method has a straightforward philosophy but drawbacks are that it requires a large computer capacity and solving a complex eigenvalue problem tends to be a time-consuming process. The mode superposition method, on the other hand, has been employed by many researchers. There have been several methods developed to analyse the multi-mode flutter in the frequency domain. Agar (1989, 1991) and Chen (1994) developed modal techniques to solve the linearized quadratic eigen-equations. As a development of the p-K method which has been used in the field of aircraft industry, Namini et al. (1992) and Cheng (1995) presented a more general numerical procedure called the p-K-F method to determine the pre- and post-flutter behaviour by solution to the modal equations. Further to these, Lin and Yang (1983), Jones and Scanlan (1991), Tanaka et al. (1992), Jain et al. (1996) and so on directly utilize the determinant search method to calculate the complex eigenvalues in a general term of the impedance matrix.

(2) Formulation of flutter equation

Actual calculation procedure in detail is explained elsewhere, such as Miyata & Yamada (1990) and Ge & Tanaka (1999). However, the general formulation of 3D flutter analysis can be briefly outlined as follows.

The equations of motion of a bridge that is discretized as a n-degree-of-freedom structure can be formulated as follows:

$$[M_s]\{\ddot{\delta}\}+[C_s]\{\dot{\delta}\}+[K_s]\{\delta\}=[F_v]\{\dot{\delta}\}+[F_d]\{\delta\} \qquad (9)$$

where $[M_s]$, $[C_s]$ and $[K_s]$ are the mass, damping and stiffness matrices of the structure, $\{\delta\}$ is a structural deflection vector, $[F_v]$ and $[F_d]$ are the velocity and displacement parts of the unsteady aerodynamic force matrix, respectively. The unsteady aerodynamic force components were defined earlier by eq. (13) of 2.3. The static action of wind and the aerodynamic gust forces on the right-hand side of the equation can be excluded for the flutter analysis. From (9), the system equation can be very simply

$$[M]\{\ddot{\delta}\}+[C]\{\dot{\delta}\}+[K]\{\delta\}=0 \qquad (10)$$

where $[M]=[M_s]$, $[C]=[C_s]-[F_v]$ and $[K]=[K_s]-[F_d]$.

If the made superposition method is considered, eq. (10) can be rewritten as follows:

$$[\tilde{M}]\{\ddot{\Phi}\}+[\tilde{C}]\{\dot{\Phi}\}+[\tilde{K}]\{\Phi\}=0 \qquad (11)$$

where $$[\tilde{M}]=[X]^T[M][X],\quad [\tilde{C}]=[X]^T[C][X],\quad [\tilde{K}]=[X]^T[K][X] \qquad (12)$$

are the generalized mass, damping and stiffness matrices, respectively. The displacement vector is now expressed by

$$\{\delta\}=[X]\{\Phi\} \qquad (13)$$

where $[X]$ and $\{\Phi\}$ are called the mode matrix and general coordinate vector, respectively. By assuming a simple harmonic oscillation for the general coordinate as

$$\{\Phi(t)\}=\{\Phi\}\exp(\lambda t) \qquad \lambda=\lambda_R+i\lambda_I \qquad (14)$$

the flutter conditions are given by

$$\left|\lambda^2[\tilde{M}]+\lambda[\tilde{C}]+[\tilde{K}]\right|=0 \qquad (15)$$

Corresponding circular frequency ω and the damping ratio ς are defined from the complex eigen-value as

$$\omega = \sqrt{\lambda_R^2 + \lambda_I^2} \qquad \varsigma = \frac{\lambda_R}{\sqrt{\lambda_R^2 + \lambda_I^2}} \tag{16}$$

Flutter critical speed $\overline{U}_F$ is decided from $\varsigma = 0$ and ω_F is decided from the corresponding λ_I.

(3) Mode participation

Almost all 3D flutter analyses are carried out in the frequency domain and are based on the idea of mode superposition. The assumption is that a dynamic coupling between the natural modes takes place through the self-excited aerodynamic forces. However, it should be noted that there are some fundamental questions regarding this assumption. First of all, there is a question of how many and which natural modes are participating to the instability. Particularly, when the structure is very large and/or when the structure is under construction and its full stiffness is not reached yet, there can be more than two vibration modes contributing to the instability. Secondly, this mode combination is only an approximate expression of the flutter mode anyway and there is no reason why it has to be always true. Particularly, when the contributing modes are lacking in their geometrical affinity, the flutter vibration mode could be quite complicated. In view of this, it is desirable to develop a more comprehensive and accurate procedure to do flutter mode analysis and improve the understanding of the aerodynamic instability of cable-supported bridges.

Ge and Tanaka (1999) investigated the issue of mode participation by considering the participation of both multiple natural modes and full natural modes of vibration which are particularly important for long-span cable-supported bridges. Both the multi-mode and full-mode flutter analysis methods employed the general expression of linear unsteady aerodynamic forces, which include 18 dimensionless aerodynamic derivatives considering vertical bending, pitching torsion as well as lateral bending and their mode interactions. The multi-mode approach uses a multi-degree-of-freedom model technique and includes the self-excited aerodynamic force interaction in the structural equations of motion to produce an asymmetrical eigenvalue problem with the order of the number of natural modes participating in flutter oscillation. The eigenvalue solution of the characteristic matrix involved is indicative of the nature of pre-selected possible oscillations that can exist at a given wind speed For the full-mode approach, it is unnecessary to assume the flutter oscillation mode as a combination of a few natural modes of the target structure. Indeed, this approach formulates the asymmetric eigenvalue priblem including the entire natural modes and representing all possible system oscillations, but only solves the first several characteristic roots which contain the most important one corresponding to the lowest flutter speed.

Comparison of numerical results based on the two methods indicated that there may be a significant conservatism in the two-mode method that assumes only the fundamental flexural and torsional natural modes to participate in the flutter response, and that the multi-mode analysis including enough number of natural modes can approach an approximate solution to the full-mode analysis with good accuracy.

3.4 Galloping

Aerodynamic instability in translational motion normal to wind is sometimes observed in structures with aerodynamically bluff cross-sections such as towers, cranes and ice-covered cables, and is called galloping because of its violent feature. It is a self-excited motion in which the structural motion itself is the cause of creating the negative aerodynamic damping. The main difference in characteristics of this phenomenon from the previously described flutter instability is in the fact that a) the response amplitude of galloping tends to grow to a much greater magnitude than the linear dimension of the cross-section, often leading to the structural destruction; b) the vibration tends to be strongly non-linear as a result; and c) the response is often strongly influenced by the existence of flow turbulence, in the sense that turbulence could trigger the instability which does not exist otherwise.

Since the galloping motion is usually with very large amplitude at high wind speed, it is known that the response is predictable by applying the quasi-steady analysis, only if the aerodynamic forces on the given structural section are clearly identified. A well-known criterion for instability, introduced by Den Hartog (1933), is given by

$$\left\{\frac{dC_L}{d\alpha}+C_D\right\}_{\alpha=0}<0 \tag{17}$$

For the bridge girders, particularly for a deck-on-box section, this condition is sometimes satisfied when the depth of the box is substantial, such as more than a quarter of the bridge deck width.

One of the characteristic points of galloping that are different from flutter type of instability is its strong non-linearity. Since the dynamic displacement for this case is considered to be large, the direction of wind against the bridge deck will have a relative angle of attack defined by

$$\alpha=\tan^{-1}\left(\dot{z}/\overline{U}\right) \tag{18}$$

The aerodynamic lift for this case is then replaced by a lateral force, taken positive in the direction of $-z$, which is defined by

$$F_z(\alpha)=-(L\cos\alpha+D\sin\alpha)=\frac{\rho\overline{U}^2}{2}\cdot d\cdot C_{Fz}(\alpha) \tag{19}$$

where, the lift and drag forces are defined by

$$L(\alpha)=\frac{\rho\overline{U}_{rel}^2}{2}\cdot d\cdot C_L(\alpha) \qquad D(\alpha)=\frac{\rho\overline{U}_{rel}^2}{2}\cdot d\cdot C_D(\alpha) \qquad \overline{U}_{rel}=\overline{U}\sec\alpha$$

and hence the lateral force coefficient is given by

$$C_{Fz}(\alpha)=-(C_L+C_D\tan\alpha)\cdot\sec\alpha \tag{20}$$

and $$\frac{dC_{Fz}}{d\alpha} = -\left\{\frac{dC_L}{d\alpha} + C_D\left(1 + 2\tan^2\alpha\right)\right\}\sec\alpha - \left(C_L + \frac{dC_D}{d\alpha}\right)\tan\alpha\cdot\sec\alpha$$

The lateral force excites the vibration when $dC_{Fz}/d\alpha$ at $\alpha = 0$ is positive, which gives the Den Hartog's criterion given in eq.(17) as a necessary condition for instability. By substituting eq.(18) to (20)

$$C_{Fz}(\alpha) = \sum_{i=odd} A_i \cdot \left(\frac{\dot{z}}{\overline{U}}\right)^i + \sum_{j=even} A_j \cdot \left(\frac{\dot{z}}{\overline{U}}\right)^j \cdot \frac{\dot{z}}{|\dot{z}|} \qquad (21)$$

In many cases, the first mode of vibration would be predominant in response and hence

$$Q_i(t) = \int_L L(y,t)\psi_i(y)dy \approx \frac{\rho\overline{U}d}{2} A_1\dot{q}_1 \int_L \psi_1^2(y)dy \qquad (22)$$

Hence, as a first order equation,

$$\ddot{q}_1 + 2\omega_1\left(\varsigma_1 - \frac{\rho\overline{U}d}{4\omega_1 m_e}A_1\right)\dot{q}_1 + \omega_1^2 q_1 = 0 \qquad (23)$$

which leads to a refined form of the Den Hartog criterion as follows:

$$\left\{\frac{dC_L}{d\alpha} + C_D\right\}_{\alpha=0} < \frac{4\omega_1 m_e}{\rho\overline{U}d}\cdot\varsigma_1 \qquad (24)$$

m_e above is an equivalent mass. Further, the non-linear equation of motion is expressed by

$$\ddot{z} + \omega_1^2 z + F(\dot{z}) = 0 \qquad (25)$$

where $$F(\dot{z}) = 2\varsigma_1\omega_1\dot{z} - \frac{\rho\overline{U}^2 d}{2m}\left\{\sum_{i=odd} A_i\left(\frac{\dot{z}}{\overline{U}}\right)^i + \sum_{j=even} A_j\left(\frac{\dot{z}}{\overline{U}}\right)^j \cdot \frac{\dot{z}}{|\dot{z}|}\right\} \qquad (26)$$

From the energz principle $$W = \oint F(\dot{z})dz(t) = 0 \qquad (27)$$

which will decide the nonlinear limit cycle for a range of wind speed.

3.5 Instability in Torsion

Analysis of torsional instability, considering a SDOF system, should be parallel to SDOF galloping. However, its quasi-steady analysis is not so straightforward because of the difficulty in taking the effective angle of attack. Analyses were attempted by Modi and later by Nakayama & Mizota and well summarized by Blevins (1990).

In order to avoid any possible ambiguity, it makes more sense to use unsteady aerodynamic forces. Only relevant terms are A_2^* and A_3^* of the pitching moment. Hence, the equation of motion is

$$\ddot{\alpha} + 2\varsigma_\alpha \omega_\alpha \dot{\alpha} + \omega_\alpha^2 \alpha = \frac{\rho \overline{U}^2}{2J} B^2 \left\{ K A_2^* \frac{B\dot{\alpha}}{\overline{U}} + K^2 A_3^* \alpha \right\} \tag{28}$$

where, as before, the aerodynamic coefficients A_2^* and A_3^* are assumed to be functions of reduced frequency $K = \omega B / \overline{U}$. If no coupling with any other modes are assumed, $\omega = \omega_\alpha$ and hence the critical condition for the onset of instability is defined by

$$A_2^* = \frac{4J\varsigma_\alpha}{\rho B^4} \tag{29}$$

References:

Agar, T.J.A., Aerodynamic flutter analysis of suspension bridges by a modal technique, *J. Engng Structures* (11) 1989, pp.75-82.

Agar, T.J.A., Dynamic instability of suspension bridges, *Comput. Struct.* (41) 6, 1991, pp.1321-1328.

Bleich, F., Dynamic instability of truss-stiffened suspension bridges under wind action, *Trans. ASCE* (114) 1949, pp.1177-1222.

Blevins, R.D., *Flow Induced Vibration*, Van Nostrand Reinhold, 1920 (2nd ed.).

Boonyapingyo, V., Yamada, H. & Miyata, T., Eind-induced nonlinear lateral-torsional buckling of cable-stayed bridges, *Proc. ASCE* (120) ST2, 1994, pp.486-506.

Bucher, C.G. & Lin, Y.K., Stochastic stability of bridges considering coupled modes, *Proc. ASCE* (114) EM12, 1988, pp.2055-2071 & (115) EM2, 1989, pp.384-400.

Chen, Z.Q., The three dimensional analysis of behavior investigation on the critical flutter state of bridges, *Proc. Int Symp. on Cable-stayed Bridges*, Shanghai, 1994, pp.302-307.

Cheng, S.H., A 3D finite element flutter analysis of long span bridges, *M.Eng. thesis, Tongji University*, Shanghai, 1995 (in Chinese).

Den Hartog, J.P., Transmission line vibration due to sleet, *AIEE Transaction* (51) 1932, pp.1074-1076.

Diana, G., Cheli, F., Zasso, A.Collina, A. & Brownjohn, J., Suspension bridge parameter identification in full scale tests, *JWEIA* (41) 1992, pp.165-176.

Dowell, E.H. (ed.), *A Modern Course in Aeroelasticity*, Kluwer Academic Pub., 1989 (2nd ed.).

Fujino, Y., Wilde, K., Masubawa, J. & Bhartio, Rational function approximation of aerodynamic forces on bridge deck and ist application to active control of flutter, *Proc. 9th ICWE*, New Delhi (2) 1995, pp.994-1005.

Fung, Y.C., *An Introduction to the Theory of Aeroelasticity*, Dover, 1969.

Ge, Y.J. & Tanaka, H., Aerodynamic flutter analysis of cable-supported bridges by multi-mode and full-mode approaches, *JWEIA* (86) 1999, pp.123-153.

Hodges, D.H. & Pierce, G.A., *Introduction to Structural Dynamics and Aeroelasticity*, Cambridge Univ. Press, 2002.
Jain, A., Jones, N.P. & Scanlan, R.H., Coupled flutter and buffeting analysis of long-span bridges, *Proc. ASCE* (122) ST7, 1996, pp.716-725.
Jones, N.P. & Scanlan, R.H., Issues in the multi-mode aerodynamic analysis of cable-stayed bridges, *Infrastructure'91, International*, 1991.
King, J.P.C., Davenport, A.G. & Larose, G.L., A study of wind effects for the Storebælt Bridge tender design, Denmark, *UWO Research Report*, BLWT-SS31-1991, Dec., 1991.
Kovacs, I., Svensson, H.S. & Jordet, E., Analytical aerodynamic investigation of the cable-stayed Helgeland Bridge, *Proc. ASCE* (118) ST1, 1992, pp.147-168.
Lin, Y.K. & Li, Q.C., New stochastic theory for bridge stability in turbulent flow, *Proc. ASCE* (119) EM1, 1993, pp.113-127.
Lin, Y.K. & Yang, J.N., Multi-mode bridge response to wind excitation, *Proc. ASCE* (109) EM2, 1983, pp.586-603.
Miyata, T., Yamada, H., Boonyapinyo, V. & Santos, J.C., Analytical investigation on the response of a very long suspension bridge under gusty wind, *Proc. 9th ICWE* (2) New Delhi, 1995, pp.1006-1017.
Namini, A., Albrecht, P. & Bosch, H., Finite element-based flutter analysis of cable-suspended bridges, *Proc. ASCE* (118) ST6, 1992, pp.1509-1526.
Poulsen, N.K., Damsgaard, A. & Reinhold, T.A., Determination of flutter derivatives for the Great Belt Bridge, *Proc. 8th ICWE* (2) London, Ont., 1991, pp.153-164.
Scanlan, R.H., Béliveau, J.G. & Budlong, K.S., Indicial aerodynamic functions for bridge decks, *Proc. ASCE* (100) EM4, 1974, pp.657-672.
Scanlan, R.H. & Rosenbaum, R., *Aircraft Vibration and Flutter*, Macmillan, New York, 1951; Dover, New York, 1968.
Scanlan, R.H. & Sabzevari, A., Aerodynamic stability of suspension bridges, *Proc. ASCE* (94) EM2, 1968, pp.489-519.
Selberg, A., Aerodynamic effects on suspension bridges, *Proc. 1st ICWE*, Teddington (2) 1963, pp.462-486.
Tanaka, H., Yamamura, N. & Tatsumi, M., Coupled mode flutter analysis using flutter derivatives, *JWEIA* (42) 1992, pp.1279-1290.
Theodorsen, T., General theory of aerodynamic instability and the mechanism of flutter, *NACA Report* No.496, 1935.
Theodorsen, T. & Garrick, I.E., Mechanism of flutter: A theoretical and experimental investigation of the flutter problem, *NACA TR*685, 1940.
Tiffany, S.H. & Adams, W.M., Non-linear programming extensions to rational function approximation methods for unsteady aerodynamic forces, *NASA TP* 2776, 1988.
Ukeguchi, N., Sakata, H. & Nishitani, H., An investigation of aeroelastic instability of suspension bridges, *Proc. Int. Symp. on Suspension Bridges*, Libon, 1966, pp.273-284.
Xie, J.M., Bridge flutter theory and research of flutter characteristics of cable-stayed bridges, *Ph.D. thesis, Tongji University*, Shanghai, 1985 (in Chinese).

Chapter 4 Buffeting

4.1 General Characteristics

Buffeting is dynamic structural response caused by wind turbulence, which either inherently exists in natural wind or was created by existence of upstream objects. It is usually considered and analyzed as a forced vibration caused by time-dependent aerodynamic forces due to velocity fluctuation. Buffeting is a stochastic vibration, consisting of a wide range of frequency components, and its amplitude is randomly fluctuating. However, the buffeting of bridge decks often appears as a narrow-band response only in the first couple of modes and quite random in its amplitude. It generally increases in parabolic manner with the mean wind speed. The peak response amplitude is usually four times or so greater than the root-mean-square response.

Consequence of having buffeting vibration is usually not catastrophic to the structure but long-time influence of it such as fatigue damage can be a serious engineering concern.

4.2 Analytical Prediction

(1) <u>Two-dimensional quasi-steady assumption</u>

By applying a conventional quasi-steady aerodynamics and the concept of strip theory, the two-dimensional aerodynamic lift force per unit deck length can be approximately expressed as

$$L(y,t)=\frac{\rho\overline{U}^2}{2}B\frac{dC_L}{d\alpha}\frac{w-\dot{z}}{\overline{U}} \tag{1}$$

in which, $dC_L/d\alpha$ is the lift slope and $w(t)$ is the vertical component of the velocity vector. Eq.(1) is obtained by replacing the lift coefficient by the product of the lift slope and the instantaneous angle of attack, $(w-\dot{z})/\overline{U}$. Eq.(1) results in the aerodynamic damping of

$$\varsigma_{ai}=\frac{\rho\overline{U}B}{4\omega_i M_i}\frac{dC_L}{d\alpha}\int_L \psi_i^2(y)dy \tag{2}$$

and the buffeting force corresponding to the vertical bending of the bridge deck as

$$Q_i(t)=\frac{\rho\overline{U}B}{2}\frac{dC_L}{d\alpha}\int_L w(y,t)\psi_i(y)dy \tag{3}$$

By taking the autocorrelation of eq.(3) and applying Fourier transform, the spectral density function of $Q_i(t)$ can be obtained as follows:

$$G_{Qi}(f) = \left(\frac{\rho \bar{U} B}{2} \frac{dC_L}{d\alpha}\right)^2 \int_L \int_L |X_a(y_1, y_2; f)|^2 G_w(y_1, y_2; f) \psi_i(y_1) \psi_i(y_2) dy_1 dy_2 \tag{4}$$

(2) Aerodynamic admittance and Joint acceptance

In eq.(4), there appears a new function X_a, which represents the overall effectiveness of the aerodynamic lift force in exciting the structure. It is primarily a function of frequency and the span-wise correlation of lift forces assumed in the strip theory and can be put together with the lateral correlation of velocity as

$$|X_a(y_1, y_2; f)|^2 G_w(y_1, y_2; f) \approx |X_a(f)|^2 G_w(f) \tilde{R}_L(y_1, y_2; f)$$

and hence

$$G_{Qi}(f) \approx \left(\frac{\rho \bar{U} B}{2} \frac{dC_L}{d\alpha}\right)^2 |X_a(f)|^2 G_w(f) |J_i(f)|^2 \tag{5}$$

where

$$|J_i(f)|^2 = \int_L \int_L \tilde{R}_L(y_1, y_2; f) \psi_i(y_1) \psi_i(y_2) dy_1 dy_2 \tag{6}$$

is referred to as the joint acceptance function. $\tilde{R}_L(y_1, y_2; f)$ is the correlation coefficient of the lift force, and is usually approximated as

$$\tilde{R}_L(y_1, y_2; f) \approx \exp\left\{-c\left(\frac{f \Delta y}{\bar{U}}\right)^k\right\} \qquad \text{where} \qquad \Delta y = |y_1 - y_2| \tag{7}$$

The force correlation has been often assumed to be represented by the velocity correlation. However, in reality, it has been observed that the lift forces tend to be better correlated than the velocity components, which means that the calculated response based on this assumption can be somewhat less than in reality. $|X_a(f)|^2$ is called the aerodynamic admittance function.

[Example 1] Horizontal line-like structures under drag excitation

Consider the buffeting response of a horizontal beam of length L, mass per unit length m and lateral bending stiffness EI. The beam is exposed to a turbulent wind approaching normal to the beam axis, inducing horizontal bending motion due to fluctuating drag. The equation of motion is

$$m\ddot{x} + (EIx'')'' = p(y, t)$$

By expressing the response as $x(y,t) = \sum_r \phi_r(y) q_r(t)$ the modal quantities are introduced:

$$M_r = \int_L m(y) \phi_r^2(y) dy \qquad K_r = (2\pi f_r)^2 M_r$$

$$C_r = 2\varsigma_r\sqrt{M_r K_r} \qquad Q_r(t) = \int_L p(y,t)\phi_r(y)dy$$

The modal equation of motion becomes $$M_r\left(\ddot{q}_r + 2\varsigma_r\omega_r\dot{q}_r + \omega_r^2 q_r\right) = Q_r(t)$$

The mean-square response is given by $\sigma_x^2(y) = \sum_i\sum_j \overline{q_i q_j}\phi_i(y)\phi_j(y) \approx \sum_r \overline{q_r^2}\phi_r^2(y)$

where $$\overline{q_r^2} = \frac{1}{K_r^2}\int_0^\infty \left|H_r(f)\right|^2 G_{Qr}(f)df$$

$$G_{Qr}(f) = \int_L\int_L G_P(y_1,y_2;f)\phi_r(y_1)\phi_r(y_2)dy_1dy_2$$

and $$G_P(y_1,y_2;f) = G_P(f)\tilde{R}_P(y_1,y_2;f)$$

The force coherence $\tilde{R}_P(y_1,y_2;f)$ is unknown but is assumed to be the same as the velocity coherence $\tilde{R}_u(y_1,y_2;f)$ by Davenport and the same assumption has been often made. Then

$$\tilde{R}_P(y_1,y_2;f) = \tilde{R}(y_1,y_2;f) = \exp\left(-\frac{f\left|y_1 - y_2\right|}{\overline{U}}\right)$$

Hence $$G_{Qr}(f) = G_P(f)\left|J_r(f)\right|^2$$

in which $$\left|J_r(f)\right|^2 = \int_L\int_L \tilde{R}_P(y_1,y_2;f)\phi_r(y_1)\phi_r(y_2)dy_1dy_2$$

is the joint acceptance function. Substituing these expressions, the mean-square modal response becomes as follows:

$$q_r^2 = \frac{1}{K_r^2}\int_0^\infty \left|H_r(f)\right|^2 G_{Qr}(f)df = \frac{1}{K_r^2}\int_0^\infty \left|H\ \ (f)\right|^2\left|J_r(f)\right|^2 G_P(f)df$$

where

$$\left|H\ \ (f)\right|^2 = \frac{1}{\left\{1-(f/f_r)^2\right\}^2 + \left\{2\left(\varsigma_{S,r}+\varsigma_{a,r}\right)f/f_r\right\}^2}$$

$$G_P(f) = \left(\frac{2\overline{P}}{\overline{U}}\right)^2\left|X_r(f)\right|^2 G_u(f)$$

$\varsigma_{S,r}$ and $\varsigma_{a,r}$ are the structural and aerodynamic damping, respectively. The aerodynamic damping for the r-th mode is approximately given, based on the quasi-steady theory, by

$$\varsigma_{a,r} = \frac{\rho A C_D\overline{U}}{2\omega_r m_r} \qquad \text{where} \qquad m_r = \frac{\int_L m(y)\phi_r^2(y)dy}{\int_L \phi_r^2(y)dy}$$

The aerodynamic admittance function $\left|X_r(f)\right|^2$ needs to be defined in one way or another.
A few important comments should be remembered for this analysis as follows:

1. Mode-coupling terms are ignored, though this should not have too much influence.
2. Spanwise force coherence would be probably higher than assumed here.
3. Aerodynamic admittance: is this a scape goat?
4. For the unsteady aerodynamic forces, it is better to use the measured derivatives, if possible.

[Example 2] Horizontal line-like structure under lift excitation

Consider this time the same beam as the previous example, but buffeting excitation due to lift force. By expressing the response as

$$z(y,t) = \sum_r q_r(t)\phi_r(y)B$$

the modal equation of motion is

$$\ddot{q}_r + 2\left(\varsigma_{S,r} + \varsigma_{a,r}\right)\omega_r \dot{q}_r + \omega_r^2 q_r = \frac{Q_r(t)}{M_r}$$

in which $$M_r = \int_L m(y)\phi_r^2(y)dy$$

The aerodynamic damping is expressed, by using the Scanlan type aerodynamic derivatives, as

$$\varsigma_{a,r} = -\frac{H_1^*}{2\mu_r}\int_L \phi_r^2(y)dy$$

in which $\mu_r = M_r / L\rho B^2$ is the modal mass ratio and the derivative H_1^* is a function of reduced frequency $K = B\omega_r / \overline{U}$. If the quasi-steady approach is taken as before,

$$\varsigma_{a,r} = \frac{1}{4\mu_r L}\frac{1}{K}\frac{dC_L}{d\alpha}\int_L \phi_r^2(y)dy$$

The generalized buffeting force can be formulated as

$$Q_r(t) = \frac{\rho\overline{U}}{2}\frac{dC_L}{d\alpha}\int_L w(y,t)\phi_r(y)dy$$

Auto-correlation of $Q_r(t)$ is

$$R_{Qr}(\tau) = \left(\frac{\rho\overline{U}}{2}\frac{dC_L}{d\alpha}\right)^2 \int_L\int_L \overline{w(y_1,t)w(u_2,t+\tau)}\phi_r(y_1)\phi(y_2)dy_1dy_2$$

By applying Fourier transform, the spectral density function of $Q_r(t)$ can be obtained. Considering the concept of aerodynamic admittance again,

$$G_{Qr}(f) = \left(\frac{\rho \overline{U}}{2}\frac{dC_L}{d\alpha}\right)^2 \left|\mathrm{X}_r(f)\right|^2 \int_L \int_L C_w(y_1, y_2; f)\phi_r(y_1)\phi_r(y_2)dy_1 dy_2$$

in which $C_w(y_1, y_2; f) = G_w(f)R_w(y_1, y_2; f)$ is the co-spectrum of velocity component $w(t)$. Again, the use of velocity correlation instead of the force correlation is usually the practice here. It is an approximation which is probably not right and will, most likely, lead to the underestimation of the structural response. The modal response spectrum is

$$G_{qr}(f) = \frac{\left|H\ \ (f)\right|^2}{K_r^2} G_{Qr}(f)$$

in which $\left|H_r(f)\right|^2 = \dfrac{1}{\left\{1-(f/f_r)^2\right\}^2 + \left\{2(\varsigma_{S,r}+\varsigma_{a,r})f/f_r\right\}^2}$

hence $\sigma_{qr}^2 = \int_0^\infty G_{qr}(f)df = \left(\dfrac{\rho B\overline{U}}{2K_r}\dfrac{dC_L}{d\alpha}\right)^2 \int_0^\infty G_w(f)\left|J_r(f)\right|^2 \left|H_r(f)\right|^2 df$

where the joint acceptance function is defined as

$$\left|J_r(f)\right|^2 = \int_L \int_L \widetilde{R}_w(y_1, y_2; f)\phi_r(y_1)\phi\ \ (y_2)dy_1 dy_2$$

and the mean-square response is given by $\sigma_z^2(y) \approx \sum_r \sigma_{qr}^2 \phi_r^2(y)$

[Example 3] Along-wind response of vertical line-like structure

Consider now a thin vertical structure, such as a tower, of height H, exposed to a boundary layer wind. The mean speed distribution is generally given by

$$\overline{U}(z) = \overline{U}_H\left(\frac{z}{H}\right)^\alpha$$

Applying the modal analysis as before,

$$x(y,t) = \sum_r \phi_r(z)q_r(t) \qquad \text{and} \qquad \sigma_x^2(z) \approx \sum_r \overline{q_r^2}\phi_r^2(z)$$

The expressions leading to $\overline{q_r^2}$ are the same as before, except the aerodynamic damping can be approximately given by

$$\varsigma_{a,r} \approx \frac{1}{M_r \omega_r} \int_0^H \frac{\overline{P}(z)}{\overline{U}(z)} \phi_r^2(z) dz \qquad \overline{P}(z) = \frac{\rho \overline{D} C_D}{2} \overline{U}^2(z)$$

Spectral density for the generalized force $Q_r(t)$ is given by

$$G_{Qr}(f) = \int_0^H \int_0^H G_P(z_1, z_2; f) \phi_r(z_1) \phi_2(z_2) dz_1 dz_2$$

where

$$G_P(z_1, z_2; f) = \sqrt{G_P(z_1, f) G_P(z_2, f)} \cdot \tilde{R}_P(z_1, z_2; f)$$

in which

$$G_P(z, f) = \left\{ \frac{2\overline{P}(z)}{\overline{U}(z)} \right\}^2 \left| X_a(f) \right|^2 G_u(z, f) \qquad \text{where}$$

$$G_u(z, f) \approx G_u(H, f)$$

and

$$\tilde{R}_P(z_1, z_2; f) \approx \tilde{R}_u(z_1, z_2; f) \approx \exp\left\{ -c_V \frac{f|z_1 - z_2|}{\overline{U}(z_m)} \right\} \qquad z_m = \frac{z_1 + z_2}{2}$$

Hence

$$\sqrt{G_P(z_1 f) G_P(z_2, f)} = 4 \frac{\overline{P}(z_1)}{\overline{U}(z_1)} \frac{\overline{P}(z_2)}{\overline{U}(z_2)} \left| X_a(f) \right|^2 G_u(f)$$

and

$$\frac{\overline{P}(z)}{\overline{U}(z)} = \frac{\rho \overline{D} C_D}{2} \overline{U}(z) = \frac{\overline{P}_H}{\overline{U}_H} \frac{\overline{U}(z)}{\overline{U}_H} \qquad \overline{P}_H = \frac{\rho \overline{D} C_D}{2} \overline{U}_H^2$$

Substituting these expressions

$$G_{Qr}(f) \approx \left\{ \frac{2\overline{P}_H}{\overline{U}_H} \right\}^2 G_u(f) \left| X_a(f) \right|^2 \int_0^H \int_0^H \tilde{R}_u(z_1, z_2; f) \phi_r(z_1) \phi_r(z_2) \frac{\overline{U}(z_1) \overline{U}(z_2)}{\overline{U}_H^2} dz_1 dz_2$$

$$\left| J_r(f) \right|^2 = \int_0^H \int_0^H \frac{\overline{U}(z_1) \overline{U}(z_2)}{\overline{U}_H^2} \exp\left\{ -c_V \frac{f|z_1 - z_2|}{\overline{U}_m} \right\} \phi_r(z_1) \phi_r(z_2) dz_1 dz_2$$

$$\approx \frac{1}{(1+\alpha)^2} \frac{1}{1 + \frac{c_V}{3} \frac{fH}{\overline{U}_H}} \qquad \text{when} \qquad \phi(z) = \frac{z}{H} \qquad c_V = 8 \text{ (say)}$$

[Example 4] Vertical structure with horizontal extent

In reality, it becomes probably necessary to consider a substantial width of the structure in the above analysis. As a result, the joint acceptance function is now considered in horizontal direction as well as the vertical direction as follows:

$$G_Q(f) = \left(\frac{2\overline{P}_H}{\overline{U}_H}\right)^2 |J_V(f)|^2 |J_H(f)|^2 G_u(f)$$

where

$$|J_V(f)|^2 \approx \frac{1}{(1+\alpha)^2} \frac{1}{1+\frac{8}{3}\frac{fH}{\overline{U}_H}} \quad \text{and} \quad |J_H(f)|^2 \approx \frac{1}{1+10\frac{fB}{\overline{U}_H}} \text{ (say)}$$

Hence

$$\left(\frac{\sigma_x}{\overline{X}}\right)^2 = 16(1+\alpha)^2 I_u^2 \int_0^\infty |J_V(f)|^2 |J_H(f)|^2 \frac{G_u(f)}{\sigma_u^2} df$$

$$\approx 16(1+\alpha)^2 I_u^2 \left[|J_V(f_0)|^2 |J_H(f_0)|^2 \frac{G_u(f_0)}{\sigma_u^2} \int_0^\infty |H(f)|^2 df + \int_0^\infty |J_V(f)|^2 |J_H(f)|^2 \frac{G_u(f)}{\sigma_u^2} \right]$$

and

$$\int_0^\infty |H(f)|^2 df = \frac{\pi f_0}{4\varsigma_S}$$ f_0 = eigen frequency, ς_S = structural damping

$$\int_0^\infty |J_V(f)|^2 |J_H(f)|^2 \frac{G_u(f)}{\sigma_u^2} df \approx \int_{-\infty}^{\ln f} \frac{f G_u(f)}{\sigma_u^2} d(\ln f) \qquad f = \frac{3\overline{U}_H}{8H}$$

This formulation has been adopted by the National Building Code of Canada for the consideration of wind load on tall buildings.

4.3 Aerodynamic Admittance

Aerodynamic admittance is a transfer function to express how effectively the frequency characteristics of velocity fluctuation are picked up by the aerodynamic force components. Naturally, it depends upon the geometrical configuration of the body exposed to the flow turbulence. Even if an ideally two-dimensional strip assumption is considered, since there are two velocity components (u, w) and each of them has its own effects on three force components (L, D, M_p), six different admittance functions are conceivable for each cross-section of the body, though probably only three of them would have practical significance.

It is very difficult to make analytical estimation of these functions, though there are a few cases considered as follows:

Sears function

A classical example is an aerofoil that is facing a sinusoidal change of w-component. Sears (1941) formulated this case as follows:

$$L = \frac{\rho \overline{U}^2}{2} B \frac{dC_L}{d\alpha} \frac{w(t)}{\overline{U}} \Theta(k) \qquad \Theta(k) = \text{the Sears function}$$

where $k = \frac{\pi f B}{\overline{U}}$ and $w(t) = w_0 \sin \omega t$. The Sears function is analytically given by

$$\Theta(k) = \{J_0(k) - iJ_1(k)\}C(k) + iJ_1(k) \qquad C(k) = F(k) + iG(k)$$

or

$$|\Theta(k)|^2 = (J_0^2 + J_1^2)(F^2 + G^2) + J_1^2 + 2J_0 J_1 G - 2J_1^2 F$$

$$\approx \frac{1}{1 + 2\pi k} \qquad \text{[Liepmann, 1952]}$$

Davenport's formulation

The admittance function between $u(t)$ and drag force $D(t)$ was considered by Davenport (1964) by integrating the velocity correlation over the surface. When the pressure correlation over a flat surface placed normal to the flow is approximated by

$$\tilde{R}_u(f) \approx \exp\left(-k \frac{f\Delta}{\overline{U}}\right) \qquad k \approx 7 \text{ (say)}$$

The admittance function is

$$|\mathrm{X}(f)|^2 = \frac{1}{A^2} \int_0^D \int_0^D \int_0^B \int_0^B \tilde{R}_u(\Delta y) \tilde{R}_u(\Delta z) dy_1 dy_2 dz_1 dz_2$$

where

$$\Delta y = |y_1 - y_2| \quad \text{and} \quad \Delta z = |z_1 - z_2|$$

When $B = D = \sqrt{A}$ (a square plate), this formulation results in

$$|\mathrm{X}(f)|^2 = \left\{ \frac{2}{(k\xi)^2} \left(k\xi - 1 + e^{-k\xi}\right) \right\}^2 \qquad \xi = \frac{f\sqrt{A}}{\overline{U}}$$

Vickery's expression

Following a similar concept as before, Vickery (1965) came up with an expression as follows:

$$|\mathrm{X}(f)|^2 = \frac{1}{\left\{1 + \left(2f\sqrt{A}/\overline{U}\right)^{4/3}\right\}^2}$$

Measured Results

There have been a number of attempts to measure the aerodynamic admittance functions experimentally. The method in general is to take the ratio of the total force spectrum on a section model to the velocity spectrum detected simultaneously. However, since the testing conditions cannot be perfectly two-dimensional, often there is a problem of having two different effects on the results mixed up: two-dimensional frequency transfer effects of the sectional force at any particular section and the spanwise coherence of it. In order to avoid this problem, the pressure distribution around the sections along very narrow strips has to be detected to measure both of these effects separately. The development of a fast pressure-scanning device has made it possible only recently.

There are indications that actual 2D admittance may be much less than it has been believed but, at the same time, the spanwise force correlation seems to be much higher than that of velocity components.

4.4 Peak Factor

The largest instantaneous value of a stationary random function within a specific sampling period can be estimated from the statistical characteristics of the process as a ratio to the value of the standard deviation. Consider first a stationary random process $x(t)$ having a normal probability distribution with the mean a_x and standard deviation σ_x. It is convenient to define the reduced variate $\eta = (x - a_x)/\sigma_x$, in which case the probability density of the process is

$$P(\eta) = \frac{1}{\sqrt{2\pi}} \exp(-\eta^2) \qquad (1)$$

The expression for the cumulative distribution function for the maxima of the stationary random process was first derived by Cartwright and Longuet-Higgins. They have shown that, for a large value of η, and $\varepsilon \neq 1$, the distribution function $q(\eta)$ can be approximately given by

$$q(\eta) \approx \sqrt{1-\varepsilon^2} \exp\left(-\frac{\eta^2}{2}\right) \qquad (2)$$

in which

$$\varepsilon = \sqrt{1 - \frac{m_2^2}{m_0 m_4}} \qquad \text{and} \qquad m_r = \int_0^\infty n^r G(n) dn \qquad (3)$$

where $G(n)$ is the power spectrum of the random process. Davenport used this expression and also by applying the Rice's theory to give the number of maxima, N, during a given period, T, as

$$N = \sqrt{m_4/m_2} \qquad (N \to \infty) \qquad (4)$$

reached the probability density for the largest maxima as

$$P_{\max}(\eta)d\eta = \exp(-\xi)d\xi \tag{5}$$

where $\xi = Nq(\eta) = \nu T \cdot \exp\left(-\frac{\eta^2}{2}\right)$ and $\nu = \sqrt{\frac{m_2}{m_0}}$ (6)

or, inversely

$$\eta = \sqrt{2\log_e \nu T - 2\log_e \xi}$$

$$= \sqrt{2\log_e \nu T} - \frac{\log_e \xi}{\sqrt{2\log_e \nu T}} - \frac{(\log_e \xi)^2}{2(2\log_e \nu T)^{3/2}} + \dots \tag{7}$$

Using these expressions, certain properties of the distribution can be decided. The mean, for example, is

$$\overline{\eta_{\max}} = \int_{-\infty}^{\infty} \eta P_{\max}(\eta)d\eta = \int_{-\infty}^{\infty} \eta e^{-\xi} d\xi = \sqrt{2\log_e \nu T} + \frac{\gamma}{\sqrt{2\log_e \nu T}} \tag{8}$$

where $\gamma = 0.5772...$ is the Euler's constant and T is the sampling period. Since the mean square value is expressed as

$$\overline{\eta_{\max}^2} = \int_{-\infty}^{\infty} \eta^2 e^{-\xi} d\xi$$

the standard deviation is given by

$$\sigma(\eta_{\max}) = \overline{\eta_{\max}^2} - \left(\overline{\eta_{\max}}\right)^2 = \frac{\pi}{\sqrt{6}}\sqrt{2\log_e \nu T} \tag{9}$$

The mode, which is found by the maximum of equation (5), is given by

$$\text{mode}\,(\eta_{\max}) = \sqrt{2\log_e \nu T} \tag{10}$$

and the probability density is $\sqrt{2\log_e \nu T}\big/ e$.

Davenport has commented on this theory as follows: ”The quantity, ν , can be interpreted physically as the frequency at which most of the energy in the spectrum is concentrated. Thus, with lightly damped systems, this will generally be close to the natural frequency when we are talking about the gust induced structural response, for example. Furthermore, in wind-loading problems, we are generally concerned with predicting the largest value likely to occur within a period such as an hour. These conditions suggest that, in the main, the values of νT of practical interest lie between 10^2 and 10^4. The probability density functions for νT = 10^2, 10^3 and 10^4 are shown in the figure below. For comparison, the distribution of the population is also shown in the figure. The figure emphasizes the narrowness of the distribution of largest values, particularly for larger values of νT . It points to the fact that, in many problems, it is probably sufficient to assume the largest value equal to the mean largest value and ignore the variabiliy. From this figure, it is seen that in practical cases the peak value during an hour is likely to be 3.5–4.5 standard deviations in excess of the mean value." [Davenport 1964]

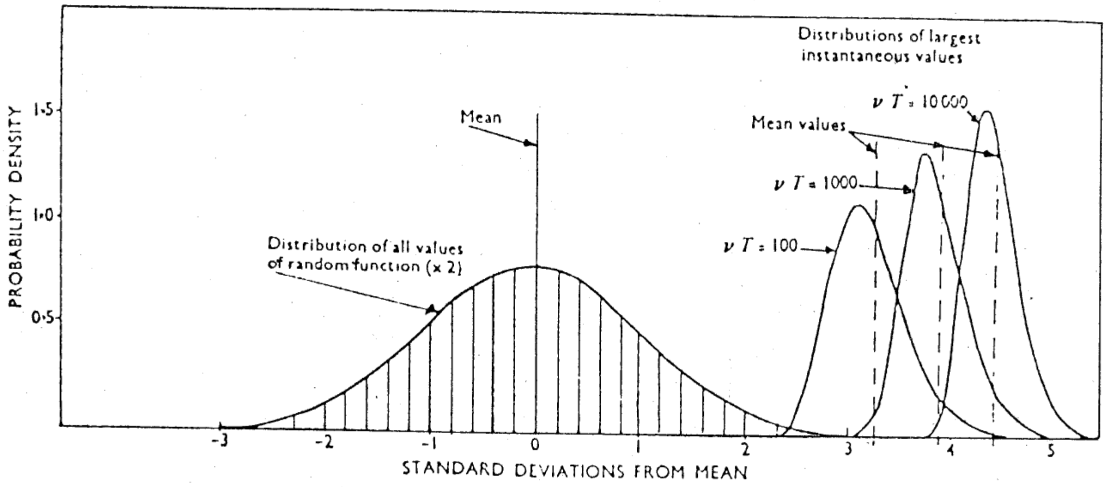

Relationship of distribution of largest instantaneous values of random process to the distribution of all values for different values of νT .

4.5 Time Domain Analysis

The formulation of buffeting analysis was first developed in the time domain just like any other dynamic analysis. However, its development has been done by linearizing them and solving them in the frequency domain and this practice is still going on. In more recent years, the development of computer-aided flying and the active flutter control of aircraft wings have pushed the need to express the unsteady aerodynamic forces in time variant manners. Very efficient algorithms have been developed in the time domain to perform the servo-control of flaps based on aerodynamic data obtained experimentally in the frequency domain.

In the field of bridge aerodynamics, too, the frequency domain approach has been predominantly applied to solve the problem of wind effects even if the original formulation was in the time domain. As briefly stated in 3.2, in 1970s, Scanlan et al. first worked on solving the problem entirely in the time domain, introducing the inditial functions, which were put forward earlier in the aeronautical field. It is, however, only recently that much effort has been invested in developing efficient time domain formulation of the unsteady aerodynamic forces that could be combined with finite element models of the structure and could include all the nonlinearitis that have been omitted in the past. This development has been justified with the planning of very long bridges such as the bridge over the Stretto di Messina and the Akashi Kaikyo.

The problem of the formulation of time varying wind load in the time domain can be summarised as follows:

1. The bridge deck is excited by the instantaneous wind turbulence at a certain time t but is also influenced by what happened between the eddies in the flow and the deck at time $t-\tau$. It is to say that the wind loading involves a memory effect or that there exists a phase lag between the excitations and actual aerodynamic forces themselves. In the frequency domain this memory effect is expressed by aerodynamic admittance functions.

2. A moving fluid induces the initial forcing on a deck. At the same time, however, the motion of a deck interacts with the fluid media and induces additional forces, which are not in phase with the body motion. These motion-dependent, self-excited forces can be expressed in one or several degrees of freedom, either independent of or coupling with each other.

3. The aerodynamic forces are far from being fully correlated along the bridge span. The span-wise correlation of the approaching wind fluctuations, combined with the mode shapes of the deck, governs the spanwise distribution of the aerodynamic forcing. Also, the spanwise coherence of the aerodynamic forces is not necessarily identical to that of the approaching flow turbulence, as opposed to what has been often implied by the strip assumption. It appears that the spanwise coherence of the forces also depends upon the deck geometry, its aspect ratio in particular, length scales of turbulence and turbulence intensity.

4. The simulation of the approaching wind has also its own share of difficulties. An adequate simulation should model all the one-point and two-point statistics of the wind fluctuations. Locally, it should respect the first and second moments for each wind component as well as autospectra and cross-spectra of all velocity components. A discussion of this aspect is found in the literature. Needless to say

this is a subject of primary importance because , no matter how good the wind loading algorithm is, if the input wind field is not adequate, the output will suffer significantly.

A brief literature review regarding the time domain analyses in bridge aerodynamics is given below. The approaches found in literature can be classified in five categories: 1) quasi-steady aerodynamics; 2) corrected quasi-steady aerodynamics; 3) indicial functions (Fourier transform); 4) rational function approximations (Laplace transform); and 5) equivalent oscillator (neural network and black box).

Miyata et al. (1995) clearly presented the advantages of the time domain approach for the prediction of the wind action on long span bridges when combined with a finite element modelling of the structure. The formulation used here is fairly simple and very much along the line of the original formulation by Davenport. Quasi-steady aerodynamics are assumed as well as the strip assumption. Kovacs et al. (1992) has a similar approach except that the finite element model of the structure includes structural nonlinearities for large deflections in order to evaluate the ultimate state conditions. Though the limitations of these approaches with quasi-steady aerodynamics are numerous, Miyata et al. (1995) obtained an impressively good agreement of their results with the wind tunnel test results for a very large suspension bridge. The limitations are: a) non-inclusion of the motion-induced forces besides the quasi-steady expression of the aerodynamic dymping in the wind load model; b) memory function expressed as an aerodynamic admittance filtering the wind field simulation; c) inadequate representation of the spanwise coherence of the forces; and d) the assumption that the centre of the aerodynamic lift is fixed at a quarter of the deck width from the deck centreline. This last assumption allows the inclusion of the torsional motion in the definition of the apparent angle of attack or in the relative wind velocity as shown in 2.2. The position of the aerodynamic centre is known to vary with reduced velocity.

The work by Diana et al. (1992-95) in relation to the studies for the proposed bridge over the Stretto di Messina has taken a similar approach with the exception that some of the above limitations have been removed by the development of a "corrected" quasi-steady theory. Here, the motion-induced forces are fully included in the formulation of the aerodynamic forces via the experimentally determined aerodynamic derivatives. The location of the aerodynamic centre is also determined from the aerodynamic derivatives. Note that Diana et al. have proposed a different normalization of the aerodynamic derivatives so that they can be interpreted as a deviation from the quasi-steady expression. At high reduced velocities, the process is almost quasi-steady and the aerodynamic derivatives, by their definition, tend to be unity.

To include the motion-induced forces, Diana et al. (1992) proposed an equivalent linearization, for each reduced velocity, of the following type:

$$C_L^*(\alpha_e) = C_{Ls}(\alpha_0) + \int_{\alpha 0}^{\alpha e} K_L^* d\alpha_z \qquad (1)$$

where $C_L^*(\alpha_e) =$ corrected aerodynamic force coefficient;

$C_{Ls}(\alpha_0) =$ static coefficient at angle α_0 of the equilibrium position; and

$K_L^* =$ aerodynamic derivatives (v.g., lift slope varying with reduced velocity).

Here α_e is defined as the apparent angle of attack based on the relationship

$$\alpha_e = \alpha - \frac{\dot{z}}{\overline{U}} - n\frac{B\dot{\alpha}}{\overline{U}} \tag{2}$$

where z and α represent respectively a vertical displacement and rotation of the deck, B the deck width, $\overline{U}$ the mean wind speed, and n is the position of the aerodynamic centre which is the function of reduced velocity. The formulation has been proved to be adequate in many ways, except when it deals with the response in higher vibration modes. The limitations attributed to the memory effects and the spanwise coherence of the forces have not been dealt with by Diana.

In a series of papers spanning over several years, Scanlan et al. (1972-75) described the use of indicial functions for the inclusion of the motion-induced forces in the time domain formulation of the aerodynamic forces. The formulation of self-excited force F_{Ls} can be read as follows:

$$F_{Ls} = \frac{\rho\overline{U}^2 B}{2}\frac{dC_L}{d\alpha}\int_0^s \left\{\Phi_L(s-\tau)\alpha'(\tau) + \Psi_L(s-\tau)\frac{z''(\tau)}{B}\right\}d\tau \tag{3}$$

where $\quad s = \dfrac{\overline{U}t}{B} \qquad (...)' \equiv \dfrac{d}{ds}$

$\Phi_L(s) =$ indicial response function due to a step change in angle of attack, and
$\Psi_L(s) =$ indicial response function associated with a step change in vertical velocity.

$\Phi_L(s)$ and $\Psi_L(s)$ could be in the form of

$$\Phi_L(s) = c_0 + c_1 \cdot \exp(c_2 s) + c_3 \cdot \exp(c_4 s) + ... \tag{4}$$

where the coefficients c_i are extracted by nonlinear least-square fitting of the experimentally obtained aerodynamic derivatives. Even though this approach appears to be efficient, very few examples of its application can be found in the literature.

More recently, Lin and Li (1993) proposed another model for the self-excited forces on a bridge deck based on the idea of indicial functions. The self-excited loads are expressed in terms of convolution integrals of response functions due to a unit impulse displacement, vertical and angular. These impulse response functions are obtained from the inverse Fourier transform of the frequency response functions of the form for the moment due to the change of the angle of attack α, for example:

$$\tilde{F}_{Ms}(\omega) = \rho B^2 \overline{U}^2 \left\{ c_1 + i \cdot c_2 \frac{\omega B}{\overline{U}} + \sum_{j,k} \frac{i \cdot c_j \frac{\omega B}{\overline{U}}}{c_k + i \cdot \frac{\omega B}{\overline{U}}} \right\} \tag{5}$$

$$F_{Ms}(\omega) = \rho B^2 \overline{U}^4 \omega^2 \left[A_3^*(K) + i \cdot A_2^*(K) \right] \tag{6}$$

where the coefficients c_j are obtained from nonlinear fitting of the experimentally determined aerodynamic derivatives $A_j^*(K)$ and $H_j^*(K)$. Li & He (1993, 1995) have presented a method to experimentally determine the coefficients c_j and consequently the impulse response functions. A complete example of the use of this formulation is given by Xiang et al. (1995) for the motion-induced forces. Comparisons are made between time domain predictuions and wind tunnel test results for the Shanton Bay Bridge. The agreement is remarkable, even though here also the buffeting forces are calculated using quasi-steady aerodynamics.

Fujino et al (1995), in dealing with the problem of active control of flutter for bridges, have formulated a method to express the motion-induced forces in the time domain. This method is directly inspired by the work in the aerospace industry. Rational function approximations are used to express the equation of motion of the deck in a linear time invariant state-space from where the unsteady aerodynamic forces do not depend explicitly on reduced velocity. The aerodynamic derivatives obtained from experiments are stored in tabular form in the reduced frequency domain and are approximated in the Laplace domain by rational functions and a series of coefficients. The rational functions are then inverse Laplace transformed to the time domain to solve the state-spaceequation of motion, Tiffany & Adams (1988). The level of accuracy is a function of the number of aerodynamic states used for the approximation, but once the numerical problems are solved this method appears to be effective and is currently used in aerospace applications, for example by Tewari & Brink-Spulink (1992).

Li & He (1995) have also presented a formulation of the unsteady forces that includes rational approximations for the motion-induced forces and the buffeting forces are expressed by convolution integral of impulse aerodynamic transfer functions determined experimentally from wind tunnel tests. An example of the calculations is given but no comparisons with measured aeroelastic response of a physical model are made. This method appears to be the most complete of the above described approach. Yagi's analysis (1997) is along the same line though the work was apparently carried out independent of any of the above.

Finally, Diana et al. (1995) have initiated research on new methods to express the aerodynamic forces in the time domain including buffeting, motion-induced forces and vortex-shedding forces using numerical models comprised of the bridge deck and an equivalent oscillator. The new methods include "black-box model", a neural network model and sophisticated parameter identification algorithms using an extended Kalman filter. Preliminary evaluations of the methods have shown satisfactory results, especially for nonlinear phenomena such as vortex-shedding induced oscillations.

References:

Béliveau, J.G., *Proc. 2nd US Nat. Conf. on Wind Engng*, Fort Collins, 1975, Paper IV-21.

Cartwright, D.E. & Longuet-Higgins, M.S., Statistical distribution of the maxima of a random function, *Proc. Roy. Soc.* (A237) 1956, pp.212-232.
Chen, X.Z., Matsumoto, M. & Kareem, A, Time domain flutter and buffeting response analysis of bridges, *Proc. ASCE* (126) EM1, 2000, pp.7-16.
Chen, X.Z., Matsumoto, M. & Kareem, A., Aerodynamic coupling effects on flutter and buffeting of bridges, *Proc. ASCE* (126) EM1, 2000, pp.17-26.
Davenport, A.G., The buffeting of suspension bridge by storm winds, *Proc. ASCE* (83) ST3, 1962, pp.233-268.
Davenport, A.G., Note on the distribution of the largest value of a random function with application to gust loading, *Proc. ICE* (28) 1964, pp.187-196.
Davenport, A.G. & Wardlaw, R.L., *LR416*, NRCC, 1964.
Diana, G. et al., Suspension bridge parameters identification in full scale tests, *JWEIA* (41) 1992, pp.165-176.
Diana, G. et al., Comparison between wind tunnel test on a full aeroelastic model of the proposed Messina Bridge and numerical results, Pt.II, *Proc. 3rd Asia-Pasific Symp. on Wind Engng*, Hong Kong, 1993, Vol.1, pp.137-142.
Diana, G., Cheli, F. & Resta, F., Time domain aeroelastic force identification on bridge decks, *Proc. 9th ICWE*, New Delhi, 1995, Vol.2, pp.938-949.
ESDU, *Fluctuating loads and dynamic response of bodies and structures in fluid flow - background information*, Item No.77032, Engineering Science Data Unit, 1985 (amend.B).
Falco, M., Curami, A. & Zasso, A., Nonlinear effects in sectional model aeroelastic parameters identification, *JWEIA* (42) 1992, pp.1321-1332.
Fujino, Y., Wilde, K., Masukawa, J. & Bhartia, B., Rational function approximation of aerodynamic forces on bridge deck and its application to active control of flutter, *Proc. 9th ICWE*, New Delhi, 1995, Vol.2, pp.994-1005.
Irwin, P.A., Wind tunnel and analytical investigations of the response of Lions' Gate Bridge to a turbulent wind, *LTR-LA*-210, NRCC, 1977.
Jakobsen, J.B., Fluctuating wind load and response of a line-like structure with emphasis on motion-induced wind forces, *Ph.D. thesis*, Norges Tekniske Høgskole, 1995.
Kovacs, I., Svensson, H.S. & Jordet, E., Analytical aerodynamic investigation of the cable-stayed Helgeland Bridge, *Proc. ASCE* (118) ST1, 1992, pp.147-168.
Larose, G.L., The response of suspension bridge deck to turbulent wind: the taut strip approach, *M.E.Sc. thesis*, Univ. of Western Ontario, 1992.
Larose, G.L., *Ph.D. thesis*, Technical University of Denmark, June 1997.
Li, M.S., Buffeting response of large bridges in atmospheric turbulence, Ph.D. thesis, Southwestern Jiatong University, Chengdu, 1993.
Li, M.S. & He, D.X., Buffeting response of large bridges, *Proc. 9th ICWE*, New Delhi, 1995, Vol.2, pp.893-904.
Liepmann, H.W., On the application of statistical concepts to the buffeting problem, *JAS* (19) 12, 1952, pp.793-800.
Lin, Y.K. & Li, Q.C., New stochastic theory for bridge stability in turbulent flow, *Proc. ASCE* (119) EM1, 1993, pp.113-127.
Mann, J., The spatial structure of neutral atmospheric surface-layer turbulence, *JFM* (273) 1994.
Miyata, T. et al., Analytical investigation on the response of a long suspension bridge under gusty wind, *Proc. 9th ICWE*, New Delhi, Jan. 1995, Vol.2, pp.1006-1017.
Rice, S.O., Mathematical analysis of random noise, *Bell Tech.* (18) 1944, pp.282-232 & (19) 1945, pp.46-156.

Scanlan, R.H., Béliveau, J.G. & Budlong, K.S., Flutter and aerodynamic response considerations for bluff objects in a smooth flow, *Proc. IUTAM-IAHR Symp. on Flow-Induced Structural Vibrations*, Karlsruhe, 1972, pp.339-354.

Scanlan, R.H., Béliveau, J.G. & Budlong, K.S., *Proc. ASCE* (100) EM4, 1974, pp.657-672.

Tanaka, H. et al., Modelling of wind action on bridges, *DMI Res. Rept*. 94869, Danish Maritime Institute, Mar. 1996.

Tewari, A. & Brink-Spulink, J., Multiple-pole rational function approximations for unsteady aerodynamics, *J. Aerocraft* (30) 3, 1992, pp.426-428.

Tiffany, S.H. & Adams, W.M., Nonlinear programming extensions to rational function approximation methods for unsteady aerodynamic forces, *NASA Tech. Paper* 2776, 1988.

Xiang, H.F., Liu, C.H. & Gu, M., Time domain analysis for coupled buffeting response of long span bridges, *Proc. 9th ICWE*, New Delhi, 1995, Vol.2, pp.881-892.

Yagi, T., *D.Tech. thesis*, Kungl Tekniska Högskolan, Stockholm, 1997.

Vickery, B.J., *NPL Aero Rept*.1143, 1965.

Chapter 5 Vortex Induced Oscillation

5.1 General Characteristics

Vortex induced vibration is induced by vortices of air flow created by the interaction of wind and the structure. When an aerodynamically bluff body is exposed to wind, a trail of alternating vortices, the Kármán vortices, is often found in its wake, formed by the flow separated from the body. There is also a fluctuating lift force acting on the body corresponding to the formation of vortices. As a result, when the frequency of vortex formation is close to the structure's eigen-frequency, there will be a resonant vibration. This is the most fundamental concept of vortex excitation. However, once the vibration starts, the body motion itself will influence on the flow behaviour, which results in the more complicated interaction of flow and structure.

Unlike the case of buffeting, the vortex excitation is usually observed in one or more limited wind speed ranges and its amplitude is limited without divergence. The vibration is usually characterised by a narrow-band frequency spectrum and somewhat regular amplitude. The bridge deck usually vibrates in vertical bending but sometimes in torsion, too. The phenomenon is known to be sensitive to the magnitude of structural damping and also to the existence of wind turbulence. Truss-stiffened bridges are, unless they are equipped with high-solidity railings or parapets, expected to be free of any serious vortex excitation.

Vortex induced oscillation of bridge decks has been so frequently observed that it usually consists of the primary concern when the wind stability of bridge is considered. It is often regarded as a relatively easy matter that can be determined by carrying out simple section model wind tunnel tests. It is mainly because the design criteria applied to this phenomenon often simply ask if a section is "good" or "bad", meaning whether or not any appreciable vortex induced response would be expected in possible wind speed range for a given structural damping. However, for more exact assessment, the prediction has to indicate the level of actual response qualitatively in relation to damping and wind characteristics.

Obviously the most reliable method of prediction at this point is to use an aeroelastic model of the whole bridge with properly simulated natural wind conditions. A possible problem for this case is the wind speed. Often the available wind speed range of the wind tunnel is too high for the proper measurement. On the other hand, if the section model tests are projected, question still remains if a reliable response prediction is obtainable from the test results.

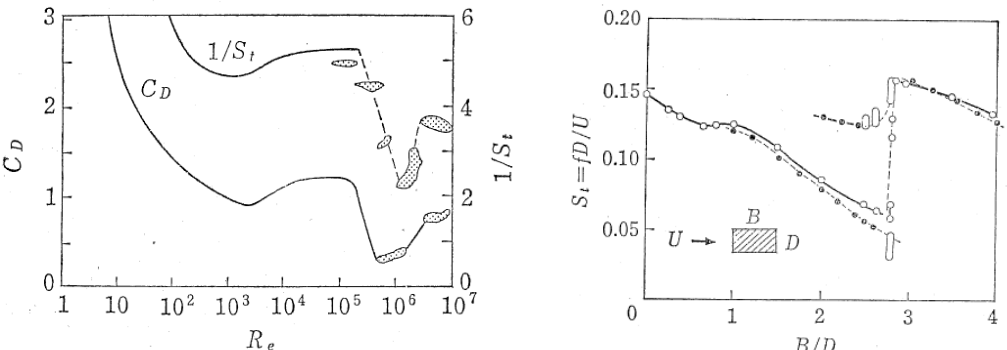

(a) Circular cylinder (b) Rectangular prisms

Fig.5.1 Strouhal number versus Reynolds number.

5.2 Analytical Prediction

(1) <u>Forced vibration model</u>

The most classical understanding of vortex shedding excitation is to consider it as a resonance with the aerodynamic forces caused by the periodic shedding of vortices alternately from the upper and lower surfaces of the deck. From this understanding, the following two most fundamental dimensionless parameters are derived:

$$St = \frac{f \cdot d}{\overline{U}} = \text{Strouhal number} \tag{1}$$

$$Sc = \frac{m\varsigma}{\rho d^2} = \text{Scruton number} \tag{2}$$

where $f =$ the frequency of vortex formation, which coincides with the natural frequency

$d =$ a representative linear dimension of the deck cross-section, usually the depth

$\overline{U} =$ the mean wind speed

$m =$ the deck mass per unit deck length

$\varsigma =$ the critical damping ratio of the structure, and

$\rho =$ the air density.

Considering ordinary plate-girder or box-girder bridge decks, the Strouhal number is typically in the range of 0.07 to 0.14. The simplest analysis is to assume a simple harmonic fluctuating force

$$\hat{L}(y,t) = \frac{\rho \overline{U}^2}{2} \cdot d \cdot \hat{C}_L \sin(2\pi f_S t) \tag{3}$$

which works on a two-dimensional section of the bridge all through the span. Also, the lift forces are assumed to be fully correlated along the bridge span. The peak response amplitude $\hat{z}$, if it is the case, is simply given by

$$\frac{\hat{z}}{d} = \left(\frac{U_R}{4\pi}\right)^2 \frac{\hat{C}_L}{Sc} \qquad \text{where} \qquad U_R = \frac{1}{St} = \frac{\overline{U}}{f \cdot d} \tag{4}$$

$\hat{C}_L$ is a function of the cross-sectional shape, the Reynolds number, the scale of turbulence and the structural aspect ratio, but is typically in the range of 0.2 to 0.4 and is independent of the response amplitude as a first approximation. Note that the deck mass may not be constant along the span in reality. Generally speaking, there is also effect of vibration mode, $\psi_i(y)$. Considering these factors, m in (2) should be replaced by an effective mass defined as follows:

$$m_e = \frac{\int_L m(y)\psi_i^2(y)dy}{\int_L \psi_i^2(y)dy} \tag{5}$$

(2) Factors to influence on the behaviour

There are some deviations from the above explanation when the vortex excitation is observed in reality. Three significant issues are as follows:

Frequency Locking: From eq.(1), the frequency of vortex formation is proportional to the mean wind speed. However, once the vibration starts, the motion of the body tends to control the flow pattern around the body and, as a result, the vortex shedding becomes synchronized with the vibration frequency, which does not follow the Strouhal law. The vortex frequency stays constant over a specific range of wind speed. This situation is called the locked-in phenomenon, which indicates the aspect of self-excited vibration rather than a simple forced vibration and resonance.

Correlation length: The vortex excitation mechanism is not really uniformly distributed along the whole bridge span; i.e., the cross-correlation of the exciting forces decreases along the bridge axis. Because of the lock-in effects, the excitation force has its maximum at the point of the antinode of the mode shape. The general tendency is that the correlation increases with the increasing vibration amplitude and decreases with the flow turbulence.

Flow turbulence: The flow turbulence existing in the approaching wind tends to disorganize the regular pattern of excitation forces and thus decreases the response level. This is generally observed in all wind tunnel tests for vortex excitation and, as a result, there is almost always a high expectation of engineers that the vortex shedding excitation observed in wind tunnel tests could be averted, or at least less in magnitude, in reality because of the wind turbulence which inherently exist in natural wind. Past experience is that the flow turbulence at the bridge site is not necessarily always so much as it is estimated for buffeting prediction, and the magnitude of vortex excitation can be just as high as it is predicted by wind tunnel tests with smooth flow.

(3) More refined method

Experience has shown that even when the flow is smooth and d is uniform, the fluctuating lift force is not strictly periodical but has a narrow-band spectrum over frequencies adjacent to the Strouhal frequency, f_S, where f_S is again defined by $St \cdot \overline{U}/d$. Large scale turbulence in approaching flow can be considered as a slowly varying mean speed, $\overline{U}$, which affects on the central frequency f_S. Thus, if the force fluctuation in smooth flow is sinusoidal, Gaussian turbulence would cause the Gaussian form spectrum of the lift force. Hence,

$$\frac{f \cdot G_L(f)}{\sigma_L^2} = \frac{f/f_S}{b\sqrt{\pi}} \exp\left\{-\left(\frac{1-f/f_S}{b}\right)^2\right\} \tag{6}$$

where $\sigma_L =$ rms lift force
$b =$ a bandwidth parameter.

The bandwidth parameter b also primarily depends on the large scale turbulence. The full-scale experience indicates the approximate expression of $b = 0.10 + 2\sigma_u/\overline{U}$. It also suggests a fairly narrow-band, typically 80% of the variance lying within a frequency range of $\pm 20\%$ of f_S. The above spectrum is expected to fit over the frequency range of $f_S(1 \pm b)$ (Vickery 1994).

The spectrum of $Q_i(t)$ can be given in terms of the spectrum of $L(y,t)$ and its normalized co-spectrum as follows:

$$G_{Qi}(f) = \int_L \int_L \sqrt{G_L(y_1, f) G_L(y_2, f)} \cdot \tilde{R}_L(y_1, y_2) \psi_i(y_1) \psi_i(y_2) dy_1 dy_2 \tag{7}$$

in which, $G_L(y,f)$ is given by eq.(6). $\tilde{R}_L(y_1, y_2)$ is the span-wise correlation of the fluctuating lift forces acting on a stationary structure. The peak amplitude is typically given by two times rms for a well-developed vortex shedding excitation.

Span-wise correlation:

The span-wise correlation decays with turbulence and improves significantly with the increase of vibration amplitudes. However, where the amplitudes of structural motion are large enough to have significant effects of them, the effect of motion-dependent aerodynamic damping becomes even more predominant in determining the response level. The measured correlation for the case of vortex excitation of bridge decks is badly missing. If any new experimental results would become available, the reference should be made to them. With the absence of any reliable information, it can be taken as unity for the given span length, as a conservative assumption.

Aspect ratio, turbulence etc.:

The Strouhal number is dependent upon the surface roughness, Reynolds number, flow turbulence and the aspect ratio $\Lambda = l/d$ of the structure. A wishful idea here is that very little effects are expected of Reynolds number at its practical range. The effect of aspect ratio is indicated in some references. The Strouhal number for typical highway bridge sections is usually in the range of $1/6.5$ to $1/13$ and tends to decrease slightly with roughness and increase with turbulence intensity.

The lift force coefficient is considered to be strongly influenced by the intensity of turbulence and also by the scales of turbulence when they are of the same order or less than the width of the structure. Not much is known on these points for typical bridge deck sections. Equivalent knowledge for chimneys is better available.

The proposed British code in the lest of references has suggested to formulate a characteristic excitation parameter, $C_L/(St)^2$. The order of magnitude of the rms lift coefficient, σ_{CL} , is known to be 0.1 to 0.2.

Motion induced forces:

The motion dependent forces can be represented by

$$L_z(y,t) = \frac{\rho \overline{U}^2}{2} \left(\frac{\omega d}{\overline{U}} \right)^2 \left\{ H_4^* z + H_1^* \frac{\dot{z}}{\omega} \right\} \tag{8}$$

where, generally speaking, the aerodynamic coefficients or derivatives H_1^*, H_4^* are amplitude dependent. They can be decided only by experimental means. H_1^* would decide the magnitude of aerodynamic damping.

The application of this idea particularly for cylindrical chimney stacks is more elaborated, for example, by Vickery (1994) and Ruscheweyh (1994).

5.3 Typical box sections applicable to bridges

The critical reduced speed to give the maximum response for typical box sections has been suggested as follows (Wyatt 1981):

B/D	$(U/fD)_{cr}$
<1.25	6.5
1.25–10	5.5+0.8·B/D
>10	13.5

B and D in this table indicate the width and depth of the box girders, and $\overline{U}$ is the mean wind speed. Exact prediction of dynamic response amplitude is difficult unless the aerodynamic lift force is exactly known. However, based on the past experience, a simple analysis has been proposed by the Hanshin Expressway Authority, Japan, as follows (Miyata 1997):

Consider a typical box-girder highway bridge. Applying 2D analysis,

$$m\ddot{y} + c\dot{y} + ky = \frac{\rho \overline{U}^2}{2} BC_L \frac{\dot{y}}{\overline{U}} \qquad \text{where} \qquad C_L \approx 0.625 \left(\frac{D}{B} \right)^2 \frac{B}{y} \tag{1}$$

which leads to the peak response amplitude of

$$\hat{y} = \frac{\rho \overline{U} B^2 C_L}{8\pi m f \varsigma} \tag{2}$$

Since $\left(\overline{U}/fD\right)_{cr} \approx 1.67\alpha$, (2) can be written as $$\hat{y} = K_R \frac{\alpha\rho D^2 B}{8\pi m\varsigma} \quad (3)$$

where K_R = Factor to consider the effect of flow turbulence (≤ 1)

and
$$\begin{aligned} \alpha &= 1.8 - 0.125 \cdot Sc \qquad (Sc < 4.8) \\ &= 1.2 \qquad\qquad\qquad\; (Sc > 4.8) \end{aligned} \quad (4)$$

Further to this analysis, the wind-tunnel experience has indicated the following range of maximum response amplitude:

$$\begin{aligned} \frac{y}{B} \cdot \frac{m\varsigma}{\rho BD} &\leq 0.024 \qquad (B/D \leq 5) \\ &\leq \frac{0.12}{B/D} \qquad (5 < B/D < 13) \end{aligned} \quad (5)$$

5.4 Control and Suppression

Structural vibration could be reduced by installation of vibration dampers, for example. However, in the evolution of the design of modern large bridges, there has been considerable development of aerodynamic performance of road decks, such as the use of shallower and/or closed sections and various edge treatments, to reduce, if not completely suppress, the dynamic bridge response. It is difficult to come up with a comprehensive theory regarding what would be the aerodynamically better cross-sections, but a practically important technique is to learn through the past experiences. Wardlaw (1992) has given a good review of successful experience, which is really a treasure box in this respect.

Generally speaking, the following statements could be made:

a) Instability of the bridge deck is often induced corresponding to the vortex formation at the sharp corners of the deck cross-section. If the deck has an open cross-section, therefore, it is usually a good idea to at least partially close it, or exrtend the sleeves or fairings from the sharp edges.
b) Another possibility is to install spanwise vertical buffles longitudinally inside the cavity, such as the space between the edge plates or boxes. They help reducing the formation of vortices.
c) Edge fairings are often found to be effective in reducing vortex excitation. They can be of a triangle shape pointing outside, or more streamlined.
d) The tower legs often have rectangular cross-sections, which tend to be subjected to vortex excitation. Installation of small vanes around the corner or removal of a sharp corner edge by giving a small cut-out is known to be effective in improving the aerodynamic performance.
e) In any of these provisions, the wind-tunnel is an indispensable tool for determining which method is effective and how their size should be.

References:

Advances in Wind Engineering (Krishna ed.) Wiley Eastern Ltd., 1994, pp.205-233.

Cook, N.J., *The designer's guide to wind loading of building structures* (2 vols.) Butterworths, 1985 & 1990.

Miyata, T. (ed.), *Wind Engineering of Structures*, JSSC, 1997 (in Japanese).

Ruscheweyh, H., Vortex excited vibrations, *Wind-Excited Vibrations of Structures* (Sockel ed.) Springer-Verlag, 1994.

Ruscheweyh, H., *Dynamische Windwirkung an Bauwerken* (2 vols.) Bauverlag GmbH, 1982.

Vickery, B.J., The response of chimneys and tower-like structures to wind loading, *Recent* Wardlaw, R.L., The improvement of aerodynamic performance, *Aerodynamics of Large Bridges* (Larsen ed.) Balkema, 1992, pp.59-70.

Wyatt, T.A. & Scruton, C., *Bridge Aerodynamics* (Wyatt ed.) Thomas Telford, 1981, pp.22-25.

Chapter 6 Cable Aerodynamics

6.1 Classification of Cable Vibrations due to Wind

The development of cable-stayed bridges as a structural choice for medium to long span bridges has been remarkable through the closing decades of the last century. As an essential component of the bridge superstructure, stay cables play an important role in the dynamic behaviour of cable-stayed bridges. Cables are extremely vulnerable to wind excitation mainly due to its low mechanical damping. Many efforts have been made during the past years to clarify the mechanisms of, and find solutions to, various types of wind-induced cable vibrations to alleviate engineering problems. Furthermore, with a rapid development of span length in cable-stayed bridges, even new types of instability particularly of the inclined cables have been identified, such as the rain-wind vibration, high-speed vortex excitation, and the dry inclined cable galloping, which have been all new challenges to bridge engineers. The purpose of the present chapter is to attempt a comprehensive state-of-the-art review of various types of wind-induced cable vibrations.

The wind-induced cable vibrations can be categorized into several groups, depending mainly upon their excitation mechanisms but also somehow upon their historical context. They can be as follows:

a) Vortex induced vibration, or aeolian oscillation;
b) Buffeting due to wind gust;
c) Classical galloping typically observed in cables with iced accretion;
d) Wake interference, or wake galloping and resonant buffeting;
e) Parametric excitation due to support motion;
f) Reynolds number related drag instability;
g) Rain-wind induced vibration;
h) High-speed vortex excitation; and
i) Dry inclined cable galloping.

The first two types of vibration are generally small in amplitude and possible fatigue failure would be the only engineering concern associated with them. The last three types are mainly related to inclined cables, such as bridge stay cables, and the rain-wind induced vibration is the one most frequently observed in reality. The excitation mechanism of rain-wind vibration has been made clearer in recent years, and some effective control methods have been successfully applied in practice. However, the last two types of motion are still much less understood and require more intensive research attention. The dry inclined cable galloping, in particular, would cause a very strong concern since they are to result in undesirably large amplitude motion and yet it is not fully understood precisely under what conditions this would occur and why.

6.2 Vortex Induced Vibration, or Aeolian Oscillation

This is a small amplitude vibration caused by vortex shedding and takes its name from the aeolian harp, an ancient Greek instrument functioned on the same mechanical principle. The basic mechanism of excitation is a resonance to the frequency of vortex shedding f_V, which is given by

$$f_V = St \cdot \frac{\overline{U}}{D} \qquad (1)$$

where $\overline{U}$ = the mean wind speed, D = the outer diameter of the cable. St is the Strouhal number, which is approximately 0.19 ~ 0.20 for a circular cross-section and the Reynolds number of ~10^5 or less. As a typical example, if D = 0.16 m and St = 0.19 are assumed, for the mean wind speed of $\overline{U}$ = 5~25 m/s, corresponding vortex shedding frequency is in the range of f_V = 10~50 Hz. Since the cable's fundamental frequency is often in the range of 0.2~2 Hz, the resonance occurs only with much higher harmonic modes with vibration frequencies of 10~50 Hz, where the mechanical self-damping is likely to be quite high. The maximum vibration amplitude usually does not exceed one cable diameter, peak-peak. Wind turbulence generally tends to reduce the response amplitude, even down to a half compared to the exposure to smooth air flow (Ehsan et al. 1990).

The same mechanism of wind excitation can cause much more serious engineering problems for towers, chimneys and bridge road decks. Both experimental and analytical investigation has been devoted to this topic and their outcomes have been reflected to the design codes in practice. However, vortex shedding excitation of cables is not a major concern for engineers except that it may cause fatigue damages near the cable clamps. For the case of power transmission lines, it is a common practice to install the Stockbridge-type dampers (Leblond & Hardy 1999) or helical surface rods around the conductor. It is noteworthy that the Stockbridge dampers also contribute in possible twist of cables but they also have serious problems of failure due to fatigue. For bridge cables, the viscous dampers are more commonly used. A novel device, the passive damper cable, has been proposed recently (Sauter et al. 2001). The slack nature of the damper cable exhibits large static hysteresis caused by inter-strand friction of the cable during bending motion, which is said to dissipate energy effectively.

6.3 Buffeting due to Wind Gust

Gust induced random vibration is generally not a very serious concern for structural cables except for the power transmission lines. There are a few fundamental references such as (ASCE Committee 1984) in this respect. The basic idea of its recommendation is to come up with a gust response factor for the prediction of dynamic response by a conventional buffeting analysis in the frequency domain. The procedure is based upon an earlier publication by Davenport (1979). Further improvement of its contents should include particularly the spanwise force correlation, wind yaw angle effects, and the longitudinal loads along the cable span.
For bridge cables, buffeting is generally a less serious problem. High tension of bridge stay cables generally helps to limit the amplitude of buffeting. Sometimes buffeting is observed as a result of wake interference, where the existence of upstream objects is the cause of disturbance for the downstream cables. Electric wires along the main cable of the Golden Gate Bridge exhibited vibration a couple of decades ago, which was probably buffeting of this kind. It has been pointed out (Virlogeux 1998) that wake buffeting could produce aerodynamic instability in bridges

when there are two parallel cable planes. If the time required for the wind flow to travel from the upstream plane to the downstream plane of cables is equal to a half of a cycle of the torsional vibration of the deck, it is conceivable that cable buffeting can enhance the deck vibration and cause the bridge instability, though, in the authors' knowledge, this has never been an issue in reality. This mechanism is touched again in 6.5 below.

6.4 Galloping of Iced Cables

The accretion of ice on a conductor modifies its cross-sectional geometry and hence its aerodynamic characteristics. This may result in an aerodynamically induced instability called galloping. The motion is principally in vertical direction with a low frequency, typically less than 1 Hz, and a large amplitude such as 10~20 m, large enough to cause serious design and operational problems. The primary reason of this mechanism is a significant negative slope in the lift force curve against the angle of attack, α, which gives the exciting lift force in the same direction as the cable motion. Thus, energy from the surrounding airflow is fed continuously to the system, leading to an unstable motion similar to flutter. The instability criterion is given by the well-known Den Hartog criterion (1932); which is

$$\frac{\partial C_L}{\partial \alpha} + C_D < 0 \tag{2}$$

where C_L and C_D are the lift and drag force coefficients, respectively.

However, strictly speaking, since the drag force also slightly depends on the angle of attack, the path of the cable motion tends to follow an elliptical trace. Furthermore, the instability is known to be triggered by aerodynamic coupling with torsion (Lilien 1997). On the other hand, the static deflection due to drag force and pitching moment under high wind speed can effectively change the aerodynamic characteristics of the cross-section, which could even stabilize the cable (Novak & Tanaka 1974). A similar behaviour for the case of non-circular cable sections has been also discussed by Fujino et al. (1997). Since the dynamic amplitude of galloping tends to be so large, the cable behaviour becomes strongly nonlinear. Unlike torsional flutter, wind turbulence does not necessarily work as a stabilizing factor for galloping (Novak & Tanaka 1974). Engineering problems are not restricted to the power conductors. Some studies (Novak et al. 1978) have shown that the same mechanism of excitation may have resulted galloping of heavy guy cables, leading to the collapse of a guyed tower. It has been reported that the violent vibration of bridge stay cables observed at the Ørsund link between Denmark and Sweden in February 2004 was likely to be galloping caused by snow and sleet accumulation on cable surface (Larsen 2005).
A comprehensive list of the references related to the research on galloping has been presented by Lilien (1997). The analysis itself of galloping does not involve too much theoretical difficulties in principle. However, it needs to be supported by reliable aerodynamic data for a range of realistic natural ice shapes formed under various weather conditions of interest. The collection of this information will greatly assist the theoretical study of galloping.

6.5 Vibrations Caused by Wake Interference

The dynamic behaviour of structures excited by wind can be drastically altered by their proximity to its neighbouring structures. These mechanisms that lead to aerodynamic excitation do not even exist for a single isolated structure. Much research on this category of fluid-structure interaction has been motivated by problems encountered with the closely spaced tubes exposed to internal flow of heat exchangers and also with bundled conductors used in high voltage electric power transmission lines. There are, however, some other examples of proximity effects also related to spaced cables, slender towers and chimneys. Due to the complexity of flow pattern around closely spaced structures, several different driving mechanisms can arise. Zdravkovich (1997), for example, has studied various cases of aerodynamic interaction between two circular cylinders (Fig.1) located close to each other quite extensively.

Of particular importance, in the present context, is the case when two circular cylinders are placed in staggered arrangements. The predominant response is a) resonant buffeting, where the vortex wake of an upstream body is resonant with a natural frequency of a structure submerged in the wake; and b) wake galloping, where lift and drag forces excitig in the wake shear flow leading to a coupled 2DOF instability of a submerged cylinders.

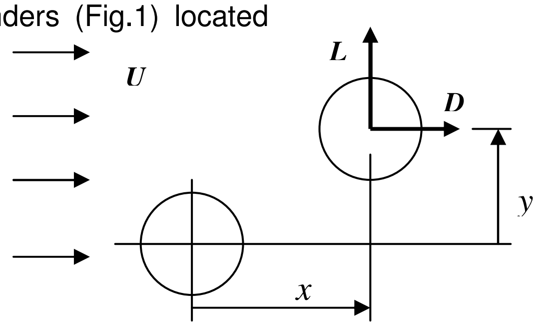

Fig.1

Wake interference galloping occurs when two cylinders are either closely or largely spaced. For close spacings, the flow around two cylinders is significantly altered by aerodynamic interference between two cylinders. Stay cable vibrations of the Yobuko Bridge (Yoshimura et al, 1995) was of this kind. Extensive studies of instability of closely spaced cylinders have been conducted, particularly for heat exchanger bundles (Chen, 1987) and bridge stay cables (Yoshimura et al. 1995, for example). Instability is observed in the range of $-2 < y/D < 2$ and $1 < x/D < 4$. It starts at the critical reduced velocity of $\left(\overline{U}/fD\right)_{cr} \approx 40$, which typically corresponds to the flow speed of 5 ~ 20 m/s, and follows generally an elliptical trajectory with the maximum amplitude of less than 3D. The motion is known to be sensitive to the Scruton number, $Sc = m\varsigma/\left(\rho D^2\right)$ and becomes hardly recognizable at $Sc > 50$. To reduce the vibration amplitude, the installation of viscous dampers at cable ends or connecting the adjacent cables by cross-ties have been practiced. However, these methods are not effective for longer cables.

As spacing increases, the interference effects diminish until the next “large spacing” instability range, $8 < y/D < 20$, is reached, where the interference effects are only on the downstream cylinder and the flow around the upstream structure is no longer affected by the second cable. The interference effects of largely spaced structures have attracted less research attention except for the wake galloping of bundled conductors and a good comprehensive reference of both analyses and test results is presented by Wardlaw (1994). The transmission of electric power in very high voltage requires suspension of conductors in bundles to avoid a corona discharge to ground. The separation of parallel conductors, typically in the range of 10 ~ 20 conductor diameters, is maintained by the use of spacers that usually divide the span into 50 ~

60 m subspans. This becomes the reason of having a distinctively different type of cable vibration called subspan oscillation caused by wake interference.

If the upstream cable is fixed, the downstream conductor would move in an elliptic path with the long axis nearly horizontal. Amplitudes become large enough that conductors could clash. Although it is the downstream conductor that becomes aerodynamically unstable, the field observations report the existence of anti-phase motion of a conductor pair with both cables having similar amplitudes and with the frequency in the range of 1 ~ 4 Hz. This is in contrast to the vortex shedding excitation which takes place at higher frequencies of 10 ~ 50 Hz, and the large amplitude galloping of iced conductors at the frequency less than 1 Hz.

The aerodynamic mechanism of this vibration was extensively investigated in 1970s and is fairly well understood by now. Research activities included aerodynamic force measurements (Warlaw & Cooper, 1974) and mathematical analyses (Simpson & Flowers 1977, for example). It has been found that the presence of wind velocity gradient across the wake of the windward object would induce position-dependent lift and drag forces on the downstream cable. The most sensitive region for this excitation is approximately at a quarter of the width of the wake from its outer edge shear layer, where the lift force reaches its maximum.

A conventional practice of suppressing this type of motion is with spacer-dampers that are flexible and often installed at unequal intervals. However, the impact of the damper provided by the spacers on the instability is still not clear. Opposite conclusions were drawn from different studies. The use of low level damping has been recommended by a Hydro-Quebec study (Hardy & Bourdon 1979), while Price and Paidoussis (1984) has advised to use very high level of damping.

The unexpected wake-induced flutter was observed recently (Toriumi et al. 1999) on the hanger ropes of the Akashi Kaikyo Bridge in Japan. Cable distance was 9D for this case, normal to the bridge axis. Spiral ropes of 10 mm in diameter were used to wind up the hanger ropes to suppress both the wake-induced flutter and vortex shedding excitation effectively.

6.6 Parametric Excitation

Vibrations of stay cables can be excited by motion of the anchorage points, as it was first pointed out by Kovács and Leohardt (1982). This is sometimes observed in cable-supported structures such as cable-stayed bridges and guyed towers. One of the important points in particular is the fact that a cable can be excited not only with its natural frequency but also with the excitation frequency which is two times its own natural frequency.

The most likely cases are when the excitation frequency is approximately twice or equal to the first natural frequency of the cable. This is only an indirect aerodynamic excitation of cables. Nevertheless, it can be a serious issue and should be briefly mentioned here. Because of its low structural damping, the cable motion can develop to large amplitude even if the end excitation is small. Also, since the bridge stay cables present a wide range of natural frequencies, there is a good possibility of some of the cables resonating with the movements of the deck or pylons due to wind or traffic loads. Parametric excitation of bridge stay-cables including nonlinear characteristics and varieties of parameter changes is an interesting research topic but is not fully investigated yet (Gani & Tanaka 2005). However, it is also said that the stay cable vibration is likely to stay linear because of very small sag and small end motions (Liu et al. 2005). It has been reported that the stay cables of the Second Severn Crossing experienced severe vibration apparently because of this reason. When the cross-ties were installed to alleviate the cable vibration, the bridge deck started vibrating, since now it has lost an effective TMD (Stubler et al. 1999). For the case of the Normandy Bridge, the problem was removed by adding cross-ties between stay cables to avoid resonant vibrations (Virlogeux 1995).

6.7 Reynolds Number Related Drag Instability

This phenomenon was observed about four decades ago on a stranded wire conductor crossing the Severn River in England. The vibration was severe enough to cause numerous electrical faults due to the clashing between conductors. There was apparently no vertical conductor motion associated with it. A very interesting fact was that the wind speed and direction at which the instability occurred was confined to rather narrow bands. The physical dimensions involved in the case are as follows: main span length = 1,619 m, the sag = 80.5 m, cable diameter = 43 mm and cable mass = 6.40 kg/m. Vibration frequency was found in the range of 0.128 ~ 0.130, which approximately corresponds to the first asymmetric mode in lateral sway. The vibration was observed at the mean wind speed 13 to 15 m/s and most of the time the mean wind direction was 10 ^{o} to 25 ^{o} deviated from the normal to the span. Results from extensive studies (Davis et al. 1963; Richards 1965) pointed out that this unusual instability was due to the sensitivity of the drag force to the Reynolds number.

As it has been well-recognized, the aerodynamics of cylindrical bodies is highly sensitive to the change of the flow speed near the critical Reynolds number. Though the critical Reynolds number is influenced by the roughness and texture of the body surface as well as the flow turbulence, it is characterized by a sudden drop of the drag force with the increase in wind speed. If the cable is swinging back and forth parallel to the wind direction, and if the change in the relative wind speed takes place at this sensitive speed range, it is possible to have the induced aerodynamic force acting in the same direction as the body motion, and thus generate the negative aerodynamic damping. In case of a smooth circular section, this “drag crisis” occurs at the Reynolde number range of 2 ~ 5×10^5. Considering the cable diameter to be the order of 50 ~ 150 mm, possibility of having this instability is at the wind speed of 20 ~ 60 m/s, which is possible to take place but has never been reported as a problem in reality.

For the case of the Severn crossing, the helical stranding of conductors featured two influences on the aerodynamic characteristics. First, the critical Reynolds number for the conductor was about an order of magnitude lower than that of the smooth circular cylinder, down to 2.6 ~ 4.0×10^4 because of the characteristic roughness. Second, in oblique winds, the lay of the strands streamlined the flow on surface in which the wind was more parallel to the stranding and roughened the opposite surface. This deflected the flow streamlines and generated a mechanism for lift. The effect was further amplified at the critical Reynolds number when the mechanism of drag damping was also active. This mechanism caused a large amplitude motion and the clashing. As a countermeasure, the conductor was wrapped in PVC tape to eliminate the unfavourable impact of the stranded surface.

Considering the range of Reynolds number and possible cable dimensions, similar instability is conceivable for bridge stay cables, too. However, so far no particular case has been attributed to this mechanism.

6.8 Rain-Wind Induced Vibration

Rain-wind induced cable vibration has been most frequently reported for bridge cable vibration. It was first addressed by Hikami (1986) when the stay-cables of the Meiko-Nishi Bridge in Japan experienced annoying vibrations. The most curious part was that it was observed under certain wind conditions, but only when it was raining. The observed vibration amplitude was up to approximately 2D, D being the cable diameter, which was typically 14 cm, and under the wind of 8 ~ 14 m/s. A simple analysis led to the conclusion that the observed vibration was not any of the known types. The observed frequency was 1 ~ 3 Hz, which was well below the Strouhal frequency for the vortex shedding excitation. The cables were too far apart in distance to cause any aerodynamic interference. The observed cable vibrations were hence assumed to be a new type of instability, which is caused by the combined action of rain and wind.

After this new type of excitation mechanism was reported, it became clear that, in fact, there had been some other cable vibrations reported earlier for other bridges, which could have been classified into the same category. Some of the reported cases of this type of cable vibration are given in Table 1. Other reported cases oscillation of overhead conductors (Hardy & Bourdon 1979), inclined hangers of the Humber Suspension Bridge (Zasso et al. 1992) and even vertical hangers of two arch bridges (Ruscheweyh & Verwiebe 1995; Verwiebe 1998) all observed under rain and wind conditions. In the case of the arch bridges, the violent vibration of the vertical hangers caused fatigue damage at its welded connection to the gusset plate.

Table 1: Reported cases of rain-wind induced cable vibration

Bridge Name	Country	Observed Year	Max. Double Amplitude	References
Köehlbrand	Germany	1974	about 1 m	Ruscheweyh & Hirsch 1974
Brottonne	France	1977	about 0.6 m	Wianecki 1979
Meiko-Nishi	Japan	1984	0.55 m	Hikami 1986 & 1988
Farø	Denmark	1985	about 2 m	Langsoe & Larsen 1987
Aratsu	Japan	1988	about 0.6 m	Yoshimura et al. 1989 & 1995
Tenpozan	Japan	—	close to 2 m	Miyasaka et al. 1987 Ohshima & Nanjo 1987
Ben Ahin	Belgium	1988	about 1 m	Cremer et al.1995 Lilien & Pinto da Costa 1994

Burlington	Vermont	1990's	?	Virlogeux 1998
Glebe Island	Australia	1990's	?	Virlogeux 1998
Nampu	China	1992	?	Cheng (personal communication)
Yangpu	China	1995	?	Gu et al. 1998
Erasmus	Holland	1996	about 1.4 m	Geurts et al. 1998
Ørsund	Denmark Sweden	2001	„large"	Larsen & Lafrenière 2005
Cochrane	Alabama	2002-04	about 1.5 m	Irwin et al. 1999 & 2005

The characteristics and some specific conditions of this type of vibrations through field observations and wind tunnel tests can be summarized as follows (Hikami & Shiraishi 1988; Yoshimura et al. 1989; Main et al. 2001; Matsumoto 1998; Stubler et al. 1999; Matsumoto et al. 2001):

Moderate rain – neither light drizzle nor a downpour is conductive to such vibrations.
Wind speed of 6 ~ 18 m/s, with the majority of the cases in 8 ~ 12 m/s.
Cable frequency of 0.6 ~ 3.0 Hz.
Cable diameters ranging from 140 mm to 225 mm.
Reynolds number of 6×10^4 ~ 2×10^5, which is the transition range from sub-critical to critical.
Cables located in the leeward side of the pylons, most of the case.
Cable inclination of 20 ^{o}~ 45^o from horizontal, in many cases.
Wind direction of 20^o ~ 60^o relative to the plane of the cable.

The cause of this vibration is considered to be in two steps. First, the formation of upper water rivulet on the cable surface seems to be a key factor (Hikami 1986; Yamada et al. 1991). It is formed as a result of a sensitive equilibrium between gravity, capillary and aerodynamic forces. The water rivulet effectively alters the geometrical cross-section of the cable and hence the aerodynamic forces on it. Depending on the location and size of the rivulet, it tends to give a negative slope of lift curve against the small change in the angle of attack and also significantly reduce the drag force, which results in the Den Hartog type galloping instability (Yamaguchi 1990). Also, once the cable is set to motion, the upper rivulet tends to oscillate along the cable surface in circumferential direction and this motion can be aerodynamically coupled with the flexural oscillation of the cable, making the modal aerodynamic damping negative. Naturally, it is expected to intensify the vibration (Hikami 1986; Yamaguchi 1990; Ruscheweyh 1999). Contrary to this explanation, Bosdogianni & Olivari (1996) do not believe the motion of liquid rivulets has any influence on the instability. More research on the second triggering factor, in fact, identified three fundamentally different excitation mechanisms associated with along-wind, cross-wind and mainly across-wind cable vibration under rain and wind conditions (Verwiebe 1998; Verwiebe & Ruscheweyh 1998). They essentially depend on the cable orientation and wind speed. An approximate method to estimate the amplitude of rain-wind induced vibration is suggested. A recent finding by Flamand (2001) reveals the dependence of excitation on the thickness of the thin water film moving on the cable surface, and the link between the thickness and surface speed of the water.

There are many other studies on this topic. Yamaguchi's work (1990) indicates that this instability is essentially a galloping. Geurts et al. (1999) developed a numerical model based on SDOF galloping theory to predict the rain-wind induced cable response for the Erasmus Bridge. Thus obtained analytical results of vibration amplitude approximately agreed with the field data. In the model proposed by Xu and Wang (2001), the interaction between wind, cable and rivulet was considered. The predicted steady-state response showed that the main characteristics of an inclined cable with moving rivulet, such as velocity-restricted and amplitude-restricted, could be captured. The analytical study by Gu and Lu (2001) pointed out the importance of initial rivulet position in generating the cable instability. The "unstable zone" of initial rivulet position and the "dangerous zone" of instantaneous rivulet position were identified for cables of different natural frequencies. Matsumoto (1995 etc.) on the other hand finds that the air flow component along the cable is the essential cause of this vibration.

Various kinds of structural and aerodynamic means have been developed to suppress and prevent the vibration. Increase of the system damping by installation of oil dampers (Yoshimura et al. 1989), hydraulic dampers (Geurts et al. 1999), viscous-friction dampers (Kovacs et al. 1999), or connecting some of the longest cables by using cross-ties (Langsø & Larsen 1987; Hikami & Shiraishi 1988; Kusakabe et al. 1995; Virlogeux 1998) are found to be effective structural means. The installation of TMD on the vertical hanger of an arch bridge (Ruscheweyh & Verwiebe 1995) was also proven to be effective. As for developing the aerodynamic measures, the main idea is to break up the formation of the upper water rivulet. Thus, various methods have been proposed and applied to the bridge cables, such as the use of helical wire whirling on the cable surface (Flamand 1994; Bosdogianni & Olivari 1996), the adoption of a dimpled cable surface (Kobayashi et al. 1995; Virlogeux. 1998), or the use of an axially protuberated surface (Saito et al, 1994). All these have proven to be effective and successful in the field to various extents. The effect of cable surface roughness has been also investigated by the wind tunnel tests (Miyata et al. 1994). A more recent proposal (Verwiebe & Ruscheweyh 1998) of deflecting the water on cable surface to control the motion needs further development.

Regarding the amount of damping required to control it, Irwin (1997) has suggested that the vibration can be reduced to a harmless level if the Scruton number is greater than 10, i.e.,

$$Sc = \frac{m\varsigma}{\rho D^2} > 10 \tag{3}$$

where, $m =$ cable mass per unit length, $\varsigma =$ the critical damping ratio, $\rho =$ air density, and $D =$ cable diameter. This statement is also supported by experience in Japan (Yamada 1997). Considering $D = 15$ ~ 20 cm and $m = 100$ kg/m for a bridge stay cable, for example, this is equivalent to the structural damping of approximately ς = 0.5% or more.

6.9 High-Speed Vortex Excitation of Dry, Inclined Cables

Although majority of the observed stay cable vibration belongs to the rain-wind induced type, it has been found both in field and wind tunnel tests that dry inclined cables can also undergo large amplitude oscillation without precipitation. Matsumoto et al. (1989) reported the observations of cable vibrations without rain but with characteristics of rain-wind vibrations, up to the maximum amplitude of 23 cm at the wind speed 40 m/s during a typhoon. Matsumoto et al. (1995) further explained that these vibrations occurred for the cables of the Higashi-Kobe Bridge, too. These phenomena were not properly explained by any known mechanisms and were attributed to the high-speed vortex shedding excitation because, compared to the normal Kármán vortex-induced vibration, the observed instability occurred at much higher reduced wind velocity ranges in multiples of 20, i.e., $U_R = 20, 40, 60 \ldots$.

Matsumoto (1998) tried to explain the mechanism of this vibration with the concept of 3D Kármán vortex interaction. When wind goes over an inclined cable, the vortices are generally shed in the wake. Besides, because wind is oblique to the cable, an axial airflow also exists, which may form and shed axial vortices along the cable. The axial flow, which interrupts the fluid interaction between the two separated shear layers in the wake, plays a role similar to a splitter plate, and behaves like an "air-curtain" or "base-bleed" (Matsumoto et al. 1990). They explained that it was the fluid interaction between the axial and the Kármán vortices, as well as the cable motion that caused this high-speed vortex excitation. In the experimental studies carried out by them, the frequency of the axial vortex shedding was found to be equal to 1/3 of the Kármán vortex shedding. Consequently, the Kármán vortex was amplified with the every third vortex, which correlates well with the observed fact that the instability occurred only at the discrete reduced wind velocity of 20, 40, 60.... The intermittently amplified Kármán vortices also well explained the beating phenomenon observed in the tests (Matsumoto 1998; Cheng & Tanaka 2002) and on Meiko-Nishi Bridge (Matsumoto 1998).

As a means to suppress the vibration, Matsumoto has suggested the use of discrete elliptical plates attached on the cable surface (Matsumoto et al. 1995a). By doing so, not only the formation of the axial flow, but also the formation of upper rivulet is prevented. Thus, this aerodynamic countermeasure helps to control both rain-wind induced vibration and high-speed vortex shedding. However, any of damping devices would also effectively work, similar to any other wind excitation of cables.

Although studies have been carried out to investigate this type of vibration for several years, and progress seems to be encouraging as the excitation mechanism gradually becomes clear, there are still lots of unknowns to satisfactorily explain the phenomenon and make proper predictions. The exact damping level required to suppress or eliminate the motion should be quantitatively predicted. Since the suggested 3D vortex shedding mechanism strongly depends on end conditions at the wind tunnel tests and also the yaw angle of the cable against wind, it is important to compare the conditions between the cable model tests and the full-scale observation of real bridge cables.

6.10 Dry Inclined Cable Galloping

(1) Beginning

Galloping of dry inclined cable is a relatively new term and its concept has become clearer only recently. First it appeared as a side product of the study on rain-wind vibration. There have been some experimental studies carried out (Saito et al. 1994; Miyata et al. 1994; Matsumoto et al. 1995b & 2005; Cheng et al. 2002 & 2003) to investigate this phenomenon and, so far, it has been observed only in wind tunnel tests. Results obtained from these studies show that if the wind is oblique, the instability of the cables, which are inclined to wind (Fig.1), could have similar response characteristics as galloping. The results are found to be very sensitive to the model end conditions in the wind tunnel tests and thus sometimes it is difficult even to reproduce it. However, if it takes place in reality as predicted, it would be a very serious engineering problem. Although this type of cable motion has never been clearly observed on real bridges, some field observations in fact are said to be better explained with galloping than calling them rain-wind induced vibration (Virlogeux 1998; Irwin et al. 1999).

An instability criterion to indicate the critical wind speed originally suggested by Saito et al (1994) for this instability is approximately given by (Fig.2)

$$(U_R)_{cr} \approx 35\sqrt{Sc} \tag{1}$$

where $U_R = \overline{U}/(fD)$ is the reduced wind speed, and $Sc = m\varsigma/(\rho D^2)$ is the Scruton number. According to Saito, this criterion is applicable to the cases where the angle between cable axis and wind direction is 30° to 60°. It imposed a difficult design condition for bridge stay cables with a typical diameter of 150 to 200 mm, since it would place so many bridge stay cables into a category of "prone to galloping". The reality, however, is that many existing stay cables seem to be surviving without suffering this instability. Further investigation was urgently required under these circumstances.

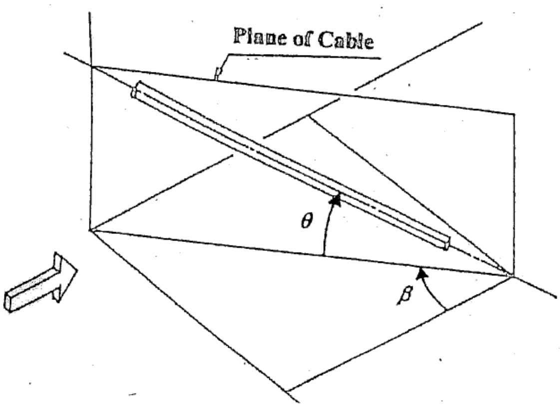

Fig.1 Inclined cable.

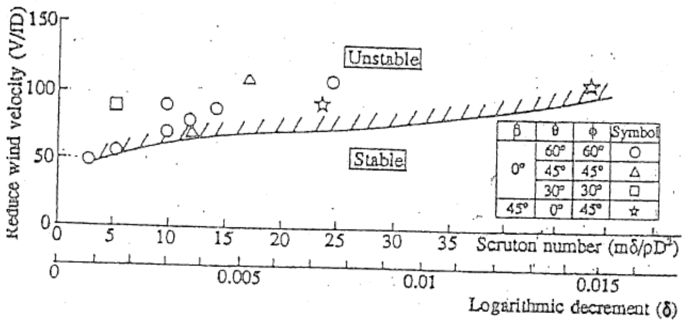

Fig.2 Saito's criterion

It is now required that a more refined stability criterion for the dry inclined cable galloping, and the range of the physical parameters associated with the suggested criterion should be established. In order to evaluate if the Den Hartog galloping criterion is applicable to explain the phenomenon, aerodynamic forces acting on the inclined cable need to be measured.

There are a few interesting issues raised in relation to the excitation mechanism of this instability. One of them is the role of the air flow along the cable axis and possible interaction of it with the Kármán vortices behind the cable. It has been suggested by Matsumoto et al. (1995), who also indicate that the axial flow in fact has a significant role in rain-wind vibration, too. By introducing an artificial axial flow in the experiment, Matsumoto et al (1995) showed that the existence of axial flow could induce negative slope of the lift force, and galloping of dry inclined cable would occur when the velocity of the axial flow was 30% more than that of the approaching flow. A question then is whether or not this artificially imposed axial flow well represents the air flow situation behind an inclined cable in reality.

Another significant fact is, as pointed out by Larose and Zan (2001), that the instability is observed clearly in the critical Reynolds number range. It is certainly interesting to note that all of observed rain-wind vibration has occurred almost exactly at the critical Reynolds number. A question is then why and how it relates to the instability, including the dry cable galloping.

(2) Two test series - Ottawa and Milano

Ottawa Project by NRCC/UO/RWDI

A series of wind tunnel investigation on inclined cable vibrations took place in Ottawa recently (Cheng et al. 2002 & 2003) as a collaborative effort between the University of Ottawa, RWDI Inc. and the National Research Council Canada. The study consisted of two phases: the dynamic model test for response measurement and the static pressure model to investigate the aerodynamic forces on the cable. The dynamic model was a section of a full-size stay cable with a total length of 6.7 m, a diameter of 0.16 m, and a linear mass of 60.8 kg/m. The model was inclined against wind with equivalent angles of $\phi = 35^o$ to 60^o and $\alpha = 0^o$ to 60^o, where $\phi =$ the cable-wind angle, which is the angle of wind plane relative to the cylinder axis, and $\alpha =$ the angle between wind plane and the vibration plane. They successfully reproduced high-speed vortex excitation and one particular case ($\phi = 60^o$ and $\alpha = 54.7^o$) in which the dry inclined cable galloping appeared at the wind speed of 32 m/s. The geometrical set-up of the model is equivalent to a real bridge cable inclined and yawed both 45^o to the mean wind direction and the Scruton number was $m\delta/(\rho D^2) = 11$.

In Fig.3, their test results are compared with the stability criterion suggested earlier by Saito et al. (1994) and also some other experimental results obtained in Japan (Miyata et al. 1994; Honda et al. 1995). It is evident that Saito's criterion for the onset of instability is much more conservative than other experimental results.

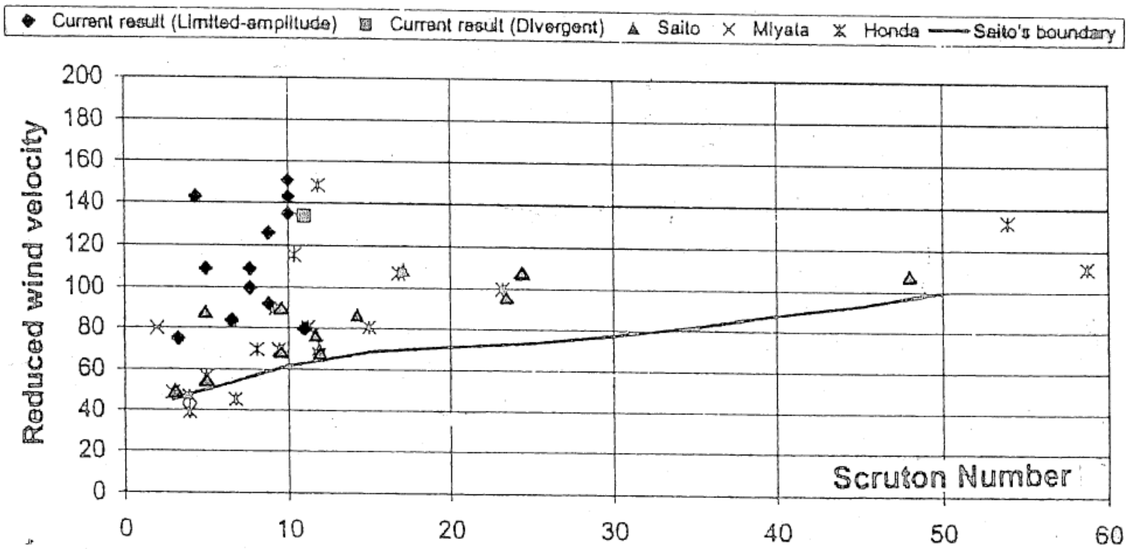

Fig.3 Various dynamic test results of inclined cables

The force measurement results clearly indicate that the tendency toward instability, or galloping, takes place at particular combinations of vertical inclination and horizontal yaw angle, and also at the wind speed corresponding to the critical Reynolds number, where the Den Hartog instability criterion is satisfied as a result of a negative slope of the lift force with the angle of incidence and significant reduction of drag force (Cheng et al. 2003). Further to this, an observed indication toward instability with and without the span-wise force correlation is discussed in conjunction with the appearance of amplitude-limited, high-speed vortex excitation phenomena (Cheng & Tanaka 2005).

Further to these results, Macdonald (2005) introduced a more generalized 2D instability criterion, which was applied to this particular case and showed an excellent agreement with the test results. His theoretical criteria are given in **2.3** below in more detail.

Milano Campaign

In 2004, by using a very large wind tunnel at the Politecnico di Milano, a 6m long, 316mm diameter cylinder was rigidly supported horizontally with a variable horizontal yaw angle for the measurement of cross-sectional aerodynamic forces and their span-wise coherence. A particular emphasis was placed on finding the aerodynamic behaviour in the critical Reynolds number range. There were a number of extremely interesting findings from this series of tests but some of the findings particularly related to inclined cable galloping are as follows (Larose et al. 2005):

1. The existence of the asymmetric, single bubble regime at $\mathrm{Re} = 1.6 \times 10^5$ on an inclined cylinder, which was previously observed in the Ottawa study in smooth flow, was confirmed in 2.5% turbulence, which is a good representation of the situation of bridge cables in the field.
2. As was the case in the Ottawa study, the cross-sectional lift forces were found distinctly different at different location along the cylinder, even if they were only one diameter apart.

3. In this Reynolds number range, a nonlinear change of lift force due to change in wind speed, which could explain partly a quasi-steady cause of instability.
4. A complete set of steady and unsteady aerodynamic forces on a yawed stay cable mode in the critical Reynolds number range was obtained, which consists of a complementary tests of the Ottawa study.

(3) Critical Issues

Onset Criteria

As it was mentioned earlier in **2.2**, Macdonald (2005) has tried a general quasi-steady analysis of inclined cable galloping, including the effect of Reynolds number variation, and derived a general 2D criterion for galloping instability given as follows:

$$Z_s = \frac{\varsigma_s m f_n}{\nu/\rho} > R\left[\frac{\mathrm{Re}}{16\pi}\left\{-h(C_D)+\sqrt{g^2(C_D)+g^2(C_L)-h^2(C_L)}\right\}\right] \qquad (2)$$

where $\rho =$ the air density, $\mathrm{Re} = \frac{DU}{\nu} =$ Reynolds number, $D =$ cable diameter, $C_D =$ drag coefficient, $C_L =$ lift coefficient, $\omega_n = 2\pi f_n =$ circular natural frequency, $\varsigma_s =$ the structural damping ratio, $m =$ cable mass per unit length, and $U =$ wind speed. $R[...]$ indicates the real part. Also

$$g(C_F) = C_F\left(2\sin\phi - \frac{1}{\sin\phi}\right) + \frac{\partial C_F}{\partial \mathrm{Re}}\mathrm{Re}\cdot\sin\phi + \frac{\partial C_F}{\partial\phi}\cos\phi \qquad (3a)$$

$$h(C_F) = g(C_F) + \frac{2C_F}{\sin\phi} \qquad (3b)$$

in which C_F is either C_D or C_L and $\phi =$ the cable-wind angle, defined as the angle between a flow velocity relative to the cylinder axis. The definition of aerodynamic forces and their coefficients follow the following equation. The angle relationship is explained in Figs.4&5.

$$F_x = \frac{\rho U_R^2 D}{2}\left(C_D\cos\alpha_R - C_L\sin\alpha_R\right) \qquad (4)$$

where $U_R =$ the magnitude of the relative velocity, and $\alpha_R =$ the relative angle of attack.

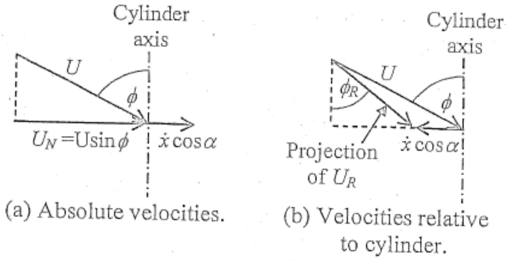

Fig.4 Cable-wind plane

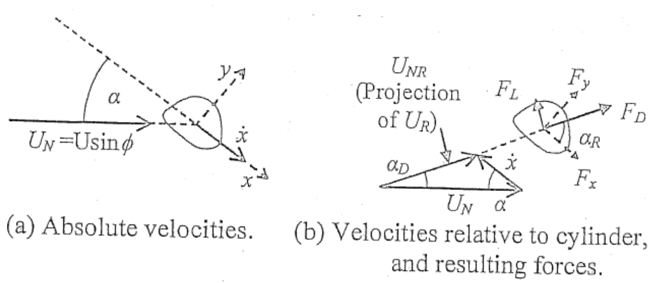

Fig.5 The plane normal to the cylinder.

It is important to note that the right hand side of the criterion (2) is a function of Re and ϕ only and independent of the direction of cable motion. Note also that the expression (2) is simplified for a circular cylinder. More general expression and its derivation are given in Macdonald & Larose (*to be published in J. Fluids & Structures*). Detailed measurement of both lift and drag force components for an inclined cylinder in the critical Reynolds number range was carried out by Larose et al. (2003). It is interesting to note that Macdonald has predicted, based on this analysis and available aerodynamic data, that another instability area, which exists when the cable-wind angle is between 75^0 and 90^0. A practical importance of this analysis is in the fact that the magnitude of aerodynamic negative damping can be actually calculated, and hence, the additional damping to the system to suppress any instability can be predicted.

Critical Reynolds Number

Larose and Zan (2001) particularly emphasized the sensitivity of cable vibrations to Reynolds number. It is certainly interesting to note that all of observed rain-wind vibration has occurred almost exclusively in the critical Reynolds number range. The case of dry inclined cable galloping investigated by the Ottawa group was again at the critical Reynolds number. It is also extremely interesting to note that the conventional Den Hartog criterion would indicate instability corresponding to the drag crisis in this range, but by considering the large influence of Reynolds number on force coefficients, the governing reason of inclined cable galloping is actually found to be the difference in lift force due to Re, the $\partial C_L / \partial \mathrm{Re}$ term (Larose & Macdonald). The critical Reynolds number is sensitive to the presence of surface roughness, flow turbulence, motion of the cable and a flow angle not perpendicular to the cylinder axis. More recent study further indicate the fact that the effects of Reynolds number on aerodynamic force distribution and resulted cable motion are highly dependent upon the orientation of the body to the mean flow direction (Larose et al. 2003, MacDonald 2005).

The state-of-of-the-art regarding this particular instability, as of 2005, is that

1) Galloping of dry inclined cable does exist as a possible instability;
2) It is a unique aerodynamic phenomenon for a cable, which is inclined against wind;
3) Instability takes place in the critical Reynolds number range;
4) There are a few specific geometrical positions where the cable could become unstable;
5) Additional damping required to suppress the instability could be predicted by eq.(2).

References:

Bosdogianni, A. & Olivari, D., Wind- and rain- induced oscillations of cables of stayed bridges, *JWEIA* (64) 1996, pp.171-185.

Chen, S.S., A general theory for dynamic instability of tube arrays in cross flow, J. Fluids & Structures (1) 1987, pp.35-53.

Cheng, S.H. & Tanaka, H., Aerodynamics of dry inclined cables, *Proc. 2nd Int. Conf. Advances in Wind & Structures*, Pusan, Korea, 2002, pp.361-368.

Cheng, S.H., Tanaka, H., Irwin, P.A. & Jakobsen, J.B., Aerodynamic instability of inclined cables, *Proc. 5th ISCD*, Santa Margherita, 2003, pp.69-76.

Cheng, S.H. et al., Divergent motion of cables exposed to skewed wind, *Proc. 5th ISCD*, Santa Margherita, 2003, pp.271-278.

Cheng, S.H. & Tanaka, H., Correlation of aerodynamic forces on an inclined circular cylinder, *Wind & Structures, An International Journal* (8) 2, 2005, pp.135-146.

Committee on Electrical Transmission Structures, *Guidelines for transmission line structural loading*, ASCE Structural Division, 1984.

Davenport, A.G., Gust response factors for transmission line loading, *Proc. 5th ICWE*, Fort Collins, Colrado, 1979, pp.899-910.

Davis, D.A., Richards, D.J.W. & Scriven, R.A., Investigation of conductor oscillation on the 275 KV crossing over the River Severn and Wye, *Proc. IEE* (110) 1963, pp.205-219.

Den Hartog, J.P., Transmission line vibration due to sleet, *AIEE Transaction* (51) 1932, pp.1074-1076.

Ehsan, F., Scanlan, R.H. & Bosch, H.R., Modelling spanwise correction effects in the vortex-induced response of flexible bridges, *JWEIA* (36) 1990.

Flamand, O., Rain-wind induced vibration of cables, *Proc. Int. Conf. on Cable-stayed & Suspension Bridges*, Deauville (2) 1994, pp.523-531.

Flamand, O., An explanation of the rain-wind induced vibration of inclined stays, *Proc. 4th ISCD*, Montreal, 2001, pp.69-76.

Gani, F. & Tanaka, H., Parametric excitation of stay-cables, *presented to the 6th ISCD*, Chaleston, South Carolina, 2005.

Geurts, C. & Staalduinen, P., Estimation of the effects of rain-wind induced vibration in the design stage of inclined stay cables, *Wind Engineering into the 21st Century*, (eds. Larsen, Larose & Livesey) Balkema, 1999, pp.885-892.

Gu, M. & Lu, Q., Theoretical analysis of wind-rain induced vibration of cables of cable-stayed bridges, *Proc. 5th Asia-Pacific Conf. on Wind Eng'ng*, Kyoto, 2001, pp.125-128.

Hardy, C. & Bourdon, P., The influence of spacer dynamic properties in the control of bundle conductor motion, *IEEE PES Summer Meeting*, Vancouver, 1979.

Hikami, Y., Rain vibrations of cables of cable stayed bridge, *JAWE J. Wind Eng'ng* (27) 1986.

Hikami, Y. & Shiraishi, N., Rain-wind induced vibrations of cables in cable-stayed bridges, *JWEIA* (29) 1988, pp.409-418.

Honda, A., Yamanaka, T., Fujiwara, T. & Saito, T., Wind tunnel test on rain-induced vibration of the stay-cable, *Proc. 1st ISCD*, Liège, 1995, pp.255-262.

Irwin, P.A., Wind vibrations of cables on cable-stayed bridges, Building to Last: *Proc. ASCE Structural Congress XV*, Portland, Oregon, 1997, pp.383-387.

Irwin, P.A., Nedim, A. & Telang, N., Wind induced stay cable vibrations – A case study, *Proc. 3rd ISCD*, Trondheim, 1999, pp.171-176.

Kobayashi, H., Minami, Y. & Miki, M., Prevention of rain-wind induced vibration of an inclined cable by surface processing, *Proc.9th ICWE*, New Delhi, 1995, pp.753-758.

Kovács, I. & Leonhardt, A., Zur frage der Seilschwingungen und der Seildämpfung, *Die Bautechnik* (10) 1982, pp.325-332.

Kovács, I. Strommen, E. & Hjorth-Hansen, E., Damping devices against cable oscillations on Suuingesund Bridge, *Proc.3rd ISCD*, Trondheim, 1999, pp.145-150.

Kusakabe, T., Yokoyama, K., Kanazaki, T. & Sekiya, M., The effects of cable cross ties for wind-induced vibration, *Proc. 9th ICWE*, New Delhi, 1995, pp.783-792.

Langsø, H. & Larsen, O., Generating mechanisms for cable-stay oscillations at the Farø Bridge, *Proc. Int. Conf. on Cable-stayed Bridges*, Bangkok, 1987, pp.1023-1033.

Larose, G.L., Jakobsen, J.B. & Savage, M.G., Wind-tunnel experiments on an inclined and yawed stay-cable model in the critical Reynolds number range, *Proc. 5th ISCD*, Santa Margherita, 2003, pp.279-286.

Larose, G.L., Savage, M.G. & Jakobsen, J.B., Wind tunnel experiments on an inclined and yawed circular cylinder in the critical Reynolds number range, *Proc. 11th ICWE*, Lubbock, Texas, 2003 (2) pp.1705-1712.

Larose, G.L. & Zan, S.J., The aerodynamic forces on the stay cables of cable-stayed bridges in the critical Reynolds number range, *Proc. 4th ISCD*, Montreal, 2001, pp.77-84.

Larose, G.L., Zasso, A. & Grappino, S., Experiments on a yawed stay cable in turbulent flow in the critical Reynolds number range, *Proc. 6th ISCD*, Charleston, 2005.

Larsen, A. & Lafrenière, A., Application of a limit cycle oscillator model to bridge cable galloping, *Proc. 6th ISCD*, Charleston, South Carolina, Sept. 2005.

Leblond, A. & Hardy, C., On the estimation of a $\theta \leq 45°$ complex matrix of symmetric Stockbridge-type dampers, *Proc. 3rd ISCD*, Trondheim, 1999, pp.139-144.

Lilien, J.L., Galloping of overhead electrical lines, mechanisms, wind tunnel experiments - field measurements, *Proc. 2nd ISCD*, Tokyo, 1997, pp.37-48.

Liu, M.Y., Zuo, D. & Jones, N.P., Deck-induced stay cable vibrations: Field observations and analytical model, *Proc. 6th ISCD*, Charleston, South Carolina, Sept. 2005.

MacDonald, J.H.G., Quasi-steady analysis of inclined cable galloping in the critical Reynolds number range, *Proc. the 6th ISCD*, Charleston, South Carolina, Sept. 2005.

Macdonald, J.H.G. & Larose, G.L., Quasi-steady analysis of dry inclined cable galloping in the critical Reynolds number range, *Proc. UK Wind Engineering Society*, Cranfield, 2004.

Macdonald, J.H.G. & Larose, G.L., A unified approach to aerodynamic damping and drag/lift instabilities, and its application to dry inclined cable galloping, accepted for publication in *J. Fluids & Structures*.

Main, J.A., Jones, N.P. & Yamaguchi, H., Characterization of rain-wind induced stay-cable vibrations from full-scale measurements, *Proc. 4th ISCD*, Montreal, 2001, pp.235-242.

Matsumoto, M., Yokoyama, K., Miyata, T., Fujino, Y. & Yamaguchi, H., Wind-induced cable vibration of cable-stayed bridges in Japan, *Proc. Canada-Japan Workshop on Bridge Aerodynamics*, Ottawa, 1989, pp.101-110.

Matsumoto, M., Shiraishi, N., Kitazawa, M., Knisely, C., Shirato, H., Kim, Y. & Tsujii, M., Aerodynamic behaviour of inclined circular cylinders-cable aerodynamics, *JWEIA* (33) 1990, pp.63-72.

Matsumoto, M., Ishizaki, H., Kitazawa, M., Aoki, J. & Fujii, D., Cable aerodynamics and its stabilization, *Proc. ISCD*, Liege, 1995, pp.289-296.

Matsumoto, M., Yagi, T., Oishi, T. & Adachi, Y., Effects of axial flow and Kármán vortex interferences on dry-state cable galloping of inclined stay-cables, *Proc. 6th ISCD*, Charleston, 2005.

Matsumoto, M., Yamagishi, M. Aoki, J. & Shiraishi, N., Various mechanism of inclined cable aerodynamics, *Proc. 9th ICWE*, New Delhi, 1995, pp.759-770.

Matsumoto, M., Observed behaviour of prototype cable vibration and its generation mechanism, *Bridge Aerodynamics*, (eds. Larsen & Esdahl) Balkema, 1998, pp.189-211.

Matsumoto, M., Shirato, H., Yagi, T. Jones, N.P. & Hayashi, T., Field observation system of cable aerodynamics in natural wind, *Proc. 4th ISCD*, Montreal, 2001, pp.219-225.
Miyata, T., Yamada, H. & Hojo, T., Aerodynamic response of PE stay cables with pattern-indented surface, *Proc. Int. Conf. on Cable-stayed & Suspension Bridges*, Deauville, 1994, (2) pp.515-522.
Novak, M. & Tanaka, H., Effect of turbulence on galloping instability, *Proc. ASCE* (100) EM1, 1974, pp.27-47.
Novak, M., Davenport, A.G. & Tanaka, H., Vibrations of towers due to galloping of iced guy cables, *Proc. ASCE* (104) EM2, 1978, pp.457-473.
Price, S.J. & Paidoussis, M.P., The aerodynamic forces acting on groups of two and three circular cylinders when subject to a cross-flow, *JWEIA* (17) 1984, pp.329-347.
Richards, D.J.W., Aerodynamic properties of the Severn Crossing conductor, *Proc. 1st ICWE*, Teddington, 1963 (2) pp.688-765.
Ruscheweyh, H. & Verwiebe, C., Rain-wind-induced vibrations of steel bars, *Proc. ISCD*, Liege, 1995, pp.469-472.
Ruscheweyh, H., The mechanism of rain-wind-induced vibration, *Wind Engineering into the 21st Century* (eds. Larsen, Larose & Livesey) Balkema, 1999, pp.1041-1047.
Saito, T., Matsumoto, M. & Kitazawa, M., Rain-wind excitation of cables on cable-stayed Higashi-Kobe Bridge and cable vibration control, *Proc. Int. Conf. on Cable-stayed & Suspension Bridges*, Deauville, 1994 (2) pp.507-514.
Sauter, D., Liu, Q., Hagedorn, P. & Rahman, A., On the vortex-excited vibrations of stay-cables, *Proc. the 4th ISCD*, Montreal, 2001, pp.277-284.
Stubler, J. Ladret, P., Domage, J.B. & Peltier, M., Bridge stay-cable vibration: Phenomena, criteria and damper technology, *Proc. 3rd ISCD*, Troudheim, 1999, pp.163-170.
Toriumi, R., Furuya, N., Takeguchi, M., Miyazaki, M. & Saito, Z., A study on wind-induced vibration of parallel suspenders observed at the Akashi-Kaikyou Bridge, *Proc. 3rd Int. Symp. on Cable Dynamics*, Trondheim, 1999, pp.177-182.
Verwiebe, C., Rain-wind-induced vibrations of cables and bars, *Bridge Aerodynamic* (eds. Larsen & Esdahl) Balkema, 1998, pp.255-263.
Verwiebe, C. & Ruscheweyh, H., Recent research results concerning the excitation mechanisms of rain-wind-induced vibrations, *JWEIA* (74/76) 1998, pp.1005-1013.
Virlogeux, M., Cable vibrations in cable-stayed bridges, *Bridge Aerodynamic* (eds. Larsen & Esdahl) Balkema, 1998, pp.213-233.
Wardlaw, R.L. & Cooper, K.R.,, Mechanisms and alleviation of wind-induced structural vibrations, *Proc. 2nd Symp. on Applications of Solid Mechanics*, Hamilton, Ont., 1974, pp.369-399.
Wardlaw, R.L., Interference and proximity effects, *Wind-excited Vibrations of Structures* (ed. Sockel) Springer-Verlag, 1994, pp.321-363.
Xu, Y.L. & Wang, L.Y., Analytical study of wind-rain-induced cable vibration, *The 5th Asia-Pacific Conference on Wind Engineering*, Kyoto, 2001, pp.109-112.
Yamada, Y., Shiraishi, N., Toki, K., Matsumoto, M., Matsuhashi, K., Kitazawa, M. & Ishizaki, H., Earthquake-resistant and wind-resistant design of the Higashi-Kobe Bridge, *Cable-stayed Bridges: Recent Development and Their Future* (eds. Ito et al.) Elsevier, 1991, pp.397-416.
Yamaguchi, H., Analytical study on growth mechanism of rain vibration of cables, *JWEIA* (33) 1990, pp.73-80.
Yoshimura, T., Inoue, A., Kaji, K. & Savage, M.G., A study on the aerodynamic stability of the Aratsu Bridge, *Proc. Japan-Canada Workshop on Bridge Aerodynamics*, Ottawa, 1989, pp.41-50.

Yoshimura, T., Savage, M. & Tanaka, H., Wind-induced vibrations of bridge stay-cables. *Proc. 1st ISCD*, Liege, 1995, pp.437-444.

Zasso, A., Bocciolone, M. & Browonjohn, J., Rain-wind Aeroelastic instability of the inclined hangers of a suspension bridge. *Proc. Inaugural Conf. Wind Eng'ng Society*, Cambridge, 1992.

Zdravkovich, M.M., *Flow around circular cylinders*, Oxford Univ. Press, 1997.

(cf) JWEIA = Journal of Wind Engineering and Industrial Aerodynamics
ICWE = International Conference on Wind Engineering or its former bodies.
ISCD = International Symposium on Cable Dynamics

Chapter 7 Wind Tunnel Tests

7.1 Similitude Requirements

(1) General

When the likely effects of wind upon a bridge need to be examined, it is often a practice to undertake wind tunnel tests. Modelling techniques employed in these testings may vary but the similitude requirements for testing are considered to have been well established and practiced for quite some time. An alternative to this is to make a prediction of wind effects based on quasi-theoretical mathematical models which are often based on empirical knowledge. Depending on the problems, it is also possible to apply the techniques of computational fluid dynamics though the scope of its application is still somewhat limited. Whichever the employed modelling technique is, it is important to remember that an experimental or theoretical model can never perfectly satisfy the similitude requirements. It means that an appropriate interpretation of the results is always essential for the prediction of the results in reality.

Structural analyses, for example, using large capacity computers are generally regarded to be fairly accurate. However, no matter how accurate the calculation is, obviously the adequacy of the outcome largely depends on the way the structure and its boundary conditions are mathematically formulated to prepare inputs for the computers. Inclusion of aerodynamic factors in this process never makes the problem easier.

The experimental simulation is even more complicated. The general requirement for modelling a physical phenomenon is essentially the same in any wind engineering problem. The concern is typically the behaviour of wind flow in a certain space and its interaction with the geometrical and/or mechanical characteristics of the boundaries of the field of concern. For correct modelling in these problems, based on Buckingham Π–theorem, it is required that a set of dimensionless parameters which consist of suitable combinations of the reference quantities are invariant in model and prototype and with them the governing equations are also rendered dimensionless. Various boundary conditions have to be also maintained in dimensionless form. There is no danger of overemphasizing the importance of this principle since most of the wind engineering problems cannot be solved with theoretical approaches alone.

For correct modelling, all of the dimensionless parameters in the prototype must be duplicated in the model. However, almost invariably, complete duplication of the parameters is impracticable. As a matter of fact, all the requirements can be satisfied only when model and prototype are identical. Hence, the decision must be made as to which parameters could be relaxed, or distorted to what extent, for each testing based on the understanding of the phenomenon and the knowledge of dominant parameters. The weak laws should be relaxed. Perhaps only a part of the entire process can be simulated to clarify the unknown mechanism. Or, analytical means may be able to substitute the deficit in physical modelling.

(2) Similitude Requirements

Geometrical consistency

First of all, it is required that the model and prototype are to be geometrically similar, which means that all linear dimensions must be applied the same scaling factor. The linear dimensions involved are as follows:

Linear dimensions of the structure to be modelled and other structures;
Linear dimensions of the surrounding topography;
Surface roughness of the structures involved;
Linear dimensions of wind flow, including the ground surface roughness, scales of turbulence, depth of the atmospheric boundary layer etc.

Often in reality, it is difficult to reproduce the structural details in model scale, when the linear scaling is exagerated and this is one outstanding cause of inaccuracy in physical model study.

Kinematic consistency

The flow field is defined by six variables; three velocity components (u, v, w), air density ρ_a (kg/m^3), pressure p (N/m^2) and temperature T (^{o}K), all given as functions of space and time variables (x, y, z, t). However, in case of bridge dynamics, ρ and T are generally deemed constants. Hence, the flow conditions are decided by four equations; three components of momentum conservation (Navier-Stokes equations) and mass conservation (continuity) equation as follows:

$$\frac{D}{Dt}\{V\} = -\frac{\Delta p}{\rho_a} + \nu \cdot \nabla^2 \{V\} \qquad \text{[Navier-Stokes]} \qquad (1)$$

$$\nabla\{V\} = 0 \qquad \text{[Continuity]} \qquad (2)$$

in which $\{V\} = (u, v, w) =$ velocity vector (m/s)
$\nu =$ kinematic viscosity (m^2/s)

The structural behaviour is influenced by many variables but, ignoring the temperature effects, major parameters are as follows:

$L =$ linear dimensions of the structure (m)
$\rho_m =$ the material density (kg/m^3)
$g =$ the acceleration due to gravity (≈ 9.8 m/s^2)
$E =$ Young's modulus (N/m^2)
$\varsigma =$ the structural damping ratio

Considering these properties, the dimensionless parameters to be considered for physical simulation are given as follows:

$$\mathrm{Re} = \frac{VL}{\nu} \quad \text{(Reynolds number)} \qquad Fr = \frac{V}{\sqrt{gL}} \quad \text{(Froude number)}$$

$\dfrac{\rho_m}{\rho_a}$ (Density ratio) $Ca = \dfrac{E}{\rho_a V^2}$ (Cauchy number)

(3)

ς (Structural damping)

Boundary Conditions

As the boundary conditions, the following factors need to be considered:

Pressure gradient:		$p(x, y, z_g)$
Approaching flow:	Mean flow speed	$\overline{U}(y, z \le z_g)$
	Spectral quantities	$G_{jj}(y, z; f) \quad (j = u, v, w)$
	Cross-correlations	$R_{ij}(\Delta x, \Delta y, \Delta z; f)$

$(i, j = u, v, w)$

Geometrical shape of the test section boundaries.

Simulation of these factors particulraly with wind tunnel facilities is discussed in 7.2.

(3) <u>Discussion on dimensionless parameters</u>

It is generally not possible to satisfy all of the requirements. Just as an example, consider $\mathrm{Re} = VL/\nu$ and $Fr = V/\sqrt{gL}$. If ν and g are common between the model and prototype, both of these requirements are simultaneously satisfied when, and only when, two systems have exactly the same V and L between them. In other words, these systems have to be identical. If the requirements are not perfectly satisfied, it is important to know the limit of availability of each similitude and also possible influence on outcomes when a condition is relaxed or distorted.

Reynolds number

Reynolds number can be defined as the ratio of the fluid inertia force to the fluid viscous force. In most of wind tunnel tests, it is impracticable to satisfy Reynolds number similitude. Indeed the viscous forces are usually at least an order of magnitude smaller and relatively unimportant compared to the inertia forces. However, the consequence of the distorsion of this requirement must be examined carefully. The following three points are of particular importance:

1) It is well known that the flow pattern around a circular cylinder is very sensitive to the change of Re because of the shift of flow separation points with it. There is a corresponding change of the wake width and the drag force as well as the frequency of vortex formation. It is important that, in modelling a structure with smooth curved surface geometry, these effects are properly taken into consideration. It should be noted that the critical Reynolds number is also

dependent on the surface roughness of the solid boundary as well as the turbulence level in the approaching air flow.

2) In case of the flow around the sections with sharp corners, the flow separation points do not move and the flow pattern is less sensitive to a change of the Reynolds number. However, a broad wake after separation from the upstream corners may reattached to the body surface, depending on the aspect ratio of the body cross-section or the length of the after-body. The flow reattachment, of course, results a reduction of drag force and increase of the Strouhal number, $St = fd/V$, in general. The critical aspect ratio of the body, at which this change occurs, depends on the Reynolds number as well as the corner radius and the air stream turbulence level. It should be also noted that this factor is influenced by the wind tunnel blockage ratio.

3) In the problems involving effects of wind turbulence, it is essential to simulate the velocity spectra correctly. Townsend (1976) has pointed out that "geometrically similar flows are expected to be dynamically and structurally similar, if their Reynolds numbers are large enough to allow turbulent flow". However, it should be remembered that the Reynolds number does play a part in the existence of the inertia subrange of its energy spectra. As the Reynolds number increases, the high frequency end of the distribution will be extended so that the total dissipation of the turbulence energy remains unchanged. On the other hand, when the Reynolds number is small, the ratio of the size of the dissipating eddies to the representative size of the predominant eddies becomes highly dependent on viscosity. A result of this is an inaccurate simulation of turbulence structure due to narrower-than-necessary inertia subrange.

Froude number

Froude number is the ratio of fluid inertia force to vertical force due to gravity and/or buoyancy. Consequently, the Froude similitude becomes important for the cases such as dissipation of airborne particles or wind-induced response of cable-supported structures where gravity is a dominant factor. For aeroelastic testing, often Froude scaling becomes the only available matching parameter for the flow itself. Whenever the influence of gravitational field needs to be considered, this requirement cannot be waived. However, depending on the nature of the problem, when the restoring force of the structure is strictly provided by the elastic force, even this similitude can be relaxed. As a result, the time scale would be most likely decided by the frequency scaling.

Density ratio

The ratio of structural density ρ_m to air density ρ_a has to be consistent. Here, ρ_m is not necessarily the density of the used materials but the apparent density of the structure as a whole. Therefore the requirement is often satisfied in terms of mass ratio, μ , as follows:

$$\frac{\rho_m}{\rho_a} = \frac{\rho_m L^2}{\rho_a L^2} \Rightarrow \frac{m}{\rho_a B^2} = \mu \tag{4}$$

For the case of a bridge model, $m =$ mass of the bridge per unit length, and $B =$ the deck width. If it is a problem in torsion, the mass parameter becomes $J/\rho_a B^4 = \mu(r/B)^2$ instead of μ, where J represents the polar mass moment of inertia per unit length of the structure.

Cauchy number

The Cauchy number, which is the ratio of elastic force to the inertia force of the fluid, can be interpreted in the following way:

$$Ca = \frac{E}{\rho_a V^2} = \frac{EL^4/L^2}{\rho_a V^2 L^2} \Rightarrow \frac{mL^4 \cdot \omega^2/L^2}{\rho_a V^2 L^2} = \left(\frac{\omega L}{V}\right)^2 \frac{m}{\rho_a L^2} \Rightarrow \frac{\mu}{V_R^2} \tag{5}$$

Since the mass ratio is already a requirement, this implies the consistency of the reduced velocity

$$V_R = \frac{V}{fL} \tag{6}$$

or the inverse of it, reduced frequency, $f_R = fL/V$, as a similitude parameter. This becomes one of the fundamental requirements in aeroelastic testing of structures. Usually it is not difficult to do testing over a wide range of reduced velocity to cover the equivalent range in reality.

Critical damping ratio

The maginitude of structural damping is obviously an important parameter for the prediction of structural dynamic response. The problem, however, is that its magnitude is uncertain even for the existing structures. Naturally the wind tunnel tests are usually carried out for a range of damping ratio. Mass and damping are two most important factors in the design and construction of wind tunnel models and these two requirements have been sometimes combined together as the Scruton number, or the mass-damping parameter, defined by

$$Sc = \frac{m\varsigma}{\rho_a d^2} \tag{7}$$

The concept of this parameter was originally introduced by a simple analytical model to demonstrate the peak amplitude of vortex-induced response, and it should be remembered that the Scruton number does not necessarily always work as a good single parameter to describe the response characteristics. Mass and damping parameters have to be, generally speaking, examined separately (Tanaka & Yamada 1987).

(cf.) Note that the Scruton number is sometimes defined as $Sc = 2m\delta/(\rho_a d^2)$, which is 4π times the number defined by (7).

7.2 Wind Tunnel Simulation of Natural Wind

(1) General principle and its history

Nobody would do model testing of a structure without considering the external loading conditions as realistic as possible together with those of the structure itself. For the testing of bridges, however, the wind action was often considered to be simply a uniformly smooth air flow, with or without small angle of attack deviated from parallel to the ground, and always normal to the longitudinal bridge axis. This simplified loading condition is something like a consideration of earthquake excitation by a simple harmonic ground motion, which may be a faily conservative assumption but not without exceptions.

Early wind tunnel studies of model buildings in 1930s and '40s indicated significant influence of wind turbulence on test results such as the pressure distribution patterns. It was about the same time when Prandtl's boundary layer theory was applied by meteorologists to explain the structure of the lower atmosphere. However, the most fundamental principle for wind tunnel tests in this regard was not clealy recognized until the following statement was made by Martin Jensen:

> "The natural wind is turbulent, and the phenomena...take place in the boundary layer of the wind, and, as should be emphasized, are highly dependent on the nature of this boundary layer......The correct model test with phenomena in the wind must be carried out in a turbulent boundary layer, and the model-law requires that this boundary layer be to scale as regards the velocity profile." (Jensen 1958)

Following the collapse of Tacoma Narrows, there was a significant contribution by aeronautical engineers towards the experimental aerodynamics with civil engineering applications. At the same time, it became a general practice to do testing of structures such as bridges in a conventional aeronautical wind tunnel where the air flow is smooth and uniform rather than simulated natural winds. It could be said that it was a "side effect" of the contribution by aeronautical prejudices. Jensen's micrometeorological consideration was followed up by Davenport's formulation of codified natural wind characteristics and physical simulation of it in early 1960s. It was a significant impact to the practice in this engineering field (Davenport & Isyumov 1967).

(2) Characteristics of natural wind

The similitude requirements of wind characteristics for physical wind tunnels and mathematical simulation models have been extensively discussed by both meteorologists and wind engineers (Plate 1982 etc.). The simulation of wind can be considered in two categories: a) the average characteristics of the turbulent boundary layer wind, which is approaching to the site of each project; and b) the wind structure at the immediate proximity of the structure, which is largely influenced by the particular topographical conditions including surrounding structures. These two are sometimes referred to as the far field and near field simulation, respectively.

For convenience, let us take x-coordinate horizontally along the mean wind, which is assumed normal to the longitudinal bridge axis, and z-coordinate vertically upward. The y-coordinate is hence along the bridge. The wind field characteristics for testing of bridge are generally defined by the following parameters:

Mean speed distribution	$\overline{U}(y,z)$		
Turbulence intensities	$I_u(y,z)$	$I_v(y,z)$	$I_w(y,z)$
Velocity spectra	$G_u(f)$	$G_v(f)$	$G_w(f)$
Velocity correlations	$R_{uu}(\Delta y, \Delta z)$	$R_{ww}(\Delta y, \Delta z)$	

For all of these factors, the general homogeneity of the flow field is required over some length in x-direction, when the model is rotated to observe the effect of horizontal skew angle.

There have been a number of studies that present good summary of these natural wind characteristics (Counihan 1973; ESDU 1986). A simple mathematical model of the atmospheric turbulence at elevation z, assuming neutral stability, can be given typically as follows:

Turbulence Intensities

$$I_u = \frac{1}{\log_e(z/z_0)} \qquad I_v = 0.8 \cdot I_u \qquad I_w = 0.5 \cdot I_u$$

Scales of Turbulence

$$L_u^x = 2.93z \qquad L_u^y = L_u^z = 0.98z \qquad L_v^x = L_v^y = L_v^z = 0.73z$$

and $L_w^x = L_w^y = L_w^z = 0.37z$

Velocity Spectra

$$\frac{fG_u(f)}{\sigma_u^2} = \frac{22n}{(1+33n)^{5/3}} \qquad \frac{fG_v(f)}{\sigma_v^2} = \frac{6.3n}{(1+9.5n)^{5/3}}$$

and $\frac{fG_w(f)}{\sigma_w^2} = \frac{1.3n}{1+5.3n^{5/3}}$ in which $n = \frac{fz}{\overline{U}(z)}$

Coherence Functions

$$\gamma_{ii}(f,\Delta r_j) \approx \exp\left(-k_{ij}\frac{f\cdot\Delta r_j}{\overline{U}(z)}\right) \qquad (i = u,v,w;\ j = x,y,z)$$

A problem of so-called Davenport-type coherence above is the fact that the coherence function of this model goes to unity at zero frequency, whereas the field measurements indicate that they should be less than one. ESDU (1986) is also following this functional form. As opposed to them, the historically well-known model proposed by von Kármán (1948) is known to agree well with the field measurement, particularly in the low frequency range.

(3) Boundary layer wind tunnels

Jensen's Experiment

Using a long wind tunel ($L = 5.5$m, width 0.6m) whose floor coated by various roughness, Jensen produced the turbulent boundary layer flows of various roughness length z_0 as shown in the table, together with the boundary layer thickness, which was found to be given by approximately $\delta(x) = z_0^{0.2}\cdot 0.341x^{0.8}$ when $2\times10^3 < \mathrm{Re} < 5\times10^5$.

Floor coating	z_o (cm)	δ(cm)
Glazed cardboard sheets	1.5×10^{-3}	10
Smooth masonite plates	$0.9–1.8\times10^{-3}$	10
Sandpaper	2.5×10^{-2}	12
Corrugated paper (h=0.35cm, λ=0.90cm)	$4.1–6.7\times10^{-2}$	14
Small broken stones (1.5 to 2cm)	0.37	15
Wooden fillets, 2.5cm(h)×2.0cm(w) 15-20 cm spacing, angled ≤20°	0.41	20
Large broken stones (3 to 6cm)	0.86	22
"Model of a city" 7.0cm(h)×2.9cm(w) rows across the tunnel, angled ≤20°	3.50	30

Jensen did measurement of wind induced pressure around a building ($h = 160$ cm) in the field where z_0 = 0.95 cm. Then he placed a 1:20 scaled model of it in his wind tunnel and tried to reproduce the wind induced pressure distribution as shown in the next page. What he found was when h/z_0 is consistent to the full scale value, the correct pressure distribution was observed.

From these results, Jensen concluded that the phenomena induced by natural wind can be reproduced only when the model tests are performed in a boundary layer which was created in a similar way as the case of natural wind and also when the linear scale of its turbulence coincides with the linear scaling of other models placed in it. h/z_0 is now called Jensen number after his name.

Jensen's idea on the experimental simulation of atmospheric boundary layer in a wind tunnel was largely extended by Davenport in Canada and Cermak in USA in the 1960s.

Development of BLWT

Since then, the simulation of natural wind and research in various wind engineering fields have made a significant progress. The idea of boundary layer simulation is now firmly established as one of the most fundamental requirements that must be satisfied in any experimental or analytical simulation of the wind engineering problems.

The boundary layer wind tunnel Davenport first established at the University of Western Ontario has a working section of about 24m long, 2.4m wide and an adjustable height, variable from 1.7m at the entrance to 2.3m at the end. The adjustment of the roof height allowed control over pressure gradients along the tunnel length. The adjustable stable wind speed range was 0.5 to 15 m/s. The simulation of atmospheric boundary layer flow under neutral condition was made by placing various roughness coverages on the wind tunnel floor. The representative power-law exponents were in the range up to 0.34 and the available linear scale compared to natural wind was typically 1:400 to 1:500.

Other methods of producing velocity profiles

There have been a number of attempts to artificially create a thick boundary layer without losing the required characteristics. They include the use of graded gauze, grid of rods, plates and other types of vortex generators, fences and other roughnesses in the upstream section. More sophisticated methods are, for example, the use of counter-jets and pulsating grids, which tend to be very expensive.

Amongst these, one of the most successful is the use of triangular spires at the entrance of wind tunnel test section. The particular technique was developed mostly at the Low Speed Aerodynamics Laboratory of the National Research Council Canada. The work was initiated in 1968 by Templin with the object to generate a thick boundary layer without having a long upwind fetch, thereby enabling the full potential of aeronautical wind tunnels to be realized for wind engineering purposes. It was further developed by Standen, Campbell et al. and more or less completed by Irwin (1979).
The original idea was to design the spire shape to obtain the desired power-law wind profile with an acceptable lateral uniformity at a distance approximately six spire

heights downstream. No considerations of the turbulence characteristics produced as a result entered into the calculation. Campbel and Standen were successful in producing a simulated mean flow profile but their calculation needed further improvement. Furthermore the desired shape of spires was still disputable. After many experiments, Irwin concluded that a straight triangle should be the reasonable choice and indicated the following calculation for the design of them.

Distorsion of similitude requirements and its consequences

Distorsion of boundary layer simulation, even if all the general characteristics of the atmospheric boundary layer flow are assumed to be well defined, can enter the modelling procedure in two ways: First, because the required flow cannot be defined very well due to inhomogeneities in the terrain surrounding the site to be modelled, and secondly because the flow simulation itself may have distorsions inherent in its methodology.

Obviously some problems are more sensitive to some boundary layer parameters than to others and some problems may involove other flow parameters as well. The discussion here is limited mostly to the structural problems and the subject of modelling pollutant dispersion is not being considered.

In order to make an effective discussion, it is convenient to classify both wind environment and structures into groups as a basic framework. For the establishment of wind environment, the general practice now is to develop the background boundary layer over a relatively homogeneous terrain (far field simulation) and then modify it by the detailed surroundings of the site in question typically for a radius of 300 to 500 m (near field simulation). The far field simulation is to produce the overall characteristics of the boundary at the site as they have been discussed throu this chapter. The near field, on the other hand, is to provide the intimate complex interaction which are largely inhomogeneous and intractable to precise definition. A useful classification of structures a detailed discussion on various aspects of simulation problems within this framework have been given by Surry (1982).

7.3 Mathematical Simulations

The application of numerical simulation techniques in the field of wind engineering or related fields has taken various steps through its history and it is probably fair to say that only recently it has come to rather realistic stages.

The first application of numerical analysis to fluid mechanics was to obtain solution of inviscid, or potential flow equations described in terms of complex potential $w(x, y) = \varphi + i\psi$, which was possible only for laminar flow. The next development was to solve the Navier-Stokes equation directly by applying various numerical integration techniques. Of course for this case, a proper turbulence model has to be introduced for the expression of Reynolds stresses.

Fundamental equations

Description of incompressible flows, whatever they are, can be given by the following equations:

$$\frac{\partial u_i}{\partial t} + u_j \frac{\partial u_i}{\partial x_j} = -\frac{1}{\rho}\frac{\partial p}{\partial x_i} + \frac{\partial}{\partial x_j}\left(\nu \frac{\partial u_i}{\partial x_j}\right) \qquad \text{[NS]} \qquad (1)$$

$$\frac{\partial u_i}{\partial x_i} = 0 \qquad \text{[Cont]} \qquad (2)$$

With p and T not much far away from the standard status, the minimum scale of turbulence, typically the depth of viscous sublayer, is far greater than the average of molecular free path. It means that it is very unlikely that the flow turbulence cannot be described by the Navier-Stokes equation. Turbulence can be considered essentially as a phenomenon of continuous media. Note that there are micro worlds which do not know turbulence, such as the motion of bacteria or spermatozoa. The mechanics of them is completely described as viscous laminar flow.

The combination of above equations describes all the possible turbulent phenomena but numerical analysis of these equations does not necessarily give all the correct solutions. Because in numerical analyses, continuous physical quantities are approximated by discrete quantities and hence give an equivalent cut-off frequency of low-pass filter corresponding to the mesh-size of different grid adopted for the calculation.

In general, it is necessary to consider very high frequency fluctuations of velocity to grasp the characteristics of turbulence and therefore requires very high quality computers.

Introducing $p \rightarrow \overline{P} + p(t)$ and $u_i \rightarrow \overline{U}_i + u_i(t)$, the following Reynolds equation is obtained:

$$\frac{\partial \overline{U}_i}{\partial t} + \overline{U}_j \frac{\partial \overline{U}_i}{\partial x_j} = -\frac{1}{\rho}\frac{\partial \overline{P}}{\partial x_i} + \frac{\partial}{\partial x_j}\left(\nu \frac{\partial \overline{U}_i}{\partial x_j} - \overline{u_i u_j}\right) \qquad (3)$$

The last term, corresponding to the Reynolds stress terms, expresses dispersion of momentum caused by velocity fluctuations.

Eq.(3) describes the averaged field of turbulence; meaning that fine fluctuations are not given by this equation and spacial gradient of wind velocity and pressure are relatively mild. Hence it is easier to use (3) than (1) for the application of finite difference method. Many attempts of numerical simulation starts with this equation.

Discussion on viscosity term

By introducing the representative length scale L and the velocity scale V and putting

$$u_i^* = \frac{u_i}{V} \qquad x_i^* = \frac{x_i}{L} \qquad t^* = \frac{tV}{L} \qquad p^* = \frac{p}{\rho_a V^2}$$

and $\mathrm{Re} = VL/\nu$, eq.(1) becomes

$$\frac{\partial u_i^*}{\partial t^*} + u_j^* \frac{\partial u_i^*}{\partial x_j^*} = -\frac{\partial p^*}{\partial x_i^*} + \frac{1}{\mathrm{Re}} \frac{\partial^2 u_i^*}{\partial x_j \partial x_j} \tag{4}$$

The last term of eq.(4), dispersion due to molecular viscosity, is inversely proportional to Re. It means when $\mathrm{Re} \to \infty$, the effect of molecular viscosity cannot be observed well.

When eq.(3) is used, usually eddy viscosity K_m is introduced to model the Reynolds stresses. For this case, as $K_m \sim VL$,

$$\mathrm{Re} = \frac{VL}{K_m} \sim 1$$

One of the most important characteristics of turbulence is the existance of various scales of eddies and their cascading process. The minimum scale of eddies is called "Kolmogorov's micro-scale η" and is given by approximately

$$\eta \sim \left(\frac{\nu^3}{\varepsilon} \right)^{1/4}$$

where ε = the rate of viscous dissipation per unit time and unit mass, or defined by

$$\varepsilon = \nu \overline{\frac{\partial u_i}{\partial x_j} \frac{\partial u_i}{\partial x_j}}$$

and hence its unit is m^2/s^3. Eddies dissipate as heat energy at this scale due to viscosity. ε is related to the energy transfer mechanism at larger scale than η and is approximately valued by

$$\varepsilon \sim V^3/L$$

where $V \sim \sigma_u$ and $L \sim L_u^x$, for example. Therefore $\dfrac{\eta}{L} \sim (\mathrm{Re})^{-3/4}$ where $\mathrm{Re} = \dfrac{VL}{\nu}$. η and L are the most important linear scales in the numerical simulation of turbulent flows.

Problem of direct simulation

If the turbulent flow field is solved, it means that the mechanism of energy dissipation needs to be included as a part of the solution and this can be done only at the scale of η. If the mesh-size h(say) of finite difference is much greater than η, this mechanism will not be discussed in this solution. At least it needs to be $h \sim \eta$. Therefore $h/L \sim (\mathrm{Re})^{-3/4}$.

If L is the linear size of the space numerically simulated, $L/h = N$ is the number of mesh (grid) in one direction. In 3D field, the number of grid is $N = (L/h)^3$, or

Re	10^4	10^6	10^8
N	10^9	10^{13}	10^{18}

In practical wind engineering problems, $\mathrm{Re} > 10^6$. $\therefore$ $N > 10^{13}$. Turbulence simulation models are needed because of this reason.

(cf.) If Navier-Stokes and continuity equations are considered under proper initial conditions and boundary conditions at each grid point to calculate velocity and pressure, and the required mathematical operations for this process is 10^2 (say), and repeat this 10^2 times, meaning 10^2 steps go ahead in time, and required time for each mathematical operation is 10^{-6} sec. (say), the total calculation time is

$$10^{13} \times 10^2 \times 10^2 \times 10^{-6} = 10^{11}(\mathrm{sec}) = 1.16 \times 10^6\, days \approx 3200\, years\,!$$

Reynolds stresses are simulated by various assumptions: $\sim K_m \dfrac{\partial u_i}{\partial x_j}$ where $K_m \propto u_{ij}$ etc.

Coarse graining: to consider the space average of quantities for certain mesh area → "Large Eddy Simulation" etc.

7.4 Wind Tunnel Testing Techniques

(1) Full bridge model tests

Started following the Tacome failure
Successful in 1) reproducing the failure mechanism, 2) designing a stable bridge, and 3) establishing the method for the followers. However, not quantitatively...
Mechanically equivalent model

The overall stiffness of the bridge girder is provided by a few spinal stiffening bars and the geometrical configuration of the girder is made up by short modules of non-structural material. The distribution of mass and mass moment of inertia can be easily adjusted by attaching additional weights at any conveniently hidden locations. The towers can be made in much the same way as the girder. The axial stiffness of main cables has to be properly simulated. The result is usually the use of a very thin piano wires and the cable mass needs to be adjusted by attached discrete masses to them.

The scale ratio for a long span bridge is often very much limited because of the availability of large wind tunnels and the linear scale of turbulence created in the wind tunnel. Regarding the latter requirement, if the Kaimal type spectrum is assumed for u-component turbulence, the perfect matching of this component may not be practically achievable with the present state-of-the-art.

The model design procedure is as follows:

1. Dynamic FEM analysis to decide eigen frequencies ω_j and mode shapes $\phi_j(x)$.
2. Dynamic analysis in model scale to decide the boundary conditions, degree of simplifications etc.
3. Froudse similitude ($\lambda_V = \sqrt{\lambda_L}$) is required particularly for suspension bridges.
4. Simulation of mass, mass moment of inertis and stiffness.
5. Simulation of cables for axial stiffness, mass and drag force.

(2) Sectional model tests

The idea is to make use of a rigid, shape-wise representative segment of the bridge as an analog device for extracting wind loads (Hjorth-Hansen 1992). By definition, any spanwise variations of the structure and wind characteristics are ignored in this testing method. The model can be almost immobile or given a forced motion for measuring the reactions at its support, or freely suspended in given air flow for the response measurement. The tests usually consider only vertical bending and torsional motion. However, it is possible to include the drag-wise sway as well. The wind flow can be either smooth or with turbulence, but it is difficult to include the turbulence effects with good accuracy, particularly of low frequency range.

Required similitude includes usually the following items:

a) Geometrical configuration of the bridge deck;

b) Mass parameters: $\mu = m/\rho B^2$ and $\nu = \mu(r/B)^2$

c) Structural damping: ς_T and ς_V

d) Reduced velocity: $\overline{U}/f_T B$ or $\overline{U}/f_V B$

e) Frequency ratio: f_T/f_V

f) Location of the centre of rotation.

where $m, r, B =$ the linear mass, radius of gyration and width of the bridge deck;
$\rho =$ air density;
$\varsigma_T, \varsigma_V =$ critical damping ratio in torsion and vertical bending;
$f_T, f_V =$ eigen frequencies in torsion and vertical bending.

The Reynolds number effects will have to be ignored but it is not any worse regarding this particular issue than other testing methods anyways. It should be, however, noted that Reynolds number does have influence, generally speaking, on bridge response and measured aerodynamic forces (Matsuda et al. 2003).

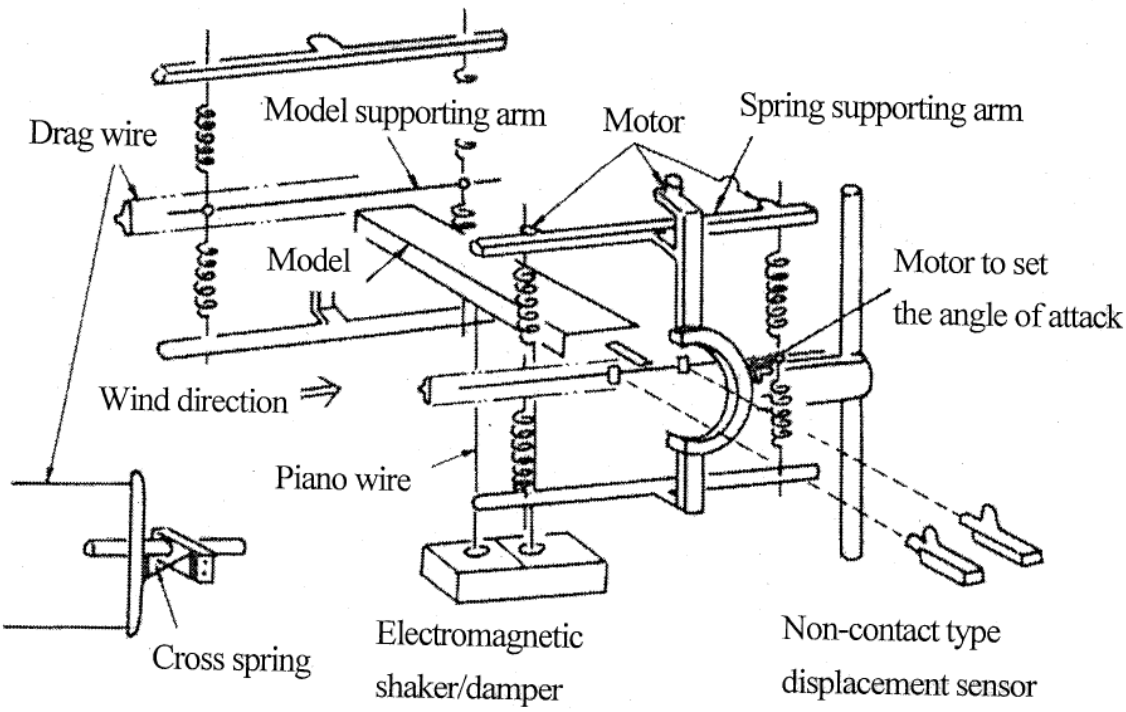

Fig.1 Typical set-up of a dynamic rig

The aerodynamic force coefficients in lift, drag and pitching moment, and all 18 motion-dependent flutter derivatives can be effectively measured by using a section model. The dynamic tests are usually effective in making prediction of aerodynamic instability, both in torsion and galloping, and exploring a possibility of vortex-shedding excitation. However, considerable interpretation efforts would be required for buffeting prediction.

There expected to be some errors pertaining to the oncoming flow, which is difficult to be perfectly two-dimensional. Beacuse the model needs to be supported from outside the wind tunnel walls, there is a possibility of air flow leaking through these holes. There have been various attempts to prevent or reduce the effects of the end-leakage. It is also necessary to give certain aspect ratio to the model to maintain the two-dimensional characteristics of testing.

Regarding the design of suspension rigs, drag wires, vibrational mode in torsion, device to control system's damping and some other practical hints for maintaining good accuracy in measurement, there is an excellent review article presented by Hjorth-Hansen (1992).

(3) Taut strip model tests

The use of a taut strip model was proposed to fill in a gap between two conventional testing methods, the sectional model method and full bridge model method. The idea is to have a simulated bridge deck in terms of its geometrical shape and mass distribution but its stiffness being provided only by stretched wires between anchorages. The geometrical scale of the deck has to be chosen in conformity with the linear scaling of wind turbulence. The simulation of main cables, which is often difficult with large scaling, is altogether given up. Since the stretched wires would vibrate with a half sine wave mode shape, the obtained test results have to be treated properly for the prediction of actual bridge response, considering the anticipated mode shapes of the bridge. Frequency in vertical bending is tuned by wire tension, whereas its ratio to the torsional frequency is controlled largely by the separation of two wire and also by addition of an elastic tube located at the centre of twist.

This technique was first introduced by Davenport (1972) as a means to take a second look at te experiments carried out at the early stage of suspension bridge aerodynamics, including this time their 3D response characteristics to simulated turbulent wind. A chief objective of the taut strip model method is a simulation of the dynamic characteristics of the bridge road deck with the consistent linear scaling factor as the simulated natural wind, and yet not going to the complexity of manufacturing a full bridge model. Inevitably there are inaccuracy in structural simulation. Since the main cables are not simulated at all, any gravitational acceleration effects and associated structural nonlinearity is altogether ignored. An ironical advantage is an almost free choice of length scale and time scale independent of each other. It means that both of Reynolds and Froude similitude are violated.

The fundamental response characteristics of taut strip models have been examined to confirm that the response in general are in good agreement with buffeting and flutter theories for which the aerodynamic derivatives and aerodynamic admittance functions are assumed to be more or less known. In fact it is one of the advantages offered by this method that when the taut strip model results are used as input to the buffeting theory, the complication of defining the aerodynamic admittance function is avoided. Also a possible complication due to nonlinearity of aerodynamic derivatives need not be considered either (Tanaka & Davenport 1982).

More recent development of high speed scanning technique for the measurement of wind induced pressure fluctuations made it possible to apply this testing method to more versatile objectives. In relation to the aerodynamic study of the Storebælt Bridge, a taut strip model was used for the measurement of unsteady aerodynamic deivatives, aerodynamic admittance function and space correlation of lift forces (Davenport et al. 1992).

References:

Cermak, J.E., Advances in physical modeling for wind engineering, *Proc. ASCE* (113) EM5, 1987.

Davenport, A.G. & Isyumov, N., The application of the boundary layer wind tunnel to the prediction of wind loading, *Proc. 2nd ICWE*, Ottawa, 1967, pp.201-230.

Davenport, A.G., King, J.P.C. & Larose, G.L., Taut strip model tests, *Aerodynamics of Large Bridges*, (ed. Larsen) 1992, pp.113-124.

ESDU, *Characteristics of Atmospheric Turbulence Near the Ground*, ESDU Item No.86010, Engineering Sciences Data Unit, 1986.

Hjorth-Hansen, E., Section model tests, *Aerodynamics of Large Bridges*, (ed. Larsen) 1992, pp.95-112.

Irwin, P.A., Full aeroelastic model tests, *Aerodynamics of Large Bridges*, (ed. Larsen) 1992, pp.125-135.

Irwin, P.A., Design and Use of Spires for Natural Wind Simulation, *JWEIA* (7) 1981, pp.361-366.

Jensen, M., The model-law for phenomena in natural winds, *Ingeniøren*, Int. ed. (2) 4, 1958, pp.121-128.

Kármán, T. von, Progress in the statistical theory of turbulence, *Proc. Nat. Academy of Science* (34) 1948, pp.530-539.

Matsuda, K., Cooper, K.R. & Tanaka, H., The analysis of wind-induced static displacements and flutter for long-span suspension bridges using steady and unsteady aerodynamic forces measured at high Reynolds numbers, *Proc. 11th ICWE*, Lubbock, Texas, 2003 (1) pp.649-656.

Panofsky, H.A. & Dutton, J.A., *Atmospheric Turbulence: Models and Methods for Engineering Applications*, John Wiley & Sons, 1984.

Plate, E.J. (ed.) *Engineering Meteorology*, Elsevier, 1982.

Surry, D., Consequences of distorsions in the flow including mismatching scales and intensities of turbulence, *Proc. Int. Workshop on Wind Tunnel Modelling Criteria and Techniques in Civil Engineering Applications*, Gaithersburg, MA, 1982, pp.137-185.

Tanaka, H., Similitude and modelling in bridge aerodynamics, *Aerodynamics of Large Bridges*, (ed. Larsen) 1992, pp.83-94.

Tanaka, H. & Davenport, A.G., Response of taut strip models to turbulent wind, *Proc. ASCE* (108) EM1, 1982.

Tanaka, H. & Yamada, H., Mass and damping simulation for the modelling of aeroelastic responses, *Proc. Int. Conf. on Flow Induced Vibrations*, Bowness-on-Windermere, May 1987, pp.103-110.

Townsend, A.A., *The Structure of Turbulent Shear Flow*, Cambridge Univ. Press, 1976 (2nd ed.).